# Functional MRI of Focal and Generalised Interictal Epileptiform Discharges

**Khalid Hamandi BSc MB BS MRCP**

DEPARTMENT OF CLINICAL AND EXPERIMENTAL EPILEPSY

INSTITUTE OF NEUROLOGY

UCL

THESIS SUBMITTED FOR THE DEGREE OF DOCTOR OF PHILOSOPHY

2007





ProQuest LLC
789 East Eisenhower Parkway
P.O. Box 1346
Ann Arbor, MI 48106-1346

**Personal Contribution**

I, Khalid Hamandi, confirm that I am the sole author of this thesis. The work presented here is my own. Information derived from other sources is indicated and referenced. Although the work reflects the contributions of a team of researchers, I have outlined my individual contribution below and those of co-researchers who made a significant contribution to the work.

I was responsible for recruitment, experimental set up, data acquisition and analysis. I personally reviewed and coded the all the EEGs. I performed all data pre-processing steps, storage and archiving of data. I performed all data analysis aside from the quantitative perfusion analysis (Chapter 4) and the frequency analysis algorithm set up by Helmut Laufs, I interrogated the results and the presentation of findings and interpretation is my own. I was responsible for producing all the figures and graphical presentation of the data. All results and interpretations were presented by myself and developed following discussions at regular supervision meetings. Afraim Salek-Haddadi recruited and scanned the first 26 patients in the GSW series (Chapter 3), although I carried out all pre-processing and analysis for the work presented here.

**Abstract**

Localizing the source of epileptic discharges is important in gaining a greater understanding of the disease, classifying epilepsy, and identifying areas suitable for potentially curable surgical resection. Functional imaging measures haemodynamic, metabolic or neurochemical correlates to localise neural activity. Combining EEG with functional MRI (EEG-fMRI) allows the localisation of haemodynamic correlates of neuronal events recorded on surface EEG. The work in this thesis aims to identify the spatial haemodynamic correlates of interictal epileptiform discharges (IED) in patients with epilepsy using EEG-fMRI. Five studies form the main body of this thesis. In the first study, 46 patients with frequent generalised spike wave activity (GSW) were studied with EEG-fMRI on a 1.5 Tesla scanner. The main finding was of a characteristic pattern of fMRI signal decrease in frontal, parietal and posterior cingulate cortex, areas of association cortex, during GSW. In the second study, 4 patients from this first series were re-studied with a 3 Tesla scanner. A high degree of reproducibility was seen in the spatial distribution of fMRI changes. Perfusion MRI with an arterial spin label sequence was used that showed a decrease in blood flow to these areas during GSW. In the third study, a novel method for the analysis of fMRI data in epilepsy, temporal clustering analysis (TCA) was assessed. The technique was confounded by subject motion, and we were unable to reliably detect correlates of IED. The fourth study moves away from correlating visually identified IEDs on the EEG, and correlates power fluctuations in the delta frequency band with simultaneously acquired fMRI. Finally a combination of EEG-fMRI and MR tractography were used to study a patient with temporal lobe epilepsy. The issues surrounding potential use of EEG-fMRI as a clinical tool are discussed.

*"One marked characteristic of the literature dealing with the cerebral circulation is, we think, the contradictory nature of the results which have been obtained by different investigators.*

*There is no reason, we imagine, for doubting that the cause of these discrepancies is to be found in the great difficulty of avoiding the sources of error which plentifully surround the subject, and in overcoming certain technical difficulties which we shall refer to. The ease with which one can obtain results upon certain points, on taking up the subject, is itself, we believe, apt to make the enquirer careless in controlling the sources of error, which , it may be noted, are some of them not at first sight obvious. We must on this account say more about the technology of our subject than would be necessary were the subject a simpler one"*

From C. S. Roy and C.S. Sherrington (1890). On the Regulation of the Blood-Supply of the Brain [Roy and Sherrington 1890].

**Table of contents**

**Acknowledgement**

I would like to thank my supervisors Professors Louis Lemieux and David Fish for their skilful insight, advice and guidance. I also thank Professor John Duncan for his clinical oversight, unparalleled enthusiasm and encouragement.

Afraim Salek-Haddadi, who was my predecessor in this work, laid much of the foundations for the methods used and with his Matlab programming skills developed many of the scripts used. I was again fortunate when Helmut Laufs joined the group with his technical computing and SPM talents. I thank them both for the scripts they wrote and their time and patience in taking me to a level of reasonable computer literacy. I thank other members of the EEG-fMRI group, Adam Liston and Joseph Suresh Paul and in particular David Carmichael for his sterling efforts with the perfusion fMRI.

Philip Allen, Nathan Thoms, Gareth Balke and Terry Thompson at the engineering laboratory at the NHNN were always available for help, advice and EEG repairs.

Shelagh Smith and Mathew Walker taught me most of what I know about EEG. The EEG technicians Joan Adams, Linda McCauly, Fiona Walker at NSE, and Catherine Scott at NHNN were always available for help and advice with EEG interpretation.

I thank the radiographers at NSE, Philia Bartlett and Jane Burdett for their patience and time, and putting up with the quirks of EEG-fMRI. I thank Mark Symms for physics support. I thank Ray Dolan for his support in getting scanner time at the FIL and Ulrike Nöth for running the scanner and providing the perfusion sequence and analysis.

I thank the consultants, clinical research fellows and physicists at the Department of Clinical and Experimental Epilepsy for their friendship and good company.

Thank you to the Wellcome Trust for providing my salary for three years as well as the funding for this research.

Lastly to my wife and children for all the fun they bring.

List of Figures

List of Tables

Abbreviations

| | |
|---|---|
| AED | Antiepileptic drug |
| ANOVA | Analysis of variance |
| ASL | Arterial spin labeling |
| AVM | Arteriovenous malformation |
| BA | Brodmann area |
| BOLD | Blood oxygenation level-dependent |
| CAE | Childhood Absence Epilepsy |
| CNS | Central nervous system |
| CPS | Complex partial seizure |
| CSF | Cerebrospinal fluid |
| CT | Computed tomography |
| DNET | Dysembryoplastic neuroepithelial tumour |
| ECG | Electrocardiogram |
| EEG | Electroencephalography |
| EPI | Echo planar imaging |
| FE | Frequency encoding |
| FDG | Flouro-2-deoxyglucose |
| fMRI | Functional magnetic resonance imaging |
| FWHM | Full width half maximum |
| GTCS | Generalised tonic-clonic seizures |
| HRF | Haemodynamic response function |
| HS | Hippocampal sclerosis |
| ICEES | International classification of the epilepsies and epileptic syndromes |

| | |
|---|---|
| **ICES** | **International classification of epileptic seizures** |
| **IGE** | **Idiopathic generalized epilepsy** |
| **ILAE** | **International league against epilepsy** |
| **JAE** | **Juvenile absence epilepsy** |
| **JME** | **Juvenile myoclonic epilepsy** |
| **MCD** | **Malformations of cortical development** |
| **MNI** | **Montreal neurological institute** |
| **MRI** | **Magnetic resonance imaging** |
| **MTL** | **Medial temporal lobe** |
| **MTLE** | **Medial temporal lobe epilepsy** |
| **NIRS** | **Near infrared spectroscopy** |
| **NMR** | **Nuclear magnetic resonance** |
| **PD** | **Proton density** |
| **PET** | **Positron emission tomography** |
| **RF** | **Radiofrequency** |
| **ROI** | **Region of interest** |
| **SNR** | **Signal to noise ratio** |
| **SPECT** | **Single photon emission computed tomography** |
| **SPM** | **Statistical parametric mapping** |
| **SPS** | **Simple partial seizure** |
| **SS** | **Slice selection** |
| **TE** | **Echo time** |
| **TCD** | **Transcranial Doppler** |
| **TR** | **Repetition time** |
| **TLE** | **Temporal lobe epilepsy** |

**Associated Publications**

**Original Articles**

Hamandi K, Laufs H, Nöth U, Carmichael DW, Duncan JS, Lemieux L. BOLD and perfusion changes during epileptic generalised spike wave activity. *In press, Neuroimage.*

Hamandi K, Powell HWR, Laufs H, Symms MR, Barker GJ, Parker GJM, Lemieux L, Duncan JS. Combined EEG-fMRI and tractography to visualise propagation of epileptic activity. *Submitted Journal of Neurology Neurosurgery and Psychiatry.*

Laufs H, Hamandi K, Salek-Haddadi A, Kleinschmidt AK, Duncan JS, Lemieux L. Temporal lobe interictal epileptic discharges affect cerebral activity in "default mode" brain regions. Hum Brain Mapp. 2006 28(10) 1023-1032.

Salek-Haddadi A, Diehl B, Hamandi K, Merschhemke M, Liston A, Friston K, Duncan JS, Fish DR, Lemieux L. Hemodynamic correlates of epileptiform discharges: an EEG-fMRI study of 63 patients with focal epilepsy. Brain Res. 2006 9;1088(1):148-66.

Laufs H, Hamandi K, Walker MC, Scott C, Smith S, Duncan JS, Lemieux L. EEG-fMRI mapping of asymmetrical delta activity in a patient with refractory epilepsy is concordant with the epileptogenic region determined by intracranial EEG. Magn Reson Imaging. 2006 May;24(4):367-71.

Hamandi K, Salek-Haddadi A, Laufs H, Liston A, Friston K, Fish DR, Duncan

JS, Lemieux L. EEG-fMRI of idiopathic and secondarily generalized epilepsies. Neuroimage. 2006 Jul 15;31(4):1700-10.

Liston AD, De Munck JC, Hamandi K, Laufs H, Ossenblok P, Duncan JS, Lemieux L. Analysis of EEG-fMRI data in focal epilepsy based on automated spike classification and Signal Space Projection. Neuroimage. 2006 Jul 1;31(3):1015-24.

Laufs H, Lengler U, Hamandi K, Kleinschmidt A, Krakow K. Linking generalized spike-and-wave discharges and resting state brain activity by using EEG/fMRI in a patient with absence seizures. Epilepsia. 2006 Feb;47(2):444-8.

Liston AD, Lund TE, Salek-Haddadi A, Hamandi K, Friston KJ, Lemieux L. Modelling cardiac signal as a confound in EEG-fMRI and its application in focal epilepsy studies. Neuroimage. 2006 Apr 15;30(3):827-34.

Hamandi K, Salek Haddadi A, Liston A, Laufs H, Fish DR, Lemieux L. fMRI temporal clustering analysis in patients with frequent interictal epileptiform discharges: comparison with EEG-driven analysis. Neuroimage. 2005 May 15;26(1):309-16.

Liston AD, Salek-Haddadi A, Kiebel SJ, Hamandi K, Turner R, Lemieux L. The MR detection of neuronal depolarization during 3-Hz spike-and-wave complexes in generalized epilepsy. Magn Reson Imaging. 2004 Dec;22(10):1441-4.

**Review Articles**

Hamandi K, Salek-Haddadi A, Fish DR, Lemieux L. EEG/functional MRI in epilepsy: The Queen Square Experience. J Clin Neurophysiol. 2004 Jul-Aug;21(4):241-8. Review.

Hamandi K, Powell HWR. Advances in imaging technology in epilepsy. Progress in Neurology and Psychiatry 2004;8(4):11-13

**Book Chapters**

Hamandi K, Duncan JS. fMRI in the Evaluation of the Ictal Onset Zone. In Textbook of Epilepsy Surgery. Eds: Hans Luders, William Bingaman, Imad Najm. Taylor and Francis Medical Books. *In press*

Matthias J. Koepp, Khalid Hamandi, Systems and networks in myoclonic seizures and epilepsies. in Progress in Epileptic Disorders: Generalised seizures: from clinical phenomenology to underlying systems and networks. Eds Edouard Hirsch, Frederick Andermann, Patrick Chauvel, Jerome Engel, Fernando Lopes da Silva, Hans Luders. John Libby, ISBN : 2-7420-0621-4.

**Conference Abstracts**

Hamandi K, Laufs H, Carmichael D, Nöth U, Paul JS, Duncan JS, Lemieux L. BOLD and ASL fMRI of generalised spike wave activity. NeuroImage. Volume 31, Supplement 1 (2006). 12th Annual Meeting of the Organization for Human Brain Mapping, Florence, Italy.

Hamandi K, Salek Haddadi A, Laufs H, Duncan JS, Fish DR, Lemieux L. functional MRI of Spike Wave Activity in Idiopathic and Secondary Generalised Epilepsy. J Neurol Neurosurg Psychiatry 2006; 77: 126-142. Proceedings of Clinical Neurosciences, Torquay, Devon, 7–9 September 2005.

Hamandi K, Powell HWR, Salek-Haddadi A, Boulby PA, Lemiux L, Parker GJM, Symms MR, Fish DR, Duncan JS. EEG-fMRI and MR Tractography. Advanced Structural and Functional Imaging in a Patient with Refractory Temporal Lobe Epilepsy. J Neurol Neurosurg Psychiatry 2006; 77: 126-142. Proceedings of Clinical Neurosciences, Torquay, Devon, 7–9 September 2005.

Hamandi K, Laufs H, Salek-Haddadi A, Liston A, Duncan JS, Fish DR, Lemieux L. Functional MRI of Spike Wave Activity. Epilepsia September 2005 - Vol. 46 Issue s6:p472. 26th IEC PROCEEDINGS 26th International Epilepsy Congress Paris, France.

Hamandi K, Laufs H, Salek-Haddadi A, Duncan JS, Fish DR, Lemieux L. Functional MRI of Generalised Spike Wave Activity. NeuroImage Volume 26, Supplement 1

pp. 1-104 (2005). 11th Annual Meeting of the Organization for Human Brain Mapping, Toronto, Canada.

Hamandi K, Salek-Haddadi A, Liston A, Fish DR, Duncan JS, Lemieux L. Evaluation of temporal cluster analysis in patients with epilepsy using simultaneous EEG/fMRI. NeuroImage Volume 22, Supplement 1 (2004). 10th Annual Meeting of the Organization for Human Brain Mapping, Budapest, Hungary.

Hamandi K, Salek Haddadi A, Fish DR, Duncan JS, Lemieux L. EEG-fMRI of generalised spike wave activity. J Neurol Neurosurg Psychiatry 2004; 75: 1213-1228 (004). Association of British Neurologists' Spring Meeting, London.

## Introduction

An epileptic seizure (ictal event) is the clinical manifestation of an abnormal synchronous neuronal discharge. Epilepsy is a condition characterised by recurrent, usually unprovoked epileptic seizures. Interictal (between seizures) epileptiform discharges (IED) are defined as "distinctive waves or complexes, distinguished from background activity, and resembling those recorded in a proportion of human subjects suffering from epileptic disorders...." [International Federation of Societies for Electroencephalography and Clinical Neurophysiology 1974]. Empirically IED are divided into spikes, spike-wave, polyspike wave complexes and sharp waves. They can occur in isolation or in brief runs, of no more than a few seconds. The material presented in this thesis investigates the haemodynamic correlates of interictal epileptic discharges (IEDs) using functional MRI.

The morphology of IEDs play a role in the syndromic classification of epilepsy, along with the clinical history and seizure semiology. Classification of epilepsy involves the distinction between focal and generalised epilepsies. In focal epilepsies, IEDs indicate the "irritative zone", i.e. an area related to the location of epileptogenic tissue. Knowledge of the irritative zone guides the surgical management of suitable patients. In the generalised epilepsies, ictal and interictal discharges appear generalised at the outset typically with generalised spike-wave (GSW) or polyspike wave (pSW) being the hallmark of a number of epilepsy types.

The EEG is therefore a primary investigation in the diagnosis and characterisation of epilepsy. It is relatively inexpensive and easy to perform. It provides a continual measure of cortical activity with an excellent time resolution. EEG however lacks good spatial resolution. Visual inspection of EEG allows localisation of focal spikes

to particular brain regions. More precise localisation requires at times imprecise, mathematical models.

Functional MRI (fMRI) can localise haemodynamic correlates of neural activity to within a few millimetres. It is based on the acquisition of a time-series of brain images where the intravoxel signal is sensitive to regional cerebral haemodynamic changes driven by local neural activity. The signal-to-noise ratio of fMRI is low so repetition of the task, stimulus or recorded activity under investigation is necessary whilst fMRI images are acquired. Correlation analysis is used to produce images or maps highlighting areas of signal change temporally related to the experimental paradigm or recorded neurophysiological activity [Bandettini *et al.* 1992]. Using simultaneously recorded EEG and fMRI, haemodynamic changes to epileptiform neuronal activity measured by the surface EEG can thus be localised.

The purpose of the work described in this thesis was three fold 1) to investigate the spatial correlates of IEDs using functional MRI, 2) to make inferences about the pathophysiological basis of these changes and 3) to explain the current methodological constraints of EEG-fMRI.

# 1 Chapter 1. Background

## 1.1 Chapter Outline

The following chapter outlines the background to this thesis. The chapter begins with the clinical aspects of epilepsy relevant to this work. I give a description of the concurrent recording of EEG with fMRI (EEG-fMRI) and review the relevant literature. Subsequently I describe the techniques of EEG, MRI and other functional imaging methods that have been used to study epilepsy.

## 1.2 Introduction

Epilepsy is a common neurological disease, with an overall incidence of around 50 cases per 100 000 persons per year in developed countries and around two to four times higher in developing countries. The prevalence is about 5 – 10 cases per 1000 persons, with a lifetime prevalence of 2 to 5% [Goodridge and Shorvon 1983b;Goodridge and Shorvon 1983a;MacDonald *et al.* 2000].

Epilepsy remains a cause of considerable morbidity and mortality. Despite the often brief and transitory nature of seizures, they cause significant disability due to the unpredictable nature of the attacks, their social and economic impact, and cerebral impairment from repeated seizures. There is a risk of injury or death during a seizure. Fundamental questions regarding the neurobiology of epilepsy, reasons for its development, seizure onset and termination, and the variable response to treatments remain unanswered.

Recorded accounts of epileptic seizures date back some 3000 years, from the ancient civilisations of Mesopotamia, Egypt, China and Asia. The Hippocratic collection around 400 BC contains the famous work On the Sacred Disease; one of the earliest known records where epilepsy is considered an organic disease with the cause lying in the brain, rather than a spiritual or psychic possession [Temkin 1971]. Current concepts of epileptic activity developed with the renaissance study of anatomy and physiology. The work of the British neurologist John Hughlings Jackson in the late nineteenth century heralded the era of the modern approach to epilepsy. He recognised that seizures occurred as a result of electrochemical discharges in specific areas of the brain and that observation of seizure manifestations could be used to locate where in the brain the seizure activity arose [Critchley 1998].

The identification and measurement of electrical activity from brain tissue lead to the primary investigative tool in epilepsy - the electroencephalogram (EEG) (section 2.4). It is used in the localisation of seizure foci and the classification of seizures and syndromes.

A further revolution in the investigation and scientific understanding of epilepsy has occurred with the advent of magnetic resonance imaging (MRI). Detailed structural brain images can show subtle abnormalities responsible for seizure generation [Duncan 1997]. More recently functional imaging techniques, PET, SPECT, fMRI and EEG-fMRI are being used to further our understanding of brain function on epilepsy [Duncan 1997].

Functional imaging in epilepsy can be separated into two broad areas: 1) the study of normal brain activity, to define eloquent cortex for planning surgical resections for example motor, language and memory areas and 2) the study of ictal and interictal

activity to localise the source or networks of epileptic discharges. The second of these areas is the subject of this thesis.

## 1.3 Classification of Epilepsy

Epilepsy is not a specific disease, but a heterogeneous group of disorders manifesting the neuroanatomical and pathophysiological substrate causing the seizures. These present a diversity of seizure types, and epilepsy syndromes. Classification of these is appropriate to allow accurate communication between those caring for people with epilepsy and for research. Epilepsy is classified using two interlinked classification systems, one for seizures, and one for syndromes. These were developed by the Commission on Classification and Terminology of the International League against Epilepsy (ILAE). 1) The classification of epileptic seizures, based on the electroclinical features of observed seizures, 2) the classification of epileptic syndromes, based on the presence of different seizure types, age at onset, aetiology and associated clinical and electrophysiological findings. These are detailed in four publications,

- the international classification of epileptic seizures (ICES) [Gastaut 1970]
- revised in 1981 [ILAE 1981],
- the classification of epilepsy syndromes and epilepsies (ICEES)[ILAE 1985],
- revised in 1989 [ILAE 1989].

By design the categories are descriptive, rather than diagnostic entities. As such syndromic classification needs to be used as a guide rather than a definitive diagnostic endpoint. Some categories represent pure disease entities, eg myoclonic astatic epilepsy whilst others represent a spectrum of clinical forms e.g. idiopathic

generalised epilepsy. Despite these and other shortcomings [Engel, Jr. 2001] the ILAE classification of seizures and syndromes provides a standard terminology for use by health care workers and researchers and is used throughout this thesis.

### 1.3.1 Classification of Epileptic seizures

The international classification of epileptic seizures (ICES) was developed by a panel of international experts examining video recordings of clinical and electroencephalographic manifestations of epileptic seizures. As such it is based on a consensus of opinions on the classification of seizures into a number of categories and subcategories (Appendix 1). The first level of this system distinguishes between generalised and focal onset seizures. The next level divides seizures according to semiology; generalised seizures into absence, myoclonic, tonic, clonic, or tonic-clonic events, and focal seizures into simple partial (consciousness is preserved - maintained awareness, recall and ability to carry out commands or willed movements during the event), or complex partial (consciousness is lost). Focal seizures are divided further according to presumed neuroanatomical substrate: motor, somatosensory or special sensory, autonomic and psychic.

Absence seizures can be divided into typical absence and atypical absences. Typical absences are seen in idiopathic generalised epilepsy (see below). They consist of an alteration of consciousness, occasionally there is associated eye flickering but other motor manifestations are rare; attacks are brief usually less than 30 seconds. Characteristic EEG findings are of generalised spike wave discharges of 3-5 Hz. Atypical absences are seen in symptomatic generalised epilepsy of frontal lobe epilepsy. These are more prolonged than typical absences and often associated with

motor automatisms or other features. The EEG again show generalised spike wave but usually at a slower frequency.

Myoclonic jerks are brief muscular jerks affecting limbs and less commonly trunk.

Partial or focal seizures manifest according to the area of onset, simple partial seizures without loss of consciousness and complex partial seizures with loss of consciousness.

Generalised tonic clonic seizures can either be primary, appearing to affect all areas at onset or secondary to a focal onset.

### 1.3.2 Classification of Epilepsy Syndromes and the Epilepsies

The international classification of epilepsy syndromes and epilepsies (ICEES) (Appendix 2) supplements the ICES. A medical syndrome refers to a complex of symptoms and signs which, associated together, form a characteristic clinical picture or entity. Conversely a disease has a specific well defined common aetiology and prognosis despite individual variation [Panayiotopoulos 2002a]. The distinction, defining "epilepsies" as specific disease entities rather than "epileptic syndromes" are only possible where an understanding of the pathophysiological process is known. These remain relatively small, restricted to certain metabolic or neurodegenerative diseases of childhood or early adult life.

The dichotomy between generalised and focal is retained in the syndrome classification. The next classification level takes into account known or suspected aetiology: symptomatic (with a known underlying cause), idiopathic (occurring without known underlying disease) or cryptogenic (underlying cause that remains unknown - these are generally now referred to as 'probably symptomatic'). Two further categories are recognised, one of epilepsies and epilepsy syndromes where categorisation into focal or generalised is not possible due to a lack of clearly

distinguishing features (often the case with nocturnal seizures), and another for seizures associated with a specific situation (fever, drugs, metabolic disturbance).

A revision of this diagnostic scheme has been proposed that retains the distinction between focal and generalised epilepsies but is divided in five parts or 'axes', organised in a hierarchical fashion allowing the integration of available and new information [Engel, Jr. 2001]. The five axes are 1) ictal phenomenology, 2) seizure type 3) syndrome 4) aetiology, where known, this includes genetic defects or specific pathological substrates 5) medical impairment [Engel, Jr. 2001].

The following sections will outline the main syndromic groups relevant to this thesis and other published EEG-fMRI studies.

## 1.4 Idiopathic Generalised Epilepsy

The idiopathic generalised epilepsies (IGE) are characterised by:

- one or more of the following seizure types, typical absences, myoclonic jerks and generalised tonic-clonic seizures (GTCS),
- normal background EEG with episodes of generalised spike or polyspike and wave on EEG and,
- The absence of other neurological signs or symptoms.

The term idiopathic comes from the Greek idios, meaning on its own, i.e. without other neurological abnormality and by definition there is no identifiable cause other than a genetic predisposition; however pathological [Meencke 1985] and imaging [Woermann et al. 1999] changes have been reported.

IGE makes up one third of all epilepsies [Panayiotopoulos 2002a]. Many have a hereditary predisposition and are age related. Seizures are typically exacerbated by sleep deprivation and alcohol. Response to appropriate antiepileptic drug treatment is good in most, but not all, and treatment usually needs to be lifelong.

Further syndromic sub-classification of IGE is made on the prevalence of the different seizure types and EEG features. The inclusion of age of onset and diurnal seizure patterns are proposed by some [Andermann and Berkovic 2001]. The main subgroups seen in adults with epilepsy are

- Childhood absence epilepsy (CAE)
- Juvenile myoclonic epilepsy (JME)
- Juvenile absence epilepsy (JAE)
- Epilepsy with generalised tonic clonic seizures on awakening (EGTC)

Assignment of patients to one these groups is based on age of onset and seizure type; these can be less than clear cut with overlap between individuals. For instance absences, myoclonic jerks and GTCS occur in both JAE and JME, with a general rule that in JAE, absences predominate and myoclonic jerks are infrequent; whereas in JME myoclonic jerks predominate, and absences are mild. CAE is distinguished from JAE by earlier age at onset (4 to 10 years), severe absences without other seizure types and a good prognosis in the majority of cases [Panayiotopoulos 2002a]. It remains debated whether different clinical manifestations represent different ends of a biological continuum or a group of distinct syndromes [Berkovic *et al.* 1987].

The typical absence seizure is the hallmark of IGE. The electrophysiological hallmark of IGE is the combination a normal background EEG with paroxysmal, generalised and bilaterally synchronous generalised (GSW) spike wave discharges of around 3-4 Hertz. These are seen during typical absence seizures manifests as a transient lapse in

consciousness, with a vacant stare, sometimes with eye deviation or flickering of eyes or eyelids. The patient is unresponsive and unaware during these episodes which are typically brief, lasting 30 seconds or less, and are associated with abrupt onset of GSW [Snead, III 1995]. Interictal GSW consists a single spike wave discharge or bursts lasting up to a few seconds, without overt clinical manifestations.

## 1.5 Symptomatic Generalised Epilepsy

The symptomatic generalised epilepsies, by definition are associated with evidence of cerebral abnormality or dysfunction. Usually they are associated with multiple seizure types and often learning difficulties. Absences seizures are more prolonged than typical absences of IGE and can be associated with automatisms; they are referred to as atypical absences; background EEG is abnormal with typically slower spike wave discharges of around 2 Hz [Holmes et al. 1987]. The major condition in which atypical absences with slow spike waves are seen is Lennox-Gastaut syndrome [Gastaut *et al.* 1966;Lennox and DAVIS 1950] where they occur in combination with multiple seizure types typically including tonic seizures. Often there is a preceding history of brain damage.

Other symptomatic or cryptogenic epilepsies are typically childhood onset and associated with brain abnormalities, these are listed in appendix 2.

## 1.6 Pathogenesis of GSW

The pathogenesis of GSW has been the subject of extensive debate and research over the 5 or so decades since its first description [Gibbs *et al.* 1935].

The debate has centred around a sub-cortical origin "the centrencephalic hypothesis" [Jasper and Drooglever-Fortuyn 1947] versus a cortical origin [Marcus and Watson 1968] for GSW. Jasper and Drooglever-Fortuyn demonstrated that electrical stimulation of the midline and intralaminar nuclei of the thalamus in cats at a stimulus frequency of 3 Hz could produce bilaterally synchronous spike wave discharge (SWD) on the cortical EEG [Jasper and Drooglever-Fortuyn 1947]. According to the centrencephalic hypothesis, an abnormal discharge originating in the brainstem reticular activating system is projected from the thalamus bilaterally to cortex. The cortical hypothesis put forward by Marcus and Watson [Marcus and Watson 1966;Marcus and Watson 1968] was based on findings that cortex independent of thalamus would support GSW. These two opposing views of cortical versus subcortical origin were reconciled to an extent by Pierre Gloor. He proposed a role for both cortex and subcortical structures [Gloor 1968], with aberrant oscillatory rhythms in reciprocally connected thalamocortical loops normally involved in the generation of sleep spindles [Gloor 1968], leading to GSW.

This evidence pertaining to the pathophysiology of GSW comes almost exclusively from electrophysiological and neurochemical recordings in animals and tissue preparations [Avoli *et al.* 2001]. The following criteria need to be met for such models to be realistic: bilaterally synchronous SWD associated with behavioural arrest, head drops and nystagmus; reproducible, predictable, exacerbated by GABAergic drugs, blocked by GABAb antagonists, SWD discharges seen on in thalamus or cortex, but with the hippocampus silent. Although many of these criteria can be met, animal models of human absence seizure remain imperfect, and clearly any animal model could not be used to test the effect of discharges on higher cortical functioning in man.

A small number of intracranial studies have been reported in man in which spike-wave activity was recorded in both thalamus and cortex [Williams 1953] [Niedermeyer *et al.* 1969;Velasco *et al.* 1989] but gave no clear indication about the initiation of these discharges or their underlying pathophysiology. The spatial sampling of depth studies is limited to the immediate vicinity of the implanted electrodes, and their invasiveness, in the absence of clinical benefit precludes their current use in IGE.

More recent experimental evidence suggests that onset is within the cortex, in an area of hyper excitable cortex, that spreads to involve a critical area, before spread to the thalamus and recruitment of thalamocortical and cortico-thalamic circuits [Timofeev and Steriade 2004]. Nevertheless the primary neuroanatomical and neurochemical abnormality in IGE remains undetermined. New evidence from EEG-fMRI will be reviewed in subsequent sections and is the subject of original work presented in this thesis.

## 1.7 Focal Epilepsies

Focal epilepsies have clinical, or EEG evidence of focal seizure onset. The following table sets out conceptual entities and their definitions developed primarily for the surgical management of focal epilepsy [Rosenow and Luders 2001].

| Term | Definition | Measured by |
|---|---|---|
| **Irritative zone** | area cortex from which interictal spikes are generated | surface or depth EEG and dipole source modelling |
| **Ictal onset zone** | area of cortex that initiates or generates seizures | video EEG recordings |
| **Epileptogenic lesion** | structural brain pathology that is the direct cause of seizures | structural neuroimaging or pathological examination following surgical resection. |
| **Symptomatogenic zone** | portion of brain that produces first ictal symptoms | EEG, semiology |
| **Functional deficit zone** | cortical area producing dysfunction | History and examination (includes psychology)<br>Functional neuroimaging |
| **Epileptogenic zone** | total area of brain necessary to generate seizures and IED | Inferred from above, cannot be measured directly |

**Table 1-1 Terminology used in describing the anatomical substrate of focal epilepsy.**

In clinical practice focal epilepsies are classified according to the lobe from which seizures arise. The temporal and frontal lobe epilepsies are outlined here given their relevance to patients studied in this thesis.

### 1.7.1 Temporal Lobe Epilepsy

The commonest form of refractory localisation related epilepsy is temporal lobe epilepsy (TLE). TLE can be divided on anatomical grounds to mesial (m)TLE, part of the limbic system, and lateral (L) TLE which is neocortical.

#### 1.7.1.1 Mesial temporal lobe epilepsy

MTLE accounts for approximately 90% of TLE cases. It is important in that it is the commonest cause of refractory epilepsy and in many cases has a good outcome following resective surgery.

MTLE is characterised by the occurrence of simple and complex partial seizures and less frequent secondary generalised seizures. A history of febrile convulsions is present in 40 – 44% of patients with surgical mTLE and when present associated with good outcome from resective surgery [Janszky et al. 2003]. Onset of seizures is typically in the second decade of life often with a further seizure free period of several years with or without medication before the onset of refractory seizures.

A simple partial seizure in isolation or before progression to a complex partial seizure is often termed the aura. Manifestations include visceral, cephalic, gustatory, dysmnestic, affective, perceptual or autonomic symptoms. In cases of rapid spread to complex partial seizures the aura is not recalled. Complex partial seizures manifest with motor arrest, impairment of consciousness, oro-alimentory automatisms, and in the limbs ipisilateral automatisms and contralateral dystonic posturing.

Common pathological substrates identified on MRI include hippocampal sclerosis (HS), malignant and benign tumours (astrocytomas, gangliogliomas, dysembryoplastic neurospithelial tumours (DNET)), vascular (cavernous and venous angiomas, arteriovenous malformations (AVM)) and malformations of cortical development (MCDs) or traumatic and other injuries (infective agents, most commonly viral, and cerebrovascular disease) other developmental injuries. Seizures caused by different pathological substrates are indistinguishable on electro-clinical grounds.

In those with HS there is a good outcome to surgical treatment with anterior temporal lobectomy with approximately 2/3 of patients becoming seizure free [Berkovic *et al.* 1995] compared to 50% for neocortical epilepsy [Spencer et al. 2003].

A number of patients with TLE have no clear structural lesion on MRI; in these term 'MR negative' provides a useful frame of reference. These form an important group for further investigation. When the epilepsy is refractory to medical treatment and surgical options are being considered, although seizure freedom rates are much less (~40%) compared to those with foreign tissue lesions or hippocampal sclerosis [Berkovic *et al.* 1995].

#### 1.7.1.2 Lateral temporal lobe epilepsy

Neocortical or lateral temporal lobe epilepsy (TLE) is less common than mTLE, making up around 10% of TLE cases. Simple partial, complex partial and rarer secondary generalised seizures are characteristic. Clinical manifestations of simple partial seizures include auditory and mental hallucinations or illusions, vestibular phenomena, dreamy states and misconceptions and depend on the affected hemisphere. Language function is disturbed if the focus is in the dominant hemisphere. Anterior lateral TLE is associated with olfactory and gustatory phenomena and déjà vu. Motor manifestations include clonic movement of facial muscles, facial grimacing, limb automatisms and dystonic posturing.

Lateral TLE can be due to any of the structural causes seen mTLE, except for HS, although HS may develop as a secondary phenomenon to lateral TLE.

### 1.7.2 Frontal Lobe Epilepsy

Around 20% of intractable epilepsies are localised to the frontal lobe. Seizures vary greatly due to the size of the frontal lobe and functions it normally subserves. Seizures depend on the origin and spread of the epileptogenic focus [Niedermeyer 1998]. The frontal lobe contains the primary motor cortex, supplementary motor cortex, prefrontal cortex and the limbic and para-limbic cortices.

In general frontal lobe seizures manifest with prominent motor manifestations. These can be tonic, clonic or postural, or bilateral vigorous motor automatisms for example bicycling. Seizures are typically short, lasting seconds to less than 1 minute; they progress rapidly to secondary generalisation (over seconds). This is in contrast to TLE where complex partial seizures usually develop over several minutes, can last tens of minutes and less commonly secondarily generalise. In contrast with TLE, frontal lobe seizures occur more commonly in sleep.

Blank spells that occur in frontal lobe epilepsy (FLE) can be electro clinically indistinguishable from absences in IGE, making syndromic distinction in some cases difficult. This has implications for management as some AEDs for example carbamazepine or gabapentin, worsen IGE but not FLE.

Causes of frontal lobe epilepsy are similar to those of temporal neocortical epilepsies.

### 1.7.3 Reflex seizures and reflex epilepsies

Reflex seizures and reflex epilepsies are rare. Seizures are usually precipitated by specific stimuli that tend to be unique to the affected patient. Despite their rarity in clinical practice reflex seizures are ideal for study with EEG-fMRI, in that they

provide unique opportunities for the study of interictal and ictal discharges in a relatively controlled manner. A number of such reports have been published.

A large number of stimuli that provoke seizures have been reported in the literature [Panayiotopoulos 2002b]. Primary reading epilepsy consists seizures provoked by reading silently or aloud, typically myoclonic jerks of the jaw; GTCS can occur if the patient continues reading in the context of increasing jerks. [Koutroumanidis *et al.* 1998b].

## 1.8 The Electroencephalogram

### 1.8.1 History

In 1857 Richard Caton published his observations of brain electrical currents from recordings in dogs [Haas 2003]. These observations formed the precursor to the work of Hans Berger. Hans Berger, a German psychiatrist at the University of Jena is considered the founder of the human EEG. He demonstrated brain electrical activity in man, using scalp recording electrodes, and in 1929 introduced the term electroencephalogram (EEG) [Brazier 1980]. It took some years before the importance of Bergers discovery was realized by the clinical and scientific community, Gray Walter at the Burden Institute in Bristol is widely credited with the development of the EEG in the UK as a routine investigation in neurological disease [Cooper 1972]. It remains a primary investigation in epilepsy.

### 1.8.2 Recording the EEG

Recording the potential difference between two applied electrodes is used to measure electrical brain activity. These potentials from skin/scalp recordings are small, of the order of tens of microvolts (1/100th the amplitude of the electrocardiogram) [Morris and Luders 1985]. An EEG system consists of the electrode assembly, preamplifier and amplifier, and the writing system.

### 1.8.3 Electrode Assembly

Electrical contact between the recording equipment and the brain tissue is made with electrodes. Electrodes can be placed on the scalp (surface electrodes) or intracranialy. Scalp electrodes consist of flat metal discs that are attached to the scalp surface by conducting paste or glue. Intracranial electrodes consist of either subdural strips or grids that are placed on the brain surface or depth electrodes that are inserted into the brain parenchyma. An electrical connection at the electrode is made by means of a metal/liquid junction. In the scalp EEG an indirect contact is established by an electrolyte bridge formed by electrode gel placed between the skin and the electrode. The properties of charge and ion flow lead to an 'electrical double layer', a stationary DC voltage. Variation in this DC voltage due to motion leads to artefact [Niedermeyer and Lopes Da Silva 1998]. The electrical impedance of scalp electrodes depends on the electrical resistance of the skin/electrolyte junction, which is in turn dependent on the condition and preparation of the skin, concentration of electrode gel and time elapsed after application of gel [Niedermeyer and Lopes Da Silva 1998]. Lightweight electrode leads are used to reduce the effects of mechanical motion at the electrode scalp contact.

### 1.8.4 Electrode Placement

An international standard for electrode positions was developed to ensure uniformity and consistency of recordings over time and between centres [Jasper 1958]. This standard for electrode placement is based on measurements between specific surface cranial landmarks that ensure a constant relationship between the position of surface electrodes and underlying cortex. The most commonly used standard is the

International 10:20 system (fig 1a). The distance between electrodes is determined by dividing in equal percentages measurements between specific landmarks on the head, the nasion and inion, and head circumference. The 10 and 20 refer to the 10% or 20% interelectrode distance. A 10:10 system is used for higher density EEG, where all interelectrode distances are 10% of a distance between the cranial landmarks (figure 1b). Electrode positions are labelled with a letter (to identify the lobe they overly) and number (indicates their side and position over that lobe). Hence F, T, P, O, C represent frontal, temporal, parietal, occipital, and central; even numbers refer to the right hemisphere and odd numbers to the left hemisphere.

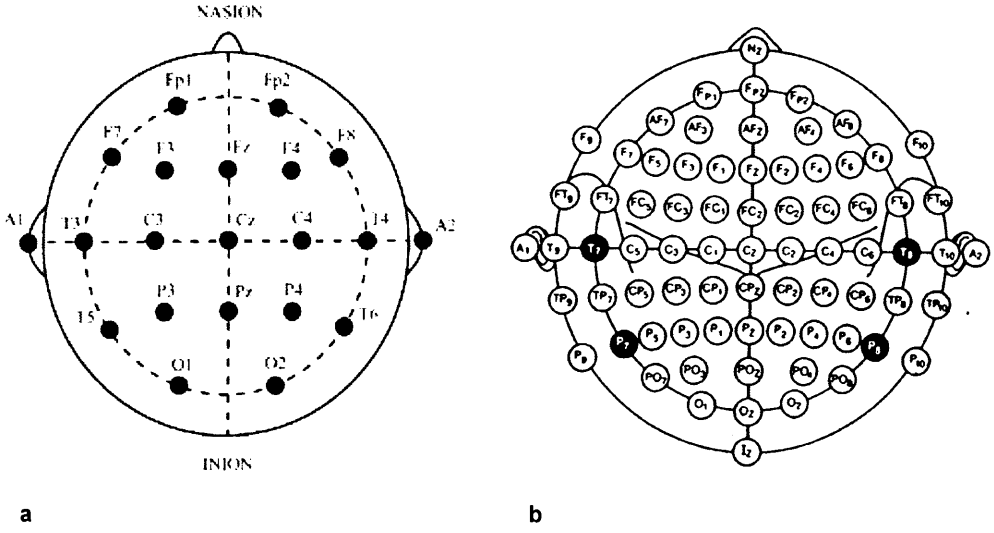


a b

**Figure 1-1 Diagram of the International 10:20 and 10:10 system for EEG electrode placement.**

### 1.8.5 Electrode Application

Electrodes can be attached to skin in a number of ways. First skin impedance is lowered by cleaning with specially designed mild abrasive cream. Electrodes can be attached by means of an electrolyte paste, (the electrode is bedded in a ball of paste

and pushed onto the scalp), and the paste creates the electrode/skin contact and holds the electrode in place. This is suitable for short recordings, 20 to 40 minutes, after which drying of paste and spread of paste due to head movement adversely effects the recording [Niedermeyer and Lopes Da Silva 1998]. A more secure method of electrode attachment uses collodion (special purpose glue). Quick drying collodion and a compressed air dryer to speed drying are used. A hole in the centre of the electrode is used for injecting electrolyte gel to secure the electrical contact with skin. An electrode cap can be used in place of single electrodes. A tight fitting cap into which electrode wells are sewn in provides a relatively rapid and secure means of acquiring scalp EEG.

### 1.8.6 Signal Recording and Amplification

Electrode leads usually pass to a preamplifier, filtering circuit and power amplifier. EEG records the change in potential difference over time between any two electrodes. The recorded signal has a frequency bandwidth. The frequency range used in standard EEG is 0.16 – 100 Hz, sometimes a lower frequency response is needed for example when recording DC shifts [Reutens 2000], or higher up to 3000Hz for brainstem auditory evoked potentials. Adjustable high pass and low pass filters allow the operator to restrict frequency response of the channel to the frequency band of interest. This is useful when interference covers frequencies outside that of EEG frequencies of interest. However if interference lies within EEG frequencies then filter adjustments will result in loss of real signal. Too narrow a recording range and information is lost, too wide irrelevant information is likely to contribute to noise.

### 1.8.7 Recording and Display

The spatial distribution of scalp potentials is achieved by simultaneous recording from multiple electrodes across the scalp. Selecting desired combinations or derivations of comparative electrodes gives a number of display montages. The standard clinical scalp EEG has 21 channels. In the research setting several times that number may be used (up to 128 or 256) [Lantz et al. 2003].

Display montages can be separated into two types:

- Referential – the difference between each electrode and a single reference electrode is shown, typically the ipsilateral ear, a central electrode (necessary in EEG-fMRI) or an average of all electrodes
- Bipolar – the difference between two adjacent scalp electrodes.

Altering the display montage allows visualisation of abnormalities and helps distinguish artefact from neurophysiological phenomena, and aids EEG localisation.

Technological advances over the last few decades, with digitisation, have revolutionised EEG techniques. These include processing, visualisation, artefact correction, storage and mathematical manipulation. Perhaps the most significant application in clinical EEG is the ability to change the montage display 'off–line' i.e. reformatting the display for different views after the recording is done. Prior to this, a number of fixed montages on a paper trace were operator selected, for each recording session. Other advantages of digital EEG, enhanced by advances in computer technology include the ability to store large amounts of data, and apply mathematical techniques for frequency analyses, filtering and colour mapping.

### 1.8.8 Basis of EEG Activity

Neural activity involves transmission of electrical current by ionic flux. The changes in potential difference resulting from neural activity are recordable at the scalp surface, or by means of depth electrodes. These changes in potential difference likely reflect the summed potential of macroscopic changes in current flow between the intracellular (the source) and extra cellular space (the sink), known as local field potentials [Niedermeyer and Lopes Da Silva 1998]. These result from synchronous (or simultaneous) changes of the membrane potential of neighbouring neurons as result of 1) synaptic transmission, leading to Excitatory Post Synaptic Potentials (EPSPs) and Inhibitory Post Synaptic Potentials (IPSPs) [Buzaki and Traub 1997] and 2) membrane oscillations from voltage dependent activation of membrane ion channels [Llinas 1988]. Fast action potentials are not thought to contribute significantly to the EEG as temporal summation of such brief events is not likely to occur [Llinas 1988].

The main generators of EEG rhythms and interictal epileptiform discharges are dendrites in the upper cortical layers. Several thousand parallel orientated dendrites have to be synchronously active to give measurable signal. Synchronous activity involving an area of at least 6 $cm^2$ is needed to produce the epileptic spike visible on surface EEG [Cooper *et al.* 1965].

The cerebral cortex is made up of a complex network of inhibitory and excitatory neurons. EEG rhythms reflect the complex interplay with and between these networks. Broadly, slow rhythms characterise a synchronous (sleep or resting state) and lower amplitude faster rhythms a less synchronised (active state) of brain activity [Buzaki and Traub 1997].

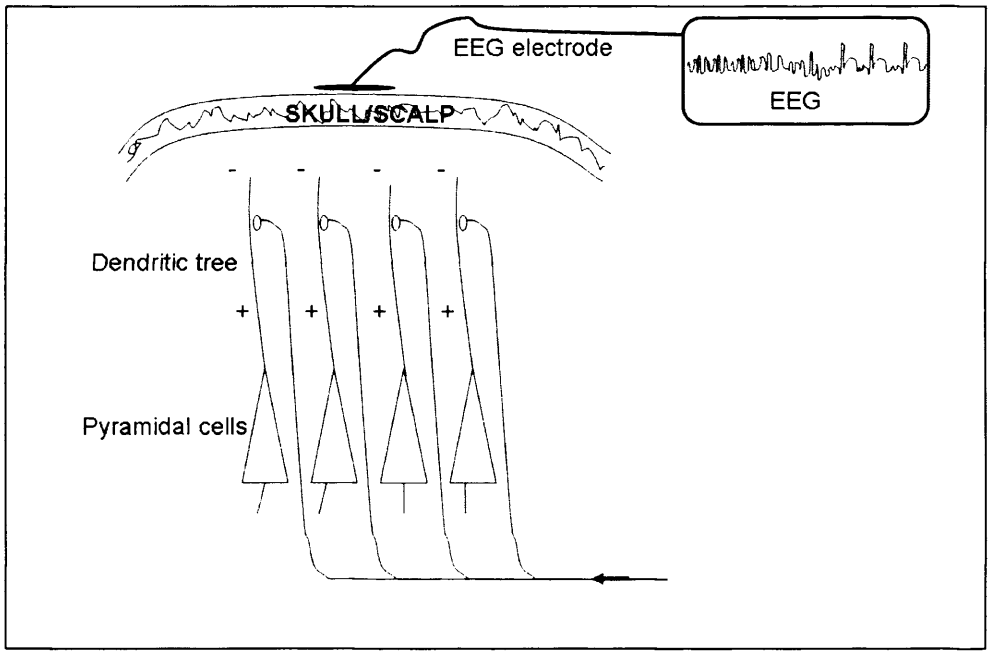


**Figure 1-2 Schematic of the physiological basis of EEG activity.**

**Electrical negativity is directed toward the outer cortex. EEG potentials are measured as the difference between two points, one on the scalp where EEG effects are strong and the other (the reference electrode) ideally isolated from the effects of interest. Some commonly used reference sites are CSV, earlobes, mastoids, tip of nose and average reference ("reference free"). Single pyramidal cell may have more than $10^4$ synapses distributed over its soma and dendrite surface. $10^5$ neurons under each square millimetre of cortical surface. Scalp EEG measures space-averaged activity of $10^7$ or more neurons implying a source area of at least a square centimetre. Scalp EEG potentials can be estimated as if generated by a dipole source.**

### 1.8.9 Normal Brain Rhythms

The normal EEG consists of variable rhythmic activity; in the human brain important physiological frequencies have a more restricted range (between 0.3 and 70 Hz). These frequencies are broken down into the following bands or ranges:

- Delta less than 4 Hz
- theta 4 – 7.5 Hz ,
- alpha 8-13 Hz,
- beta 14 – 30 Hz,
- And gamma above 30 Hz with unlimited upper range.

In the awake EEG record of normal adult brain the alpha (8-13Hz) and beta (14 – 30 Hz) rhythms predominate.

Alpha waves are found during wakefulness. They have a higher amplitude posteriorly than anteriorly and become prominent when eyes are closed. Alpha activity disappears normally with eye opening and attention (eg, mental arithmetic, stress). Alpha waves become less prominent during drowsiness and give way to a low voltage pattern of mixed slow waves (mostly theta) as sleep evolves [Markand 1990].

Beta waves are small in amplitude, usually symmetric and more evident anteriorly. Many drugs, such as barbiturates and benzodiazepines, augment beta waves.

Theta and delta waves are known collectively as slow waves. Theta waves normally are seen in sleep at any age. They are not normally seen to any great extent in awake adults. Delta waves are normally are seen in deep sleep in adults as well as in infants and children. They are abnormal in the awake adult. Often, they have the largest amplitude of all waves. Delta waves can be focal (local pathology) or diffuse (generalized dysfunction).

### 1.8.10 EEG in Epilepsy

The diagnosis of epilepsy remains a clinical one, with EEG playing a supporting role, assisting in the syndromic classification of epilepsy and in lateralisation or localisation in the pre surgical work up of focal epilepsy. The detection of specific abnormal EEG rhythms or phenomena indicates the presence of abnormal cortical activity in epilepsy. These EEG manifestations can be separated into interictal discharges (IEDs) (usually brief, occurring when there is no apparent clinical seizure activity) and ictal events (clinical seizure activity is apparent). This distinction can be difficult when "interictal" events are prolonged without overt clinical change and the term electrographic seizure is sometimes used.

#### 1.8.10.1 Interictal Discharges

The definition of IEDs is somewhat circular, "distinctive waves or complexes, distinguished from background activity, and resembling those recorded in a proportion of human subjects suffering from epileptic disorders...." [International Federation of Societies for Electroencephalography and Clinical Neurophysiology 1974]. IEDs arise from an area of cortex that is termed the irritative zone [Talairach and Bancaud 1966]. The following criteria are used in defining IEDs:

- Sharp wave - transient, clearly distinguishable from background activity, with pointed peak and a duration of 70-200 milliseconds (ms)
- Spike - same as sharp wave, but with duration of 20 to less than 70 ms
- Spike-and-slow-wave complex - Pattern consisting of a spike followed by a slow wave (classically the slow wave being of higher amplitude than the spike)

- Multiple or poly- spike-and-slow-wave complex - Same as spike-and-slow-wave complex, but with 2 or more spikes associated with one or more slow waves

IEDs need to be clearly distinguished from the background, show an abrupt change in polarity occurring during several milliseconds and have a physiological field [Walczak and Jayakar 1997].

IEDs occur unpredictably, and in most patients rarely seen in a routine 20-30 minute recording. The detection of IEDs is increased with serial recordings or prolonged ambulatory recordings to capture these infrequent events. Activation procedures with hyperventilation and photic stimulation can increase the occurrence of IEDs. Photic stimulation induces IEDs mainly in IGE, and in focal epilepsies with an occipital onset. An EEG recorded during sleep will often show IEDs where none occur during waking. A sleep deprived/sleep EEG, with continued recording after waking can reveal interictal discharges not seen on a routine EEG [Martins et al. 1984].

The cellular basis of IEDs is inferred from experimental animal models that generate events similar to IEDs. These experimental interictal discharges are characterised by the abrupt 'paroxysmal' depolarisation shift (PDS) [Jefferys 2003]. These are rapid depolarisations which make the neurons fire rapid bursts of action potentials. The PDS is the sum of simultaneous excitation from many other neurons within the same population. The PDS depends on the excitatory neurotransmitter, glutamate, and has the following components: sustained neuronal depolarisation is mediated by an influx of $Ca^{2+}$ ions, neuron firing a rapid train of action potentials after depolarisation that exceeds the threshold potential, associated with an influx of $Na^{+}$. This sustained depolarization is followed by re-polarisation and usually hyper-polarisation mediated by potassium efflux. The corresponding extra cellular field potential summed over a

large population of neurons is detected as the surface EEG spike. This consists a negative peak that corresponds to the $Ca^{2+}$ and $Na^{+}$ influx, that falls back to and then below baseline during hyperpolarisation and finally gradually returns to baseline.

Experimental models show that the conditions required for epileptic discharges to take place are excitatory (pyramidal) neurons connected into a synaptic network, the synapses need to be strong enough, and the population of neurons needs to be large enough. Many experimental models of epilepsy rely on the application of pro-convulsant drugs either directly to brain tissue or slice preparations, or systemically in high enough doses. These usually increase the synaptic strength by blocking inhibitory GABAergic synapses e.g. pentazolamide, bicuculline or penicillin. Chronic experimental models, which more closely resemble human epilepsy, and human pathological studies in focal epilepsy show increased synaptic connectivity (e.g. mossy fibre sprouting) changes in ion channel properties and alterations in synaptic properties.

1.8.10.2 The Ictal EEG

In contrast to IEDs, ictal discharges have a beginning, middle and end i.e. an evolution. Focal seizures begin with localised rhythmic EEG changes, fast activity, attenuation or sharp waves, which show spatial and temporal evolution, depending on speed of propagation, becoming bilateral in some complex partial seizures or where there is secondary generalisation. Generalised seizures begin with abnormal activity throughout both hemispheres at the same time.

Recording an ictal EEG is useful in the following situations:

- the diagnosis of epilepsy is in doubt
- classification of seizure syndrome
- localisation of ictal onset, usually in the context of pre-surgical planning

- quantification of the number of seizures occurring, if not clinically overt

Electrical manifestations of seizure activity are not always captured on surface EEG, simple partial seizures with restricted field and some complex partial - in particular frontal lobe seizures - may not show surface EEG changes. In addition muscle artefact during a seizure can obscure the electrical record.

1.8.10.3 EEG in Epilepsy Syndromes

The EEG has a crucial role to play in syndromic diagnosis as outlined by the ILEA. The distinction between focal and generalised seizures may not be apparent from the history however the presence of focal or generalised IEDs on the EEG can clarify this. The location of focal IEDs roughly corresponds to the site of seizure onset although this is not always the case.

Generalised spike wave at 3-4Hz is the hallmark of IGE. A slower GSW (<2.5Hz) is characteristic of symptomatic generalised epilepsies, e.g. Lennox Gastaut syndrome. GSW can be seen in frontal lobe epilepsy, which again can present with brief absences and generalised tonic clonic seizure; sometimes making syndromic differentiation difficult. In adults, aside from GSW of IGE or Lennox Gastaut there are no other prominent syndromic aspects to the EEG. In children characteristic EEG features are seen in the following syndromes: Landau Kleffner, Benign Epilepsy with Centro-temporal spikes, West syndrome (infantile spasms and hypsarrythmia) and familial partial epilepsy with variable foci.

1.8.10.4 Intracranial EEG

Scalp electrodes can provide good lateralisation and regional localization, are non-invasive and relatively straightforward to acquire. However they do not necessarily localise the site of onset of seizures with precision for the following reasons:

widespread surface changes, too deep sources or rapid seizure spread beyond the site of initial onset. Intracranial recordings are sometimes necessary in the presurgical work up of patients.

Two types of intracranial recording are used, depth electrodes that are inserted in to the brain parenchyma, and subdural grids or strips that are placed on the surface of the cortex under the dura.

Intracranial recordings overcome the problems of poor spatial resolution of surface EEG. The filtering effects of skull, scalp tissue and skin that limit localisation are avoided, electrodes are at a closer proximity to areas of interest, unfavourable dipole orientations are avoided, and recordings are free of muscle and movement artefact. Electrodes need to be placed at or over the presumed site of seizure onset, and only a limited number of electrodes or grids can be placed. Intracranial EEG must not be a 'fishing expedition' that hopes to catch the seizure onset zone by serendipity. A hypothesis about the site of presumed seizure onset is needed to guide the placement of intracranial electrodes.

The technique of stereo-electroencephalography (SEEG), the stereo tactic placement of depth electrodes helps precise electrode localisation [Spencer 1981]. Intracranial electrodes can be left in place for up to two weeks, to record one or more habitual seizure and thus support or refute a prior hypothesis regarding areas of seizure onset that can be surgically removed. Sub-dural grids can be used in electrocorticography, to stimulate cortex to delineate eloquent areas.

The disadvantage of intracranial recordings is that only a limited area of the brain is sampled, and EEG is recorded only from the immediate vicinity of electrode contacts. There is a risk of infection and haemorrhage, in up to 4-5% of depth electrode

implantations [Fernandez *et al.* 1997] and up to 20% of subdural electrode implantations.

1.8.10.5 Electrical and Magnetic Source Localisation

The aim of source localisation is to identify the area, or point in the brain that has generated the surface recorded EEG or megnetoencephalographic (MEG) event. Mathematical modelling is used to reconstruct potential solutions. Assumptions need to be made about the conductivities and geometry of the brain, skull, and scalp compartments. An approximation of tissue conductivity is needed and typically a homogeneous and isotropic head shape model is used [Assaf and Ebersole 1997]. Several techniques have been proposed and applied [Ebersole 1997]. The shape and magnitude of the scalp recorded voltage fields, the three-dimensional location of the electrode arrays, and high density EEG (at least 64 channels) is needed for source localisation.

The limitation of source localisation, however, is that there is no unique solution to explain the surface EEG pattern; this is known as the "inverse problem". Different source solutions can be found that result in the same field distribution. This fundamental difficulty can be addressed by imposing constraints on the solution. For example, physiological and anatomical considerations that lead to the single (or multiple) point dipole model of generators of epileptiform discharges [Cohen et al. 1990].

Other limitations include assumptions regarding volume conduction, the effects of neurophysiological propagation and the inability to distinguish between the two [Alarcon *et al.* 1994]. It is suggested that, semi empirical correlations between symptomatology, surgical outcome, and detailed presurgical modelling of the

neocortical projection patterns by combined MEG, EEG, and MRI may be more fruitful than source localization with unrealistic source models [Alarcon *et al.* 1994].

## 1.9 Magnetoencephalography (MEG)

A brief note of magnetoencephalography (MEG) is made here. It is an emerging technique for the localisation of IEDs. MEG measures the magnetic field alterations at the scalp surface induced by intracellular electrical current in pyramidal neurons. This is in contrast to EEG where changes in scalp potentials induced by electrical current in the intracellular space are measured. The magnetic fields of the brain are extremely weak, $10^1$ fT [femtotesla] for evoked cortical activity and $10^3$ fT for alpha rhythm. The ambient magnetic noise of the urban environment is of the order of $10^8$ fT. Extremely sensitive sensors and operation of the MEG system in a magnetically shielded room are therefore needed to overcome these signal to noise issues.

The key component in MEG hardware is the sensor element known as SQUID (Superconducting Quantum Interference Device). The SQUIDs transform the extremely weak magnetic fields present at the scalp surface into signals. The encapsulated sensors are immersed in liquid helium positioned about three to four cm from the cortex. MEG recordings were first made by David Cohen in 1968 [Cohen 1968]. These initial recordings were made with a single channel magnometer. Information was therefore only available from areas of cortex immediately under this single channel, clearly limiting its applicability. Whole head MEG with several hundred channels is now standard.

Recording with a very high number of channels, up to 300 to 400 channels is possible, compared to the limit of 128 or at most 256 with scalp EEG. In comparison to EEG

there is less distortion of magnetic fields by the resistive properties of the skull and scalp [Knowlton and Shih 2004]. MEG selectively detects tangential sources, thus MEG only measures electrical activity in the cerebral sulci. EEG detects both tangential and radial sources, with radial sources predominating in scalp recordings. The spatial resolution of MEG is dependent on the modelling of dipole locations [Barkley 2004a].

More recent applications of MEG include functional mapping of eloquent cortex, where paradigms originally designed for fMRI are yielding information on neural activity with a temporal resolution that would not be possible with the imaging methods that measure the haemodynamic or metabolic correlates of neural activity. Discussion of these is beyond the scope of this introduction but these methods are likely to have an important role in the future presurgical assessment in epilepsy [Knowlton and Shih 2004].

There is some debate regarding the superiority of MEG over EEG in epilepsy [Baumgartner 2004] [Barkley 2004b]. From a practical perspective the main consideration affecting the use of MEG is cost. The cost of a MEG scanner, the shielded room and analysis software more than 30 times more expensive than an EEG system with similar analysis capabilities [Lesser 2004]. In clinical practice EEG offers the advantage of long term recordings, during which patients can remain ambulant during the recording. Throughout a MEG recording the subject needs to lie as still as possible, limiting the recording time and the ability to record ictal events, although a few cases with simple partial seizures have been reported [Yoshinaga et al. 2004] [Tanaka et al. 2004]. Localisation accuracies of MEG and EEG are comparable, but MEG may be more sensitive for the localization of neocortical spikes [Baumgartner 2004]. More useful than suggesting the superiority of one technique over another is to

conclude that the techniques are complimentary and any preference depends on the question being asked and the environment in which it is tested. MEG like EEG is dependent on the spontaneous neurophysiological event of interest occurring during the recording period.

## 1.10 Magnetic Resonance Imaging

### 1.10.1 Background

The property and behaviour of nuclei placed in a magnetic field, nuclear magnetic resonance (NMR) was discovered independently by Felix Bloch at Stanford University and Edward Purcell at Harvard University in 1946. NMR was developed as a technique to study the chemical make up of compounds, by utilising the fact that different elements behave differently in electromagnetic fields. In 1971 Peter Mansfield in Nottingham University and Paul Lauterber in New York developed the theory and techniques necessary for image formation with NMR [Wood and Wehrli 1999]. In the field of medical imaging the term NMR has since been replaced with MRI (Magnetic Resonance Imaging). Advances in hardware and imaging techniques continue, in particular the development of higher strength magnets with higher image resolution, short scanner time and new scan sequences.

### 1.10.2 Principles of MRI

Image formation: excitation of nuclei

Atomic nuclei, with an odd atomic or mass number, possess a magnetisation moment associated with their nuclear spin. Under normal conditions the magnetic moments of

nuclei found in the body are randomly distributed resulting in no overall net magnetisation. Atomic nuclei placed in a static magnetic field (termed B0) will tend to align along and precess about the axis of the field (the z-axis) and are said to have longitudinal magnetisation.

The rate of precession of the nucleus (f) is given by the Lamor equation:

$$f=\gamma B_0/2\pi \qquad [1]$$

where $\gamma$ is the gyromagnetic ratio and $\mathbf{B_0}$ the magnetic field strength. The value of $\gamma$ varies between nuclear (and atomic) systems (hydrogen, lithium, carbon, etc). An MR instrument must be designed to detect signals at the resonance frequency corresponding to a specific nucleus of interest. MRI systems are tuned to the resonance frequency of hydrogen ions due to the abundance of water in the human body.

Application of a time varying magnetic field (B1), in the form of a short pulse of resonant electromagnetic field (the radiofrequency (RF) pulse), in the x-y plane, at the Larmor (resonant) frequency, for hydrogen, results in excitation, or perturbation of this equilibrium state. This rotates the magnetisation away from the z-axis, thus producing a transverse component of magnetisation. This transverse component rotates around z at the Lamor frequency. Electrical current is thus induced in a receiver coil oriented in the transverse plane.

Typical strengths of B1 are of the order $10^{-4}$ T. The strength and duration of the RF pulse are selected to rotate the magnetisation through a required angle; the flip angle. Magnetisation is often rotated through 90°.

Following RF pulse application, magnetisation gradually decays through two mechanisms: 1) to equilibrium alignment with B0 as a result of interactions with and loss of energy to surrounding molecules or the lattice, hence the term spin-lattice or

T1 relaxation. 2) Net transverse magnetisation is lost due to dephasing: the precessing protons de-phase with each other so components in the transverse plane tend to cancel, this is termed spin-spin relaxation, or T2 decay. T1 and T2 are properties of the material (and other factors, such as $B_0$) and form the basis of contrast formation in MRI, along with spin density (number of water protons per unit volume).

In addition when an object or subject is placed in the scanner magnetic field inhomogeneities develop. These inhomogeneities result in dephasing of the spins at a faster rate than by T2 alone. The term T2* characterises this phenomenon, and it is of particular relevance to functional MRI, as the oxygenation state of haemoglobin affects T2*.Areas of air/tissue interface, e.g. orbitofrontal sinuses are also susceptible to this.

Image formation: spatial encoding

Spatial encoding is the process by which MR images can be created. This is achieved mainly by modulation of the resonant frequency as a function of space. Essentially, changes in the strength of B0 alter the Lamor frequency, according to the above equation. Therefore, predetermined changes in B0 (along z) and a frequency selected RF pulse results in excitation of protons in a specific location or slice. The modulation of B0 is obtained using gradient fields. Altering B0 in one plane (the slice selection gradient), allows slice selection for excitation and signal generation. Changing B0 and RF pulses in the other two planes x-y, (known as the frequency encoding gradient, and phase encoding gradient), results in a signal with spatial encoding information in all three dimensions.

MR images are digital, consisting of picture elements commonly called pixels (2D) or voxels (3D). The MRI signal being a rapidly changing analogue signal in the radiofrequency receiver analogue-to-digital conversion produces the required digital

signal, which can be stored and manipulated on computer. The digitised raw data space is known as k-space, where the digital signal is stored; k-space is filled line by line as data is acquired. K-space data is reconstructed by a mathematical process, the Fourier Transform, which coverts the signal from the frequency to the spatial domain. This gives the voxel intensities that are converted to the MR image.

Sequences and image contrast

Alterations in the timing of the main radiofrequency pulse, repetition time (TR), and acquisition of signal, echo time (TE), weight the image in favour of particular tissue contrasts. Three basic sequence types exist; spin echo (SE), gradient echo (GE) and inversion recovery (IR). Briefly, a SE sequence involves an initial RF pulse of 90°, with a further refocusing 180° pulse at time TE/2. This rephases components of transverse magnetisation that have undergone T2 and T2* decay thus improving signal to noise and hence image quality. GE sequences start with an RF pulse (usually <90°), they use shorter TR and TE, hence scan time is shorter, however susceptibility artefacts, due to main field inhomogeneities, are more prominent. For IR sequences an initial inversion pulse of 180° is applied. This flips longitudinal magnetisation 180° (z to –z). Relaxation, or recovery, toward z occurs at a rate dependent on T1 of the tissue. There will be a time point at which longitudinal magnetisation for each tissue type passes zero. Application of the 90° excitation pulse at this point means that signal from this tissue suppressed or attenuated. An example of this is the FLAIR (FLuid Attenuated Inversion Recovery) sequence. This suppresses signal from CSF avoids partial volume effects at CSF cortex boundaries.

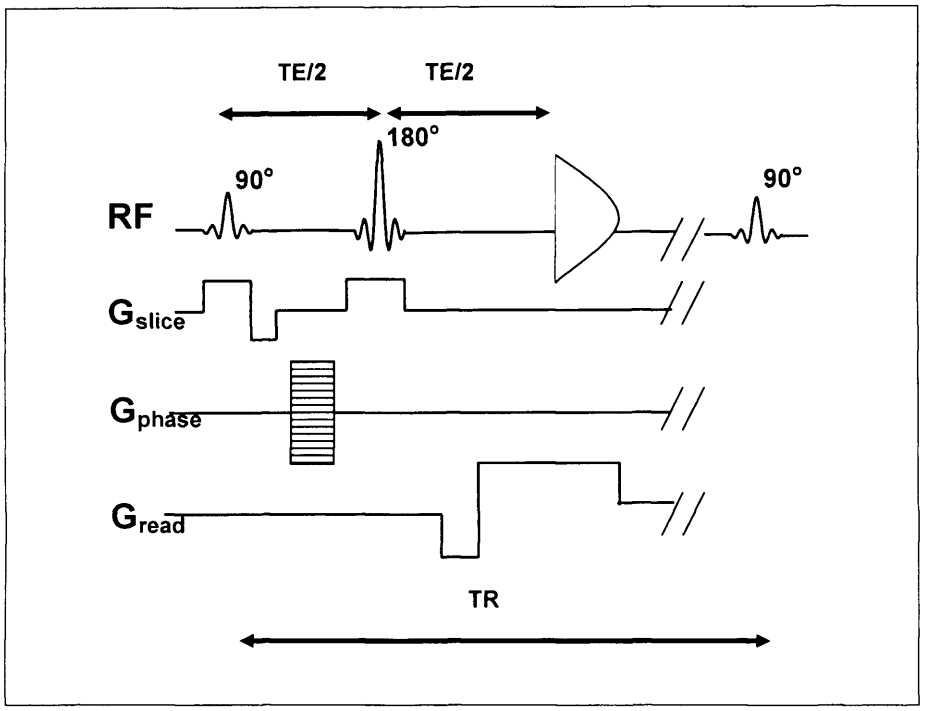


**Figure 1-3 MRI sequence diagram of gradient echo planar sequence.**

**Pulse sequence diagram showing all the gradients and RF pulses used to produce an image. The repetition time (TR) is the interval between two successive pulse cycles (i.e. the time to acquire one whole brain volume) and the echo time (TE) is the time taken from the application of the RF pulse to the measurement of the MR signal. A combination of three gradient fields; slice selection (SS, $G_{slice}$), frequency encoding (FE, $G_{read}$) and phase encoding (PE, $G_{phase}$), are used to spatially encode the protons.**

Image formation

Raw MRI data is stored in a matrix known as k-space; all points in k-space contain data for each point in the MRI image. A mathematical process known as the Fourier transform is used to convert k-space data from the frequency domain to the spatial domain. Points near the centre of k-space have low spatial frequencies and convey the

overall form of the image. Points at the periphery of k-space have high spatial frequencies and convey the fine edge detail of the image, but have little effect on image contrast. In order to use the Fourier transform to produce an image a certain amount of k-space needs to be sampled. This can be done via a number of different paths, or trajectories. The representations of image resolution and field of view are inversely related for physical image space, compared to k-space; therefore sampling a larger area of k-space leads to increased spatial resolution in the image, whereas decreasing the distance between points of k-space increases the image field of view.

### 1.10.3 Echo Planar Imaging

Spin echo sequence can take several minutes to acquire a single slice. To measure dynamic brain process a much faster acquisition is needed. Echo planar imaging (EPI) allows the acquisition of whole slices within a fraction of a second [Mansfield 1977], and hence whole-brain coverage within 2-3 seconds i.e. the timescale of the haemodynamic correlates of neural activity. This is achieved by applying a train of read gradients that produce a train of echoes following a single RF excitation pulse, rather than a single echo following each RF pulse. K-space data in conventional MRI is acquired a line at a time with each excitation pulse. During EPI k-space is acquired continuously so that all lines of k-space are filled after each excitation. This is achieved by a 'trick' of spatial encoding illustrated in the sequence diagram below.

**Figure 1-4 Echo-planar pulse sequence.**

**Illustrating the readout gradient switching that allows rapid spatial encoding.**

**From http://airto.bmap.ucla.edu/BMCweb/BMC_BIOS/MarkCohen/Papers/EPI-fMRI.html**

In most fMRI experiments performed today, a gradient echo version of EPI is preferred over spin echo EPI, due to its greater speed of acquisition.

A particular limitation of EPI is its sensitivity to field inhomogeneities because of the use of repeated, relatively weak gradients. These inhomogeneities occur at air tissue interfaces and cause the characteristic 'dropout' seen in orbitofrontal and temporal areas (figure 1.5). Inhomogeneities and hence attenuation of MR signal also depend on the intravoxel haemoglobin oxygenation levels which form the basis of most fMRI studies.

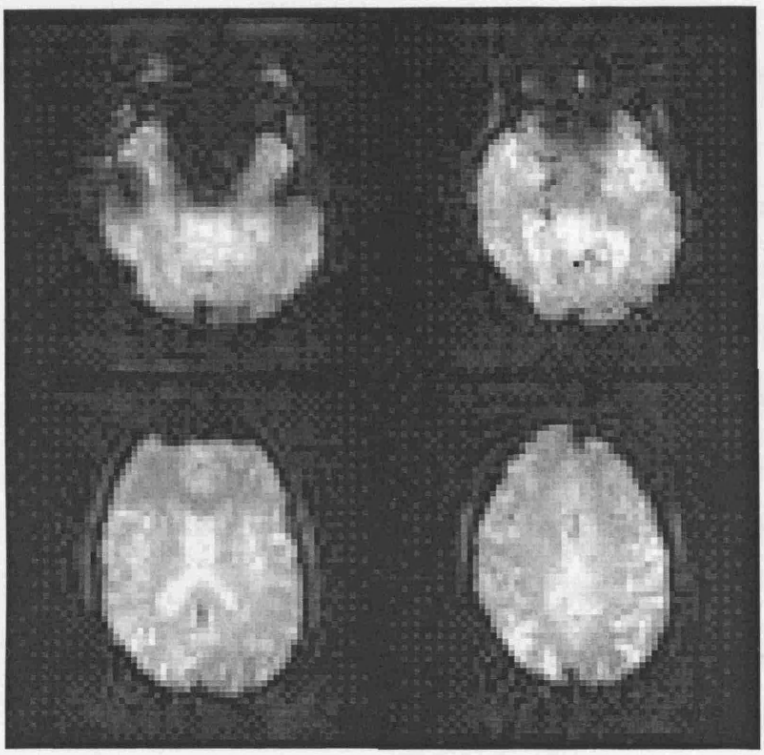

**Figure 1-5 Typical echo planar image.**

**Four representative axial slices from a BOLD gradient-echo EPI acquisition. The temporal resolution of ~3s for acquisition of the whole brain volume is obtained at the expense of spatial resolution (compared with high-resolution anatomical MRI), and regional signal dropout due to magnetic field inhomogeneity (orbitofrontal and temporal areas).**

### 1.10.4 Functional MRI and the BOLD Response

Over a century ago it was recognised that neuronal activity was associated with changes in regional cerebral blood flow [Roy and Sherrington 1890]. Hans Berger, the founder of the human EEG spent his early career looking for correlates of brain activity using haemodynamic measures; however was limited by inadequate tools [Gloor 1994]. Today the imaging techniques of SPECT, PET and fMRI, allow the

measurement of these haemodynamic changes and hence inferences about brain function in resting and experimental conditions.

The non-invasive localisation of dynamic changes in the human brain activity is made possible by 1) the magnetic properties of haemoglobin, and 2) the haemodynamic consequences of neural activity. During Blood Oxygen Level Dependent (BOLD) fMRI [Ogawa *et al.* 1990b], a time series of images that are sensitive to intravoxel deoxyhaemoglobin levels is acquired during a recording session whilst the subject undertakes a task or stimulus. Haemoglobin oxygenation then acts as an endogenous contrast agent.

During neural activity local cerebral oxygen consumption increases, this is followed over seconds by a disproportionate increase in blood flow, that greatly exceeds oxygen consumption; and to a lesser extent an increase in blood volume; resulting in an absolute decrease of local deoxyhaemoglobin. The magnetic resonance signal is sensitive to the oxygenation state of haemoglobin [Thulborn et al. 1982]. In the oxygenated state the Fe ion is "shielded" and exerts little magnetic effect on its surrounding environment; in contrast to deoxyhaemoglobin which disrupts a surrounding magnetic field [Pauling and Coryell 1936]. The different magnetic properties according to the oxygenation state of haemoglobin can therefore be exploited to give a functional contrast of neural activity.

Ogawa and colleagues observed MR signal decrease in vein and surrounding tissue in response to decreasing oxygen in inspired air in anaesthetised rats. They proposed the use of this phenomena as an endogenous contrast in the study of brain physiological activity, and introduced the term Blood Oxygen Level Dependent (BOLD) contrast [Ogawa *et al.* 1990a;Ogawa *et al.* 1990b]. Similar findings were seen in cat brain during the course of anoxia [Turner et al. 1991]. In 1992 four groups reported BOLD

signal increase or activation in response to visual or sensory stimuli [Kwong *et al.* 1992;Bandettini *et al.* 1992;Frahm *et al.* 1992;Ogawa *et al.* 1992]. Since then BOLD imaging has revolutionised the study of human brain function, primarily due its non-invasive nature.

Three phases of the BOLD response have been proposed [Buxton 2001], an initial dip, followed by a BOLD peak and subsequently a decrease in signal with a transient undershoot below baseline. The temporal characteristics of the BOLD effect may vary between sessions, regions and subjects [Aguirre et al. 1998], but are sufficiently well described by a canonical Haemodynamic Response Function (HRF) derived from data acquired following brief stimuli. This enables the efficient modelling and detection of the brief signal changes attributable to physiological stimuli or tasks [Buckner et al. 1996].

The haemodynamic response to neural activity reaches a peak at around 5 seconds from the onset of neural activity and returns to baseline over 20 to 30 seconds and can be captured in its entirety with fMRI.

Comparison of images in the active state (task or stimulus) and rest state (no task or stimulus) or between different tasks is used to generate contrast between images and hence identify areas of task related neural activity.

### 1.10.5 From Neuron to BOLD

The relationship between neural activity and blood flow changes (neurovascular coupling) remain to be fully explained. In particular, the reasons for the much greater increase in cerebral blood flow (CBF) relative to oxygen consumption (CMRO2) remain unclear [Buxton 2002]. Early observations with PET that suggest uncoupling between CBF and CMRO2 [Fox and Raichle 1986;Fox et al. 1988] were driven by

glucose metabolism. This is likely an oversimplification and further observations have led to alternative and more robust models. Notably, tight coupling, with a linear relationship between CBF and CMRO2 has been shown, possibly related to the diffusivity of oxygen from blood to brain at a given perfusion level [Hoge *et al.* 1999a;Hoge *et al.* 1999b]. Malonek and Grinvald suggested that CBF is controlled on a coarse scale and CMRO2 on a much finer scale [Malonek and Grinvald 1996]. Using near infrared spectroscopy they noted an initial increase in deoxyhaemoglobin, that was better localised to neural activity followed by a much larger decrease in deoxyhaemoglobin over a much wider spatial area - "watering the garden for the sake of one thirsty flower" [Malonek and Grinvald 1996]. An alternative hypotheses is the 'oxygen limitation model' [Buxton and Frank 1997]; a large flow change is needed to support a small increase in oxygen metabolism. This is based on two assumptions, 1) blood flow increases as a result of increased velocity rather than capillary recruitment and 2) oxygen delivery is limited at rest, i.e. only a fraction of $O_2$ molecules are extracted for metabolism due to the relationship between $O_2$ bound to haemoglobin [Buxton and Frank 1997]. Frahm et al propose weaker coupling between CBF and CMRO2 on the basis of their observations [Frahm et al. 1996]. However alternate modelling of their data, to include changes in CBV as well as CBF, can explain their findings with tight coupling throughout [Buxton 2002].

The cellular mechanisms that orchestrate these blood flow changes are yet to be fully determined [Heeger and Ress 2002]. The haemodynamic response to neural activity is likely initiated by neuronal signalling with fast neurotransmitters, i.e. the BOLD response is a reflection of neuronal signalling, rather than the energy deficit of neurons [Attwell and Iadecola 2002]. Logothetis and colleagues using simultaneous microelectrode recordings and BOLD fMRI observed that BOLD signal changes

correlate best with local field potentials, rather than axonal firing patterns [Logothetis et al. 2001], reflecting dentiritic input, and intracortical processing in a brain region, rather than synaptic output.

### 1.10.6 Experimental design

Most commonly fMRI is used to map neural responses to a particular experimental task or stimulus. This is presented either as brief events or blocks, repeated over the course of an fMRI session (typically of 10 to 20 minute duration) to improve signal to noise. Comparison is then made between scans acquired during the two states.
fMRI experiments can be divided into two main categories according to the nature of the delivered stimulus or performed task during scanning - block based designs and event related designs. In block related designs, alternating periods or blocks of task and resting states (of tens of seconds each) are performed during scanning. Because of the temporal delay and duration of the BOLD response, blocks of less than 8 seconds would fail to resolve activations, and blocks of several tens of seconds are found to be most efficient. Event related designs have certain advantages over block designs, they allow design of more intricate psychological studies accounting for such issues as subject habituation. Both block and event related designs can be used to model EEG in EEG-fMRI of epileptic activity, according to the nature of the IED. As we shall see the main constraint in EEG-fMRI is on the occurrence of these events and experimental efficiency.

### 1.10.7 Limitations of BOLD fMRI

The BOLD response is a qualitative rather than a quantitative measure of neural activity. The biological processes driving the response remain poorly understood. BOLD fMRI cannot be used to detect low frequency state-related changes because of large intersessional variability and scanner noise characteristics. Together with the slow HRF relative to neural activity, the detection power of fMRI is limited to the narrow frequency band within which most conventional fMRI paradigms operate, i.e. active and rest states alternating, or events occurring, every 20 to 30 seconds.

BOLD fMRI has relatively low signal to noise ratio. Subject cooperation, experimental design, post processing strategies and statistical frameworks are needed in the interpretation of data [Kim and Ogawa 2002]. BOLD fMRI correlates with neuronal activity to several millimetres with a temporal resolution of a few seconds. The spatial resolution is ultimately limited by the extent of recorded regional changes in cerebral blood flow relative to this activity. At 1.5T a large contribution to BOLD signal comes from draining veins, being the site of largest change in deoxyhaemoglin levels, rather than the capillary bed [Lai *et al.* 1993;Frahm *et al.* 1994]. This so called brain / vein problem could result in activation distal to the site of activity.

Motion artefacts present a serious confound in fMRI. Subject head motion results in different parts of the brain, with different signal characteristics being imaged at any one voxel over the course of the time series. The effects are most pronounced at edges of intensity difference, e.g. near the surface of the brain or ventricles. Another factor is referred to as spin history effects. Although the MR signal is not fully relaxed between excitations, a stable state is reached within the slice. Movement out of or into this slice presents different spin histories to the next RF pulse and hence different

signal is acquired. Further EPI is particularly susceptible to image distortion due to field inhomogeneities that will vary with subject motion [Jezzard and Clare 1999]. Motion is minimised by subject selection and training and the use of foam pads, restraining straps or vacuum cushions.

Post processing techniques to minimise the impact of motion will be reviewed later.

### 1.10.8 Blood Flow Measurements Using Arterial Spin Labelling

The relatively new technique of perfusion MRI, using arterial spin labelling (ASL) as a non-invasive endogenous contrast, measures CBF itself; as apposed to relative changes in blood oxygenation [Williams *et al.* 1992;Buxton and Frank 1997;Detre and Alsop 1999;Kim 1995]. ASL techniques have a higher spatial and temporal resolution than BOLD. They have been used in the investigation of the underlying mechanisms of the BOLD response [Hoge *et al.* 1999b;Hoge *et al.* 1999a] and offer a more sensitive tool for within and across subject hypotheses tests than BOLD [Aguirre *et al.* 2002]. Briefly the principle behind ASL is based on 'magnetic labelling' of arterial blood before it enters the field of view. This is achieved by a 180° RF pulse to flip the magnetisation of water in arterial blood proximal to, and prior to acquiring the image slice. After a delay to allow the tagged slice to reach the area to be imaged the tag image is made. Subsequently a control image is acquired without prior tagging. The two images are subtracted; the static signal cancels out leaving the signal from the arterial blood delivered to each voxel within the time interval between labelling and scanning. The advantage over other tracer techniques, specifically PET, is that radioisotopes are not used, allowing multiple sessions in the same subject.

### 1.10.9 Data Pre-processing and Analysis

The signal to noise ratio in fMRI is low, a few percent at 1.5 Tesla. Image analysis needs to take place within a complex statistical signal processing framework.

The work in this thesis uses the Statistical Parametric Mapping software (SPM) (http:www.fil.ion.ucl.ac.uk/SPM). The term SPM is used interchangeably throughout this thesis to refer to the software package or the resulting statistical image – statistical parametric map, from which inferences about brain function are made, depending on the context in which it appears.

The standard BOLD fMRI analysis pipeline as implemented in SPM, can be broken down into three basic steps:

1) Pre-processing. The voxels between successive temporally acquired images need to conform to the same anatomical space necessitating spatial realignment. Spatial smoothing is added to increase signal to noise. In group analyses spatial normalisation to a standard template is also needed.

2) Regression analysis. Time series at each and every voxel is correlated with the experimental paradigm. A statistical value linked to the effect of interest is obtained for each voxel.

3) Statistical inferences. A correction for multiple comparisons is needed given the large number of correlations i.e. for several tens of thousands voxels. A number of correction methods exist, the simplest being the Bonferroni correction, whereby the p values are divided by the number of observations. This is too conservative for fMRI data because of temporal and spatial autocorrelation between the data. In SPM a correction based on Gaussian random fields is used instead. In the classical approach the statistical

procedure is aimed at protecting against false positives. An appropriate level of significance (threshold) is applied resulting in a statistical parametric map.

The SPM can be colour coded and overlaid onto anatomical images for display purposes. The terms 'activation' and 'deactivation' are operationally defined as increases or decreases in the BOLD signal at these correlated voxels.

## 1.11 Functional Imaging in Epilepsy

### 1.11.1 Background

Structural brain imaging can reveal the substrate for epilepsy. MRI is the imaging modality of choice. The clinical role of MRI in epilepsy is to identify underlying pathology, such as vascular lesions, infection and tumours that require specific therapy and to assist in the formulation of syndrome and aetiological diagnosis by demonstrating focal abnormalities. Functional neuroimaging in epilepsy has a wider scope. It can be used to define either eloquent cortex using a range of experimental paradigms or to define epileptogenic areas, with a view to surgical resection or in studying the neurobiology of epilepsy.

The in vivo investigation of human brain function can be considered in terms of

1) neurophysiological recording – EEG and MEG and

2) haemodynamic or metabolic measures – fMRI, positron emission tomography (PET), single photon emission tomography (SPECT), near infrared spectroscopy (NIRS) and transcranial Doppler (TCD).

Each modality has its own merits and drawbacks in terms of resolution and invasiveness. Neurophysiological techniques have superior temporal resolution, a few hundreds of milliseconds, but limited spatial resolution, due to the "inverse problem"

of dipole modelling (see section 1.8.10.5). Imaging methods on the other hand have better spatial resolution but poorer temporal resolution, limited by the temporal resolution of acquisition process, and ultimately by the resolution of the physiological correlate being measured. Figure 1.6 and table 1.2 (below) depict some of these properties for each of the techniques:

**Figure 1-6 Temporal and spatial resolution of neuroimaging modalities.**

**The temporal and spatial resolution of neurophysiological and functional imaging modalities is shown. The sources of epileptic discharges are at the synapse and millisecond level, functional imaging modalities in human studies are inevitably many orders of magnitude above this.**

**EEG – electroencephalography, ERP – evoked response potential, fMRI – functional MRI, MEG – magnetoencephalography, PET – positron emission tomography. Adapted from Cohen and Bookheimer 1994 [Cohen and Bookheimer 1994].**

| Modality | Property measured | Temporal resolution | Spatial resolution | Invasiveness | Cost | Other considerations | |
|---|---|---|---|---|---|---|---|
| | | | | | | Pros | Cons |
| **Neurophysiological** | | | | | | | |
| Scalp EEG | Local field potential / synaptic activity | +++ | + (SEEG ++) | Minimal | Low | Widely available | Poor spatial resolution<br>Inverse problem<br>motion and other artefacts |
| Intercranial EEG | Local field potential / synaptic activity | +++ | + | High | High | High sensitivity, minimal artefact | Invasive<br>Limited sampling to vicinity of placed electrodes |
| MEG | | +++ | + | Minimal | High | Repeat session within subjects<br>Child 'friendly' | Cost<br>Inverse problem |
| **Neuroimaging** | | | | | | | |
| PET | Haemodynamic, metabolic or neurochemical | + | ++ | Moderate | High | Between session comparisons | Radiation<br>Cost<br>Limited scan sessions |
| SPECT | Haemodynamic or neurochemical | + | + | Moderate | Low | Ictal scans possible | Low temporal and spatial resolution |
| fMRI | Haemodynamic<br>Likely correlate of local field potential | ++ | ++ | Minimal | Low (after initial purchase and multiple use ) | Repeat session within subjects | Low signal to noise<br>Image distortion particularly temporal, orbitofrontal |
| NIRS | Haemodynamic | ++ | + | Minimal | Low | Non invasive | Spatial resolution |
| TCD | Haemodynamic | ++ | + | Minimal | | Non invasive | Spatial resolution |

**Table 1-2 Overview of functional neuroimaging modalities, and their relative merits.**
**MEG- magnetoencephalography, PET-positron emission tomography, SPECT-single photon emission tomography, fMRI-functional magnetic resonance imaging, NIRS-near infrared spectroscopy, TCD-transcranial Doppler. +: low, ++: average, +++ high.**

## 1.12 Positron Emission Tomography

### 1.12.1 Methods

Positron emission tomography (PET) is based on imaging the radioactive decay of specially designed radioligands (or tracers) that target a cerebral physiological process. The image acquisition process consists of: venous injection of tracer, cerebral uptake and scanning make up PET. Throughout there is radioactive decay of the tracer. The short half of the isotopes (see table 3) in the tracers necessitates an onsite cyclotron unit for their manufacture, the cost of which is a key limitation of PET.

PET images are constructed from detection of gamma rays emitted during radioisotope decay, hence localising the radioisotope in brain. PET tracers are designed using radioisotopes of commonly occurring elements in biologically active compounds involved in different cerebral processes. These include haemodynamic and metabolic, activity, neurotransnsmitter synthesis and receptor binding activity. Co registration with MRI and the application of statistical methods provide an objective evaluation [Henry et al. 1990].

Scans can be undertaken in the resting state or before, during and after predetermined experimental conditions e.g. motor or cognitive tasks, drug administration or seizure occurrence. Statistical comparison is used to identify global and regionally specific effects of experimental conditions. The quantitation of images allows comparison between scan sessions, undertaken weeks or months apart and study low frequency state changes, something which cannot be done with fMRI. However PET has a much poorer temporal resolution, of the order of tens of minutes for FDG PET. Other considerations include the invasive nature of radioactivity and the need for venous and often arterial access; high cost; and the unstable nature of the isotope.

Commonly used tracers in epilepsy, along with the processes they measure and their half life are shown in table 3.

| Tracer | Isotope | T1/2 | Process measured | Main abnormality in epilepsy |
|---|---|---|---|---|
| [18F]FDG | 18 flourine | 2 hrs | Glucose uptake | Hypometabolism of interictal lesion |
| $H_2{}^{15}O$ | 15 oxygen | 2 mins | Cerebral blood flow | Hypoperfusion of EZ, not useful clinically for resting interictal studies for focus lateralisation or localization. Due to low T1/2 |
| [11] Flumazenil | 11 carbon | | Benzodiazepine (GABAA) receptor | Decreased binding in EZ, less extensive than [18F]FDG |
| [11] C Carfentanil<br>[11] C Diprenorphine<br>[11] C Doxepin<br>N-methyl 11C Ketamine | 11 carbon | 20 mins<br>-<br>-<br>- | Opiate system<br>Mu<br>Mu- , Kappa, Delta<br>H1 ligand | No significant changes |
| [11] C α-methyl tryptophan | 11 carbon | 20 mins | Precursor to serotonin synthesis (and others) | Increased in epileptogenic tubers in TS, FCD, epileptogenic mesial temporal lobe [Natsume et al. 2003] and surgical margins in surgical failures |
| [18F]FCWAY | 18 flourine | 2 hrs | 5HT 1A receptor | Reduced in epileptogenic mesial temporal lobe [Toczek et al. 2003] |
| [11]C CNS516 | 11 carbon | 20 mins | Open calcium channel in NMDA receptor | |

**Table 1-3 Summary of PET tracers, the cerebral processes they measure and interictal changes seen in focal epilepsy.**

**[18F]FDG - flourodeoxyglucose, T1/2 – half life**

**[18F]FCWAY- (*N*-(2-[4-(2-methoxyphenyl)piperazino])-*N*-(2-pyridinyl) *trans* – 4 -fluorocyclohexanecarboxamide)**

PET can be used to measure haemodynamic (H2[15]O) or metabolic process (2-[18F] fluoro-2-deoxyglucose ([18F]FDG)) or specific receptor binding (e.g. flumazenil (FMZ)).

### 1.12.2 PET in Focal Epilepsy

Recent improvements in structural MRI acquisition (higher field strengths, better acquisition sequences, and post processing analysis) has superseded PET to a great extent [Duncan 1997]. Many PET abnormalities in those previously deemed MRI negative are now seen with high resolution MRI - a less invasive and less costly procedure.

The characteristic PET findings in focal epilepsy are of interictal temporal hypometabolism [Engel, Jr. *et al.* 1982b;Abou-Khalil *et al.* 1987;Henry *et al.* 1993;Koutroumanidis *et al.* 1998a] and decreased central benzodiazepine receptor binding [Savic *et al.* 1988;Savic *et al.* 1995;Koepp *et al.* 1996] in the epileptic focus. In mesial temporal lobe epilepsy this includes unilateral diffuse regional hypometabolism of mesial and lateral temporal areas with or without ipsilateral extra temporal hypometabolism and in some contralateral temporal hypometabolism [Engel, Jr. *et al.* 1982a;Abou-Khalil *et al.* 1987;Henry *et al.* 1993;Koutroumanidis *et al.* 1998a]. The areas of hypometabolism are more extensive than those of reduced benzodiazepine receptor binding. Chassoux et al showed a close association between the extent of hypometabolism and the pathways of ictal spread [Chassoux *et al.* 2004]. The pathological basis of temporal hypometabolism is unclear. It has been proposed that reduced transmembrane glucose transport rates and reduced mitochondrial glucose oxidation of viable neurons in sites of ictal onset are important factors [Henry and Votaw 2004].

Simultaneous EEG is necessary during PET as differences between interictal, ictal and post ictal during acquisition will confound any analysis. Ictal events lead to increases in glucose metabolism in focal lesions. In temporal lobe epilepsy this could lead to false localisation if an ictal scan has been inadvertently acquired, as comparison with the opposite side would suggest either hypometabolism in the contralateral lobe, or normalization of an area of interictal hypometabolism.

### 1.12.3 PET in IGE

Interictal FDG PET is normal in IGE. PET findings during absence seizures are contradictory. Absence seizures with spike wave discharge on EEG were associated with increased glucose metabolism [Engel, Jr. *et al.* 1985;Theodore *et al.* 1985] although one case of absence status was associated with decreased glucose metabolism [Theodore *et al.* 1985]. A further study of spike wave discharge found a trend toward increased glucose metabolism in patients with well defined primary generalised epilepsy [Ochs *et al.* 1987]. Measurement of rCBF in typical absences provoked by hyperventilation, using H2[15]O PET showed a 15 % global increase in global rCBF with an additional 4-8% increase in rCBF in the thalamus [Prevett *et al.* 1995a].

A global decrease in FMZ binding has been found [Savic et al. 1990], although a later study found FMZ distribution increased in the cerebellum and decreased in the thalamus [Savic et al. 1994]. Prevett et al found no changes in FMZ binding in CAE or JAE, or in relation to absence seizures [Prevett *et al.* 1995c] but treatment with sodium valproate was associated with reduced FMZ binding [Prevett *et al.* 1995b]. However further studies using improved methods to detect differences between IGE and controls found higher FMZ distribution in cerebral cortex, thalamus and

cerebellum, and no effect of short term VPA therapy [Koepp et al. 1997]. PET with the opioid receptor ligand, 11 C-diprenorphine showed increase in diprinorphine elimination on association cortex, suggesting an increase in opiate release in these areas after absence seizures, [Bartenstein *et al.* 1993].

## 1.13 Single Photon Emission Computed Tomography

### 1.13.1 Methods

Single photon emission computed tomography (SPECT) like $H_2O$ PET is based on injection of a radio labelled tracer, followed by acquisition of images that are sensitive to regional blood flow changes. The most commonly used SPECT tracers are 99mTc-hexamethyl-proplenamine (99mTc-HMPOA) and 99mTc-ethyl cysteinate dimmer (99mTc-ECD). SPECT scanners measure direct emission of gamma radiation from the cerebrally bound tracer. Mathematical reconstruction of multiple planar gamma ray images taken at different rotational angles produces a series of thin, cross sectional two-dimensional images of the brain. Following intravenous injection 70% of brain uptake takes place within 1 minute. Spatial resolution is poorer than PET, however a distinct advantage in epilepsy is the capability to ictal SPECT images. After crossing the blood brain barrier 99mTc-HMPOA forms a bond with glutathione that remains stable for up to six hours. Stable binding of tracer to brain proteins after injection means imaging can be deferred to some hours after the seizure and injection, eliminating problem of movement artefact and patient stability. These factors place SPECT in a unique position to study the haemodynamic correlates of seizures; with

injection taking place at the time of the seizure and imaging after the patient has recovered some hours later.

SPECT is relatively cheap to perform, hardware is more widely available, and tracers are more stable. This tracer stability, allowing transport and storage, obviates the need for an onsite cyclotron unit and its attendant costs. In addition, In contrast the short half life of PET radioligands precludes ictal studies aside from those with "fortuitous" seizures occurring at prearranged scans. Similarly fMRI of ictal events is serendipitous, arising when unplanned events occur during a scan session; with a major additional constraint that any head motion makes the data uninterpretable.

Ictal SPECT requires appropriate logistical set up. Timing of tracer injection at the onset of seizures is essential to capture the true ictal onset zone rather than areas of propagation [Ho *et al.* 1994;Laich *et al.* 1997]. Rapid identification of seizure onset, by patient reporting or EEG, is essential. Video EEG is necessary to catch this onset and measure the delay to injection. Patient activated (in those with sufficient warning) or automated devices can shorten any delay to injection [Van Paesschen *et al.* 2000] and improve results.

### 1.13.2 SPECT in Focal Epilepsy

Interictal SPECT alone has no place in the investigation of patients with epilepsy. Interictal SPECT although showing electro-clinically concordant areas of reduced CBF in some cases, is not always reliable or consistent. Interpretation of images is visual and hence subjective.

Ictal SPECT, with injection at the onset of a seizure shows intense hyper perfusion at the epileptic focus. A meta analysis of published data showed that in patients with TLE, the sensitivities of SPECT relative to diagnostic evaluation were 0.44

(interictal), 0.75 (post-ictal) and 0.97 (ictal)[Devous *et al.* 1998]. Combining data from ictal and interictal SPECT with SISCOM (Subtraction Ictal SPECT CO-registered to MRI) gives further improvements in sensitivity. Here two SPECT scans are acquired, one interictally, the other with tracer injection at the onset of a seizure. These are co-registered with the patients structural MRI and subtracted to give difference image of CBF between the ictal and interictal state. Sensitivity was improved from 0.39 to 0.88 in extra temporal lobe epilepsy [O'Brien et al. 1998] and from 0.74 to 0.93 in children. Statistical analysis with SPM makes evaluation of images more objective [Fell et al. 2005;Bruggemann et al. 2004]. A recent study of patients with non lesional temporal lobe epilepsy, found combined subtraction SPECT and [18F]FDG PET of localising value in just under half of the patients [Lee et al. 2003].

Ictal hyper perfusion to adjacent extra temporal cortex and ipsilateral basal ganglia [Newton et al. 1993] and contralateral (less so ipsilateral) cerebellar hemispheres is also seen.

SPECT may have a role in optimisation of electrode placement [Kaminska et al. 2003] [Thadani et al. 2004]. A recent compelling study of 15 patients with focal cortical dysplasia showed that SISCOM SPECT can be used to inform visual interpretation of structural MRI; to identify previously unseen or equivocal subtle lesions, this additional diagnostic information allowed formulation of hypotheses for intracranial monitoring and surgical resection; 5 of 9 who had surgery remained seizure free [Dupont *et al.* 2006].

### 1.13.3 SPECT in IGE

Yeni et al [Yeni *et al.* 2000] studied 6 patients with childhood absence epilepsy. Hyperventilation induced ictal images were compared with baseline images. Cerebral to cerebellar ratios for regions of interest were calculated for quantitative comparison between baseline and ictal / hyperventilation images. They found a diffuse increase in cerebral perfusion, throughout cortex and subcortical structures. The effects of hyperventilation on blood flow and potential regional differences, and the impact it may have had on their results were not tested; for example a hyperventilation induced decrease in cerebellar greater than cerebral perfusion would have given a similar finding.

Benbadis et al [Benbadis *et al.* 1998] studied a single patient with childhood absence epilepsy. They compared ictal SPECT scans, again by injection during a hyperventilation induced absence seizure, with a baseline study. The ictal scan showed a generalized reduction in SPECT signal which was interpreted as a reduction in cortical activity. Again the effects of hyperventilation on cerebral blood flow were not controlled for.

Kapuci et al studied 23 children with childhood absence epilepsy. 10 of the 23 had relative hypoperfusion in frontal areas on visual inspection. 13 of the 23 had relative hyper perfusion in these frontal areas during hyperventilation induced absence seizures, whilst all patients had global increased blood flow in ictal studies [Kapucu et al. 2003]. Once more the effects of hyperventilation were not formally controlled for.

Sperling and Skolnick [Sperling and Skolnick 1995] used the 133xenon method to measure GSW associated blood flow changes in a patient with generalized epilepsy and continuous spike wave discharges. They found decreased blood flow during spike wave throughout the cortex, in parietal more than frontal lobes.

## 1.14 Transcranial Doppler

### 1.14.1 Methods

Transcranial Doppler (TCD) measures blood flow velocity in intracranial arteries, typically the middle cerebral artery using an ultrasound probe [Caplan *et al.* 1990;Deppe *et al.* 2004]. The probe is placed on the side of the scalp until an arterial trace is detected. Simultaneous EEG and TCD is possible with little additional technical constraints above those of the individual techniques. An advantage of TCD over modalities described above is that it provides continuous measurements on relative blood flow changes, rather than an averaged 'snapshot' of blood flow over a period of time

### 1.14.2 TCD of GSW

Five studies of GSW using TCD have been reported.

Sanada et al [Sanada *et al.* 1988] studied 2 patients with childhood absence epilepsy, a total of 8 absences were recorded. Blood flow velocity began to decrease 7-9 seconds after the start of GSW and reached a minimum at 0-8 seconds after the end of GSW, with flow velocities returning to baseline within a minute after the end of GSW.

Klingelhofer et al [Klingelhofer *et al.* 1991] studied 3 patients with frequent GSW using simultaneous EEG and TCD. A total of 25 GSW epochs were recorded. Around 3 seconds after the onset of GSW the flow velocity on MCA decreased by 25.84% (+/- 10.45%). These changes persisted several times longer than the period of GSW.

Bode et al [Bode 1992] studied 51 children with different types of epilepsy. In 16 children, 33 seizures were captured. During absence seizures the mean flow velocity

decreased to a minimum of 46%-82% (median 71%) of the baseline values. Flow velocity increased during tonic and tonic-clonic seizures. No flow changes were seen in 35 children with generalized epileptic discharges of 5 seconds or less without clinical manifestations.

De Simone et al [De Simone *et al.* 1998] studied 5 children with frequent absence seizures. Mean flow velocity increased a few seconds before the clinical and electroencephalographic manifestations of each seizure to maximum values of 25.5-42.8% with respect to baseline within 2-3 seconds of onset; followed by a fast reduction in flow velocity to a minimum of 30.8-44.0% decrease with respect to baseline, recorded within 4-6 seconds from the end of each absence seizure.

Diehl et al [Diehl *et al.* 1998] studied 13 patients and found significant change in flow velocities in 9. Respiratory rate and end tidal $CO_2$ were measured in one patient. Four had an initial increase and a subsequent decrease. This was partially paralleled by an increase in RR and a decrease in $pCO_2$. In three patients, an increase in CBFV preceded the onset of GSW by several seconds, followed by a decrease in CBFV. Two patients showed a decrease only. They suggested that the decrease might be due to hyperventilation and hypocapnia however it is difficult to extrapolate this from only one patient.

In summary TCD studies consistently show decreases in cerebral blood flow during GSW, with changes typically exceeding the GSW epoch. In some cases this decrease is preceded by an initial increase that occurs some seconds before the onset of GSW.

The following table summarises the literature of functional imaging of GSW.

| Modality / Study | No of Patients | Epilepsy Syndrome | Methods | Findings |
|---|---|---|---|---|
| **PET** | | | | |
| [Engel, Jr. *et al.* 1985] | 4 | IGE | $^{18}$FDG PET<br>HV induced GSW vs. HV after treatment | Patterns of CMRGlc identical for ictal and interictal scans<br>But 2.5 – 3.5 diffuse increase in global CMRGlc when hyperventilation ictal scans compared to hyperventilation when seizures were controlled |
| [Theodore *et al.* 1985] | 9 | IGE | $^{18}$FDG PET | No interictal abnormalities, GSW in 3<br>Diffusely increased compared to interictal in one, and to control values in the other.<br>Decrease throughout cortical and subcortical structures in one with absence status. |
| [Ochs *et al.* 1987] | 7 | 2 IGE and 5 SGE | $^{18}$FDG PET | slight trend toward increased global CMRGlc in 2 with IGE, global CMRGlc unaffected in SGE |
| [Prevett *et al.* 1995a] | 8 | IGE | $H_2{}^{15}O$ PET<br>HV induced GSW | Mean global increase (14.9%) in blood flow absence seizures and, in addition, a focal increase in thalamic blood flow of 3.9 to 7.8%. |
| **SPECT** | | | | |
| [Yeni *et al.* 2000] | 6 | CAE | HV induced GSW vs. rest | Increase in CBF higher than baseline in HV induced seizures |
| [Nehlig *et al.* 2004] | 4 | IGE | SISCOM | One Ictal scan showed diffuse blood flow decreases.<br>Three other scans acquired during the post ictal phase show generalised blood flow increase |
| **$^{133}$Xenon** | | | | |
| [Sperling and Skolnick 1995] | 1 | SGE daily absence status | Xenon 133 method | Global decrease by 12% from baseline in CBF during GSW, regional differences, greater decrease in parietal lobe than frontal |

| | | | | |
|---|---|---|---|---|
| **EEG-fMRI** | - | | | |
| [Steinlein *et al.* 1995] | 16 | IGE | EEG-fMRI (I) 1.5 T with photic stimulation | In photosensitive patient increased cortical activation, perioroiandic attenuation, marked occipital and posterior cingulate post stimulus undershoot |
| [Salek-Haddadi *et al.* 2003b] | 1 | CAE | EEG-fMRI (C) 1.5 T | Thalamic increase, cortical decrease |
| [Aghakhani *et al.* 2004] | 15 | IGE | EEG-fMRI (C) 1.5 T | Thalamic change in 12, predominantly increase<br>Cortical anterior and posterior, increase and decrease, decrease predominates |
| [Gotman *et al.* 2005] | 15 as above | IGE | EEG-fMRI (C) 1.5 T | Group analysis of Aghakhani [Aghakhani *et al.* 2004]. Thalamic increase, 'default mode' decrease |
| **TCD** | | | | |
| [Sanada *et al.* 1988] | 2 | CAE | MCA TCD and simultaneous EEG | Flow velocity decrease 7-9 seconds after onset of GSW, trough 0-8 seconds after end GSW with rebound return to baseline after 1 minute |
| [Klingelhofer *et al.* 1991] | 3 | IGE | MCA TCD and simultaneous EEG | Flow velocity initial increase 3.41 +/- 0.98% followed by decrease 25.84 +/-10.45%, flow velocity changes outlasted GSW by several times |
| [Bode 1992] | 51 | All types | MCA TCD and simultaneous EEG | Flow velocity increase during tonic seizures. Mean flow velocity decrease 46-82% (median 71%) during absence seizures. |
| [Nehlig *et al.* 1996] | 4 | 4 IGE<br>+<br>16 GAERS rats | MCA TCD and simultaneous EEG | Flow velocity decrease by a median value of 20-24% during spontaneous absences.<br>In GAERS CBF decreased during absence status, increased 175-664% in induced convulsive seizures |
| [Diehl *et al.* 1998] | 13 | 9 IGE<br>3 F<br>1 HA | MCA TCD and simultaneous EEG | Changes in 9, 7 with IGE, 1 FE<br>4 biphasic, increase in CBF at onset of GSW followed by decrease, of which 3 initial increase peaked -0.5 to -6.0 s before the onset of GSW, followed by decrease. CBF seen only in GSW >0.8s. |
| [De Simone *et al.* 1998] | 5 | IGE | MCA TCD and simultaneous EEG | Mean flow velocity increased (25.4-42.8%) gradually 5-10 seconds before GSW, reached maximum value 2-3 sec form onset, followed by fast decrease, lowest levels 30.8-44.0 % with respect to baseline, recorded within 4-6 sec from the end of each absence seizure. Return to baseline with 15-20s. |

| | | | | |
|---|---|---|---|---|
| **NIRS** | | | | |
| [Haginoya *et al.* 2002] | 15 | All types | NIRS | 'Mild' decrease in CBV or no change with absences<br>Increase with GTCS |
| [Buchheim *et al.* 2004] | 3 | IGE | NIRS frontal cortex with simultaneous EEG | Decrease in oxy-haemoglobin, and increase in deoxy-haemoglobin (consistent with decrease in neuronal activity, started several seconds after the EEG defined absence - outlasted event by 20-30 sec. |
| **IN ANIMAL MODLES** | | | | |
| [Nehlig *et al.* 1991] | | Wistar rats | 2-[14C]deoxyglu autorad method | Increase in local CMRGlc in 52 of 59 areas studied |
| [Nehlig *et al.* 1991] | | GAERS | 2-[14C]deoxyglu autorad method + haloperidol or ethosuxamide | Response to Haloperidol – continuous GSW, difference in energy metabolism between GAERS and non-epileptic control rats was abolished<br>Response to ethosuxamide - GSW totally suppressed, rates of energy metabolism remained higher by 31-72% in all structures of epileptic rats compared to non-epileptic controls, suggests 'decreased ictal metabolism.....by the brain in rats with absence epilepsy' |
| | | WAG/Rij | EEG-fMRI (C) 7T | During spike wave seizures increased fMRI signals in focal regions including the perioral somatosensory cortex, occipital cortex spared.<br>During bicuculline-induced generalized tonic-clonic seizures fMRI increases larger and more widespread than during spike-and-wave seizures |
| [Nersesyan *et al.* 2004a] | | WAG/Rij | Laser Doppler flowmetry | Increases in CBF during GTCS; greater that increase during whisker barrel somatosensory cortex; greater than increases during SWD. Normal physiological increase lies between GSW and GTCS. Somatosensory and motor cortex intensely involved in SWD |
| [Tenney *et al.* 2003] | 10 (4.7T) | WAG/Rij | EEG-fMRI | BOLD activation in thalamus ≥4% and all cortical ROIs, no areas of deactivation. |
| [Tenney *et al.* 2004] | | GBL gamma-butyrol-acetone | EEG-fMRI | Predominantly positive BOLD change in the thalamus, sensory and parietal cortices mixed positive and negative, temporal and motor cortices only negative changes |

**Table 1-4 Summary of functional imaging studies of GSW.**

**GBL - gamma-butyrol-acetone, GAERS – Genetic Absence Epilepsy Rats from Strasbourg, MCA – middle cerebral artery, SD – Sprague-Dawley, TCD – transcranial Doppler, WAG/Rij – Wistar albino Glaxo rats from Rijswijk.**

## 1.15 EEG correlated fMRI (EEG-fMRI)

### 1.15.1 Background

EEG is the primary clinical investigation in epilepsy. Spatial resolution of surface EEG is poor and mathematical models are needed to localise putative areas generating EEG phenomena. fMRI on the other hand can visualise directly, in deep as well as superficial structures, correlates of neural activity generating EEG recorded events. Combining EEG with fMRI (EEG-fMRI) therefore is extremely attractive in studying epilepsy.

In 1993 Ives and colleagues recorded EEG in the MRI scanner in humans. They drew attention to the future potential of this technique in the investigation of epilepsy as well as the presence of artefact and safety hazards [Ives *et al.* 1993]. There followed a number of further reports of EEG recorded with fMRI in the study of patients with epilepsy [Huang-Hellinger *et al.* 1995;Seeck *et al.* 1998;Krakow *et al.* 1999;Patel *et al.* 1999]. The following section will discuss the technical issues related to recording EEG in the MRI scanner, and the acquisition of MR images in the presence of EEG recording equipment, and review applications of EEG-fMRI in epilepsy.

### 1.15.2 Practical Considerations

Interactions between the EEG equipment, the subject and the scanner need to be considered and dealt with for safe and adequate recording of both EEG and MRI.

These can be considered in terms of:

(1) Patient safety

(2) EEG artefacts: cardiac and scanner related

(3) Image artefacts caused by the EEG recording equipment.

(1) and (2) occur as a result of magnetic induction. Currents can be induced in circuit formed by the EEG leads, the EEG amplifier and the subject through three main mechanisms: the movement of electrical conducting loops (the EEG electrodes and leads) in the strong static magnetic field of the MR scanner, the changing gradient fields, and the radiofrequency pulses. The relationship between the magnitude of the effect (induced Electromotive Force (EMF)), the loop and magnetic field is defined by the Faraday Law of induction - a current is induced in an electrical conductor moving in a magnetic field, or by Lenzes law for time-varying fields around static loops.

#### 1.15.2.1 Safety

MRI is a relatively safe imaging technique. It does not involve ionising radiation and there are no clearly demonstrable adverse biological effects. The number of scans an individual can have is not limited; this is a great advantage in clinical practice and research where serial scans, or repeated experiments under varying conditions can be performed in any one subject.

The primary hazard of MRI relates to ferromagnetic attraction of the static magnetic field. MRI is contraindicated in patients with medically implanted metal objects in soft tissue (e.g. pacemakers, or aneurysm clips) or metal accidentally embedded through accidents. Motion, heating effects and the induction of electrical current could lead to serious injury or death. Similarly loose metal objects brought into the scanner room can become dangerous projectiles.

The radiofrequency pulses delivered during MRI delivers energy to tissue. The specific absorption ratio (SAR) refers to the amount of energy deposited to tissue by a particular MRI sequence. Scan sequences are limited by this SAR to prevent dangerous heating effects. At higher field strengths, rapidly switching gradient fields can induce peripheral nerve stimulation, that can be uncomfortable or painful [Ehrhardt et al. 1997]. Gradient coils generate acoustic noise during scanning and ear protection is needed for patients and anyone else in the scanner room.

Equipment used in the scanner room, e.g. for physiological monitoring, must be specially designed. Heating in wire loops in contact with patients can cause burns.

Of the three potential sources of induced current, namely (1) movement of a circuit loop in the main static field (2) the effect of rapidly changing gradient field on the circuit loop and (3) the effect of radiofrequency pulses on the circuit loop, (3) was found to be the most important potential source of danger in attaching metal electrodes and lead wires to the scalp in a 1.5T GE scanner (with its specific gradient and RF coil characteristics) [Lemieux *et al.* 1997]. Current-limiting resistors placed as near to the electrode as possible were recommended, the choice of resistor represents a trade-off with the lowest possible value to minimise signal loss that affords safety for a certain set of operational conditions. These are dictated by the size and orientation of conducting loops formed by the electrode leads and patient, the strength and frequency of the RF fields in turn related the MR sequence's energy deposition rate, the head coil, the type of EEG electrode-lead assembly and the resistor's thermal characteristics. Based on theoretical considerations, experiments in relation to the above, and accounting for the worst possible scenario in terms of conducting loops and choice of MR sequence, 10kOhm resistors for each EEG electrode were recommended [Lemieux *et al.* 1997]. It is worth noting that EPI sequences generally have very low energy deposition rates and therefore this resistor

value may be considered conservative in the context of fixed imaging protocols limited to this type of acquisition. Some consider that avoidance of loop formation in the EEG leads, by taking electrodes out through the back of the scanner bore is sufficient to prevent currents that may cause excessive heating, without the need for resistors [Lazeyras *et al.* 2001], however most commercial systems have safety resistors on the electrode set-up. No heating incidents have occurred in over 300 EEG fMRI studies at 1.5 at the National Society for Epilepsy, and none have been reported elsewhere.

1.15.2.2 EEG Quality

The EEG is exquisitely sensitive to electrode or wire motion in the scanner's strong static magnetic field. Intrinsic body motion due to respiration and the heartbeat can result in EEG artefacts [Ives *et al.* 1993;Muri *et al.* 1998].

In addition switching of the imaging gradients and RF signals during image acquisition give rise to significant perturbations in the EEG. These effects and strategies for their reduction can be considered in terms of (1) subject movement, (2) pulse artefact and (3) imaging artefact.

As a general rule the amplitude of each of these artefacts is influenced by the size and degree of movement of conducting loops in the EEG electrode assembly. Practical measures such as minimising the size of these loops, and fixation of leads by foam padding or a vacuum cushion leads to a reduction in these artefacts [Anami *et al.* 2002;Hoffmann *et al.* 2000] and twisting the leads together such that induced currents cancel out [Goldman *et al.* 2000]. Imaging artefacts can be minimised by alternating EEG and image acquisition or using the EEG-triggered approach (see below) although neither of these techniques are optimally efficient in terms of data acquisition and experimental flexibility.

EEG can also suffer drastically from the subjects head motion due to current induction. Motion of a short duration, swallowing, eye movements, blinking, coughing may obscure or mimic EEG events of interest i.e. interictal spikes, however such artefacts are short lived and usually recognisable. Post-processing strategies, visual interpretation and the use of a sensitive motion sensor to identify motion related artefact, can help in limiting the impact of motion [Hill et al. 1995], however ultimately good patient selection, patient compliance, and head immobilisation are the most important considerations.

1.15.2.3 Pulse Artefact

EEG artefacts associated with the cardiac cycle, (the ballistocardiogram) have been recognised since the earliest reports of EEG-fMRI [Ives *et al.* 1993] . Contributing factors are likely to be pulsatile head and attached lead movement with each heart beat [Ives *et al.* 1993] and to a greater extent scalp movement due to a blood flow effect in scalp arteries [Allen *et al.* 1998]. The artefact is manifest as a low amplitude regular discharge on the EEG; its close temporal relationship to the ECG facilitates its identification, but its morphology could be mistaken for interictal epileptiform discharges. Pulse artefact can be minimised by the practical measures outlined above that limit both motion of scalp and electrodes. However considerable individual variability exists and visible pulse artefact on the recorded EEG can potentially interfere with the identification of events mediated by neural activity. Digital subtraction algorithms have been developed for removing pulse artefact from the recorded EEG. These subtract an averaged pulse artefact waveform, based on the timing of the EEG peak, calculated for each electrode during a defined EEG epoch [Allen *et al.* 1998]. A similar method was proposed by Ellingson and colleagues, and validated in recordings of auditory evoked potentials [Ellingson *et al.* 2004]. One

assumption needed for this digital subtraction method is that the artefact is constant throughout the recording; this is not strictly true due to scanner drift and motion effects however synchronisation of EEG sampling with the scanner clock go some way to meet this assumption. Kim and colleagues developed a method that adds wavelet based noise removal to the digital subtraction [Kim *et al.* 2004].

1.15.2.4 Imaging Artefact

During scanning, gradient and radio frequency fields varying in time, give rise to induced currents in the EEG circuit. Gradient switching results in high amplitude, high frequency artefact that obliterate the EEG trace, with components within the physiological EEG frequencies. This is illustrated below

**Figure 1-7 EEG acquired during echo planar MRI.**
**Showing the large gradient artefact that effectively obliterates the EEG. Inset demonstrates that with a large dynamic range this artefact is measurable and after digital subtraction good quality EEG can be obtained.**

Strategies for dealing with this artefact include 1) the experimental design - alternating scan and EEG acquisition, and 2) signal processing methods - subtracting the recorded artefact from the EEG trace.

The experimental design: Three methods for MRI acquisition with EEG recording exist: spike triggered, interleaved or continuous. In spike triggered studies the patient lies in the scanner and EEG is recorded, without scanning. Scanning is only initiated after an event of interest, typically 3 to 5 seconds after an EEG spike i.e. when the peak in BOLD response is expected, and continued for some 5 – 10 seconds – "spike" scans. A similar duration of scans is acquired after a periods of background EEG, "rest" scans. A statistical comparison can then be made between spike and rest scans to identify areas of spike correlated BOLD activations [Krakow *et al.* 1999;Patel *et al.* 1999]. An interleaved EEG/fMRI sequence consists of intermittent scanning during EEG recording; the obliterated sections of EEG can be interpolated [Goldman *et al.* 2000].

Both spike triggered and interleaved methods have limitations. In spike triggered studies the temporal characteristics of fMRI acquisition and the haemodynamic response to IEDs impose constraints on scanning rate and duration of scans. A minimum time interval of the order of 15 s between scans is needed to prevent signal variation due to incomplete T1 signal decay. The maximum duration of each image acquisition (whole brain volume) needs to be less than the expected duration of the BOLD response to ensure separation of responses from events (missed on the obliterated EEG) which may occur during image acquisition, this is difficult to achieve with current imaging sequences and whole brain coverage. Continuous and simultaneous EEG-fMRI acquisition with digital artefact subtraction is now standard in EEG-fMRI studies (see following section)

Signal Processing: Reduction of gradient artefact using methods conceptually similar to that of pulse artefact subtraction have been developed [Allen *et al.* 2000]. Using a timing signal from the scanner an averaged artefact waveform is calculated over a fixed number of epochs and then subtracted from the EEG for each epoch; this is followed by adaptive noise cancellation to reduce any residual artefact. The recording system has a large dynamic range to capture low amplitude EEG and large imaging artefact; sampling is at 5 kHz [Allen *et al.* 2000].

A methodologically simpler post processing technique consists of comparing the frequency spectra of the EEG recorded before and during imaging. Differential or interfering frequencies are subtracted by use of band stop filters in the time domain or by the Fast Fourier transform (FFT) processing. In addition high and low pass filters 0.1 Hz to 40Hz to remove artefact outside the EEG frequency band are included [Hoffmann *et al.* 2000]. The FFT processing leads to higher amplitude spikes at the cost of EEG frequency data. When applied to the unaffected EEG 40% of frequencies in the frequency window were discarded [Hoffmann *et al.* 2000]. Although there was no effect on the EEG to visual inspection this technique would be suboptimal in studies based on frequency analysis of the EEG.

Again the digital artefact subtraction is adversely affected by the non-constant nature of the scanner artefact due to subject motion and jitter in slice acquisition. Strategies other than digital subtraction continue to be developed, for example by the addition of principle component analysis (PCA) [Negishi et al. 2004].

An elegant method in reducing imaging artefact is that proposed by Anami and colleagues - the stepping stone sequence [Anami et al. 2003]. Initially they recorded EEG with a 20000Hz digitisation and 3000Hz low pass filter to characterise the imaging artefact waveform. Peak artefact components corresponded to each gradient component. The EPI sequence was therefore modified to provide a window when the

artefact waveform resided around baseline. EEG sampling every 1000 μs at these time points, when the artefact waveform was at baseline, eliminated most of the imaging artefact. Any residual artefact was subtracted using an averaged artefact waveform.

The advantage of digital subtraction to reduce EEG artefact is that un-interrupted imaging and EEG recording is possible without timing constraints (for example the fMRI sequence) imposed by the combined measurements. Real-time display of good quality EEG offers the possibility of monitoring the EEG (bad electrode contacts, motion-related artefacts, sleep studies etc), the occurrence of EEG events of interest (experimental 'performance'), and the detection of seizure activity in patients with epilepsy.

#### 1.15.2.5 Image Quality

Any conducting medium placed near the subject's head (electrodes, electrode adhesive, gel, leads and current limiting resistors) can lead to image degradation by a number of possible mechanisms: firstly, signal dropout and geometric distortions can occur due to magnetic susceptibility differences and induced eddy currents, particularly in EPI; secondly, SNR degradation due to RF shielding caused by the presence of significant amounts of conducting material forming a shield around the head. In addition, electromagnetic noise emitted by the EEG recording system can lead to degradation of image signal to noise, and therefore all electronics placed in the scanner room must be RF shielded. Signal dropout due to close proximity of electrodes and leads and the scalp can be limited by choosing materials judiciously, studies of such artefact in phantoms has identified the most suitable currently available electrode assemblies [Krakow *et al.* 2000]. Even so, conductive gel can produce large image artefacts, and the minimum amount necessary for acceptable electrode impedance is recommended [Krakow *et al.* 2000].

### 1.15.3 EEG-fMRI Studies - What has been done so far?

In the decade since the first report of recording the EEG in the MRI scanner (Ives 1993) there have been a wealth of EEG-fMRI publications in the study of epilepsy and normal brain rhythms. Initial studies of EEG-fMRI in epilepsy were essentially tests of feasibility, i.e. could a BOLD activation to interictal discharges be detected and if so does this co-localise to known electro-clinical and neuroimaging findings. In a percentage of cases this is shown to be true. In order to have a more useful research and clinical tool, the basis of these changes need to be determined and close spatial localisation to the epileptogenic zone (for surgical resection) demonstrated. In the following discussion the studies have been divided into studies of focal and generalised epilepsy and ictal and interictal studies.

#### 1.15.3.1 Focal Interictal

In 1996, Warach et al first reported imaging findings of inter-ictal epileptiform activity in two patients using spike triggered fMRI. Spike and rest images were compared for percentage signal changes, several bilateral clusters of activation were noted, motion correction and statistical significance testing were not employed [Warach *et al.* 1996]. Although there was no clear correlation between the areas of activation and electroclinical findings making interpretation difficult, they nevertheless demonstrated the potential of the technique.

Krakow et al studied 24 patients using the spike triggered EEG-fMRI [Krakow *et al.* 1999;Krakow *et al.* 2001]. EEG spikes (corroborated with clinical EEG records) were identified on the pulse-artefact corrected EEG with the patient lying in the scanner, and single-volume scanning was initiated approximately 3 seconds post-event. Control scans were acquired following quiescent periods. Twelve of 24 patients showed activations consistent in location to electroclinical data. Seven of the twelve

with structural lesions had activations within or overlapping these lesions. The detection of BOLD activations was weakly dependent on the amplitude of the spikes, likely reflecting the size of neural networks involved, the morphology (recordings with different spike morphologies were less likely to show activations) and the number of events occurring during the experiment, reflecting limitations due to known signal to noise characteristics.

Patel et al studied 20 patients, again using the spike triggered approach [Patel *et al.* 1999]. Of these 20, 12 were suitable for further analysis. They used three methods of analysis, and suggested a 90% sensitivity based on activations seen in 9 out of 10 selected for individual spike analyses. Two representative cases were presented.

Seek et al used spike triggered EEG-fMRI to study a patient with frequent bilateral frontal spikes (L>R) [Seeck *et al.* 1998]. The patient had a very high frequency spike rate and the rest state was achieved by the administration of intravenous clonazepam. Three clusters of activation were described concordant with 3D source reconstruction of scalp EEG and subdural recording over the focus - an area of frontal gliosis, on subsequent resection. More widespread changes were also seen possibly as a result of benzodiazepine administration.

Lazeyras et al [Lazeyras *et al.* 2000] reported on 11 patients with refractory epilepsy, seven of whom showed significant concordant BOLD activations in spike triggered studies.

Jager et al [Jager et al. 2002] studied 10 patients with focal epilepsy and frequent discharges using a spike triggered approach. Significant focal activation was seen in 5 patients, concordant with EEG findings. The findings of signal intensity increases of up to 30% however are not compatible with physiological BOLD signal change and motion effects may have contributed [Lemieux et al. 2003].

Researchers in Montreal have published widely in EEG-fMRI. Benar et al [Benar *et al.* 2002] reported on four patients with focal epilepsy and good BOLD activations. Multiple clusters of activation were reported. No significant relationship was found between the sizes of the HRFs to the EEG spikes. Al Asmi et al have published results from 38 patients [Al Asmi *et al.* 2003]. They undertook 48 studies in 38 patients, 17 (35%) of which were not analysed due to no spikes occurring during scanning. BOLD activations concordant with electro-clinical data was seen in 39% of 31 studies i.e. 12 of 48 (25%) of studies showed BOLD activations. Patients with multi-focal spikes were less likely to show BOLD activation and the inclusion of such patients was felt to have resulted in the low yield [Al Asmi *et al.* 2003]. This data has recently been explored with further analysis. Thalamic involvement has been demonstrated in a greater extent of patients with bilateral synchrony than in those with unilateral spikes [Aghakhani *et al.* 2005]. In those with malformations of cortical development fMRI changes include activations and deactivations both within areas of heterotopia and in adjacent cortex, in addition to distant deactivation in some [Kobayashi *et al.* 2005;Kobayashi *et al.* 2006]. The Montreal group use a series of HRFs peaking from 3-9 seconds in addition to the standard HRF that peaked at 5.4 seconds, to capture temporal variations in the BOLD response. Using these multiple HRFs resulted in a higher percentage of cases with significant fMRI activations, from 45% when using the standard HRF alone, to 62.5% [Bagshaw *et al.* 2004]. The standard HRF was good at detecting positive BOLD responses, but less appropriate for negative BOLD responses, the majority of which were more accurately modelled by an HRF that peaked later than the standard [Bagshaw *et al.* 2004].

Benign childhood epilepsy with centrotemporal spikes (BECTS), is an idiopathic focal epilepsy with age related onset and benign course. The characteristic interictal EEG activity, which in part defines the syndrome, of frequent high amplitude

centrotemporal sharp waves followed by a slow wave, makes this an ideal condition for study with EEG-fMRI. Two studies report concordant fMRI activation in BECTS. A study of 7 patients revealed fMRI activation in the right perisylvian area in 3 patients, 2 patients had no IEDs during the scanning period and two others no fMRI activation despite IEDs [Boor *et al.* 2003]. EEG was recorded continuously but was obliterated during periodic scanning periods that may have obliterated events and hence reduced statistical power of the study. The second study consisted a spike triggered acquisition in a single patient; fMRI activation was seen in left inferior sensorimotor cortex [Archer *et al.* 2003b]. BOLD changes were seen in other brain areas, anterior cingulate, occipital and left frontal shown on the glass brain images. All statistical maps were thresholded at $P<0.001$ uncorrected. It was suggested that the anterior cingulate may also have a role in the generation of the surface recorded discharges [Archer *et al.* 2003b].

1.15.3.2 Generalised Interictal

The study of generalised EEG discharges is directed toward understanding the basis of these discharges and the networks involved. This is in contrast to focal studies where determining concordance with a presumed generator based on other clinical, neurophysiological or imaging data is paramount. The background EEG of idiopathic generalised epilepsy is normal, the characteristic 3Hz spike/wave is clearly identifiable from background, and is unlikely to be mistaken for pulse or movement artefact. Spike wave can occur in prolonged runs of a few seconds or more, that may induce larger BOLD signal changes.

Salek Haddadi et al [Salek-Haddadi *et al.* 2003b] recorded 4 prolonged runs of generalised spike wave activity (30 to 60 seconds each) in a patient with IGE. Thalamic activation and widespread cortical deactivation was found, supporting the

hypotheses of thalamo cortical loops involved in spike wave discharge. The basis of deactivation is yet to be determined and the temporal resolution of fMRI does not allow the temporal relationship in activity between cortex and thalamus to be determined. Again the distinction between a primary or secondary effect is not possible.

Archer et al in a study of 5 patients found posterior cingulate deactivation in association with spike wave discharge [Archer *et al.* 2003a]. All patients were sleep deprived the night prior to the study and one subject omitted their dose of diazepam on the morning of the study to increase the frequency of epileptiform activity. They proposed a putative role for the posterior cingulate in the generation of spike wave discharge. It remains unclear whether these changes are primary or secondary "downstream effects" to spike wave discharge.

Aghakhani et al studied 23 patients with IGE. Thalamic activation in association with spike wave discharge was seen in 12. Eight were excluded due to lack of GSW activity, and one for technical reasons. Data was analysed using five different HRF, the response corresponding to the highest t statistic was retained. Fourteen patients showed significant MRI responses. They had a mean rate of GSW of 46.4/hr during scanning (range 15.7 – 153). Both activation (five patients) and deactivation (nine patients) were seen in the cortex. Twelve patients showed thalamic responses, eight had bilateral activation, two had deactivation and two had both activation and deactivation. A recent group analysis of this data showed group effect of deactivation in association areas in frontal, parietal and posterior cingulate cortex [Gotman *et al.* 2005]. The following table summarises the published EEG-fMRI literature to the end of 2006.

| Study | Subject group - | Number of subjects | EEG system / EEG data recovery | MRI | Analysis software and methods | Main Findings |
|---|---|---|---|---|---|---|
| Ives *et al.* 1993 | Healthy volunteer | 1 | In-house | | n/a | Proof of principle |
| Steinlein *et al.* 1995 | Generalized and photosensitive | 16 patients 9 photosens | In-house /I | 1.5 | Baseline activation comparison | In photosensitive patient increased cortical activation, perioroiandic attenuation, marked occipital and posterior cingulate post stimulus undershoot. |
| Huang-Hellinger *et al.* 1995 | Healthy volunteer | 8 | In house / I | 1.5 | n/a | Safety, EEG and fMRI quality possible from recording in the scanner. Ballistocardiogram degrades EEG. |
| Warach *et al.* 1996 | Focal epilepsy | 2 | Optilink: Neuroscan / ST | 1.5 | Thresholded %change images | Bilateral clusters act in TLE case<br>Anterior cingulate activation in generalized |
| Seeck *et al.* 1998 | Focal epilepsy | 1 | Optilink: neuroscan / ST | 1.5 | Cross correlation analysis | Multiple activations, concordant with 3D EEG source localizations and subdural recordings |
| Symms *et al.* 1999 | Focal epilepsy | 1(4 sessions) | In house / ST | 1.5 | 2 tailed t test | Concordant, reproducible activations |
| Krakow *et al.* 1999 | Focal epilepsy | 10 | In house /ST | 1.5 | 2 tailed t test | Concordant, reproducible activations in 6/10 (60%) |
| Patel *et al.* 1999 | Focal epilepsy | 20 | Optilink: neuroscan / ST | 1.5 | Comparison spike with rest images | 9 of 10 activation corresponding to EEG focus |
| Lazeyras *et al.* 2000 | Focal epilepsy | 11 | Optilink: neuroscn / ST | 1.5 | Cross correlation | Activation confirmed clinical diagnosis in 8,<br>5/6 confirmed with intracranial EEG |
| Baudewig *et al.* 2001 | Focal epilepsy | 1 | Optilink: neuroscn / ST | 1.5 | Cross correlation | Area of signal enhancement concordant with hyper intensity seen on ictal FLAIR images in a<br>patient with non-lesional partial epilepsy |
| Krakow *et al.* 2001 | Symptomatic generalised | 1 | ENR32, schwartzer / I | 2 | Cross correlation | Unilateral insular involvement with Generalised discharges |
| Lemieux *et al.* 2001 | Focal | 24 | In house / ST | 1.5 | 2 tailed t test | 12 (50%) concordant activation, 2 discordant activation |

| | | | | | | |
|---|---|---|---|---|---|---|
| Benar *et al.* 2002 | Focal | 1 | In house / C | 1.5 | GLM | Concordant activation |
| Al Asmi *et al.* 2003 | Focal | 4 | Schwarzer / C | 1.5 | GLM | Concordant activation on 2 of 4, variability in HRF between subjects |
| Archer *et al.* 2003 | Focal | 38 (48 studies) | Schwarzer / ST C | 1.5 | GLM | Activation in 39%, concordant in 'almost all' |
| Boor *et al.* 2003 | IGE | 5 | In house / ST | 3 | 2 tailed t –test | Posterior cingulate deactivation |
| Salek-Haddadi *et al.* 2002 | BCETS | 7 | EMR16, Schwarzer / I | 1.5 | GLM | 3 of 6 activation right perisylvian area |
| Diehl *et al.* 2003 | Focal (ictal) | 1 | In house / C | 1.5 | GLM | Concordant activation with sub-clinical focal seizure |
| Salek-Haddadi *et al.* 2003 | IGE | 1 | In house / C | 1.5 | GLM | Thalamic activation, cortical deactivation |
| Aghakhani *et al.* 2004 | IGE | 15 | Schwarzer / C | 1.5 | GLM | Cortical changes in 15, thalamic in 12 |
| Aghakhani *et al.* 2005 | Focal | 64 | EMR32, Schwartzer / C | 1.5 | GLM | Thalamic activation in 55% with bilateral synchrony and 12.5% unilateral spikes |
| Federico *et al.* 2005 | Focal | 6 | In house / ST | 3 | 2 tailed t test | 4 activation within the lesion, deactivation around the lesion |
| Gotman *et al.* 2005 | IGE | 15 | Group analysis of Aghakhani 2003 | 1.5 | GLM | Thalamic activation, cortical deactivation |
| Kobayashi *et al.* 2005a | Focal | 60 (studies) | Schwartzer / C | 1.5 | GLM | Deactivation in 52 / 60 – distant to presumed epileptogenic zone |
| Kobayashi *et al.* 2005b | Focal | 14 (26 studies) | BrainProducts/ C | 1.5 | GLM | Activation and deactivation within lesion, perilesional and at distant sites |
| Salek-Haddadi *et al.* 2006 | Focal | 63 | In house / C | 1.5 | GLM | Activation in 68% near concordance with site of presumed seizure generation – more likely were good electro-clinical localization, frequent stereotyped spikes |

**Table 1-5 Summary of published EEG-fMRI studies of interictal discharges in epilepsy.**

**C – continuous EEG-fMRI, GLM – general linear model, I – interleaved EEG-fMRI, ST – spike triggered EEG-fMRI**

1.15.3.3 Ictal Studies

Major practical limitations exist in studying ictal activity with fMRI. For robust analysis a seizure needs to be captured in its entirety during a scan session and subject motion is a serious confound in fMRI analysis [Field *et al.* 2000;Hajnal *et al.* 1994]. Nevertheless a number of studies have been carried out in individual patients with frequent partial seizures. Early reports of ictal fMRI used a number of exploratory analysis methods often without concomitant EEG. These include visual inspection of image time series, cross correlation analyses and variance maps; however these lack the robustness of a formal statistical framework.

A total of 5 case reports of fMRI of ictal activity in humans have been published (table 1.5), in addition to a study using fMRI to image the pre-ictal state. These are detailed below.

Jackson et al. [Jackson *et al.* 1994] used single slice fMRI to obtain BOLD sensitive images in a 4-year old child with Rasmussen's encephalitis, and frequent motor seizures involving the right side of the face. Images were obtained every 10 s from a single slice in blocks of 10 minutes. Images were analysed by subtracting baseline images from those acquired during seizures. Analysis was by way of visual inspection. No motion correction or formal statistical analysis was applied. Signal increases were seen in left hemisphere gyri in 5 clinical seizures. A similar change was seen also during a period that was not associated with a clinical seizure, felt to be sub clinical activity. Whilst this case showed the potential of fMRI to detect seizure activity, the contribution of motion effects, caused by the single slice moving in and out of the imaging plane leading to the detected signal changes, remain a possibility.

Detre et al. [Detre *et al.* 1995] described fMRI activation with suspected sub-clinical seizure activity. The patient had right focal motor seizures, affecting face. There was no simultaneous EEG recording during fMRI and there was no clinical evidence of seizure activity. Scans were acquired every 4 seconds for 11 minutes. After standard pre-processing with realignment and spatial smoothing, images were displayed as an animated cine loop and inspected visually. Focal signal-intensity changes were seen in the posterior left frontal lobe, which correlated in both duration and spatial localization with ictal activity on previous outside scanner EEG. The patient went on to intracranial implantation and surgery. A one $cm^2$ area of cortex identified on corticography was resected; pathologic examination revealed chronic gliosis. The resected area, as seen on post operative structural MRI, showed close spatial concordance with the area of fMRI activation. Further cross-correlation analysis was used to examine time-dependent alterations in regional signal intensity that correlated with signal-intensity changes from this cortical seizure focus [Detre *et al.* 1996]. Signal changes in the left ventrolateral thalamus showed a high degree of temporal correlation with signal changes in the left frontal cortical seizure focus, suggesting functional connectivity between the thalamus and the cortical focus.

Krings et al. [Krings *et al.* 2000] reported on a patient with a right frontal glioma. She was experiencing up to five events an hour at the time of the study. A 33-s Jacksonian march involving the left leg with "calf shaking" was imaged with fMRI. One hundred and two scans were acquired with a temporal resolution of 2.2seconds per scan, i.e. around 3 minutes of scanning. An automated image realignment algorithm was used to minimize the effects of interimage motion-related artefacts. For each voxel, the percent change in T2* signal fluctuations was calculated for each time point, against a baseline (mean of MR signal of the first 20 images of a given voxel).

These were colour coded on a thermal scale, overlaid onto an anatomical image and visualized by scrolling through the functional images in an animated loop. Only voxels exhibiting percent signal changes larger than 1.5% from baseline were visualized to minimize random MR signal noise.

Three perilesional areas with signal intensity changes related to seizure activity were seen with signal changes of between 2.2 – 3.5%. The temporal evolution of signal change in each of these regions differed, beginning at 60 seconds before (an increase of up to 2.2% ), 30 seconds before (a decrease of up to 3.5) and at the onset of the seizure (an increase of up to 3.1%). The last region was in the left foot area as determined by previous motor fMRI. It is not clear from the report whether changes of similar percent changes were seen elsewhere in the brain at other times during scanning. A temporal resolution of 2.2 seconds is too slow to allow imaging of the propagation of electrical activity.

Salek-Haddadi et al reported a case of ictal fMRI based on an electrographic seizure recorded on simultaneous continuous EEG [Salek-Haddadi *et al.* 2002]. The simultaneous recording of EEG during fMRI being necessary to fully correlate ictal activity with fMRI measures. A 47 year old man with frequent partial and secondarily generalized seizures was scanned with continuous EEG and fMRI (EEG-fMRI) for 35 minutes (700 scans) as part of a study of interictal epileptiform discharges. An electrographic seizure, with a focus at F7/T3 of approximately 40 seconds occurred early into the study. Images were realigned to the same space and spatially smoothed. fMRI data was analysed according to the general linear model, with the recorded seizure as an effect of interest and the realignment parameters as nuisance covariates. An extensive area of activation was seen extending postero-inferiorly from the left insular grey matter, through the temporal lobe insula, along the superior and middle

temporal gyri to the left fusiform gyrus; anteriorly to the left inferior frontal gyrus; and superiorly up to the left inferior parietal lobule. A smaller cluster was also evident within the grey matter of the ipsilateral cingulate gyrus. The mean signal rise was 2.5% (maximum 5.5%) with a prolonged undershoot. The undershoot most likely represented more prolonged oxygen consumption, following the peak in blood flow response, than is seen in the normal physiological HRF.

#### 1.15.3.4 Reflex Epilepsies

The reflex epilepsies [Dreifuss 1998] although rare provide unique opportunities to study the epileptogenic zone with fMRI, given that ictal events can be induced during fMRI scanning; once appropriate ethical considerations and consent have been addressed.

Morocz et al [Morocz *et al.* 2003] studied a 48 year old woman with music induced complex partial seizures. Scanning took place in blocks with previously identified 'epileptogenic' music alternating with music that was known not to induce seizures. Statistical analysis revealed two patterns of BOLD signal change, one related to the actual triggering of music induced seizures in the left anterior temporal lobe, the right gyrus rectus and ventral frontal lobes, and the other related to exposure to the specific epileptogenic music in the orbitofrontal lobes only. The authors speculate that emotional processing of music in the orbito-frontal areas may have initiated the seizure cascade.

Reading epilepsy is characterized by brief jaw jerks associated with EEG spikes when reading specific texts. Generalized seizures can follow if reading persists in the face of increasing jaw jerks. Archer et al [Archer *et al.* 2003c] studied 2 patients with spike triggered fMRI and reading epilepsy. Subjects read text back projected onto a screen during fMRI scanning. EEG was recorded continuously and scanning was triggered

2.5 seconds after the occurrence of an EEG spike to acquire one brain volume. An identical 'rest' volume was acquired after a twenty second period of no spikes. fMRI of a standard reading task was also acquired using a 30 second block design of reading text versus fixating on a cross hair. Spike versus rest scans were compared by means of an unpaired t test. Reading-related spike activity was seen bilaterally in the inferior precentral gyrus, central sulcus, basal ganglia, and globus pallidus. Signal change of 2.5% in cortex and 1 % basal ganglia was seen in association with jaw jerks and spikes.

Salek-Haddadi et al (submitted) studied 9 patients with reading epilepsy using an MR-compatible system for scalp EEG, submental EMG, left-handed button press, and online audio recording to detect reading-induced orofacial myocloni (ORM). Language and motor (hand/mouth) mapping did not show any abnormalities, compared to normal subjects. One patient had abundant ORM in association with left-frontal spikes occurring on silent reading. In a further five patients, symptoms were only elicitable on reading aloud so events were self-indicated. Induced spikes or jaw jerks were associated with consistent activation patterns within left motor and pre-motor areas in five of these six patients, in Brodmann area (BA) 47 in 2/6, in the striatum (4/6) and thalamus (2/6). Taken together these studies demonstrate the potential cortical and sub-cortical circuitry involved in reading induced seizures [Koepp et al. 2004]. The following table summarizes the published ictal fMRI studies.

| Reference | Clinical data | Seizure detection | Functional MRI | Analysis | Main ictal fMRI finding |
|---|---|---|---|---|---|
| [Jackson *et al.* 1994] | 4 year old male: right sided partial motor seizures of body and face<br>**Aetiology** Rasmussen's encephalitis<br>**MRI** L hemisphere thickened cortex with abnormal signal in grey matter<br>**Routine EEG**<br>Interictal: Widespread slow and occasional L parietal spikes.<br>Ictal: Irregular slow waves over anterior frontotemporal regions preceded by twitching<br>**Sedation** IV Diazepam | Facial movement | **Scanner** 1.5T Siemens SP4000<br>**Sequence** Multi shot FLASH (TE/TR 60/85ms, matrix 62x128. FOV 230mm, flip angle 40° | Visual inspection of subtraction images and time courses extracted from subsequently selected areas | L hemisphere cortical signal increase |
| [Detre *et al.* 1995;Detre *et al.* 1996] | 25 yr old male: R focal motor seizures of face<br>**Aetiology** cryptogenic<br>**MRI** widespread left hemisphere atrophy<br>**Routine EEG** Interictal: Increased theta during wakefulness<br>Ictal: No definite ictal findings | Clinical observation | **Scanner** 1.5T GE signa<br>**Sequence** Single shot GE-EPI (TE/TR 50/4000 ms, 64x64 matrix, FOV 240mm, 16x5 mm slices no gap).<br>**Coverage** whole brain<br>**Time resolution** 4s | Visual inspection of thresholded percentage change images and time courses extracted from selected cluster.<br>Concordant areas with 3-4% signal increases | Area focal signal increase concordant with subsequently identified region on corticography |
| [Krings *et al.* 2000] | 62 yr old female, Jacksonian march L leg<br>**Aetiology** glioblastoma multiforme<br>**MRI** R central space occupying lesion<br>**Routine EEG**<br>Ictal and interictal EEG normal | None | **Scanner** 1.5T Phillips Gyroscan<br>**Sequence** Multishot GE-EPI (TE/TR 35/2200ms. Voxel size 3x5x5mm flip angle 35°<br>**Coverage** Whole brain<br>**Time resolution** 2.2s | Visual inspection of thresholded percentage change images and time courses from selected clusters | 2 perilesional areas of signal increase and one of decrease, starting 60 seconds before the onset of the seizure |

| | | | | | |
|---|---|---|---|---|---|
| [Salek-Haddadi *et al.* 2002] | 47 year old male, left fronto-temporal electrographic seizure.<br>**Aetiology** cryptogenic<br>**MRI** normal<br>**Routine EEG**<br>Interictal: Left fronto-temporal spikes | Concurrent EEG | **Scanner** 1.5 GE signa<br>**Sequence** GE-EPI (TE/TR 40/3000 64x64 matrix, FOV 240, 21x5mm interleaved slices)<br>**Coverage** Whole brain<br>**Time resolution** 3 seconds | SPM99 according to the general linear model.<br>Modelling of ictal event as boxcar with motion parameters as nuisance covariates | L fronto-temporal signal increase with subsequent prolonged undershoot before return to baseline |
| [Morocz *et al.* 2003] | 48 yr old female, music induced complex partial seizures<br>**Aetiology** cryptogenic<br>**MRI** normal<br>**Routine EEG**<br>Interictal: normal<br>Ictal: left temporal theta and high frequency | Self reporting by button press | **Scanner** 1.5T Philips Gyroscan<br>**Sequence**<br>Gradient echo PRESTO<br>TE/TR 35/5000ms, 3.75x3.75 mm, slice thickness 3.5mm flip angle 30° | SPM99, boxcar of seizure inducing music versus non-seizure inducing music; and seizure sessions versus non-seizure sessions | L temporal signal increase during music induced seizures. |

**Table 1-6 Summary of published ictal EEG-fMRI studies.**

1.15.3.5 Animal Studies

The study of ictal activity in humans is limited by the ability to capture seizures during the scan session, and the lack of independent knowledge of the seizure focus. Animal models are commonly used in the development of anti epileptic drugs, neurophysiological and histochemical studies. Well established models include the penicillin and kindled seizure models, and genetic epilepsy models.

Using EEG-fMRI Nersesyan et al [Nersesyan *et al.* 2004b] studied rat models of IGE, the WAG/Rij (a model of human absence seizure with GSW activity) and bicuculline induced tonic clonic seizures. Rats were anaesthetised during all studies. During GSW increased fMRI signal was seen in focal regions including whisker somatosensory cortex, but visual cortex was relatively spared. They drew attention to the similarities of this distribution with electrophysiological studies, where neural activity is most intense in perioral somatosensory cortex, but spare the thalamus [Nersesyan *et al.* 2004a].

Opdam et al [Opdam et al. 2002] developed a sheep model of penicillin induced focal seizures specifically for the purpose of studying ictal activity measured with fMRI and simultaneous intracranial EEG. An intracranial EEG probe was placed on the cortical surface with a penicillin delivery port. EEG acquisition was interleaved with MRI scanning. Data was analysed by means of the variance of the time series of each voxel. These variance maps were overlaid onto the raw images for anatomical localisation. Areas of greatest variance, which included the injection site and the ipsilateral amygdala, were considered to be part of a cortical – sub cortical circuit in seizure propagation. This study demonstrated a proof of principle, the main outcome being the development of a large animal model that could be studied with fMRI. Their observations of BOLD changes were preliminary. More sophisticated analysis, for

instance modelling the EEG with fMRI according to the general linear model, would be more robust to signal to noise issues and may yield clearer spatio-temporal localisations.

#### 1.15.3.6 The Pre-Ictal State

Mathematical analyses of EEG frequency components suggest the presence of a pre-ictal state [Fell et al. 2001]. Federico et al [Federico *et al.* 2005] studied the fMRI signal changes minutes prior to a seizure in three patients with frequent sleep onset seizures. Patients were sleep deprived for one night and scanned the following morning under close supervision, until a seizure occurred. There was no concurrent EEG monitoring. Images were analysed by comparing fMRI signal between two 1 minute blocks - at one minute before seizure onset compared with in one case three, and the other two five minutes before the seizure. The full signal time course of regions of interest based on differences detected in this comparative analysis was examined. Two patients showed BOLD activations ipsilateral to the site of presumed seizure onset, whilst the other had contra-lateral changes. The significant fMRI signal changes were attributed to altered neuronaly driven haemodynamics in the pre-ictal state; although without EEG it is possible that changes in sleep wake cycle that preceded the seizures may have also been captured. Comparing similarly spaced one minute blocks at other points in the time series would have given some indication of the specificity of their findings, and other possible confounding effects in the data. The use of concurrent EEG, and possibly some form of independent motion detection would be advantageous in these studies.

1.15.3.7 Studies of Normal EEG Rhythms

Determining the relationship between haemodynamic correlates of neural activity represented as normal EEG rhythms is important in understanding the neurophysiological basis of these rhythms, in addition to defining resting state changes that may have implication for paradigm based fMRI studies. Alpha rhythm (8-12 Hz), the first EEG phenomena to be described by Hans Berger, and the hallmark of the resting brain state, is the normal EEG rhythm most studied with EEG-fMRI. Laufs et al used the power time course in the alpha frequency band (8-12Hz) convolved with the HRF as a regressor in the analysis of fMRI time series in 10 subjects. They found widespread negative correlation with alpha power bilaterally in frontal and parietal cortices with sparse positive correlation, restricted to two foci in the cingulate gyrus and occipital cortex. No correlation between fMRI signal and power in the 4 to 7 Hz theta band were found[Laufs *et al.* 2003a]. Further analysis of activity fluctuations occurring in correlation with three bands of beta frequencies, beta1: 13-16Hz, beta2:17-23 Hz and beta3: 24-30Hz; found activation at (17-23Hz) of posterior cingulate, the temporal-parietal junction and dorsal medial pre-frontal cortex and at (24-30Hz) activation of anterior cingulate, and retrosplenial, temporal-parietal and pre-frontal deactivation. The results suggest distinct network activity that fluctuates between different modes, in the awake resting state, represented by specific EEG bands.

Goldman et al 2002 studied eleven healthy volunteers in the eyes closed resting state with EEG-fMRI, they present data from 4 subjects [Goldman et al. 2002]. They used an interleaved acquisition of EEG and MR scanning, as EEG was obliterated during scanning by gradient artefact. MR coverage was reduced to six slices to increase the amount of interpretable EEG for each TR period. Using a Fast Fourier Transform, the

power in the alpha band in 2.5s epochs was determined corresponding to each TR for four bipolar posterior EEG channels; this was convolved with an a priori HRF, followed by a voxel wise correlation to produce statistical maps. Using a region of interest analyses alpha power was negatively correlated in the occipital ROIs, positive correlations were seen in the thalamus and insula.

Moosmann et al used simultaneous EEG-fMRI and EEG-NIRS, to study alpha activity. Both interleaved and continuous EEG-fMRI were used, the advantages of continuous being whole brain coverage and greater significance of results in that interpolation of EEG was not necessary. Negative correlations with alpha power were found in the occipital cortex in single subject and group analyses. Positive correlations between alpha power and signal change in the thalamus were seen in some subjects.

The discrepancy between the findings of Laufs et al with fronto-parietal deactivation correlated with alpha power and those of Goldman et al and Moosmann et al of occipital deactivation and thalamic activation are unclear but may be explained as due to the resting state of the subject during the scan session, as determined by the theta to alpha power band ratio [Laufs *et al.* 2006b]. A further possibility is inadvertent/undetected eye opening during the study session, or generation of visual imagery despite the eyes closed state. This needs further investigation.

## 1.16 Conclusion

EEG-fMRI is a remarkable advance allowing the study of the haemodynamic correlates of epileptiform activity, providing localising information of interictal discharges and studying the neural correlates of normal EEG rhythms.

The aims of the work described in this thesis are to investigate the utility of EEG-fMRI in the diagnostic classification of epilepsy, the better localisation of the epileptogenic zone in localisation related epilepsy, and the spatio-temporal networks involved in interictal discharges in localisation related and idiopathic generalised epilepsy; in addition to observing the benefits of improved hardware 1.5 to 3T MRI, and multi channel EEG recording.

# 2 Chapter 2. Common Methods

## 2.1 Introduction

In the following chapter I will provide an account of general methods common to all subsequent chapters. These chapters in turn will contain more detail of methods specific to the studies they describe. I have grouped the methods into four main areas which I will deal with in turn. These are: 1) patient recruitment, 2) EEG acquisition and pre-processing, 3) fMRI acquisition and pre-processing 4) EEG-fMRI analysis.

## 2.2 Ethics and Research Governance

I familiarised myself with the following documents, detailing good research practice, informed consent and data protection issues:

- Research: the Role and Responsibilities of Doctors
- (www.gmc_uk.org/standards/research.htm)
- MRC Ethics Series: Good Research Practice (www.mrc.ac.uk)
- University College London Hospitals (UCLH) documentation on Research Governance, including Committees on the Ethics of Human Research for UCLHNHS Trust and UCL 2002; Consent and Security, A Data Protection Toolkit for Researches at UCLH 2002; and UCLH Research Governance Policies for the Conduct of Research Principle Investigators 2003 - Update 1: Adverse Events in Research, Update 2: Consent Forms for Research, and Update 3 Patient Information Sheets for Research (www.uclh.org).

I obtained ethics approval from the Joint Research Ethics Committee of the National Hospital for Neurology and Neurosurgery to recruit and carry out EEG-fMRI in adult patients with focal and generalised epilepsy (and healthy volunteers, for methods development) on the MRI scanners at the National Society for Epilepsy, Chalfont St Peter, and the Functional Imaging Laboratory, Queen Square, London. The projects were registered with the UCL data protection officer. Data was stored securely on the MRI Unit, National Society for Epilepsy network.

## 2.3 Recruitment

Patients were recruited from the Department of Clinical and Experimental Epilepsy, National Hospital for Neurology and Neurosurgery, Queen Square, London, UK and the National Society for Epilepsy, Chalfont St Peter, Buckinghamshire UK. For the studies on patients with generalised spike wave activity patients were also recruited from the department of Clinical Neurophysiology and Epilepsies, St Thomas' Hospital, London, UK. The following criteria were used in patient recruitment:

- frequent interictal epileptiform discharges on recent clinical EEG
- ability to give informed consent
- ability to tolerate MRI

Patients were identified through EEGs performed at the National Society for Epilepsy, and referrals from consultants working in the Department of Clinical and Experimental Epilepsy, Queen Square and the epilepsy unit at St Thomas Hospital London.

The clinical EEGs of potential patients were reviewed prior to their recruitment. Only those with frequent interictal discharges that were deemed of sufficient clarity to be visible on scanner EEG were included.

At the scan visit the following information was recorded from each patient:

- age
- handedness
- diagnosis (ILAE diagnostic criteria (see appendix 1 and 2)
- seizure types, (along with age of onset, semiology and frequency)
- current medication
- past medical history
- family history
- previous MRI
- previous EEG

## 2.4 Equipment and Experimental Set-up

The following diagrams illustrate the EEG equipment and scanner environment:

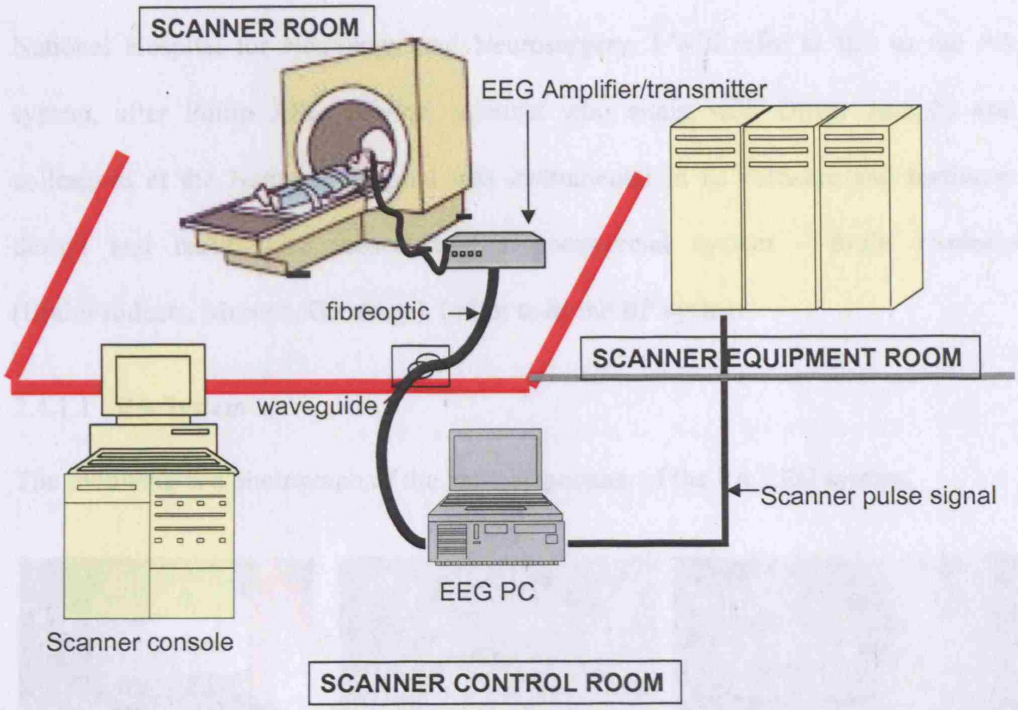


**Figure 2-1 Schematic of EEG-fMRI scanner environment.**

**Within the red lines is the scanner room. The key hardware features that allow concurrent EEG and fMRI are the shielded EEG amplifier/ transmitter and the fibre optic cable that takes the analogue signal out of the shielded room, thus preventing interference with the scanners receiver coil. The subject is visible at all times through a glass screen from the scanner control room. On-line EEG artefact subtraction allowed monitoring of the EEG during scanning.**

### 2.4.1 EEG

EEG during fMRI scanning requires specially designed hardware and software as detailed in the introductory chapter, section 2.8.2. During the course of this research two different EEG systems were used. The first was an in-house system, designed and

built at the medical engineering department of the department of neurophysiology, National Hospital for Neurology and Neurosurgery. I will refer to this as the PA system, after Philip Allen clinical scientist who along with Oliver Josephs and colleagues at the National Hospital was instrumental in its software and hardware design and build. The second was a commercial system - Brain Products (BrainProducts, Munich, Germany), I refer to as the BP system.

2.4.1.1 PA System

The following is a photograph of the key components of the PA EEG system.


**Figure 2-2 Key components of the in-house EEG system.**

**A) The components that reside within the scanner - the head box, shielded battery and main box containing the amplifier and transmitter. B) Gold disk electrodes with in line safety resistor were grouped in chains to minimize loop formation. These were applied in a bi-temporal orientation (FP2, F8, T4, T6, O2; Fp1, F7, T3, T7, O1), with one double electrode set placed in the midline (Cz, Pz) for ground and reference. C) subject in the scanner room prior to scanning, the integrity of the EEG is re-checked before the subject lies back in the scanner.**

The electrodes and a bipolar ECG channel were connected to a sixteen channel head box, and MRI compatible battery powered transmitter, and fibre optic cable to carry the analogue signal out of the scanner room. The fibre optic cable was passed through

a wave guide and connected to a remote receiver, from there to CED1401 (Cambridge Electronic Design) digitiser and Dell PC running Windows NT. All components aside from the CED were made in-house (Medical Engineering, Department of Neurophysiology, NHNN).

In a typical recording session twelve gold disc electrodes were applied according to the 10:20 system, in a bitemporal chain FP2, F8, T4,T6, O2,Fp1,F7,T3,T7,O1 with reference electrode at Pz and ground at Fz. Electrodes were attached and impedances checked outside the scanner room. The scalp was prepared with abrasive cream (Nuprep, SLE diagnostics) and electrodes attached with collodion adhesive (SLE diagnostics). Conductive electrode gel (Dracard, Crown graphic) was then applied under each electrode. The impedance across each electrode pair was measured and necessary additional adjustments made to achieve an impedance of <22kohms (of which 20 kOhm was due to the safety resistors). ECG electrodes were attached over each clavicle (areas found from experience to be optimal for recording ECG in the scanner) connected to a separate bipolar channel. Once in the scanner room with the patient seated on the scanner table, the electrodes were connected to the head box and EEG visualised on the display monitor outside the scanner room. The integrity of the EEG was monitored on line as the patient was moved into the bore of the magnet. A vacuum head cushion (a bag containing polystyrene beads that takes the shape of the head and attached electrodes before air is sucked out creating a temporary but secure mould (S&S x-ray Products, Brooklyn, NY, U.S.A.)) was used to ensure patient comfort and secure electrodes. Electrode cables were brought out of the front of the scanner bore. Cables were pushed under the scanner table mattress to minimise their movement. On-line monitoring of EEG was re-checked prior to scanning.

Scanner EEG was recorded with a sampling rate of 5000Hz, online gradient and pulse artefact subtraction algorithms [Allen *et al.* 2000] were used to monitor EEG during scanning. Subsequently the same algorithms were applied offline to allow visual analyses of the EEG, during MRI artefact subtraction the EEG was down sampled to 200Hz (to reduce the size of the data) as implemented in the software [Allen *et al.* 1998]; [Allen *et al.* 2000]. Analysis of EEG will be dealt with in the following section.

2.4.1.2 BrainProducts System



**Figure 2-3 EEG electrode cap for use with the BrainProducts EEG recording system.**

**Image from (http://www.brainproducts.com/products/)**

This commercially available system uses the artefact reduction methods developed by P Allen et al [Allen *et al.* 1998;Allen *et al.* 2000] is based on similar principles to the PA system in terms of artefact reduction. Each electrode contained a 5 kOhm safety resistor built into the cap. Key differences were an electrode cap with 32 channels arranged in the 10:10 system. Figure 2.2 shows the electrode cap used and figure 2.3 the electrode placement for the 32 channel montage.

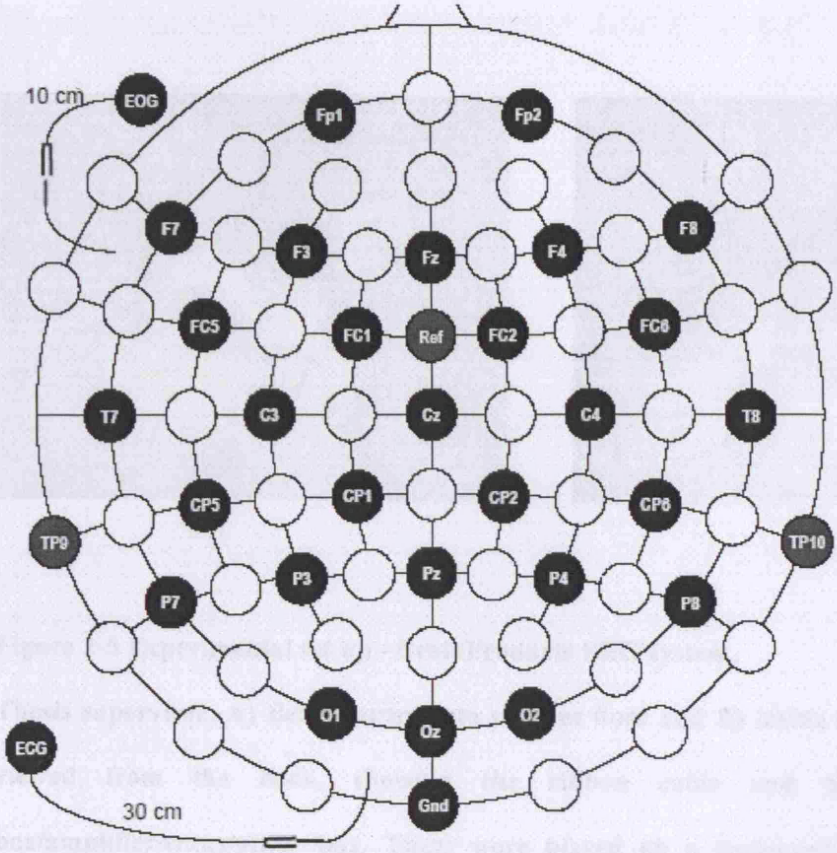


**Figure 2-4 EEG cap electrode locations.**

Key differences in the experimental set up between the PA and BP system included the use of the cap as shown above. Cap electrode cables passed posteriorly and bunched together at the vertex. These were connected to a short flat ribbon cable (around 10cm long) that was brought out of the back of the scanner bore and connected to a combined head box/amplifier/transmitter unit, as shown in figure 2.5.

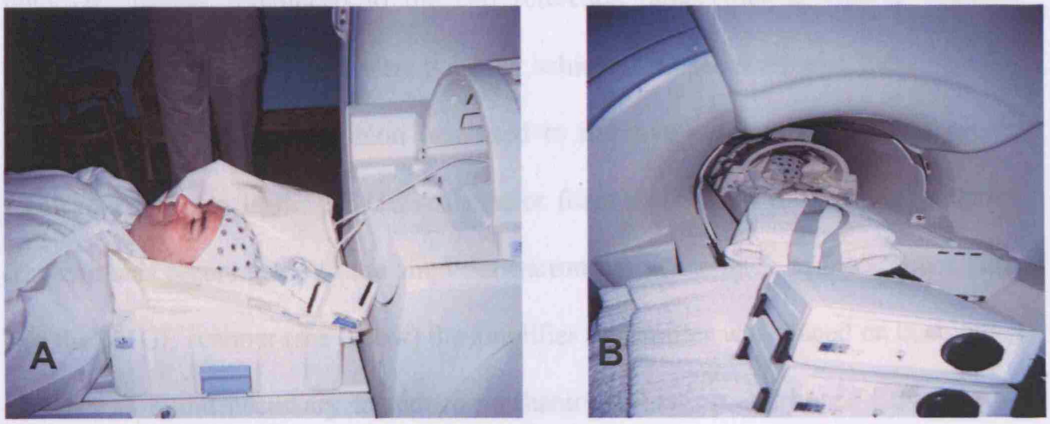


**Figure 2-5 Experimental set up - BrainProducts EEG system.**

**Thesis supervisor, A) Before entry into scanner bore and B) inside the scanner viewed from the back, showing the ribbon cable and battery/head box/amplifier/transmitter box. These were placed on a cushioned surface to minimise vibration during operation of the scanner.**

A fibre optic cable again carried the analogue signal to a remote receiver outside the scanner room; this was connected to a laptop running Windows XP Professional and the Brain Vision Recorder software (BrainProducts, Munich, Germany).

Again the placement of electrode cap and skin preparation, impedance check and baseline EEG recording were undertaken outside the scanner. After securing the cap with chest straps (these were found to be better for patient comfort than an under chin strap by self testing the two arrangements), the skin was prepared by cleaning in each electrode "placement or well" initially with alcohol and then the mildly abrasive electrode contact paste. The wells were then filled with electrode paste (ABRALYT 2000; FMS, Herrsching-Breitbrunn, Germany) using a syringe. A left "EOG" and ECG lead were attached using EEG paste (Elefix, Nihon Kohden, Hamburg,

Germany). Unlike the P Allen system the ECG electrode was built into the cap as unipolar channel referenced to the cap reference rather than a bipolar channel. Impedances of 10 – 20 kOhm were typically achieved at each scalp electrode.

Again the vacuum head cushion was used to improve patient comfort and secure electrodes and cap in the 3T GE scanner, or foam padding in the Siemens scanner. The cap was reconnected to the amplifier/transmitter at the back of the scanner bore. For the 3T GE scanner (see below) the amplifier transmitter was placed on cushioning which was found necessary to reduce mechanical vibration and hence EEG artefact during scanning. The integrity of resting EEG was checked prior to scanning. EEG sampling was again at 5000Hz, with down sampling during artefact correction.

### 2.4.2 EEG Analyses

EEGs were corrected for scanner and pulse artefact using supplied software algorithms. The P.Allen system utilised the scanner "trigger" pulse simultaneously recorded with the EEG to calculate an averaged artefact waveform. MRI artefact correction the BrainProducts system proceeded in two ways, depending on the MRI scanner used (see section 3.5). On the 3T GE scanner EEG acquisition relative to scanning was "free running", i.e. no independent measure of slice or volume acquisition was acquired; the artefact itself was used to generate "markers" of scan start (for each volume), by taking the points of steep gradient takeoff as markers of scanner artefact. On the 3T Siemens allegra the acquisition with the BrainProducts system was synchronised with the scanner clock, this gives a time locked sampling of the artefact waveform. Using the sequence TR, an average waveform can be calculated and subtracted.

During scanner artefact correction the data was down sampled to 200Hz to reduce the size of the data, and low pass filtered (40Hz P.Allen system, 70 Hz BrainProducts system). For pulse artefact subtraction the P.Allen took the peak of the QRS complex to calculate average for subtraction, the BrainProducts system required user definition of the cardiac waveform to generate markers of each peak, which could be reviewed and adjusted across the whole time series.

### 2.4.3 EEG Coding

Artefact subtracted EEGs were reviewed in both referential and bipolar montages. All EEGs were personally coded with one or more colleague (ASH, HL or MW and with assistance from EEG technicians at the National Society for Epilepsy). EEGs were visually inspected and events of interest e.g. spikes, sharp waves or the start and end of runs of generalised discharges were marked and labelled using a mouse driven cursor, and written out in a text file (PA system) or export format (BP system) that contained named events of interest according to scan time. These were imported into the Matlab workspace and saved as variables consisting of vectors of event of onsets that could be used in the analyses of the corresponding fMRI data.

### 2.4.4 MRI

Three scanners were used during the course of this research. Two were at the National Society for Epilepsy 1) a GE 1.5T signa horizon, this was decommissioned in May 2004 2) a GE 3.0T signa EXCITE that replaced the 1.5 T GE Signa horizon, and 3) the third used for 6 sessions on selected patients a 3T Siemens Allegra at the Functional Imaging Laboratory on London (chapter 4).

Standard EPI acquisition sequences were used, in addition to an Arterial Spin Label sequence for perfusion MRI on the Siemens scanner. Specific sequence details are given within each of the following chapters. In addition a volume scan was acquired for coregistration and overlay of functional maps.

The SPM2 software package (www.http.fil.ion.ucl.ac.uk\spm) was used for all pre-processing and voxel based statistical analyses.

#### 2.4.4.1 MRI Reconstruction

All raw images were transferred to a central data store on a SunFire V440 file server with 2 x 1 GHz processors, 4 GB memory and 2 attached RAID[1] arrays with 6.8TB useable disk space (Sun Microsystems).

Using scripts developed in-house the images were reconstructed and the 4D functional images (X,Y,Z,time) converted to create a series of 3D volumes, with one volume (or image) for each time point in the Analyse format (/www.mayo.edu/) - required by SPM. The Analyse format is based on each image in the time series comprising two files (these share the same name but differ in their ending) 1) the image file (image_name.img) containing the numbers that make up the information on the image and 2) the header file (image_name.hdr) containing information about the img file, as fields of text, floating point, integer and other information about the acquisition sequence, parameters and other user defined inputs.

#### 2.4.4.2 MRI Pre-Processing

There is no single standard pre-processing procedure in functional neuroimaging. The order and choice of steps depends on the aims of the study and the acquisition

[1] RAID = Redundant Array of Independent (orig. Inexpensive) Disks meaning that data is stored on say 4 disks and a checksum is written on a 5th disk, so that if ever one disk goes down the data can be recovered automatically using the other 3 disks and the checksum (parity) disk

sequence. Nevertheless there are standard components or steps to pre-processing which are outlined here; more specific details of what was done are given in the individual chapters. These steps are 1) slice timing correction (optional), realignment, spatial normalisation (optional) and spatial smoothing (variable parameters according to study aims).

Each pre-processing step creates 1) a transformation matrix saved in a Matlab file with the same name as each image in the time series (i.e. image_name.mat)[2] and 2) when specified re-writes each image after this transformation images is applied. The re-written images are prefixed with a letter according to the following convention, a – slice timing correction, r – realignment, w – normalization, s – smoothing (e.g. a time series that has been slice timing corrected, realigned, normalized and smoothed are named swraImage_name.hdr and swraImage_name.img).

#### 2.4.4.3 EEG-fMRI Analyses

The following section will outline the methods using the SPM2 software package to analyse fMRI data and correlate with the simultaneously recorded EEG, for spatial mapping of EEG phenomena. The analysis method follows a similar route to the more

---

[2] .mat file

From www.ion.ucl.ac.uk/spm - spm_format.man 2.1 John Ashburner 99/05/16

This simply contains a 4x4 affine transformation matrix in a variable `M'. These files are normally generated by the `realignment' and `coregistration' modules. What these matrixes contain is a mapping from the voxel coordinates (x0,y0,z0) (where the first voxel is at coordinate (1,1,1)), to coordinates in millimeters (x1,y1,z1). By default, the the new coordinate system is derived from the `origin' and `vox' fields of the image header.

x1 = M(1,1)*x0 + M(1,2)*y0 + M(1,3)*z0 + M(1,4)
y1 = M(2,1)*x0 + M(2,2)*y0 + M(2,3)*z0 + M(2,4)
z1 = M(3,1)*x0 + M(3,2)*y0 + M(3,3)*z0 + M(3,4)

Assuming that image1 has a transformation matrix M1, and image2 has a transformation matrix M2, the mapping from image1 to image2 is: M2\M1 (ie. from the coordinate system of image1 into millimeters, followed by a mapping from millimeters into the space of image2).

These `.mat' files allow several realignment or coregistration steps to be combined into a single operation (without the necessity of resampling the images several times). The `.mat' files are also used by the spatial normalisation module.

from spm_format.man 2.1 John Ashburner 99/05/16

commonly used paradigm based - event related and boxcar - fMRI with the exception that the experiment is not 'designed', and spontaneously occurring, unpredictable post hoc identified events or epochs on the simultaneously recorded EEG are correlated with the fMRI data.

SPM uses a mass univariate approach, i.e. it makes an analysis of variance separately at each and every voxel. Parametric statistical models are assumed at each voxel, using the General Linear Model to describe the data in terms of experimental (i.e. the EEG events of interest) and confounding (e.g. subject motion, physiological noise and low frequency drifts). Classical statistical inference is used to test hypotheses that are expressed in terms of GLM parameters. These parameters are visualised using an image made up of voxels of thresholded statistical values - the Statistical Parametric Map SPM[t], SPM[Z], SPM[F].

The statistical correlation is applied at each and every voxel (typically several tens of thousands). A correction for multiple comparisons is therefore needed; without which false positive errors would be at unacceptable levels. SPM uses a correction based on Gaussian Random Field theory (referred to as a family wise error correction or FWE); an alternative would be a Bonferroni correction however this is too stringent for fMRI given that there is temporal and spatial correlation between the voxel time series.

In summary (adapted from M.Brett, www.mrc-cbu.cam.ac.uk/Imaging/Common/spmstats) SPM:

- does an analysis of variance separately at each voxel;
- makes t statistics from the results of this analysis, for each voxel;
- works out a Z score equivalent for the t statistic;
- shows you an image of the t statistics

- allows a correction for multiple comparisons to the significance of the t statistics

This statistical analysis can be broken down into the following steps,

- setting up the design matrix i.e. user defined regressors and other confounds, from the simultaneously recorded EEG and motion parameters generated by the image realignment step; and configuring this to the data
- estimating the statistics at each voxel
- Interrogating the statistics.

The "standard" analysis used in this thesis is described below according to prompts and entries in the SPM graphical user interface (GUI), although a number of analyses were run using a batch script.

The design matrix is made up of the events if interest derived from the simultaneously recorded EEG, convolved with a canonical haemodynamic response function and its' temporal and/or dispersion derivative. In addition events of no interest were also included to better model the noise in the data. In this thesis we used the six realignment parameters, and their first order expansion to cover the non-linear effects of motion [Lund *et al.* 2005], to give a total of 24 motion regressors. This model was configured with the fMRI data and a high pass filter 128 seconds to remove low frequency drifts, and an autocorrelation AR(1) applied to account for correlation between successive scans or data points.

Statistical results were displayed as thresholded maps, typically an F-test to identify regions of significant activations, with a family wise error correction for multiple comparisons.

The direction of the detected signal change was identified using t-tests and plots of the peristimulus time histogram. Group analyses were undertaken which are discussed further in the relevant chapters.

All analysis involved whole brain coverage, no global normalisation was applied, no masking was used, and no post-hoc statistical analyses were undertaken on region of interest.

# 3 Chapter 3. EEG-fMRI of Generalised Spike Wave

## 3.1 Abstract

Thirty patients with idiopathic generalised epilepsy (IGE) and sixteen with secondary generalised epilepsy (SGE) were studied with EEG-fMRI. Thirty six patients had GSW during scanning (25 IGE, 11 SGE). Twenty five patients (15 IGE, 10 SGE) had significant GSW related Blood oxygen level (BOLD) signal changes. This was seen in the thalamus in 16 patients (7 (43%) IGE; 9 (90%) SGE) and symmetrically in frontal cortex in 23 (13 (86%) IGE, 10 (90%) SGE) and parietal cortex 20 patients (10 (67%) IGE, 10 (90%) SGE) and posterior cingulate cortex / precuneus in 20 patients (10 (67%) IGE, 10 (90%) SGE). The higher number of BOLD changes in SGE was likely due to higher experimental efficiency - the median number of GSW epochs per session being 8 in IGE and 45 in SGE.

At the single subject level thalamic BOLD changes were predominantly positive and cortical changes predominantly negative. A group analysis showed: in IGE a negative BOLD response in frontal, parietal and posterior cingulate cortex and a small positive response in the thalamus and in SGE a thalamic and mesial frontal activation. The observed changes reflect the known role of the thalamus in the generation of GSW, the cortical changes reflected alteration of activity in association cortex, or resting state brain activity that is consistent with the clinical manifestation of absence seizures. SPMs did not distinguish between distinct syndromic groups.

## 3.2 Introduction and Aims

EEG-fMRI was used to identify the haemodynamic correlates of GSW in IGE and SGE and to determine whether differences in activation patterns between IGE, its sub syndromes Juvenile myoclonic epilepsy (JME), Juvenile absence epilepsy (JAE), childhood absence epilepsy (CAE) and epilepsy with generalised tonic clonic seizures only (EGTCS) and SGE could be used as clinical or pathophysiological markers.

## 3.3 Materials and Methods

### 3.3.1 Patients

Forty six patients, 30 with IGE and 16 with SGE, and frequent GSW discharges on recent interictal EEG were recruited from the epilepsy clinics at the National Hospital for Neurology and Neurosurgery, London, the National Society for Epilepsy, Chalfont St Peter and St Thomas' Hospital, London.

Patients were grouped according to the ILAE 1989 classification scheme [ILAE 1989] (see Appendix 1). These were IGE and its sub classifications - juvenile myoclonic epilepsy (JME), juvenile absence epilepsy (JAE), childhood absence epilepsy (CAE), and epilepsy with generalized tonic clonic seizures only (EGTCS) - and secondary generalized epilepsy (SGE). The latter group had one or more of the following: atypical absences, an abnormal background EEG, and irregular GSW. In one patient there was electrographic evidence of a unilateral frontal focus (patient 43). All patients had normal structural MRI.

Thirty five minutes of simultaneous EEG-fMRI were acquired for each subject. In 13 patients two successive 35 minute scan sessions at the same sitting were acquired, giving 59 sessions in 46 patients.

### 3.3.2 EEG acquisition

Ten channels of EEG referenced to Pz and two channels of precordial ECG were recorded using in house recording equipment [Allen *et al.* 1998;Allen *et al.* 2000]. See Common Methods, section 2.4.1.1.

### 3.3.3 MRI acquisition

A 1.5T GE Horizon echospeed MRI scanner (Milwaukee, Wisc.) was used to acquire 700 BOLD sensitive echo-planar images (EPI) images (TE/TR 40/3000, 21 interleaved axial slices (acquired parallel to the intercommissural line), slice thickness 5 mm, FOV 24 x 24 cm, 64x64 matrix) over a 35 minute session with continuous, simultaneous EEG. An additional four images were acquired at the start of each session and discarded to allow for T1 equilibration effects. Foam padding or a vacuum head cushion was used to help secure the EEG leads, minimize motion, and improve patient comfort.

### 3.3.4 Data Analyses

#### 3.3.4.1 Single Subject Analysis

Images were 1) slice-time corrected to the middle slice, 2) spatially realigned to the first scan of the series, 3) spatially normalized to the Montreal Neurological Institute

(MNI) template supplied by SPM (the ICBM152), and 4) spatially smoothed using an isotropic Gaussian kernel (10 mm full width at half maximum).

The artefact corrected EEG was reviewed off-line and the onset and offset of GSW epochs identified with respect to the fMRI time series (see sections 2.4.2 and 2.4.3) These were used to construct a boxcar model of the active (GSW) versus rest (background) EEG state. This model was convolved with a canonical haemodynamic response function (HRF, (peak at 6 seconds relative to onset, delay of undershoot 16 seconds and length of kernel 32 seconds)), its time and dispersion derivatives, to form regressors testing for GSW-related BOLD changes.

The temporal derivative (TD) and dispersion derivative (DD) were used to accommodate variations in the canonical HRF [Handwerker et al. 2004] [Henson *et al.* 2002].

The spatial realignment parameters and their first order expansion were included as effects of no interest to model the linear and non-linear effects of motion [Friston *et al.* 1996;Lund *et al.* 2005].

Data and design matrices were high pass filtered at 128 seconds cut-off. An auto regression (AR(1)) model was used to estimate the intrinsic autocorrelation of the data [Friston et al. 2000]. No global scaling or normalization was performed, as this could introduce artifactual activation or deactivations.

An F-contrast was used to assess the variance at each voxel explained by GSW. The resulting SPMs were thresholded at $p<0.05$ using the correction for multiple comparisons based on Gaussian random field theory [Friston *et al.* 1991].

The contrast estimate pertaining to the canonical HRF [Henson *et al.* 2002] was used to ascertain the direction of the BOLD response at the global maxima and at the local

maxima of frontal, posterior superior parietal, and posterior cingulate cortices (see results table 3.2).

3.3.4.2 Group Analysis

A random effects group analysis was performed on each of the groups IGE, and SGE using the following two stage procedure to infer the average pattern at a population level [Friston et al. 1999]. This was done by taking the parameter estimates of GSW associated changes from the single-subject analyses to a 'second level' random effects group analysis using a one-way analysis of variance (after Henson and Penny ftp://ftp.fil.ion.ucl.ac.uk/spm/data/rfx-multiple/rfx-multiple.htm).

For a random effects group analysis balanced designs are required between sessions. If not then the assumption of homoscendacity is violated, i.e. errors may not be identical or independent. Nevertheless inferential statistics and the general linear model are robust to such violations, particularly if the number of events falls within one magnitude of each other [Karl Friston, personnal communication]. Friston et al showed this in functional imaging studies where this is satisfied [Friston et al. 2005]. In order to meet this criteria we selected patient sessions in which the number of GSW events fell within one order of magnitude of each other (see table 3.2, sessions marked *), giving 18 IGE cases and 10 SGE cases for the group analyses. Group analysis were also undertaken for the sub-groups JME and JAE although the smaller numbers, 7 and 9 respectively would make valid inferences more difficult [Desmond and Glover 2002].

The random effects group analysis was implemented by a one way analysis of variance (ANOVA) using SPM2. No grand mean scaling was applied. A non-sphericity correction was applied over the number of subjects. In order to take more than contrast per subject to the second level, i.e. the HRF and its two partial

derivatives, account was made for correlation and unequal variance between these contrasts [Glaser et al. 2001].

An F contrast at this second (i.e. the between subject) level was used to test for the variance explained by GSW across the groups for IGE and SGE.

## 3.4 Results

### 3.4.1 Clinical Features

See table 3.1 for the patients' clinical features. Good quality EEG was obtained following pulse and gradient artefact subtraction, allowing identification of epileptiform discharges (for examples see figure 3.1).

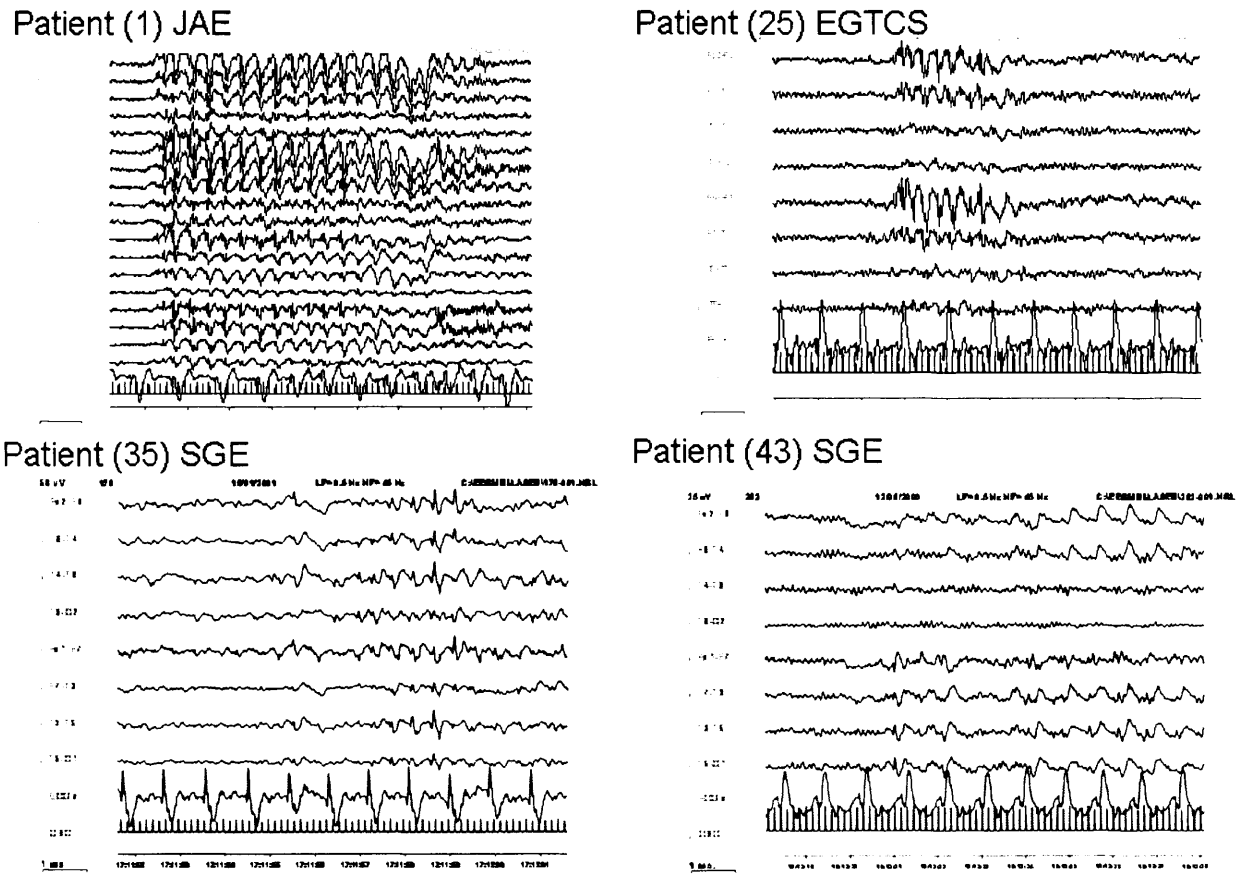


**Figure 3-1 GSW in artefact corrected EEG from 1.5T BOLD fMRI sessions.**

**4 representative subjects are shown.**

**JAE – juvenile absence epilepsy, EGTCS – epilepsy with generalised tonic clonic seizures only, SGE – secondarily generalized epilepsy, patient #43, SGE with evidence of L frontal epileptogenicity. ECG electrocardiogram, OSC scanner slice pulse used for EEG artefact correction and EEG-fMRI synchronization (7/second).**

| | ID no | Age (yrs) | Seizure type frequency (age onset/yrs) | Antiepileptic Drugs | Frequency of GSW (Hz) |
|---|---|---|---|---|---|
| JAE | | | | | |
| | 1 | 19 | Abs daily (11) GTCS 5/yr (15) | LEV, LTG | 2.5–3 |
| | 2* | 24 | Abs 15 d (10) GTCS 4/yr (13) | CBZ, ESM, LTG, TPM | 3 |
| | 3* | 18 | Abs (10) GTCS 2/mth (14) | LTG | 3-4 |
| | 4 | 43 | Abs 2/wk (9) GTCS 5/yr (9) | CBZ, LTG | 3 |
| | 5* | 43 | Abs daily (8) GTCS 4 /yr (13) | CLB, LTG, VPA | 3 |
| | 6* | 22 | Abs 4-5 wk (9) GTCS 6/yr (16) | LTG, VPA | 4 |
| | 7 | 22 | Abs 2-3 day (8) GTCS 2/mth (19) | ESM, LTG, TPM | 3-4 |
| | 8 | 54 | Abs 1/mth (19) GTCS none for 10yrs (19) | CBZ, PHT, PB, VPA | 3-4 |
| | 9* | 18 | Abs weekly (15) | Nil | 2.5-3 |
| | 10 | 19 | Abs daily (7) GTCS <1 yr (7) | CBZ, VPA | 2.5-3 |
| | 11 | 33 | Abs daily (teens) | LTG, VPA | 3 |
| | 12 † | 33 | Abs 10/day (10) GTCS 5/yr (14) | LTG, VPA | 3 |
| | 13 † | 37 | Abs 1/mth (4) GTCS 2/yr (11) | LTG, OXC, PB, VPA | 3 |
| | 14*† | 36 | Abs weekly (3) GTCS 3 in total (6) | LTG | 3 |
| Age range: 18-54 yrs, mean 30, median 28.5. Sex ratio M: F - 4:3. | | | | | |
| JME | | | | | |
| | 15 | 55 | Abs resolved (13) GTCS 1-2/yr (13) MJ 2-3/wk (teens) | CLB, LEV, LTG | 3 |
| | 16‡ | 20 | Abs daily (13) GTCS 2/mth (13) MJ daily (18), | CLN, TPM, VPA | 2-3 |
| | 17* | 59 | GTCS 1/wk (5) MJ several/wk(10) | CBZ, PB, VPA | 4 |
| | 18 | 20 | Abs 3/d (<10) GTCS 1/mth (13) MJ resolved (14) | LEV | 3 |
| | 19 | 41 | Abs nil GTCS 1/mth (15) MJ resolved (15) | CLB, LTG, PHT, VPA | 3 |
| | 20* | 18 | Abs 2-3/wk (15) GTCS<1/yr(16) MJ daily(15) | LEV, LMT, VPA | 4-5 |
| | 21* | 37 | Abs 10 d (7) GTCS 2/yr (12) MJ (teens), | CLB, GBP, VPA | 2-3 |
| | 22 | 18 | Abs nil GTCS 1/yr (14) MJ resolved (14) | VPA | 3 |
| | 23*† | 20 | Abs 3 wk (19), GTCS 1/yr (18) MJ daily (18), | CLN, LTG | 2-3 |
| Age range 18-59 yrs, mean 34, median 33. M:F - 5:4 | | | | | |
| EGTCS | | | | | |
| | 24 | 33 | GTCS free 2 yrs (11) | LTG | 4 |
| | 25* | 34 | GTCS 3 in total (12) | CBZ | 3 |
| | 26 | 32 | GTCS 4 in total (22) | CBZ, CLN | 3-4 |
| | 27† | 21 | GTCS 1/mth (1) | CLB, LTG, VPA | 2.5 - 3 |
| | 28† | 48 | GTCS 1<10yrs (7) | VPA | 2-3 |
| | 29*† | 24 | GTCS 1 in total | Nil | 2-3 |
| Age range 21-48, mean 32, median 32. M:F 2:1 | | | | | |
| CAE | | | | | |
| | 30 | 23 | Abs 10/d (4) GTCS 1/mth (12) | LEV | 3 |
| | 31‡ | 26 | Abs 15/d (8) | Nil | 3 |
| | 32‡ | 53 | Abs several/day (10) | DZP | 4 |
| Age range 26-53 yrs, mean 34, median 26. M:F 8:5 | | | | | |

| | | | | | |
|---|---|---|---|---|---|
| SGE | | | | | |
| | 33 | 29 | Abs daily (20) GTCS <1 yr (23) | LTG, VPA | 2-3 abn bkgd |
| | 34 | 29 | Abs 3/d (16) GTCS <1 yr (14) | ACE, CBZ, VPA | 1.5-2 |
| | 35 | 21 | Abs daily (10) GTCS <1 yr (10) tonic1/wk (10) | ACE, CBZ, CLN | 2-3 |
| | 36 | 19 | Abs 6-8/ d ( 7) GTCS 6/yr (7) | LEV, LTG, TGB | 3 abn bkgd |
| | 37 | 22 | Abs 2/wk (8) GTCS resolved (9) MJ 2/wk | CLN, LTG, OXC, VPA | 2-3 |
| | 38 | 26 | GTCS 2-3/yr (14) drop attacks 6/yr (26) | LTG, TPM | 2-3 |
| | 39 | 26 | Abs 2-3/wk (9) GTCS <1/yr (12) atonic sz 1/wk (10) | CLN, LTG, OXC | 2 abn bkgd |
| | 40 | 74 | Abs daily (teens) GTCS 2/mth(14) | PHT, TPM | 2.5-3 |
| | 41 | 22 | GTCS 6/mth (11) | CBZ, TPM | 3 |
| | 42 | 38 | Abs 10-20/d (7) GTCS 0-4/mth (11) | CBZ, LEV | 2-3 |
| | 43 | 21 | Abs 8/mth (13) GTCS 4/yr (18) | CBZ, LEV, VPA | 2 L>R, max F3 |
| | 44† | 40 | Abs 1-2/mth (11) GTCS 2/yr, (11) | CBZ, PHT, TGB | 3 |
| | 45† | 19 | GTCS 2/mth (2) | LTG, TPM | 2-3 abn bkgd |
| | 46*† | 47 | Abs 15/d (2) GTCS 3/mth (4) | PHT | 3-4 |
| Age range 19-74 yrs, mean 31, median 26. M:F 4:3 | | | | | |

**Table 3-1 Clinical details of patients with GSW studied with EEG-fMRI at 1.5T. This shows ILAE diagnostic categories, showing seizure type and frequency, age at onset, medication at time of study and frequency of GSW. Structural MRI in all patients was normal. The sub classification of IGE is often a source of debate, with a degree of overlap between syndromes, and some would therefore argue they represent a continuum rather than specific disease entities. For example patient #10, whilst the age of onset 7 years might suggest CAE, we prefer to classify as JAE on the basis of GTCS occurring with the onset of epilepsy, similarly patient #32 whilst the age of onset of 10 might suggest JAE has never had a GTCS, this would be unusual for JAE, hence we include them in CAE [Panayiotopoulos 2002a]. Nevertheless within the population studied distinct syndromes (or distinct ends of a spectrum) were present in most cases. JAE, Juvenile absence epilepsy; JME, Juvenile Myoclonic Epilepsy; EGTCS, idiopathic generalized epilepsy with generalized tonic clonic seizures only; SGE. secondary generalized epilepsy; abs, absence seizures; MJ, myoclonic jerks; GTCS, generalized tonic clonic seizures; ACE, actetazolamide; CBZ,**

**carbamazepine; CLB, clobazam; CLN, clonazepam; DZP, diazepam; ESM, ethosuxamide; GBP, gabapentin; LEV, leviteracetam; LTG, lamotrigine; OXC, oxcarbazapine; PB, phenobarbitone; PHT, phenytoin; TGB, tiagabine; TPM, topiramate; VPA, sodium valproate; M, male; F, female; abn, abnormal; bkgd, background; F3, left frontal electrode; d, day; wk, week; mth, month; yr, year; sz, seizure. * Patients studied in two successive sessions, † patients in whom no GSW was seen during scanning, ‡ patients excluded due to correlated motion.**

### 3.4.2 Single Subject Results

In 16 sessions (10 patients, marked † in table 1) no GSW was seen; these sessions were not considered further. Three further patients were excluded due to suspected correlation between head motion and GSW events (marked ‡ in table 1) (one of these (patient 31) was restudied at 3T, and on the basis of similar findings of this repeat analysis (see chapter 4) this exclusion was over conservative, however has little effect on the overall results and conclusions, and the patient would not have been entered into the group analysis because of the large number of GSW events (that would unbalance the design). The rate of occurrence of GSW events in the remaining 40 sessions (in 33 patients) varied between 1 and 189 per 35-minute scan session (mean 28, median 11). Table 3.2 details the areas of fMRI and direction of signal change.

Significant BOLD signal changes were seen in 25 patients, (29 sessions, 73% of sessions containing GSW): in thalamus (15 patients), frontal cortex (FC) (23 patients), posterior parietal cortex (PPC) (19 patients) and PCC / precuneus (20 patients), with one or typically more of these areas involved in each case (table 2). In addition to these areas, BOLD change was also seen, in some patients in basal ganglia, cerebellum, brainstem, the sagittal sinus, or all lobes. The following table details the single subject GSW related BOLD changes.

| Diagnostic category | Id No. | No. of GSW Events | Duration of GSW events. Median (range) (seconds) | Regions of significant fMRI signal change | | | | |
|---|---|---|---|---|---|---|---|---|
| | | | | Thalamus | Frontal | Parietal | Posterior cingulate / precuneus | Other |
| JAE | 1* | 9 | 2.1 (1.6-8.1) | - | ↑ B (L m) | ↓ B | ↑B | ↑ ss, cereb, temp |
| | 2a | 3 | 7.3 (4.4-7.7) | - | ↑ B (L m) | ↓ B | - | ↑ L temp |
| | 2b | 1 | 5.9 | - | ↑ R m | - | - | ↑ B temp |
| | 3* | 7 | 1.3 (0.9-3.3) | ↓ R | ↕ B | - | - | ↕ B head caudate (R m) |
| | 4* | 4 | 2.6 (1.0-3.0) | - | - | - | - | - |
| | 5a | 18 | 0.6 (0.4-3.6) | ↑ B | ↑ B | - | ↑ B | ↑ ss, cereb (R m), B occ |
| | 5b* | 16 | 0.7 (0.4-1.7) | - | - | - | ↕ B | ↑ cereb (L m), B occ |
| | 6a | 4 | 1.9 (1.3-3.0) | - | - | - | - | - |
| | 6b* | 17 | 1.3 (0.4-4.3) | - | - | - | - | ↓ L inf occ m |
| | 7 | 2 | 4.3 (3.4-5.3) | ↑ B | ↑ B (L m) | ↑ R | - | ↑ ss |
| | 8* | 8 | 2.1 (1.0-5.3) | - | ↓ B (L m) | ↓ B. | ↓ B | - |
| | 9a* | 8 | 1.9 (0.7-3.6) | - | ↕ B | ↓ B | ↓ B | ↑ ss m |
| | 9b | 2 | 0.6 (0.6-0.7) | - | - | - | - | - |
| | 10* | 11 | 1.3 (0.9-2.6) | - | - | - | - | - |
| | 11 | 189 | 1.6 (0.3-73.9) | ↕ B | ↓ B (L m) | ↓ B | ↓ B | ↓ ss, cereb |
| JME | 15* | 17 | 0.7 (0.4-5.3) | - | - | - | - | ↓ occ m,↕ R BS |
| | 17a* | 7 | 1.4 (1.1-1.6) | - | - | - | - | - |
| | 17b | 1 | 1.4 | - | - | - | - | - |
| | 18* | 25 | 1.3 (0.4-3.4) | ↑ B (L m) | ↑ B | - | ↑ B | ↑ occ, B temp |
| | 19* | 4 | 0.6 (0.6-0.9) | - | - | - | - | - |
| | 20* | 7 | 1.6 (0.7-1.7) | - | - | - | - | - |
| | 21a | 60 | 1.4 (0.4-8.4) | ↓ B (L m) | ↓ B | ↓ B | ↓ B | ↓ BS |
| | 21b | 89 | 1.0 (0.3-5.4) | ↑ B | ↓ B | ↓ R | ↓ B | ↑ BS m |
| | 22* | 11 | 9 (2.4-15.7) | - | ↓ B | ↓ B (L m) | ↓ B | - |

| | | | | | | | | |
|---|---|---|---|---|---|---|---|---|
| IGE-GTCS | 24* | 6 | 1.1 (0.9-1.7) | - | - | - | - | - |
| | 25a | 33 | 1.6 (0.6-3.9) | - | ↓ B | ↓ B (L m) | ↓ B | - |
| | 25b* | 24 | 1.4 (0.6-4.1) | - | ↓ B | ↓ B (L m) | - | - |
| | 26* | 5 | 1.1 (0.7-1.4) | - | - | - | - | - |
| CAE | 32* | 17 | 2.1 | ↑ B | ↓ B | ↓ B | ↓ B | ↑ cereb m |
| SGE | 33* | 25 | 1.1 (0.3-2.0) | ↕ R | ↓ B | ↓ B (R m) | ↓ B | - |
| | 34* | 55 | 13.7 (1.0-82.4) | ↑ B | ↓ B | ↕ B | ↓ B (R m) | ↓ all lobes, cereb, BS, BG |
| | 35* | 32 | 10.9 (1.3-82.4) | ↓ B | ↓ B (L m) | ↓ B | ↓ B | ↓ ss, cereb., temp, BS |
| | 36* | 9 | 7.1 (5.0-12.6) | - | ↑ B (R m) | ↓ B | ↓ B | ↑ ss, ↓ BS |
| | 37* | 78 | 2.6 (0.6-15.0) | ↕ B | ↑ B | - | ↑ B (L m) | ↕ occ |
| | 38* | 43 | 5.7 (0.7-12.3) | ↑ B (R m) | ↑ B | ↑ B | ↑ B | ↑ ss, cereb, ↕ BS |
| | 39* | 68 | 6.6 (0.4-39) | ↑ B (R m) | ↑ B | ↑ B | ↑ B | ↑ cereb, temp, BS, BG |
| | 40 | 3 | 6.9 (1.9-8.6) | - | - | - | - | - |
| | 41* | 46 | 0.7 (0.3-12.9) | ↕ B | ↓ B midline (L m) | ↓ B | ↓ B | ↓ cereb, ↑ BS, temp, occ |
| | 42* | 57 | 4.1 (1.1-24.6) | - | ↓ B | ↓ B (R m) | ↓ B | ↓ temp |
| | 43* | 46 | 5.2 (1.1-29.3) | ↑ L | ↓ B + area of L ↑ | ↓ B (R m) | ↓ B | ↓ BS |

**Table 3-2 Single subject GSW associated BOLD responses at 1.5T.**

**Table shows the number and duration of GSW epochs, and regions of significant BOLD signal change labelled in accordance with direction of HRF loading. All SPMs corrected for multiple comparisons using random field theory ($p<0.05$). Id no – identification number, corresponds to that in table 1. (a) and (b) are given for those studied with two sessions. ↑ - increase, ↓ - decrease, ↕ - biphasic. B - bilateral, L - left, R - right, m - global maxima, BG - basal ganglia, BS - brainstem, BG - basal ganglia, cereb – cerebellum, temp - temporal lobes, occ - occipital lobes, ss - sagittal sinus (draining vein). *indicates sessions included in second level group analysis.**

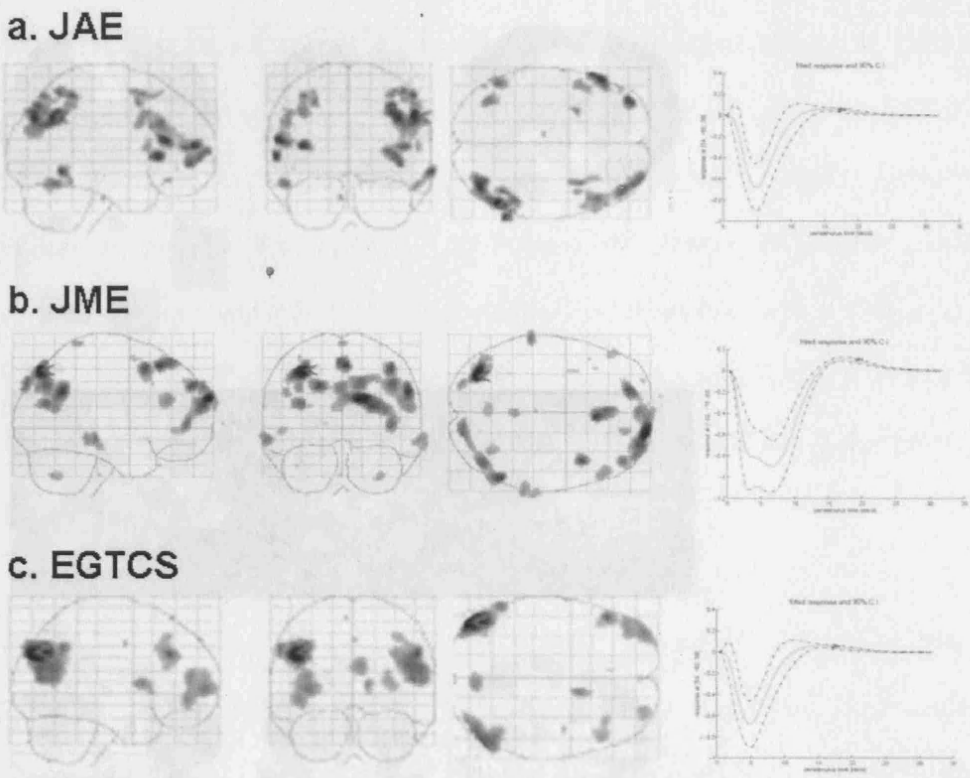


**Figure 3-2 Single subject GSW associated BOLD changes at 1.5T in IGE.**

**Mean intensity projections SPM[F] from single subject SPM analyses in 3 patients with IGE. This shows cortical signal change with GSW involving symmetrical bi-frontal, bi-parietal, posterior cingulate/precuneus in three patients with different diagnostic syndromes a) patient #10, JAE, b) patient #22 JME c) patient #25 IGE-GTCS. The fitted response for each global maximum (marked with red arrow on the SPM) is plotted on the right indicating the peristimulus time course and percent signal change. (SPMs corrected $p < 0.05$).**

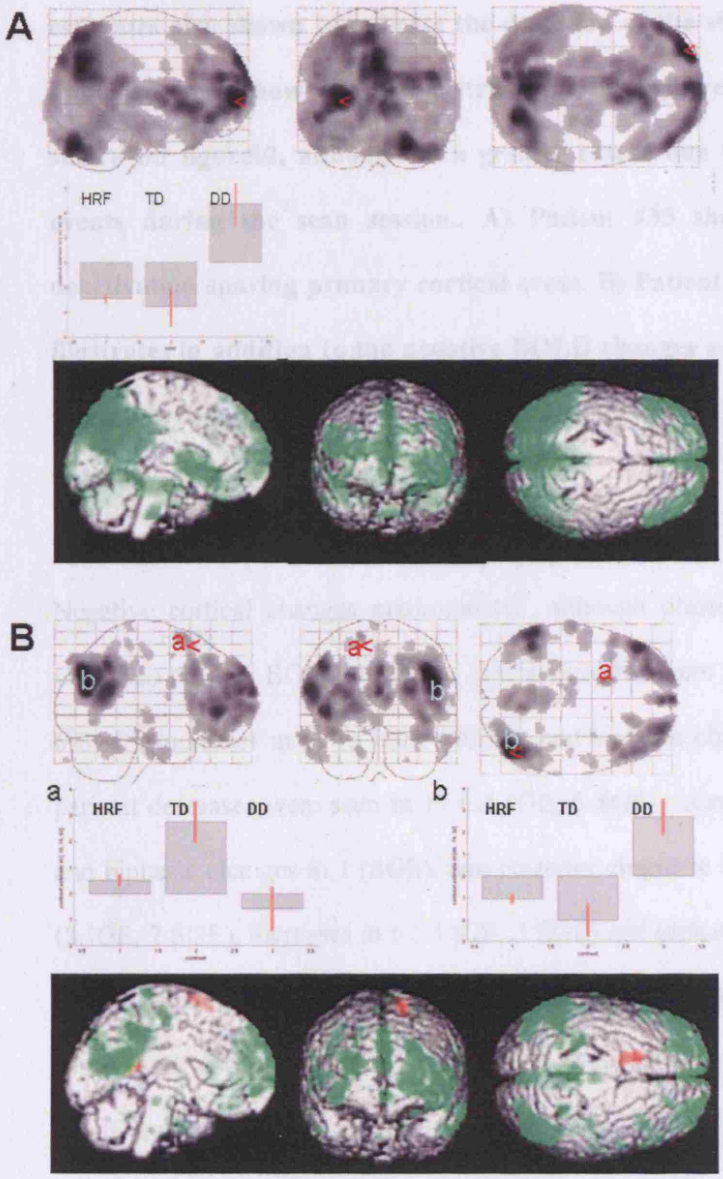


**Figure 3-3 Single subject GSW associated BOLD changes at 1.5T in SGE.**

**Mean intensity projections SPM [F] from single subject SPM analyses in 2 patients with SGE.**

**The EEG from these patients (#35 and #43) is shown in figure 3.1. A colour coded overlay of SPM [t] (red-activation and green deactivation) onto the surface render is shown for display purposes and a plot of the weighting on the contrast**

**estimates also shown to indicate the direction of the signal change at the areas indicated, both show a similar distribution on negative BOLD to the IGE cases shown on figure 2, although to a greater extent due to the higher number of events during the scan session.. A) Patient #35 shows widespread cortical deactivation sparing primary cortical areas. B) Patient #43 is also shown as this illustrates in addition to the negative BOLD changes a small area of left frontal activation concordant with the EEG abnormality (SPMs corrected, $p < 0.05$), this was reproducible at 3T (see chapter 4).**

Negative cortical changes predominated, although positive, and biphasic changes, were also present. BOLD decreases in frontal cortex were seen in 14 sessions (8 IGE, 6 SGE), increases in 10 (5 IGE, 5 SGE), and biphasic changes in 2 (IGE), posterior parietal decreases were seen in 17 (11 IGE, 6 SGE), increases in 3 (1 IGE, 2 SGE), and biphasic changes in 1 (SGE), and posterior cingulate / precuneus decreases in 15 (8 IGE, 7 SGE), increases in 6 ( 3 IGE, 3 SGE) and biphasic changes in 1. The signal change in the thalamus was positive in 9 sessions, biphasic in 4 and negative in 3 sessions. In patient 43, with SGE and EEG evidence of left frontal epileptogenicity a small area of frontal activation was seen in addition to a more widespread fronto-parietal cortical negative response.

### 3.4.3 Group Results

Figure 3.4 – 3.5 shows the SPM[F] for the HRF parameter estimate for the group analyses of the IGE, SGE and the two separate IGE subgroups JAE and JME.

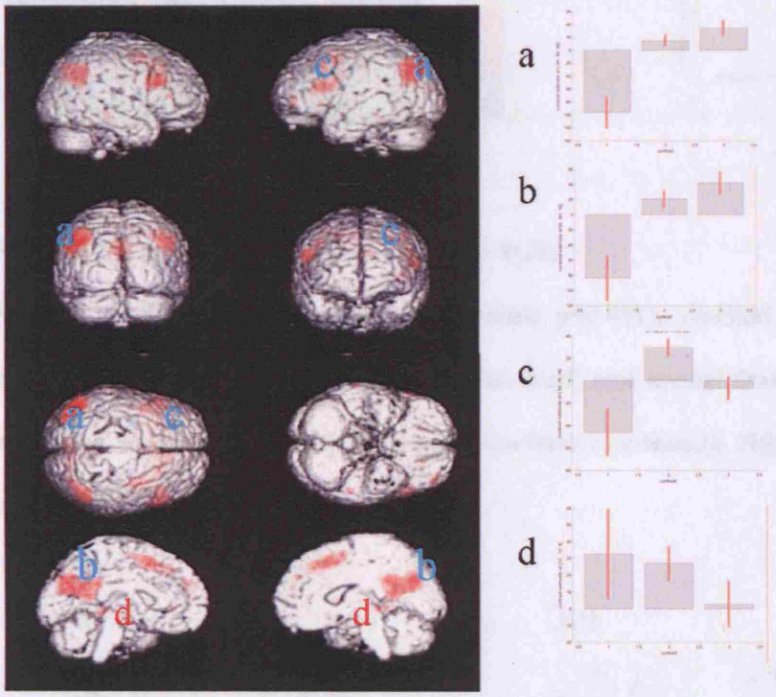


**Figure 3-4 The BOLD response to GSW in IGE.**

**SPM[F] for IGE group analysis (uncorrected p<0.001), overlaid onto 3-d canonical brain surface render. This shows bilateral parietal [46 -51 32] and [-44 -62 34] and posterior cingulate / precuneus deactivation and [6 -48 17] thalamic activation [12 -11 4]. The right panel shows the weighting on the three parameter estimate HRF, temporal derivative and dispersion derivative at each of the labelled local maxima.**

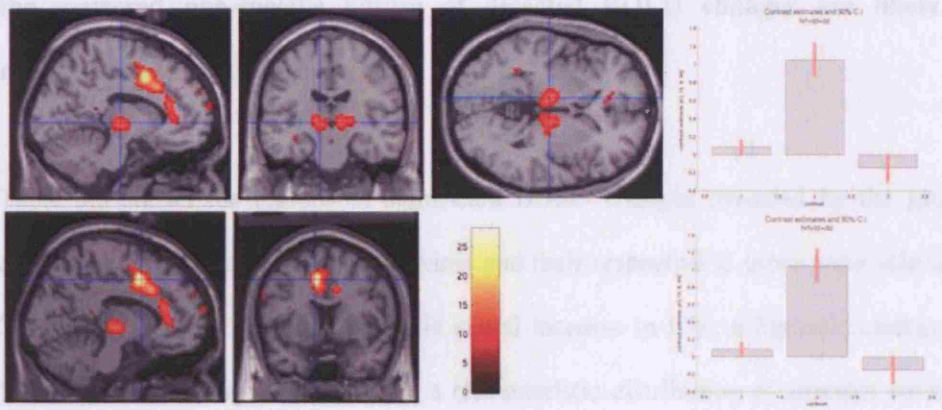

**Figure 3-5 The BOLD response to GSW in SGE.**

**SPM[F] for SGE group analysis (uncorrected p<0.001), overlaid onto template brain slices. This shows thalamic activation (red) and mesial frontal activation, weighting was maximal on the temporal derivative, although HRF was positive indicating activation.**

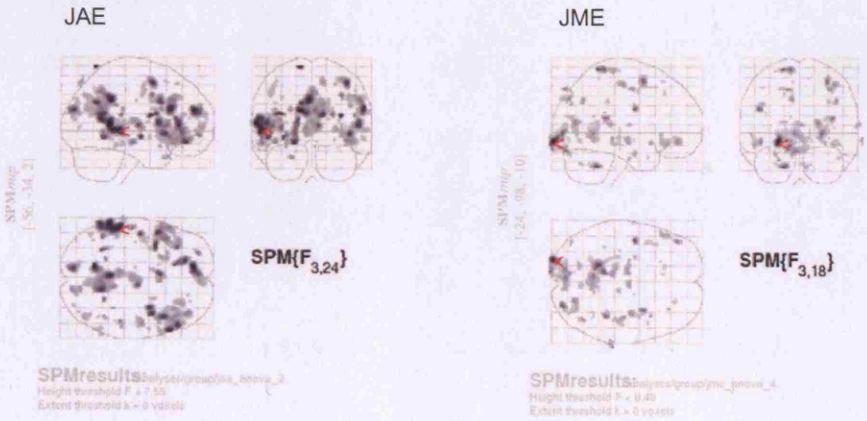


**Figure 3-6 BOLD findings in JAE and JME.**

**SPM[t] for the HRF parameter estimate for the JAE and JME subgroups (uncorrected p<0.001). The JAE map shows cortical deactivation similar to the**

**IGE group, however maps were not felt amenable to reasonable interpretation, the scattered non-specific nature of detected BOLD changes are likely a reflection on the small sample size.**

Table 3.3 shows the regions of significant BOLD changes revealed by the group analysis, coordinates for all local maxima and their respective Z score were selected. This shows a group effect of thalamic signal increase in IGE, a biphasic change in SGE, and cortical signal decrease in a characteristic distribution of superior parietal cortex, posterior cingulate cortex and frontal cortex in the IGE group and medial frontal cortex / anterior cingulate increase in the SGE group and biphasic thalamic change in the SGE group. In addition there was 'activation' in the ventricular system in the IGE group analysis.

IGE group analysis

| Region | | MNI x,y,z | Peak Z score | Weighting on contrast estimate |
|---|---|---|---|---|
| Parietal | | | | |
| L | Angular Gyrus | -44, -62, 34 | 5.96 | ↓ |
| R | Supramarginal Gyrus | 46, -51, 32 | 5.86 | ↓ |
| R | Posterior Cingulate | 6, -48, 17 | 5.23 | ↓ |
| Frontal | | | | |
| L | Inferior Frontal Gyrus | -51, 16, 16 | 4.75 | ↓ |
| L | Inferior Frontal Gyrus | -50, 26, -15 | 4.11 | ↓ |
| R | Inferior Frontal Gyrus | 53, 35, 7 | 3.86 | ↕ |
| L | Inferior Frontal Gyrus | -38, 49, 1 | 3.82 | ↓ |
| R | Middle Frontal Gyrus | 53, 23, 23 | 5.47 | ↓ |
| L | Superior Frontal Gyrus | -12, 61, 23 | 3.76 | ↓ |
| R | Superior Frontal Gyrus | 18, 48, 29 | 3.59 | ↓ |
| Temporal | | | | |
| L | Fusiform Gyrus | -51, -34, -20 | 4.21 | ↓ |
| R | Middle Temporal Gyrus | 67, -28, -12 | 4.51 | ↓ |
| L | Middle Temporal Gyrus | -46, -52, 3 | 3.78 | ↕ |
| L | Parahippocampal Gyrus | -16, -10, -13 | 3.98 | ↕ |
| Subcortical | | | | |
| L | Caudate | -14, 10, 5 | 4.68 | ↓ |
| R | Caudate | 10, 8, 5 | 4.13 | ↓ |
| R | Thalamus | 12, -11, 4 | 3.67 | ↑ |

B. SGE group analysis

| Region | x,y,x | Peak Z score | Weighting on contrast estimate |
|---|---|---|---|
| Frontal | | | |
| L Cingulate Gyrus | -8, 10, 42 | 5.56 | ↑ |
| L Anterior Cingulate | -8, 33, 2 | 3.94 | ↕ |
| L Inferior Frontal Gyrus | -50, 5, 27 | 3.98 | ↕ |
| R Cingulate Gyrus | 10, 9, 33 | 3.89 | ↕ |
| Subcortical | | | |
| L Thalamus | -14, -15, 4 | 4.15 | ↕ |
| R Thalamus | 10, -15, 3 | 3.92 | ↕ |

**Table 3-3 Group GSW associated BOLD responses at 1.5T.**

**Brain regions that showed significant GSW related change from random effects group analysis. A: IGE cases and B: SGE cases. The weighting on the contrast is given to show the direction of BOLD signal change. L, left; R, right; hrf, canonical haemodynamic response; td, temporal derivative.**

## 3.5 Discussion

BOLD signal changes were detected in 73% of sessions. Those with no BOLD response had 7 events or less, all of which were of less than 2 seconds duration.

The prevalent finding in individual subject and group analyses was of thalamic activation and cortical negative BOLD response (NBR). Thalamic signal change was seen in less than half of patients with IGE and almost all patients with SGE. This is likely due to the greater occurrence of GSW events in SGE cases compared to IGE (median SGE 44.5 versus IGE 8), and tended to be seen in those individual IGE cases with a higher number or longer duration of GSW. BOLD changes spared primary cortical areas; changes were present in frontal, parietal and temporal association areas. At the single subject level similar BOLD responses were seen across IGE syndromes and in SGE, suggesting that the predominant BOLD findings represent generic changes associated with GSW per se rather than syndrome specific patterns. This is unlikely to be due to syndrome misclassification [Berkovic *et al.* 1987] given the similarity of our findings in cases with very clear syndromic differences.

One striking feature of the results is the lack of changes in the primary cortices, except in a few cases, the primary visual cortex. Aghakhani et al (2004) similarly, found the cortical BOLD changes predominantly in a frontal and posterior distribution, similar to those seen here. They highlighted the symmetrical nature of their findings as well as the predominance of negative changes in cortex as seen here. They performed a second (between-subject) level random effects analysis to look for population effects specific to GSW (a similar analysis to that done here) on the Aghakhani et al data presented in a further publication Gotman et al 2005 [Gotman 2005].

The results of individual analyses, the case studies (first-level) and the group (second-level) analysis are complementary. The case-studies reflect subject-specific haemodynamic correlates of GSW, inferred relative to the precision with which haemodynamics can be measured (i.e., within-subject error). These analyses disclose the degree of inter-subject variability and similarities within different nosological subgroups. This sort of analysis would be employed in any potential clinical application. The second-level analysis asks a different question: what are the GSW correlates that are common to all subjects? In this context inter-subject variability is treated as a random effect and the commonalities are measured against this variability. The object here is to identify generic features that may point to a more mechanistic understanding of the functional anatomy of GSW.

The selection of patients for this study was necessarily biased to those at the severe end of the spectrum often referred for optimization of medical treatment. Rarely were patients on no medication. Carbamazepine (CBZ) and gabapentin (GBP) are known to increase the amount of GSW in patients with IGE [Kochen et al. 2002]; however they are used if the initial diagnosis is incorrect, or, in some, improvements in generalized seizures are seen despite the relative contraindication. It is notable that 7 of 34 of our IGE patients with frequent discharges were taking CBZ or GBP at the time of the study. In the other EEG-fMRI studies 4 of 15 were taking CBZ in (Aghakhani et al. 2004) and 4 of 5 in (Archer et al.2003). The effect of anti epileptic medication on the neurovascular response is not known, although any effect may be lessened by the fact that comparisons made here are within sessions. Even with optimal patient selection, the unpredictability and in cases paucity of GSW during scan sessions remains a limitation of EEG-fMRI.

Activating procedures such as hyperventilation could be employed but are likely to introduce confounds due to variable effects on cerebral circulation and the BOLD response [Kemna and Posse 2001], whilst photic stimulation, sleep deprivation or drug withdrawal would run the risk of provoking generalized tonic clonic seizures.

Patient age was not a consideration in the inclusion criteria; four patients were over 50 (#8,#15,#17,#32). The absence of the typical BOLD pattern in patients #15 and #17 may reflect differences in sleep needs and resting states in elderly people, or differences in the neurovascular response and hence neuronaly driven BOLD signal changes in the age group. This would warrant a detailed study in a larger group of subjects.

It is not possible to infer causality of the BOLD changes relative to the modelled covariate, GSW; they may represent areas generating GSW, or alternatively reflect areas secondarily affected by GSW. This difficulty in inferring causality is in contrast to paradigm driven fMRI where it is generally safe to assume a primary association between the task or stimulus and the observed fMRI changes; in addition a prior hypothesis about a relatively well defined location of expected neural activity usually exits. In GSW however we have little prior anatomical hypothesis regarding the spatial extent of BOLD changes. Nevertheless the thalamic activation seen here represents subcortical activity necessary for the maintenance of GSW [Avoli *et al.* 2001;Meeren *et al.* 2002], and the lack of thalamic activation in a number of cases may reflect low sensitivity of the model at 1.5 T [Laufs *et al.* 2006c].

The left frontal cortical activation in case 43 (figure 3.3) most likely represents an area of initiation of GSW given its concordance with the left frontal EEG onset of GSW (figure 3.1d). This area of frontal activation was reproducible at 3T (see chapter 4).

The cortical distribution of signal change, frontal cortex, posterior and posterior cingulate / precuneus, comprises areas of association cortex. Marcus Raichle coined the term "default mode" areas, to refer to a putative network that is "tonically" active when the brain is at rest, in an organized, baseline level of activity, a [Raichle *et al.* 2001;Mazoyer *et al.* 2001]. This default mode concept came from observations of consistent deactivations in these areas on meta analyses of different task related paradigms in fMRI, and independent PET measurements of increased blood flow to these areas during awake conscious rest [Raichle *et al.* 2001]. Activity in these areas as measured by PET is also altered during sleep, coma and anaesthesia [Laureys *et al.* 2004]. Default mode areas most likely represent part of a neural network subserving human awareness [Laureys *et al.* 2004]. This study, and others [Archer *et al.* 2003a] [Aghakhani *et al.* 2004;Laufs *et al.* 2006c], shows alteration of activity in these regions during GSW, which would be consistent with the clinical manifestation of absence seizures. Further evidence of involvement of these areas in GSW comes from PET findings suggesting increased opioid release in association neocortex, most marked in parietal cortex and posterior cingulate, following absence seizures [Bartenstein *et al.* 1993].

A number of lines of evidence suggest that BOLD negative responses represent a reduction in neural activity. In visual cortex, a reduction of BOLD signal, elicited by stimulating part of the visual field is due, primarily, to a reduction of neuronal activity [Shmuel et al. 2002]. A decrease in BOLD signal is seen in the occipital cortex during auditory induced saccades [Wenzel *et al.* 2000], a manipulation known to suppress neuronal activity [Duffy and Burchfiel 1975]. BOLD decreases have also been observed in the context of neuronal synchronization, modulated by sub-cortical structures [Parkes *et al.* 2004]. Visual stimulation during sleep leads to occipital

BOLD negative responses, confirmed as a decrease in rCBF with H215O PET [Born *et al.* 2002]. Similarly auditory BOLD negative responses occur on auditory stimulation during sleep, the amplitude and extent of which correlate positively with measures of EEG synchronization in sleep [Czisch *et al.* 2004].

Although the majority of cases showed cortical negative response a number of cases showed activation or biphasic time courses in the same areas. These did not differ significantly (2-sample t-tests, all $p > 0.8$) from those with negative response in terms of the frequency of GSW, the number of events, their median duration or total duration during the scan session. Cortical activations at the single subject level were seen in a greater proportion of SGE than IGE patients. This would explain the absence of widespread cortical change in the SGE group analysis, where positive signal changes in some subjects and negative in others in the same region lead to a loss of this effect at the group level.

Cortical fMRI signal increases were seen in some of Aghakhani EEG-fMRI GSW series [Aghakhani *et al.* 2004]. In TCD an initial increase was seen prior to the more prolonged decrease [Diehl *et al.* 1998] [De Simone *et al.* 1998]. Similarly, SPECT and PET showed increases as well as decreases in cortical activity to spike wave [Engel, Jr. *et al.* 1985] [Theodore *et al.* 1985] [Ochs *et al.* 1987] [Prevett *et al.* 1995a] [Yeni *et al.* 2000]. The likely explanation for these apparent contradictory findings is that the temporal resolution of these functional imaging modalities undersample the true haemodynamic variation to GSW. In addition the terms "activation" and "deactivation" are operational terms applied to BOLD fMRI signal increases and decreases respectively. The terms have their origins in the field of PET [Friston et al. 1990], in which measures are quantitative and more direct. They reflect measured vascular or metabolic responses from which inferences about neuronal activity are

made. The term negative BOLD response (NBR) has been proposed rather than deactivation as the neural correlates of these responses are not yet clear [Parkes *et al.* 2004]. In fMRI the modelling of signal changes is relative, i.e. a comparison between two states [Bandettini *et al.* 1992]. Given that here and elsewhere [Aghakhani *et al.* 2004;Salek-Haddadi *et al.* 2003b]) GSW is modelled against an implicit baseline, i.e. active (GSW) against rest (background resting state activity), and 2) changes occur in areas of association cortex, then the level of arousal or sleep reflecting resting state activity in these regions may affect the direction of detected BOLD signal changes. A negative response is therefore seen where there is a decrease or interruption of awake resting state activity; if however the patient is drowsy or asleep activity in these areas may be lower than that engendered by GSW thus giving rise to activations.

### 3.6 Conclusion

The main BOLD fMRI correlates of GSW consisted of widespread cortical negative response in areas associated with normal brain activity during conscious rest. These likely reflect a decrease in neural activity, as a result of either synchronization or inhibition of cortical activity due to thalamo-cortical interactions. This is in keeping with the clinical features of absence seizures, i.e. a brief alteration of consciousness with minimal somatosensory or motor manifestations.

# 4 Chapter 4. Three Tesla ASL and BOLD of Generalised Spike Wave

## 4.1 Abstract

Four patients were selected from the previous study for repeat EEG-fMRI at 3-Tesla, with BOLD fMRI and arterial spin label (ASL) fMRI. BOLD deactivations or Negative BOLD responses (NBR) were seen in all cases involving frontal, parietal and posterior cingulate cortex, with a high degree of concordance with the 1.5T study. BOLD activation was seen in two patients with secondary generalised epilepsy, in thalamus and left frontal cortex in one and in mesial frontal cortex in the other; in keeping with electro-clinical features of their epilepsy. No BOLD activations were seen in one patient with idiopathic generalised epilepsy and likely artifactual ventricular activation was seen in the other. BOLD activations in two patients were consistent with areas generating GSW and epileptic seizures, whereas NBR and decreased cerebral perfusion was anatomically consistent with an alteration of normal resting state brain activity during GSW.

## 4.2 Introduction and Aims

In the previous chapter GSW associated BOLD changes were described. Widespread BOLD deactivations, which will be referred to hereon in as negative BOLD responses (NBR) were seen in frontal, parietal and posterior cingulate cortex at the group level and where BOLD were present in the majority of single subject analyses. In this first study there was wide intersubject variability across all subjects but good between

session concordance in those patients studied over two sessions. In order to better understand these findings and assess the potential increased contribution of fMRI at the higher field strength of 3 Tesla, 4 patients with very frequent GSW from the initial cohort of 46 patients were selected for study with EEG-fMRI at 3 Tesla using BOLD and the newly developed method of arterial spin labelling (ASL) or perfusion fMRI . The aims of the study were:

1) to repeat EEG-fMRI with BOLD contrast at 3T

2) to validate in our setting ASL MRI as a functional imaging tool and use this to assess the contribution of blood flow changes to the BOLD response, and in particular the negative BOLD responses (NBR).

3) to assess any observed gains between 1.5T and 3T

The basis of NBR [Czisch *et al.* 2004] is not fully understood. BOLD responses arise from regional changes in deoxyhaemoglobin concentration due mainly to changes in cerebral blood flow, with an additional effect of alterations in blood volume and oxygen extraction [Ogawa *et al.* 1990a]. NBR is due to either an absolute decrease in cerebral blood flow or an increase in oxygen consumption that exceeds any blood flow increase [Wade 2002]. Mathematical modelling suggests that NBR represent neuronal deactivation or active inhibition of cortical areas [Kilner et al. 2005]. A decrease in BOLD signal is seen in the occipital cortex during auditory induced saccades [Wenzel *et al.* 2000], a manipulation known to suppress neuronal activity [Duffy and Burchfiel 1975]. BOLD decreases have also been observed in the context of neuronal synchronization, modulated by sub-cortical structures [Parkes *et al.* 2004]. Visual stimulation during sleep leads to occipital NBR, confirmed as a decrease in regional cerebral blood flow (rCBF) with positron emission tomography [Born *et al.* 2002]. Similarly auditory NBR occur on auditory stimulation during

sleep, the amplitude and extent of which correlate positively with measures of EEG synchronization in sleep [Czisch *et al.* 2004].

Arterial spin labelling (ASL) fMRI can measure cerebral perfusion by use of magnetically labelled in flowing arterial blood as an endogenous tracer [Wong *et al.* 1997]. This is achieved by modifying the magnetisation of arterial H-protons proximal to the tissue of interest. Subtraction of sequentially acquired images, with arterial spin labelling (label image), and without arterial spin labelling (control images) provides a measure of both relative and quantitative changes in rCBF. This can detect changes in blood flow correlated with neural activity in response to a task or stimulus [Wang *et al.* 2003;Garraux *et al.* 2005;Aguirre *et al.* 2002]. ASL fMRI, like BOLD fMRI, uses echoplanar techniques for imaging. Images acquired during the ASL sequence therefore also contain BOLD contrast such that both BOLD and perfusion effects can be estimated from ASL data [Wong *et al.* 1997].

## 4.3 Materials and Methods

### 4.3.1 Finger Tapping Paradigm

A self paced finger tapping paradigm was used to validate and develop the methods for the functional analysis of ASL images using SPM.

A healthy volunteer (thesis author) was scanned for 20 minutes using the ASL fMRI sequence described below, whilst performing a self paced finger tap alternating left and right hand of 46 seconds (10 TRs) each.

### 4.3.2 Patients

Four patients were selected from the first 1.5T study, four of whom had GSW associated NBR in a previous EEG-fMRI study at 1.5T [Hamandi *et al.* 2006]. Two patients had SGE and two IGE (one with generalised tonic clonic seizures (EGTCS), the other childhood absence epilepsy (CAE) and juvenile myoclonic epilepsy (JME))[ILAE 1989]. The SGE patients were selected on the basis of frequent and prolonged runs of GSW – necessary for the quantitative analysis of ASL images. The IGE patients, were selected on the basis of frequent GSW, see table 3.1 for patient details.

### 4.3.3 EEG Acquisition and Processing

32 channels of surface EEG were recorded in the scanner using BrainProducts (Munich, Germany) scanner compatible hardware and software as described in Common Methods, section 2.4.1.2. Foam padding and ear defenders were used to minimize motion and improve patient comfort. Scanner and EEG clock were synchronized, such that EEG sampling relative to scanner gradient switching was constant. EEGs were corrected for image and pulse artefacts using the Vision Analyzer software (BrainProducts, Munich, Germany), by digital subtraction of an averaged artefact waveform [Allen *et al.* 1998;Allen *et al.* 2000]. The start and stop of GSW epochs were visually identified on the artefact corrected EEG, and marked according to corresponding scan number, to be used in the fMRI statistical analysis (section 2.4.3).

### 4.3.4 MRI Acquisition

Imaging was carried out on a 3T Siemens Allegra head scanner (Siemens, Erlangen, Germany) using a standard head transmit/receive coil. A T1 weighted structural scan with an isotropic resolution of 1mm using an MDEFT sequence with optimised grey matter (GM)-white matter (WM)-contrast and imaging parameters was used to create GM and WM masks [Deichmann et al. 2004].

Two thirty minute runs of functional MRI with simultaneous EEG were acquired in each patient consisting:

1) a gradient echo (BOLD sensitive) EPI time series, whole brain coverage (TR/TE 3120/40 ms, 48 slices, 500 volumes, 3x3x2mm, 1 mm inter slice gap), which we will refer to as BOLD series,

2) a pulsed arterial spin labelling (PASL) sequence (Q2TIPS) [Luh *et al.* 1999;Nöth *et al.* 2006] (figure 4.1) with the PICORE labelling scheme in which arterial spins are labelled by a 10 cm inversion slab proximal to the imaging slices (gap 6mm), which we refer to as ASL series. The scanning parameters were: FOV 22.4 cm x 22.4 cm, matrix 64 x 64, 6 axial slices (extending superiorly from the top of the corpus callosum), 4 mm slice thickness, slice gap 0.5 mm, TR 2.3 sec, (time for acquisition of a single slice was 66ms), TE 30ms. Figure 4.1 below taken from [Nöth *et al.* 2006] illustrates the ASL sequence parameters.

**Figure 4-1 Timing of perfusion and slice layout.**

**from [Nöth *et al.* 2006].**

4.3.5 MRI Processing

The SPM2 (www.fil.ion.ucl.ac.uk/SPM) software package was used for image pre-processing and analysis, with in-house software written in Matlab 6.5.0 (www.mathworks.com) for the calculation of perfusion images. BOLD and ASL series were pre-processed separately.

BOLD series: The first five images were discarded to allow for T1 equilibration effects. Images were spatially realigned, normalized to a standard EPI template based on the MNI reference brain [Ashburner and Friston 1999] and spatially smoothed (8mm full width half maximum Gaussian kernel).

ASL series: The Siemens MoCo (motion correction in frequency space before image reconstruction) series of label and control images were used for analysis.

A programme h_perfcalc.m written in Matlab 6.5.5 was used for the following calculations.

Images were realigned to the first image using SPM2. A time series of the difference images, was calculated by subtracting adjacent control and temporally adjusted label images; (a 'surround average' of preceding and following label images was used to remove effects of BOLD signal fluctuation within one TR) [Aguirre *et al.* 2002], and

expressed as a ratio of the control image to remove BOLD contrast present in both label and control images [Garraux *et al.* 2005], according to the following equation:

$$P_1, P_2, \ldots P_{(n-2)/2} = \frac{C_1 - (L_1 + L_2)/2}{C_1}, \frac{C_2 - (L_2 + L_3)/2}{C_2}, \ldots\ldots\ldots\ldots \frac{C_{(n-1)} - (L_{(n-1)} + L_{(n)}/2}{C_{(n-1)}}$$

Where P is the ratio perfusion image and C the control and L the label image.

Difference images were thresholded according to Garraux et al [Garraux *et al.* 2005], to remove abnormal flow values that did not fall within a physiological range, by retaining only 1) pairs of voxels where control signal intensity had a value greater than 80% of the global mean intensity of the control image, and 2) voxels with a fractional signal change of less than ± 5%. This ratio difference image is referred to as ASL-P (ASL-Perfusion). A corresponding BOLD sensitive time series was calculated by summation of adjacent label and control images, these will be referred to as ASL-B (ASL-BOLD).

The structural image of each patient was segmented using SPM2 into GM, WM and CSF. The mean perfusion images, perfusion time series and structural images were co-registered to a respective BOLD image for each subject, to allow masking of quantitative perfusion images with the GM map. A further time series of difference only images C1– (L1 - L2) / 2 (i.e. not expressed as a ratio) was calculated for the quantitative analysis.

### 4.3.6 Statistical Analysis

The onset and duration of epochs of GSW from the simultaneously acquired EEG were convolved with a canonical haemodynamic response function and its temporal derivative [Henson 2003]. These were entered into a design matrix along with a Volterra expansion of the 6 realignment parameters as effects of no interest [Henson

2003]. In the analysis of the ASL-P images no modelling of intrinsic autocorrelation, filtering or temporal smoothing was applied [Wang *et al.* 2003]. In the analysis of the BOLD series and the ASL-B images, an autocorrelation (AR1) correction, and a 128 Hz low pass filter were applied [Henson 2003].

For the finger tapping paradigm a standard boxcar convolved with the HRF and its temporal derivative was used in place of an EEG derived model for image analysis.

SPM by default uses an implicit mask during the statistics estimation stage of BOLD analyses based on inclusion of voxels with intensities higher than 80% of the global image mean. This was found to be unsuitable for ASL analysis, when analysing the finger tap data, in that voxel values in the subtraction images are lower within the brain than those outside. We therefore used an explicit mask from the subjects mean perfusion image to define those voxels included in the ASL-P statistical analysis. This was achieved by modifying the SPM2 script for the statistical estimation, such that the default mask was removed and a subject specific mask used instead. The subject specific mask was created by a seed and region growing segmentation method [Moran et al. 1999].

Statistical parametric maps (SPM[t]) showing contrasts for positive and negative HRF were used to map areas of GSW associated signal change. Individual analyses were thresholded at $P<0.05$ (corrected for multiple comparisons based on Gaussian random field theory) [Friston *et al.* 1991] for the BOLD time series, and $P<0.001$ (uncorrected) for the perfusion images given their lower signal to noise ratio [Loring et al. 2002].

### 4.3.7 Quantitative rCBF Analysis

Quantification was done in the following way, resulting in an image of perfusion values termed *qperf,* using in-house Matlab scripts.

qperf (slice n)=(C(n,1) x mperf (n))/SWM(1) x 1.3499

Where:

- C(n,1) is the quantification factor for slice n. This depends on the time when slice n was acquired (given that the 6 slices are acquired at different times), and field dependent relaxation times, and was given the values [4053, 4235, 4425, 4624, 4832, 5050]
- mperf is the mean of the difference images,
- and SWM the white matter signal from slice 1.
- and the value 1.3499 is derived from exp(TE/T2*blood), where TE = 30ms; and T2*blood*(at 3T) = 100ms

Absolute difference images acquired during periods of normal EEG activity (rest images) were used for the quantitative analysis. Rest images were defined as those acquired beyond 5 TRs (23 seconds) after the end of any given GSW and up to 1 TR before the start of the following GSW. These time values were chosen to avoid inclusion of images with GSW induced perfusion changes that may precede or persist longer than the EEG epoch. Transcranial Doppler studies show that perfusion changes can persist for up to a minute after the end of GSW [Sanada *et al.* 1988;Klingelhofer *et al.* 1991;De Simone *et al.* 1998;Diehl *et al.* 1998]. The value of 23 seconds was chosen to provide a sufficient number of rest images to increase the signal to noise ratio of the mean perfusion image, on the assumption that on average perfusion value were heading toward or had reached normal levels.

Using SPM2, the structural images were segmented to white matter (WM), grey matter (GM) and cerebrospinal fluid (CSF). These segmented images and the mean difference images were co registered to the same space.

The qperf image, from above, was resliced onto the segmented grey matter map and masked with the grey matter map thresholded at >0.7, to obtain grey matter perfusion. The mean of this image was taken as the absolute perfusion value.

## 4.4 Results

### 4.4.1 Finger Tapping Paradigm

Activation in the motor cortex was seen from the ASL fMRI time series during finger tapping. Figure (4.1) shows the ASL-B (blue) and ASL-P (red) for the SPM[F], i.e. BOLD and perfusion contrast for the effect of interest, either left or right finger tap, following the modified SPM analysis.

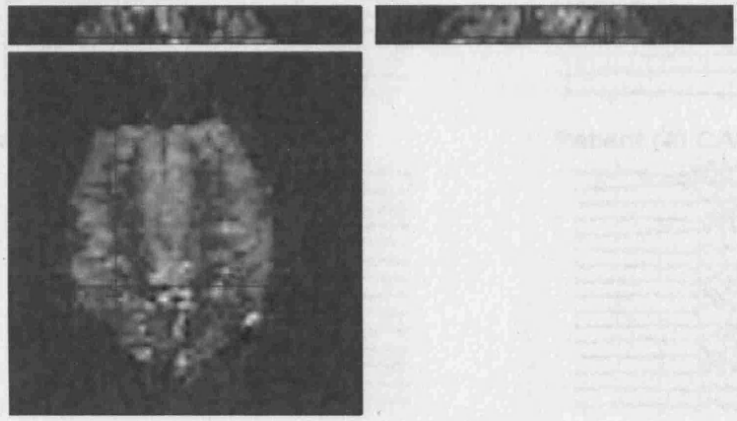

**Figure 4-2 BOLD and perfusion fMRI of self paced finger tap.**

**SPM [F] of the BOLD (ASL-B) shown in blue and perfusion (ASL-P) shown in red (uncorrected $p<0.001$) from single subject overlaid onto the mean perfusion image in native space showing expected BOLD activation and concomitant perfusion in motor cortex bilaterally.**

### 4.4.2 GSW BOLD

Good quality EEG was obtained in all scan sessions. GSW epochs were readily identified visually. Figure 4.3 shows a segment of artefact corrected EEG recorded during the BOLD fMRI demonstrating GSW for each of the subjects.

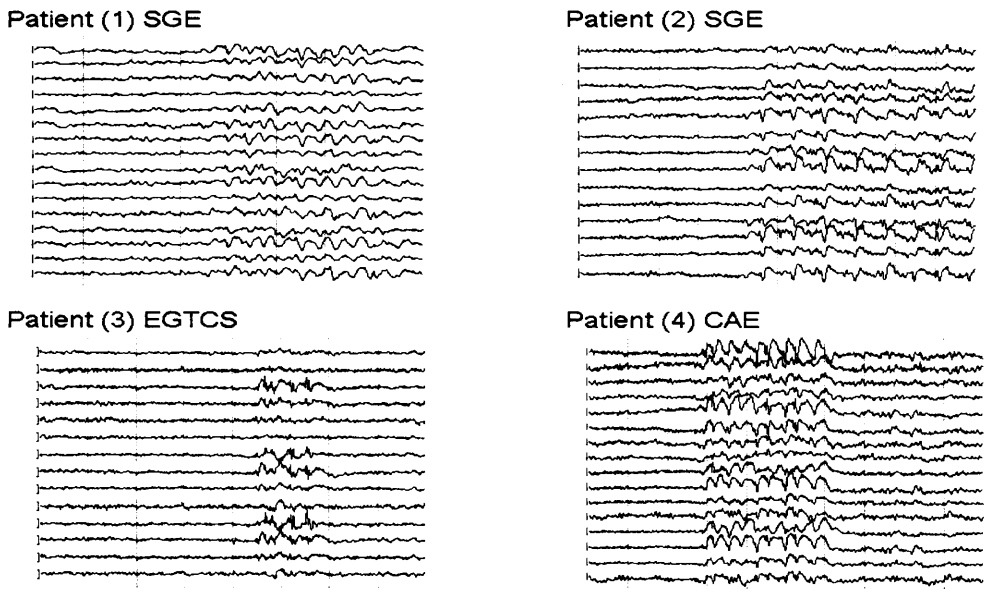


**Figure 4-3 GSW in artefact corrected EEG from 3T BOLD fMRI sessions**

**An epoch is shown for the 4 patients in whom perfusion analysis was possible. Note the activity in patient one was predominantly slow wave with admixed spikes and in patient 2 there is a left frontal lead into the GSW, both these patients had secondarily generalized epilepsy. SGE - secondary generalized epilepsy, EGTCS - epilepsy with generalized tonic clonic seizures, CAE - childhood absence epilepsy.**

| | Age | Sex | Diagnosis | Seizures type frequency / (age onset) | AEDs | Interictal EEG | GSW events number (duration range / median duration / total duration) / seconds | | |
|---|---|---|---|---|---|---|---|---|---|
| | | | | | | | 1.5T BOLD | 3T BOLD | 3T ASL |
| 1 (42) | 39 | F | SGE | Abs1 10-20 / d (9)<br>GTCS 0-4/mnth (11) | CBZ, LEV | 2-3Hz sW with admixed spikes | 57 (1.1 – 25 / 4 / 387) | 43 (1.6 – 26/ 7.4 / 387) | 38 (0.3 – 8.7 / 6.8 / 405 ) |
| 2 (43) | 21 | M | SGE | Abs 8/nmth (13)<br>GTCS 4/yr (18) | CBZ, LEV,VPA | 2-3 Hz GSW L frontal onset | 32 (1.1 – 29 / 5 / 258 ) | 40 (0.7 - 47 / 2.3 / 416) | 44 (1.7 – 41.2 / 9.8 / 564) |
| 3 (25) | 35 | M | EGTCS | GTCS 3 in total (12) | VPA | 3 Hz GSW | 33 (0.6 – 3.0 / 1.5 / 52) | 25 (0.8 – 3.0 / 1.5 / 21) | 12 (0.7 – 4.7 / 1.2 / 23) |
| 4 (31) | 30 | F | CAE | Abs 15/d (8) | None | 3 Hz GSW | 130 (0.3 – 28.7 / 3.3 / 591) | 84 (1.0 – 8.3 / 2.6 / 199 ) | 68 (0.8 – 9.8 / 2.8 / 221) |

**Table 4-1 Patient and EEG characteristics of 1.5T and 3T BOLD studies.**

**Number, median and total duration of GSW epochs during BOLD and ASL acquisitions. Abs - absences, At Abs -atypical absences, CAE - childhood absence epilepsy, EGTCS - epilepsy with generalized tonic clonic seizures, GTCS - generalized tonic-clonic seizures, SGE - secondary generalized epilepsy. CBZ - carbamazepine, LEV - levetiracetam, VPA - sodium valproate. 1 blank spells, on occasion with abnormal posturing (looks left, dystonic posturing of both arms), occasional urinary incontinence, clusters associated with thought disorder (formed illusions, distortion of perception and auditory hallucinations). The patient number in parenthesis refers to the Chpt 3 patient number in table 3.1**

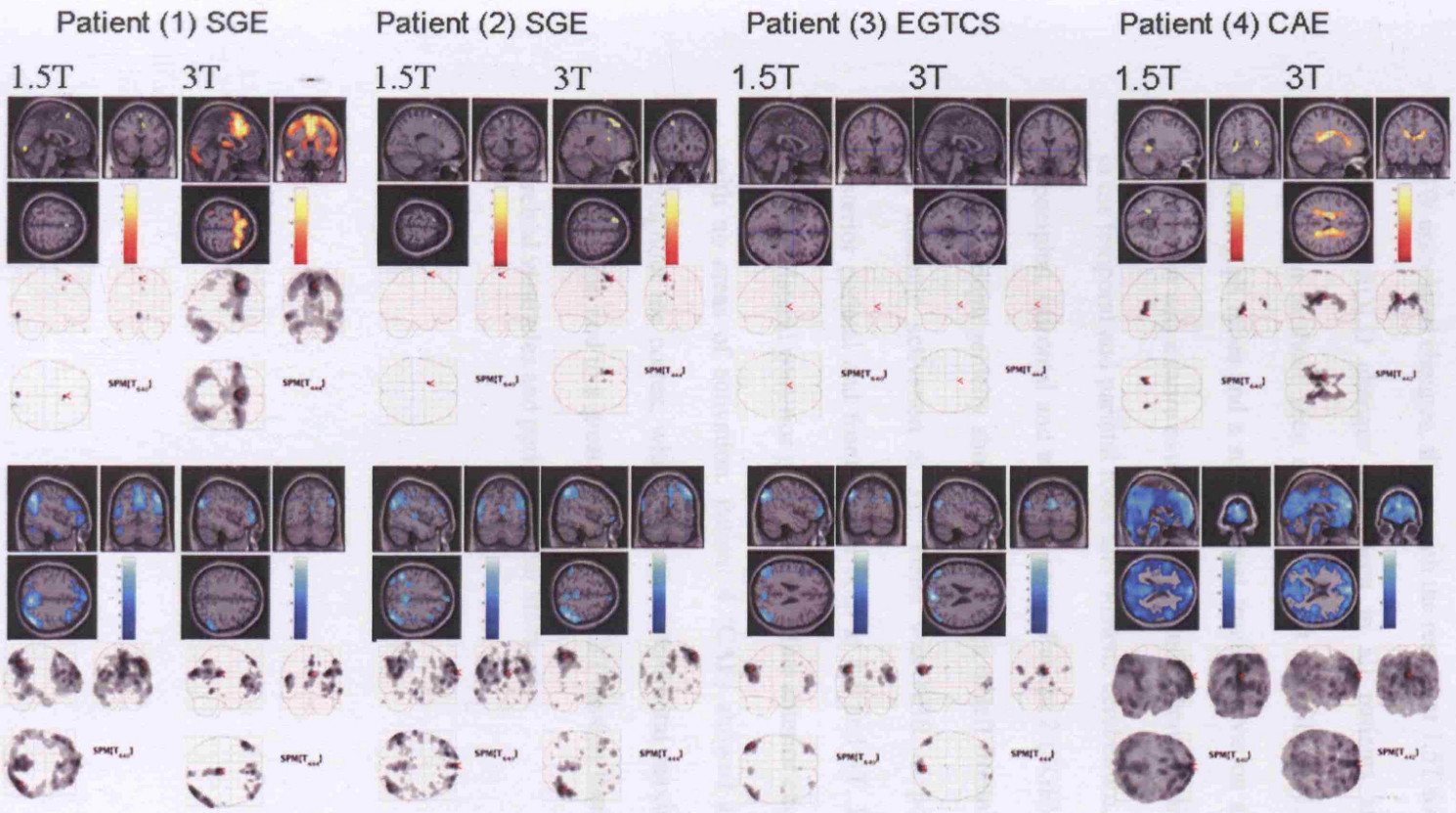


**Figure 4-4 BOLD fMRI of GSW at 1.5 and 3T.**

**SPM(t) for positive (red) and negative (blue) HRF for each of the subjects studied at 1.5 and 3T (corrected $p<0.05$ FWE). Note the striking similarity between the two sessions, acquired up to 4 years apart on two different scanners at different field strengths. The figure also demonstrates that at 3T there is no overt increase in the size of the activations seen or evidence of new "networks" not seen at 1.5T. The 'glass brain' is given for each session for further clarity.**

BOLD results Figure 4.4 and Table 4.2 show SPMs results for positive and negative GSW associated changes, shown with the results at 1.5T for comparison.

Negative BOLD changes were seen in all patients at 3T with similar spatial distribution to those seen at 1.5T. Patient 1 (SGE) at 1.5 T had widespread NBR involving all lobes and a small mesial frontal activation and left occipital activation. At 3T there was a more extensive mesial and bifrontal activation as well as activation in the temporal and parietal lobes and bilateral cerebellum, with smaller areas of NBR in occipital, bifrontal and temporal areas. Patient 2 (SGE) with EEG evidence of left frontal epileptogenicity showed a small area of left frontal activation at 1.5T and 3T, and thalamic activation at 3T. There was NBR in posterior cingulate, bilateral posterior parietal and frontal areas both at 1.5 and 3T. Patient 3 (EGTCS) showed NBR in bilateral posterior parietal and midline anterior occipital areas in both sessions with no areas of activation. Patient 4 (CAE) showed a striking widespread NBR throughout the cortex, with a mesial orbito-frontal maximum at 1.5 and 3T. In the 1.5T session and to a greater extent in the 3T session there was signal increase in the cerebral ventricles and periventricular areas.

| Patient | | Region 1.5T | MNI coordinates | Cluster size | Z score | Region 3T | MNI coordinates | Cluster size | Z score |
|---|---|---|---|---|---|---|---|---|---|
| 1) | Act | Mesial frontal | -0 16 60 | 48 | 7.04 | Mesial frontal | -2 12 50 | 16727 | >8 |
| | | L occipital | -4 -86 -8 | 115 | 5.93 | R temporal | -56 12 -10 | 867 | >8 |
| | | | | | | R cerebellum | 38 -56 -32 | 7399 | >8 |
| | | | | | | L cerebellum | -36 -70 -28 | *In above* | >8 |
| | | | | | | R superior parietal | 42 -48 50 | 411 | 6.96 |
| | | | | | | L superior parietal | -28 -32 86 | 98 | 5.74 |
| | *Deact* | *R parietal* | *46 -64 40* | *44231* | *>8* | *Cingulate gyrus* | *0 -26 26* | *956* | *>8* |
| | | *Mesial frontal* | *0 78 18* | *In above* | *>8* | *R occipital* | *42 -84 28* | *2044* | *>8* |
| | | *Precuneus* | *2 -68 38* | *In above* | *>8* | *L frontal* | *-54 3216* | *1241* | *>8* |
| | | *widespread confluent change all lobes* | | | | *Medial frontal* | *2 5048* | *310* | *>8* |
| | | | | | | *R frontal* | *48 48 2* | *1171* | *7.8* |
| | | | | | | *R temporal* | *66 -44 -8* | *201* | *7.59* |
| 2) | Act | L frontal | -16 10 70 | 36 | 6.17 | L frontal | -20 28 58 | 264 | |
| | | | | | | L thalamus | -2 -12 12 | 38 | 7.26 |
| | | | | | | L mesial frontal | -2 16 38 | 71 | 5.29 |
| | | | | | | L mesial frontal | -2 -12 40 | 37 | 5.30 |
| | | | | | | | | | 37 |
| | *Deact* | *Mesial frontal* | *0 72 20* | *8869* | *>8* | *R sup parietal* | *46 -58 52* | *2737* | *>8* |
| | | *R sup parietal* | *40 -76 40* | *7082* | *>8* | *post cingulate* | *6 -34 48* | *1661* | *7.48* |
| | | *L sup parietal* | *-48 -54 44* | *4725* | *>8* | *R front paracentral* | *-30 26 -20* | *126* | *6.81* |
| | | *L temporal* | *-66 -18 -20* | *641* | *7.61* | *L front paracentral* | *-26 58 10* | *231* | *6.74* |
| | | *L frontal paracentral* | *-2 58 -6* | *189* | *6.39* | *L frontal* | *-46 38 8* | *530* | *6.48* |
| | | *L pre frontal* | *40 20 44* | *217* | *6.23* | *L parietal (suprmarginal gyrus)* | *-64 -52 30* | *314* | *6.19* |
| 3) | Act | NIL | | | | NIL | | | |
| | *Deact* | *R parietal* | *-46 -80 34* | *1285* | *>8* | *Occipital cuneus(max)* | *4 -84 24* | *895* | *7.04* |
| | | *L parietal* | *48 -76 22* | *1380* | *7.36* | *L parietal* | *-48 -68 28* | *377* | *5.27* |
| | | *L orbitofrontal* | *-38 48 12* | *856* | *6.49* | *R frontal* | *-38 60 -8* | *313* | *5.89* |
| | | *R orbito frontal* | *28 60 12* | *329* | *6.37* | *R parietal* | *52 -68 28* | *174* | *5.52* |
| | | *Occipital cuneus* | *6 -76 22* | *346* | *6.09* | | | | |
| | | *R prefrontal* | *44 -6 42* | *61* | *5.43* | | | | |
| 4) | Act | R lateral ventricle | -26 -52 -6 | 328 | 7.74 | L caudate/ ventricle | -18 -14 26 | 6656 | >8 |
| | | L lateral ventricle | -20 -48 12 | 176 | 6.93 | Top of brain | -6 -22 82 | 279 | 7.04 |
| | *Deact* | *Widespread cortical deactivation, all lobes and cerebellum* | *0 74 20* | *165314* | *>8* | *Widespread cortical deactivation, all lobes and cerebellum* | *0 64 20* | *126584* | *>8* |

**Table 4-2 Single subject GSW associated BOLD activations and deactivations at 1.5 and 3T.**
**Details of main local maxima from SPM[t] of positive and negative HRF for the 1.5 and 3T BOLD fMRI sessions for each patient. 1.5T and 3T are shown side by side for comparison. The positive weighting on the HRF is denoted Act (activation), the negative Deact (deactivation), shown in italics. MNI coordinates, Z score and cluster size are given in each case. Act – activation, Deact – deactivation, L – left, R – right, MNI – Montreal neurological institute.**

### 4.4.3 GSW Perfusion

SPM analysis of the ASL-P and ASL-B series revealed areas of significant perfusion and BOLD change that were consistent with those derived from the 3T BOLD acquisition (figure 4.5). Patient 1 showed an increase in perfusion in mesial frontal areas and decreased perfusion in precuneus. Patient 2 showed decreases in perfusion in posterior parietal, posterior cingulate and frontal areas. Patient 3 had no significant perfusion change. Patient 4 showed widespread decrease in perfusion throughout the cortex involving posterior parietal, posterior cingulate and frontal areas with a frontal maximum. BOLD and perfusion changes are shown in figure 4.5.

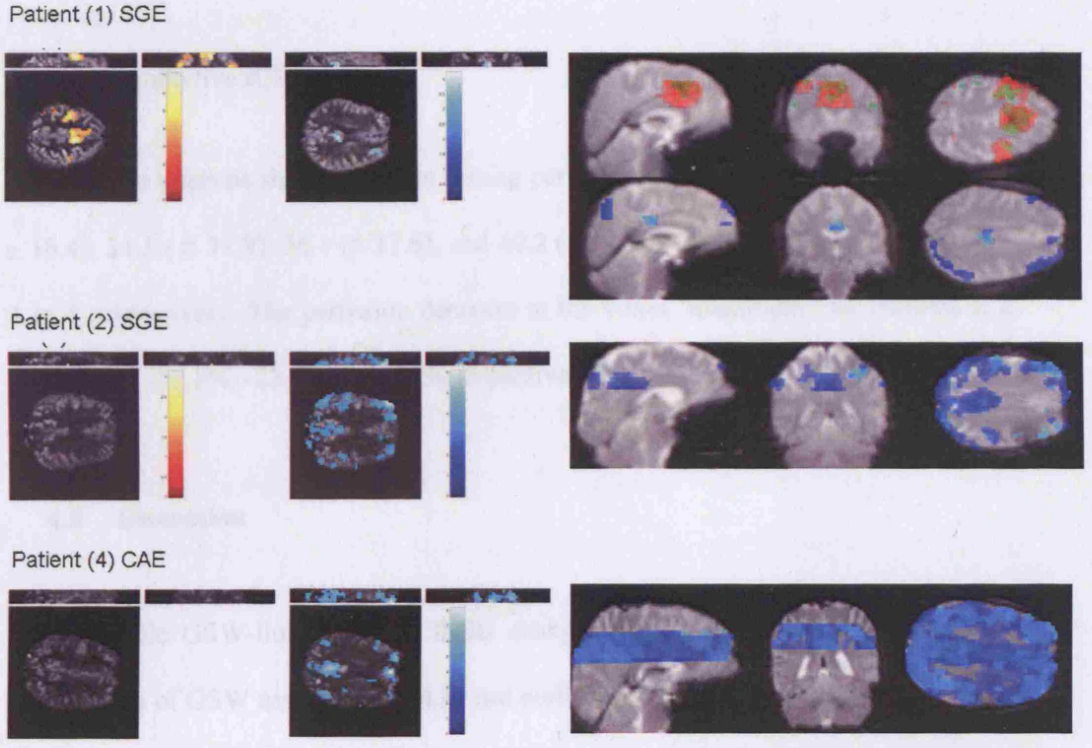


**Figure 4-5 Single subject GSW associated BOLD and CBF changes at 3T.**

**Left panel shows the SPM[t], positive (orange) and negative (blue) hrf of ASL-P cerebral blood flow during GSW. Right panel shows ASL-B, (BOLD derived from the perfusion images) activation in red and ASL-P (Perfusion changes to GSW) in green and deactivation ASL-B (blue) and ALS-P (cyan), overlaid onto the subjects EPI image demonstrating spatio-temporal correlation of BOLD and CBF.**

### 4.4.4 Quantitative rCBF

Quantitative analysis showed a mean resting perfusion across all 6 slices of 42.1 ( ± 16.4), 31.3 (± 17.9), 36.1 (± 17.6), and 40.2 ( ± 18.8) ml 100g-1 min-1 for patients 1 to 4 respectively. The perfusion decrease at the voxel 'maximum' for patients 1, 2 and 4 were -11.1%, -23.5% and -37% respectively.

## 4.5 Discussion

Reproducible GSW-linked BOLD fMRI changes were seen at 3T, with the spatial distribution of GSW associated BOLD and perfusion signal decreases, similar to those described in chapter 3. NBR were due to decreases in cerebral perfusion as shown by ASL-fMRI. The failure to see perfusion changes in patient 3 was likely due to the relatively low number of GSW epochs during recording. Quantification of perfusion images showed regional decreases of between 11% and 37% during GSW.

Cortical activations concordant with the electro-clinical diagnosis were seen in the 2 patients with SGE. In patient 1 the ictal semiology included ideational manifestations typical of prefrontal seizures suggesting orbitofrontal and anterior cingulate involvement [Niedermeyer and Lopes Da Silva 1998], the fMRI findings showed prefrontal activation. In patient 2 GSW had a left frontal onset, maximum at F3, in addition to independent left frontal discharges; the fMRI findings showed an area of left frontal activation and thalamic activation in addition to the widespread cortical deactivation.

The role of the thalamus is well established in GSW [Avoli *et al.* 2001]. Thalamic activation was seen in only one patient, (#2). The absence of thalamic activation in the

other cases may be due to a lack of sensitivity of fMRI to detect these changes. Alternatively changes in thalamic neuronal activity may have resulted in no overall correlated haemodynamic response that could be detected by fMRI.

Activation in ventricles was seen in patient 4, along with extensive cortical NBR. Suspicions of motion artefact are raised when such changes are seen, and such changes in this patient when studied at 1.5T gave some scepticism as to the validity of the results; however it is unlikely that such changes arise form gross head motion, without similar artefact seen at other tissue interfaces of brain surface. Ventricular activation in fMRI is not widely reported, although both here [Hamandi *et al.* 2006] and Gotman et al [Gotman *et al.* 2005] detected ventricular activation in fMRI group analyses of GSW. It is difficult to put this down to artefact from head motion, in that the patient did not report myoclonic jerks, and motion artefact was not evident on the simultaneously recorded EEG. Interscan motion as determined by the fMRI realignment pre-processing step, was small (<0.1mm) and we modelled variance due to motion as an effect of no interest in the analysis [Lund *et al.* 2005]. It is possible that the widespread decrease in cerebral perfusion in this case during GSW leads to an alteration in the extent of CSF pulsation, and hence ventricular wall motion that is correlated with our modelled GSW events.

The mean resting state cerebral perfusion across the whole volume in our subjects was similar to that reported in normal subjects [Garraux *et al.* 2005], and changes due to GSW of between 11 to 37% were of the same order of magnitude as cognitive and motor paradigms [Garraux *et al.* 2005] and those inferred from transcranial Doppler studies during GSW [Diehl *et al.* 1998;De Simone *et al.* 1998]. It has also been shown that the haemodynamic and metabolic responses appear preserved in response to interictal epileptiform activity [Stefanovic et al. 2005].

Extensive experimental evidence suggest that the main effect of GSW is one of cortical synchronisation, driven by reciprocal thalamo-cortical circuits [Meeren *et al.* 2002]. The BOLD and perfusion decreases seen here and by others were regionally specific involving the frontal, posterior parietal and posterior cingulate cortex. fMRI (de-)activations are only seen in areas were a measurable relative change in haemodynamics takes place. During rest areas of association cortex have a baseline level of activity which is interrupted by GSW, whereas areas of primary cortex, except for visual areas is already 'inactive' when the subject is lying still in the scanner; this may explain why primary cortical areas do not show deactivation. By contrast, areas of activation were in keeping with structures directly involved in the initiation of IEDs and seizure activity. Nersesyan et al [Nersesyan *et al.* 2004b] using simultaneous EEG and laser Doppler flowmetry found increases in CBF in somatosensory whisker barrel cortex during SWD in WAG/Rij rats, greater increases were seen during physiological stimulation and much greater increases during spontaneous and bicuculline induced generalised seizures. In animal models the majority of thalamocortical neurons are steadily hyperpolarized and inactive during cortically generated spike wave seizures, with cortical dis-facilitation or 'temporal absence of network activity' [Timofeev and Steriade 2004]. Our findings of preserved neurovascular coupling, are consistent with GSW-related NBR reflecting this decrease in neuronal activity [Shmuel *et al.* 2006].

A larger study may have added greater certainty regarding the reproducibility of GSW related BOLD changes, however difficulty was found in identifying patients with very frequent GSW particularly in IGE once appropriate treatment is commenced; as illustrated by patient 3 infrequent GSW events during scanning preclude an efficient

model for analysis of fMRI data. Patients recruited for this study were restricted to those with very frequent GSW to allow for ASL CBF measurements.

Objective assessment of sensitivity gains at 3T compared to 1.5T was not the primary aim of this study as this would be confounded by the intersession variability of BOLD-fMRI [Fera *et al.* 2004]. Nevertheless reproducible results were found in patients scanned at different field strengths on different days, up to four years apart. The perfusion changes were similar to the BOLD changes again showing consistency in results. There was however no obvious paradigm shift in going to 3T from 1.5 in these patients studied with EEG-fMRI.

## 4.6 Conclusion

BOLD fMRI changes to GSW in selected patients were reproducible after a long time interval. Perfusion measurements using ASL fMRI demonstrated that GSW associated NBR was attributable to a decrease in cerebral blood flow. This is likely due to a secondary effect of GSW on resting neuronal activity in the cortex. In selected patients with GSW of focal onset EEG-fMRI can identify this area of onset.

# 5 Chapter 5. Model Free TCA-fMRI

## 5.1 Abstract

Temporal clustering analyses (TCA) is an exploratory data driven technique that has been proposed for the analysis of resting fMRI to localise epileptiform activity without need for simultaneous EEG. Conventionally, fMRI of epileptic activity has been limited to those patients with subtle clinical events or frequent interictal epileptiform EEG discharges with simultaneous EEG recording from which a linear model is derived to make valid statistical inferences from the fMRI data. We sought to evaluate TCA by comparing the results with those of EEG correlated fMRI in eight selected cases. Cases were selected with clear epileptogenic localisation or lateralisation on the basis of concordant EEG and structural MRI findings, in addition to concordant activations seen on previous EEG derived fMRI analyses. In three, areas of activation were seen with TCA but none corresponding to the electro-clinical localisation or activations obtained with EEG driven analysis. Temporal clusters were closely coincident with times of maximal head motion. This is felt to be a serious confound to TCA; motion and physiological noise currently being impossible to isolate from epileptic activity on the basis of fMRI signal maxima alone. New techniques to localise epileptogenic activity with fMRI alone require validation with an appropriate independent measure. In the investigation of IED this is best done with simultaneous EEG recording.

## 5.2 Introduction and Aims

Analysis of fMRI data aims to identify areas of signal change associated with a task, stimulus or event of interest. The most commonly used analytical techniques are based on inferential statistics. In this a model of the expected signal change derived from a carefully designed experimental paradigm, or the timing of EEG events of interest, is fitted to and tested against the acquired fMRI data. The ability to simultaneously record good quality EEG with fMRI [Lemieux *et al.* 1997;Allen *et al.* 1998;Allen *et al.* 2000] allows this information to be obtained directly by visual inspection of the EEG. The occurrence of IEDs in patients with epilepsy, and detection on surface EEG, during the scan session therefore is central to this [Al Asmi *et al.* 2003;Krakow *et al.* 1999;Krakow *et al.* 2001]. The occurrence of events of interest is usually outside the control of the experimenter and determined only by patient selection and their resting state behaviour during scanning [Salek-Haddadi *et al.* 2003a]. In other words, 'experimental efficiency' can only be optimised through patient selection rather than experimental design. This limits patient selection to the relative few with frequent interictal discharges (ideally several per minute) that can be easily distinguished on the surface EEG. The recording of surface EEG spikes however, is dependent on the depth and a favourable dipole orientation of the electrical discharges and it is well known that frequent interictal discharges seen with intracranial depth electrodes are not always manifest on surface EEG [Niedermeyer and Lopes Da Silva 1998] confounding any linear model generated from surface EEG in these cases.

Data-driven fMRI analysis techniques, techniques that do not rely on the a priori specification of a model of the BOLD response, offer a theoretically attractive alternative to the above approach. Temporal clustering analyses (TCA) is one such

technique for obtaining activation maps when the timing of events of interest is unknown [Gao and Yee 2003;Liu *et al.* 2000;Yee and Gao 2002]. It is based on the premise that activation would cause the number of voxels reaching their individual maximum values at any given point, to rise beyond a certain threshold. It makes no assumptions with regards to the proximity of the voxels that constitute the clusters and is limited in that each voxel will reach its maximum only once in the time series. Using this approach, Morgan et al (2004) analysed resting state fMRI data in 9 patients with focal epilepsy in an attempt to localise areas of epileptiform activity, without concurrent EEG. Briefly, a histogram of the number of voxels reaching their signal maxima was plotted against time; the time points at which the number of voxels was greater than a pre-specified value (they used 100 which they subsequently found corresponded with approximately 2 standard deviations above the mean of the histogram) were taken as temporal clusters. The maxima were defined as between 102 and 110% of their baseline value over the entire time-course; we assume the rationale for this was to reduce motion effects. These 'TCA-events' were then used to perform a conventional event-related analysis using SPM99 (http://www.fil.ion.ucl.ac.uk/spm/). They investigated six patients with temporal lobe epilepsy at 1.5T, and three patients with extra temporal onset (2 frontal and 1 fronto-temporal) at 3T. A high degree of concordance between fMRI activations and electro clinical data was found, on the basis of which it was proposed that resting fMRI with temporal clustering analyses without EEG could localise epileptic activity. Whilst several analytical parameters, i.e. threshold values, definition of maxima, were selected without further justification the results of Morgan et al were striking in the concordance of fMRI activations with electro-clinical data. Their conclusion being that fMRI could detect fMRI activity without need for simultaneous EEG recording.

The following chapter describes the implementation and evaluation of TCA, as described by Morgan et al (2004), using fMRI data acquired with simultaneous EEG in patients with clearly defined focal epilepsy and frequent interictal discharges. In particular, a comparison was made between the TCA-derived and EEG-recorded events and motion was examined as a potential confound.

## 5.3 Material and Methods

*Data selection*

Eight patient sessions of previously acquired simultaneous EEG-fMRI were selected. Selection criteria included 1) patients with clear cut localisation/lateralisation on the basis of concordance between clinical seizures, EEG and structural MRI findings, and 2) concordant fMRI signal change was seen with EEG derived fMRI analyses (table 5.1) [Diehl *et al.* 2003;Lemieux *et al.* 2001;Salek-Haddadi *et al.* 2006].

*fMRI acquisition*

In seven subjects 700 (and in one 450) BOLD sensitive EPI images (TE/TR 40/3000, 21 x 5 contiguous, interleaved slices, FOV 24 x 24 cm, 64x64 matrix) had been acquired, with a 1.5T GE (Horizon Echospeed) MRI scanner with continuous, simultaneous EEG and ECG recording.

*EEG recording during fMRI*

The EEG had been recorded using in house equipment – the PA system, see methods.

*Data analysis*: Images were pre-processed using the SPM2. Images were slice-timing corrected, motion corrected using rigid-body registration [Friston *et al.* 1996], normalised to MNI template and smoothed with a Gaussian kernel (Full width at half maximum: 8mm). Linear detrending was then applied over the entire time series.

The TCA algorithm was implemented in C [script written by L Lemieux]. The methods, criteria and thresholds used by Morgan et al (2004) for TCA were adopted. For each volume, a histogram was constructed of the number of voxels reaching their maximum signal intensity. Signal maxima were taken as a signal increase of between 2% to 10% over the baseline value (initial value) as proposed by Morgan et al. (2004); temporal clusters (TCs) were taken as points that were above 2 standard deviations over the mean of the histogram. In the first instance TCA was applied to the entire fMRI time series. The TCA-derived time courses were visually compared with the fMRI time series motion realignment parameters generated from the rigid body motion correction during pre-processing, and the EEG. On visual inspection we noted close correlation between the TCA time courses and peaks in motion realignment parameters (see Results, fig 5.1). In light of this and in an attempt to make the acquisition time here more comparable with Morgan et (2004) who's fMRI sessions were 6 minutes, six-minute blocks containing least motion and occurrence of EEG events were selected, such that EEG events could be compared with TCA derived events. TCs thus derived - minus 5 seconds to account for the delay re-introduced by convolution with the haemodynamic response function (HRF) (although this was not done by Morgan et al it was felt crucial if one considers that the voxel maxima (TCs) from which onsets are derived already represent the BOLD signal) - were modelled as onsets in an event related design, convolved with the HRF and time derivative. The resulting SPM[F] were thresholded with a correction for multiple comparisons (family wise error correction, FWE < 0.05) [Friston *et al.* 1991]. The findings were compared with electro-clinical data and the statistical maps derived from the EEG-based fMRI analysis.

## 5.4 Results

Figure 5.1 shows time plots of the visually identified IEDs on the EEG recorded during the fMRI acquisition, temporal clusters obtained using TCA, and motion realignment parameters (fig 5.1).

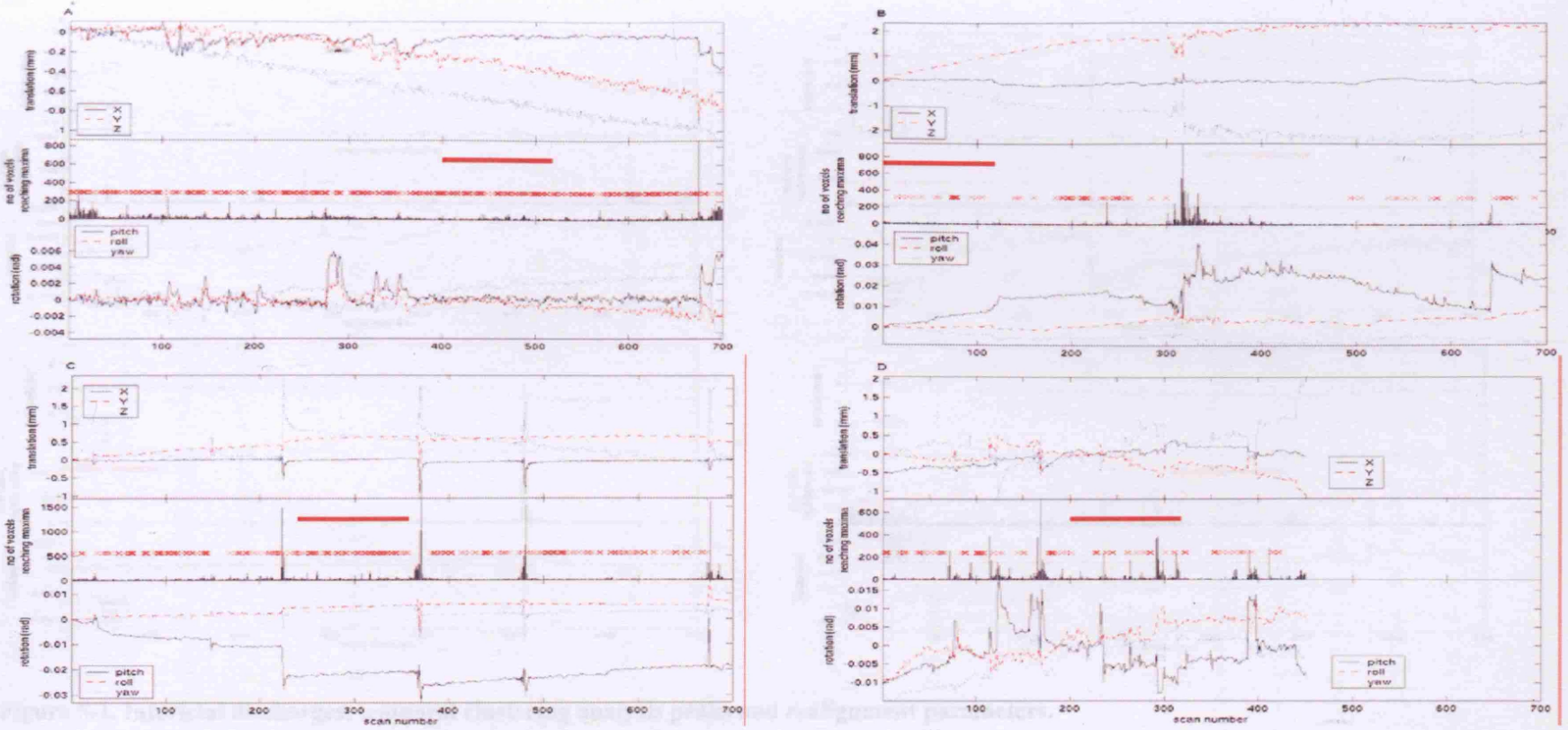
A
B
C
D
translation (mm)
X
Y
Z
no of voxels reaching maxima
rotation (rad)
pitch
roll
yaw
scan number

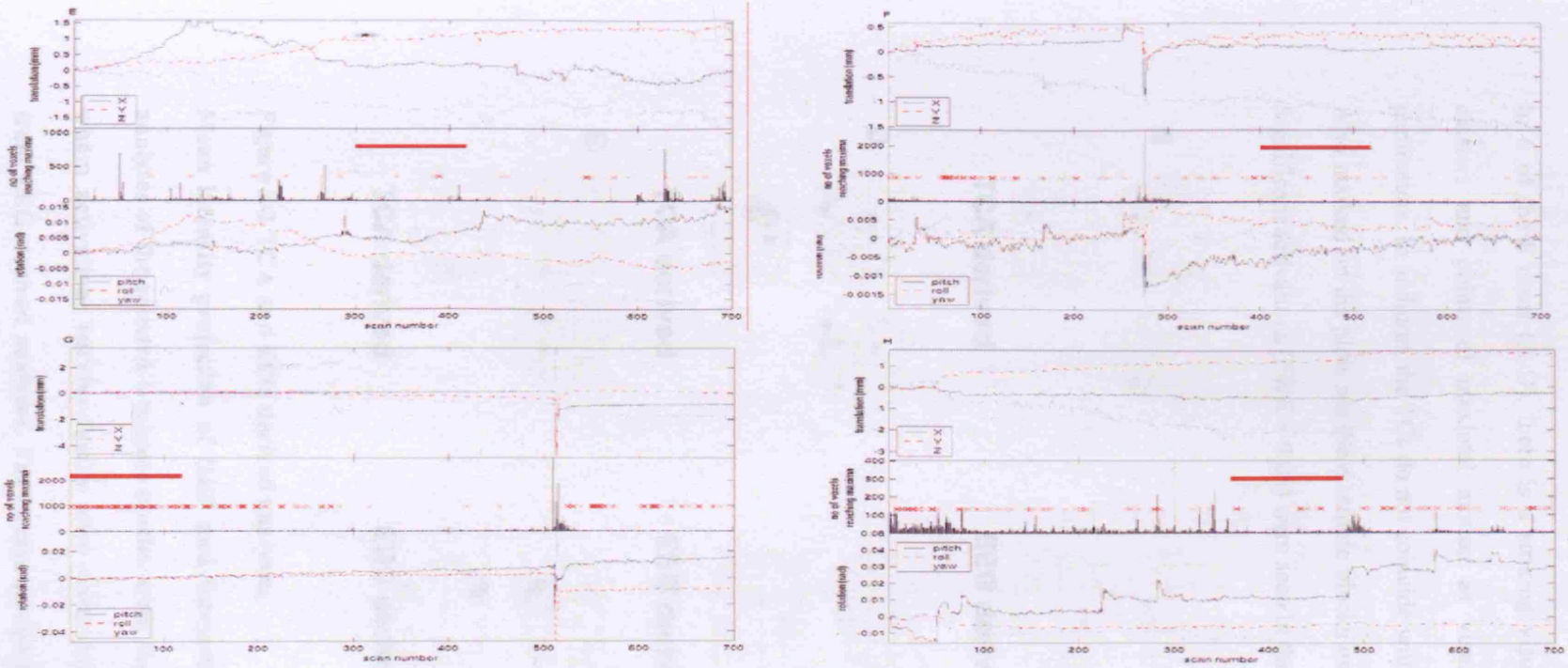

**Figure 5-1. Interictal discharges, temporal clustering analysis peaks and realignment parameters.**

**Plots from eight patients (A to H), showing points on the image time series, of visually identified EEG, against the realignment parameters and temporal clustering analysis histogram. Visually identified EEG events are marked with x. Realignment parameters (coloured lines) are generated in SPM2 from the 6 rigid body transformations in image time series realignment. Vertical black line are the histograms of TCA, the 2 standard deviation threshold is marked (.....), temporal clusters are taken as points above this line. The red bar is the 6 minute segment selected for the second TCA analyses.**

In 6 of the 8 cases (A-D), there is a striking visual correlation between temporal clusters and points of maximal motion as visualised on plots of realignment parameters. In addition, the TCs do not coincide with events identified from the EEG. Also marked on the plots are the 6 minute blocks used for the second TCA analyses. Significant activations (FWE = 0.05) were seen in three cases (figure 5.1).

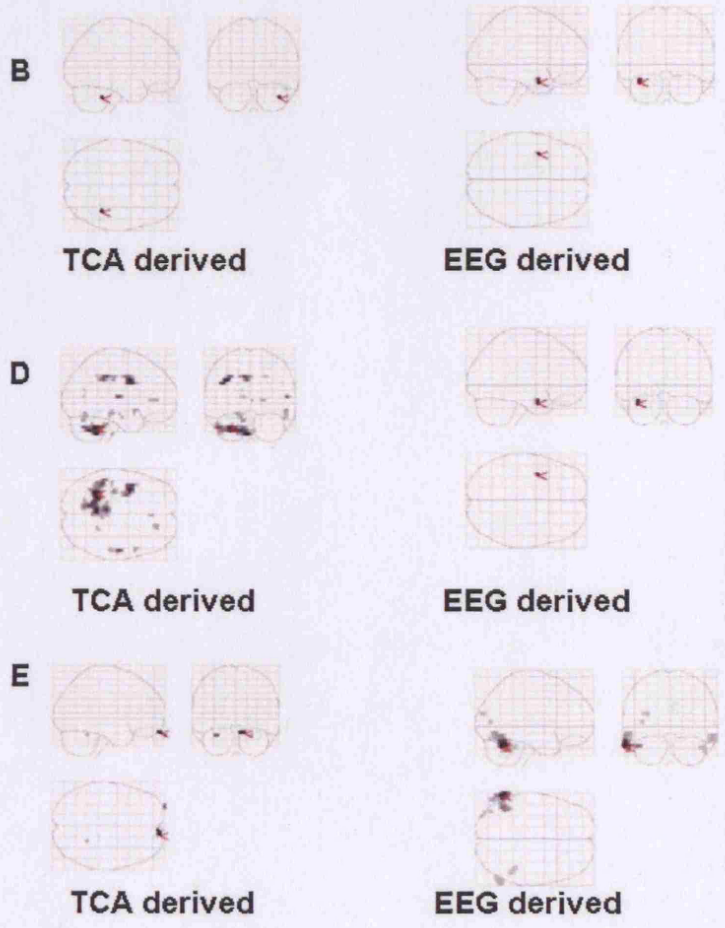


**Figure 5-2 TCA and EEG derived analyses.**

**Mean intensity projection of HRF and temporal derivative. SPMs from TCA analyses of the selected 6 minute blocks, from the three patients (B, D and E) in whom activations survive family wise error correction, compared with SPMs from EEG derived analyses. They demonstrate that activations can be detected**

**with TCA although the lack of concordance with electro-clinical data and their spatial distribution suggests they are artifactual (images thresholded FWE <0.05). Their localisation was remote from the presumed generator based on the electro-clinical data and the concordant statistical maps obtained using the linear regressor derived from the simultaneous EEG.**

| Patient | Electroclinical Lateralisation / Localisation | TCA derived fMRI Activation | Talairach coordinates | | | EEG derived fMRI activation | Talairach coordinates | | |
|---|---|---|---|---|---|---|---|---|---|
| | | | x | Y | Z | | x | y | z |
| A | L fronto-temporal | None | - | - | - | L temporal | -58 | -57 | 20 |
| B | L temporal | R cerebellum | 44 | -76 | -26 | L temporal | -37 | 1 | -20 |
| C | R fronto-parietal | None | - | - | - | R fronto-parietal, within MCD | 44 | -18 | 35 |
| D | R fronto-temporal | L cerebellum<br>L frontal<br>R parieto-temporal | -27<br>-45<br>67 | -80<br>-6<br>-40 | -20<br>49<br>0 | R frontal | 24 | 20 | 52 |
| E | bilateral posterior | midline inferior frontal | 1 | 45 | -6 | bilateral posterior | -64<br>47 | -60<br>-41 | -20<br>-23 |
| F | L temporal | None | - | - | - | L temporal | -56 | 4 | -26 |
| G | R frontal | None | - | - | - | R frontal,<br>R parietal<br>L cerebellum | 39<br>40<br>-28 | 19<br>-62<br>-71 | 41<br>47<br>-32 |
| H | L hemisphere | None | - | - | - | L temporal | -50 | -17 | -8 |

**Table 5-1. Electro-clinical localisation, EEG-fMRI derived and TCA derived activations.**

**Talairach coordinates derived from www.mrc-cbu.cam.ac.uk/Imaging/mnispace.html. (MCD – malformation of cortical development, L – left, R – right)**

## 5.5 Discussion

The aim of this study was to evaluate TCA as presented by Morgan et al [Morgan *et al.* 2004] based on their published methods in simultaneously acquired EEG-fMRI data. Their publication suggested that analysis of a relatively short fMRI recording (6 minutes) without simultaneous EEG could localise epileptogenic areas. The findings here indicate that theoretical and methodological shortcomings in the use of TCA, as proposed in detecting fMRI epileptiform activity, can lead to false activations. The cases used here were selected on the basis of having well defined focal epilepsy, in which "conventional" analysis of the fMRI data using EEG derived regressors had identified concordant activations [Salek-Haddadi *et al.* 2006]. This data should therefore facilitate comparison, in that spatially concordant fMRI activity is known to be present. The actual localisation of the epileptogenic zone, for example temporal vs. extra temporal should not affect the outcome of the method proposed. After comparison with electro-clinical data and the EEG-correlated fMRI findings, we failed to visualise interictal activity on fMRI using TCA in eight cases of focal epilepsy. In addition when the whole time series was analysed temporal clusters were closely correlated with motion events, and not IEDs, negating the validity of using these as epileptiform onsets in SPM analysis. On further visual inspection there is an apparent "inverse" correlation between TCs and EEG in some cases (see fig 5.1d), i.e. TCs are seen when no EEG events occur. This has arisen because at these times the EEG is obliterated by motion artefact, such that no EEG events are coded. TCs and EEG events are therefore mutually exclusive in instances where TCs relate to maximal motion which itself leads to an uninterruptible EEG at these points. Further,

TCs from the selected 6-minute blocks, chosen on the basis of least motion and occurrence of IEDs, when used in the analyses of fMRI data failed to detect activations concordant with electro clinical data or those obtained by GLM analysis of the whole thirty five minute session, but did result in discordant activations in three.

Head motion is a well known source of noise in fMRI and can lead to spurious activations [Field *et al.* 2000;Friston *et al.* 1996;Hajnal *et al.* 1994;Krings *et al.* 2001;Wu *et al.* 1997]. Anatomic regions that are most affected by susceptibility induced magnetic field inhomogeneities, and hence liable to motion artefact are those adjacent to bone or air, such as the mesial and inferior temporal lobes and the inferior and anterior frontal lobes, or around structural lesions [Hutton *et al.* 2002], increasing the possibility of false activations in these areas.

It is possible that the difference between these findings and those of Morgan et al is due to differences in the level of motion between the two groups. However, Morgan et al did not present any data on subject motion for comparison; in addition the degree of motion in the subjects studied here was not felt to be excessive. Further we selected 6 minute segments with least motion in an attempt to overcome this. The selection of the 2 – 10% increase from baseline (used to define the voxel maxima) which was adopted from Morgan et al may not have been suitable for this data. Although not specified as such this could be justified as a measure to exclude large signal changes due to motion. However no justification for the values Morgan et al used exists, therefore this could not be determined a priori and selection of alternative values or thresholds according to the outcome of analyses of the same dataset was not considered valid.

Again differences between the group presented here and those of Morgan et al could be argued to have resulted in the differences in results. The "gold standard" in localisation, of seizure resolution after surgery presented by Morgan et al (2004), was not present in these eight cases; however each patient was selected on the basis of clear localisation or lateralisation from concordant clinical information, structural MRI abnormalities and EEG changes, leaving little doubt as the site or side of epileptic activity. The second selection criterion of concordant fMRI activations detected by 'EEG modelled analysis' of these sessions was used to maximise the possibility of detecting this activity with TCA.

Three of eight cases presented by Morgan et al (2004) were scanned at 3T, it could be argued that with improved signal to noise TCA may be more robust, however it is increasingly recognised that the improvement in signal to noise at 3T is accompanied by a trade off with increased motion and physiological noise (Fera et al, 2004).

In addition to the potential vulnerability to signal changes associated with motion, there are a number of theoretical limitations of the proposed TCA approach as applied to the localisation of the generators of IEDs. 1) Voxels that reach local, periodic or repeated peaks of activity can only be assigned to one cluster (i.e. time point) per iteration, hence reducing sensitivity. Although methods have been proposed to overcome this using an iterative form of TCA [Gao and Yee 2003], the number of iterations is arbitrary and it is unclear whether large number of iterations are meaningful. 2) Different EEG sources cannot be separated since no spatial information is used for clustering (in contrast to EEG information used for event classification; see Diehl et al, 2003).

A more general criticism of TCA is that it uses data derived onsets as covariates, which can result in an underestimate of the noise in the data with an increased false

positive rate associated with the data-model-activation circularity. In addition the arbitrary definition and selection of maxima can result in variable parameters and thresholds; the detection of activations that "fit" prior pathophysiological hypotheses can therefore be misleading, particularly if fMRI brain coverage or slice orientation, is limited to or determined by regions of interest based on these same hypotheses. For example Morgan et al acquired 14 coronal slices (coverage 7 cm) through temporal lobes at 1.5 T in the temporal lobe group and 18 axial slices (coverage 12.6 cm) at 3 T in the extra temporal group. More complex mathematical strategies are required and have been proposed that characterise in greater detail the intrinsic structure of the data, for example independent component analyses (ICA) [McKeown *et al.* 1998;McKeown 2000].

To make a simple analogy to the non fMRI scientist, exploring voxel fMRI time series for epileptic spikes is analogous to looking at EEG disrupted by cardiac, respiratory and motion artefact with 64 x 64 x 47 = 192512 channels, albeit with spatial and temporal smoothing across these channels. The potential for false inferences is obvious.

## 5.6 Conclusion

The localisation of epileptiform activity with fMRI alone is theoretically compelling and would provide a powerful tool in localisation of epileptic activity; however novel fMRI analytical techniques need to be interpreted with some caution. In its present form TCA as described by Morgan et al was not successful in detecting BOLD changes due to epileptiform activity in cases with clearly defined localisation based on electro clinical and EEG-fMRI analyses. More sophisticated data-driven analyses

may well hold promise in epilepsy fMRI but would need to take good account of the sources of noise. This will require whole-brain coverage, predetermined analytical parameters, methods blind to electro clinical findings and validation with an independent measure i.e. concurrent EEG.

# 6 Chapter 6. EEG-fMRI of Focal Delta

## 6.1 Abstract

The majority of patients with epilepsy do not have frequent IEDs. Correlating other aspects of the interictal surface EEG with fMRI would allow clinical EEG-fMRI to be applicable to more than a highly selected group. Focal slowing on the EEG is a marker of underlying structural abnormality or epileptogenic focus. Eight patients with medically refractory focal epilepsy with focal slowing on surface EEG were studied with EEG-fMRI. Fluctuations in the delta frequency power were correlated with simultaneously recorded fMRI. In one patient with clear epochs of delta activity visual analysis of EEG was compared with an automated frequency analysis. This revealed similar findings of fMRI changes that likely reflected changes in resting brain activity, but not localising information relating to the epileptogenic zone. In the remaining patients, whilst focal slow activity was present it could not be visually coded into separate epochs. Automated frequency analysis of power fluctuations in the EEG delta band, correlated with fMRI, failed to detect any biologically meaningful changes in the simultaneously recorded fMRI data.

## 6.2 Introduction and Aims

The majority of patients with epilepsy do not have frequent IEDs. Correlation of frequency changes in the simultaneously recorded EEG may therefore provide a means for wider applicability of EEG-fMRI both in the study of the neurobiology of epilepsy and potential clinical localisation.

Focal brain abnormalities result in slowing in the overlying EEG channels. This has potential to be of localising value in focal epilepsy and may provide further avenues for analysis of EEG-fMRI data.

Delta activity is an abnormal finding in the awake adult EEG; found in any number of conditions, including structural, vascular, metabolic, infectious or epileptic abnormalities [Joynt *et al.* 1965;Gloor *et al.* 1977]. In essence focal slow is seen where there is underlying structural pathology, volume conduction, contralateral compression and transmission across commissural fibres. The pathophysiological basis of delta activity is not known. It is possible that deeply occurring IEDs, or rapid trains spikes are reflected at the surface as slow waves [Ajmone 1961]. Conversely focal slow waves can be recorded from lateral neocortical and medial temporal areas with subdural depth electrodes [Koutroumanidis *et al.* 2004].

In patients with focal epilepsy intermittent or persistent focal slow activity correlates with the area of interictal discharges [Vanrumste *et al.* 2005], the site of seizure onset as determined by epilepsy surgery [Jan *et al.* 2001], or from dipole modelling, at or near structural epileptogenic lesions [Huppertz *et al.* 2001].

In an unselected group Normand et al at the Mayo clinic found temporal intermittent delta in 33 records from 27 patients out of 12198 EEG records from a 1 year period. All those with intermittent delta had clinical seizures; with complex partial seizures, and focal temporal sharp waves in 23 [Normand *et al.* 1995]. Reiher et al found temporal intermittent delta in 45 of 127 recordings with from patients with complex partial seizures [Reiher *et al.* 1989]. Interictal delta activity appears commoner in temporal lobe epilepsy (TLE), found in 20% compared to 4% extra temporal epilepsy [Geyer *et al.* 1999]. Gambardella et al found ipsilateral delta activity in 51 of 56 TLE cases [Gambardella *et al.* 1995]. Panet-Raymond and Gotman found EEG

asymmetries that coincided with focal discrete lesions on MRI in 17 of 22 patients [Panet-Raymond and Gotman 1990]. Strong correlation between interictal regional EEG slowing and ipsilateral hypometabolism using 18FluoroDeoxyGlucose Positron Emission Tomography in patients with temporal lobe epilepsy has been found [Koutroumanidis *et al.* 1998a]; the severity of hypometabolism correlates with the amount of focal delta on the EEG [Altay *et al.* 2005]. Correlations of interictal temporal delta activity in temporal lobe epilepsy following resective surgery with pathology and outcome suggest that slow activity has a lateralising value similar to that of spiking activity [Koutroumanidis *et al.* 2004]. It was seen in patients with pathological lesions, but also those with normal imaging and non-specific pathological findings, suggesting that it is closely related to focal epileptogenesis, rather than merely a product of cortical deafferentation [Koutroumanidis *et al.* 2004].

EEG frequency analyses in EEG-fMRI have been used to show the BOLD correlates of normal brain rhythms - theta, alpha and beta [Laufs *et al.* 2003a;Laufs *et al.* 2003b;Bonmassar *et al.* 2002;Moosmann *et al.* 2003;Goncalves *et al.* 2006;Laufs *et al.* 2006b]. In a single patient with epilepsy and rhythmic delta there was spatial correlation between the delta activity associated BOLD response and the ictal onset zone as defined by intracranial EEG [Laufs *et al.* 2006a].

The aims of this study were to determine whether useful localising information could be obtained from EEG-fMRI analysis of EEG delta power fluctuations in particular the delta in patients with focal epilepsy.

## 6.3 Materials and Methods

*Patients*

Patients were selected from the epilepsy surgical programme at the NHNN, during 2005. The EEG reports of 59 patients with video telemetry for presurgical assessment were reviewed. In those where the report suggested a frequently occurring focal abnormality, the actual EEG recordings were reviewed; to assess the appearance and extent of these abnormalities. Patients who had obvious focal slow on visual inspection of the EEG record were selected. Eight patients were identified and attended for EEG-fMRI. Table 1 shows patient details.

*Data acquisition*

Simultaneous EEG and fMRI were acquired using the BrainProducts system (32 channel surface EEG cap) and a 3T horizon Echospeed scanner.

*MRI sequence*

GE Horizon Echospeed 3T, 47 slices, TE/TR 40 / 3000 ms, matrix 64 x 64, voxel size 3.75 x 3.75 x 2.5. 404 scans were acquired for each session; the first 4 were discarded to allow for T1 equilibration effects, leaving 20 minutes of data acquisition per session.

*EEG visual analysis*

All EEGs acquired during scanning were reviewed. Patient #2 had clear, distinct, left fronto-temporal delta activity, arising from background, often preceded by low amplitude spike. This case was used to compare and validate the EEG frequency analysis with the conventional EEG visual analysis. In this one case the EEG was visually coded, marking the start and stop of epochs of focal delta activity. These

were used in a boxcar design convolved with an HRF and its temporal derivative, according to the general linear model, treated in the same way as the epochs of GSW in chapters 3 and 4. In the other 7 patients no clear epochs of focal slow could be identified visually.

*EEG frequency analysis*

An automated frequency analysis of EEG-fMRI was employed using specified channels. One channel was selected on the basis of visually identified persistent or intermittent focal slow activity. Table 6.1 shows the channels used for analysis. A corresponding contralateral channel and two opposing distant channels were included in the analysis as a control for generalised changes in EEG frequency, e.g. due to alterations in vigilance, drowsiness or sleep.

The EEG was exported to the Matlab workspace using standard tools in the BrainProducts software.

*EEG-fMRI analysis*

A series of Matlab functions, developed and written in house (Helmut Laufs) [Laufs *et al.* 2006a] were used for analysis.

In addition to the manually coded analysis in one subject described above, two analyses were undertaken for each session, using the regressor as detailed below:

1) Power in the delta band 1-3Hz in a single bipolar channel of interest, selected on the basis of the patient's clinical EEG report, and visual inspection of the EEG acquired during scanning (see table 6.1),

2) power at frequency bands 1-3, 4-7, 8-12 Hz from each of the specified channels (table 6.1), in order to model potential confounding variance, for example EEG slowing due to drowsiness, or artefact in both the EEG and fMRI due to motion.

The realignment parameters and their polynomial expansion r, $r^2$, r-1 and $(r-1)^2$ were included in all analyses.

Data was high pass filtered at 128 Hz and autocorrelation function (AR1) applied.

An F-contrast for the effect of interest, i.e. focal slowing in the selected channel and t-contrasts for the positive and negative HRF was used to identify areas of BOLD correlation with changes in regional power variations in the selected frequency bands. Statistical parametric maps (SPMs) were thresholded at FWE <0.05.

| *Patient number* | *Diagnosis* | *AED* | *EEG* | *structural MRI* | *EEG from fMRI* | *Channels for analysis 1* | *Channels for analysis 2* |
|---|---|---|---|---|---|---|---|
| 1 | R-TLE | CLN TGB OXC | Anterior slow, intermixed frequent sharp and spike R: L 4:1. maximal F8 | Intrinsic abn R amygdala /uncus ?DNT | Rare R temporal spikes | n/a | n/a |
| 2 | L-F/TLE | CBZ PGB | generally slow, largely semi rhythmic theta frequent runs 2Hz delta bi-frontal L>R | NAD | Runs bilateral delta with intermixed spikes. L>R. | F3-F7 | n/a |
| 3 | R-TLE | CBZ LEV | R ant temporal intermittent slow and IEDs | R medial temporal astrocytoma | persistent R theta / delta | T8-P8 | T8-P8, T7-P7 FC1-CP1 FC2-CP2 |
| 4 | R-TLE | LEV | R temporal frequent runs of irregular theta and delta & sharpened theta waves | NAD | persistent R theta and delta | T8-P8 | T8-P8, T7-P7 FC1-CP1 FC2-CP2 |
| 5 | L-mTLE | OXC | L temporal frequent sharp waves and spike Intermixed underlying slow | L-HS | L slow | F7-T7 | F7-T7, F8-T8 FC1-CP1 FC2-CP2 |
| 6 | R-mTLE | LEV | sparse L posterior central alpha Persistent semi rhythmic theta R temporal with intermixed frequent sharp | R-HS | R temporal theta and delta | T8-P8 | T8-P8, T7-P7 FC1-CP1 FC2-CP2 |
| 7 | L-F/TLE | OXC PGB | L frequent delta and theta wide field, max antero-temporal, and frequent spikes and sharp waves | NAD | Runs left sharpened theta L>R, F7/T7 vs. F8/T8 | F7-T7 | F7-T7, F8-T8 FC1-CP1 FC2-CP2 |
| 8 | R-TLE | CBZ | Persistent R ant temp theta | R-HS | Persistent R temporal theta | F8-T8 | F8-T8, F7-T7 FC1-CP1 FC2-CP2 |

**Table 6-1. Clinical details of patients with intermittent focal slow activity.**
**Epilepsy localisation, medication at the time of the study, imaging and EEG findings.**
**TLE – temporal lobe epilepsy, mTLE – mesial temporal lobe epilepsy, F/TLE frontal or temporal (localisation not clear). CBZ – carbamazepine, CLN – clonazepam, LEV – leviteracetam, OXC – oxcarbazapine, PGB – pregabalin, TGB – tiagabine.**

## 6.4 Results

Visual inspection of EEG from the one patient (patient #1) scanned with the PA system found it to be of insufficient quality to warrant further frequency analysis, this case will not be considered further. Good quality EEG was recorded in all 7 cases acquired with the commercial BrainProducts system, with persistent or intermittent focal delta activity ipisilateral to the presumed epileptogenic lesion, as seen on routine and EEG telemetry recorded prior to the EEG-fMRI session.

Patient #2 was treated as a separate case in that the slow wave occurred in epochs clearly distinguishable from background (see figure 6.1). The start and stop of slow wave epoch were visually identified and marked and used as boxcar in the analysis of fMRI. The automated frequency analysis was then undertaken as described in the methods section.

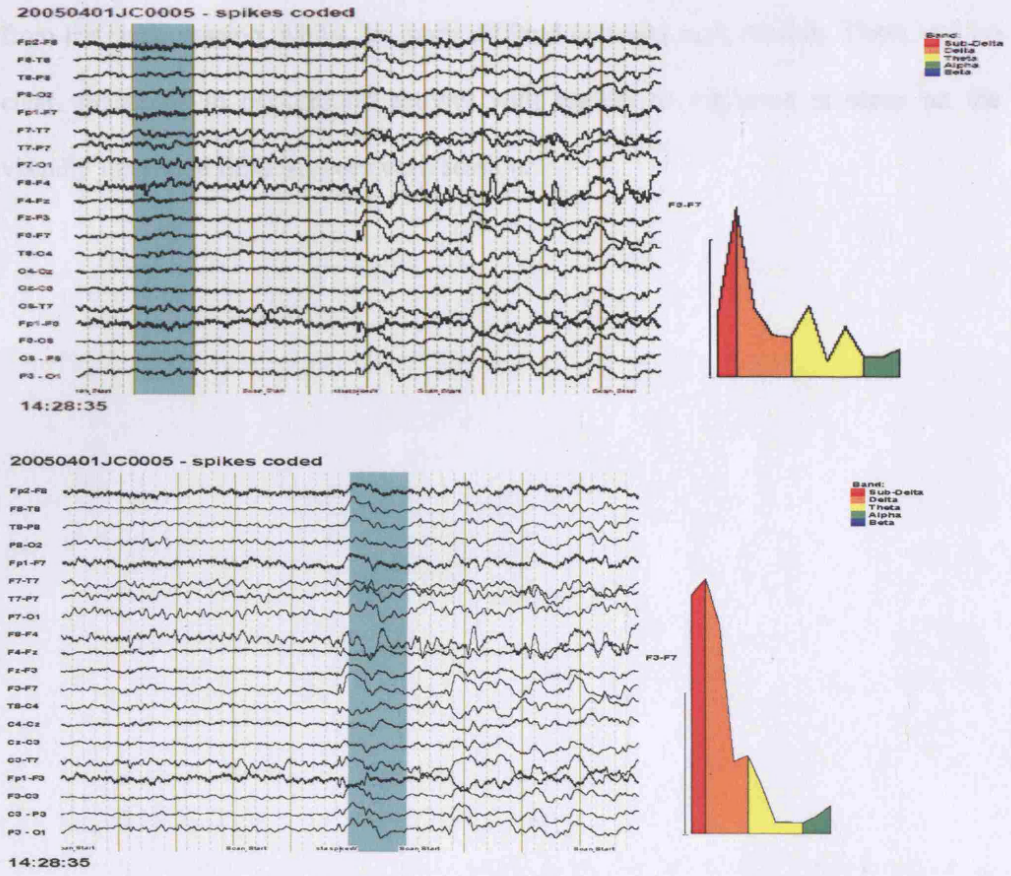


**Figure 6-1 Fronto-temporal delta on fMRI artefact corrected EEG.**

**From patient 1, on the right is the FFT of the 1 second epoch, marked with blue highlight. Normal background - upper tracing - and epoch of focal slow - lower tracing - showing increase of delta power and loss of alpha power in the lower tracing.**

Figure 6.2 shows the results from the visual analysis of EEG and the frequency analysis from each of the two recording sessions. Session 1 showed deactivation in mainly visual and to a lesser extent auditory cortex and activation in periventricular areas. Session 2 showed deactivation in bilateral posterior parietal, posterior cingulate and frontal areas, with areas of activation bilaterally in posterior frontal lobes. Similar

SPMs were obtained between the visually coded and automated frequency analysis from the same session, whilst the maps differed between each session. There was no clear difference in background activity with respect to vigilance or sleep on the visually inspected EEG between each session.

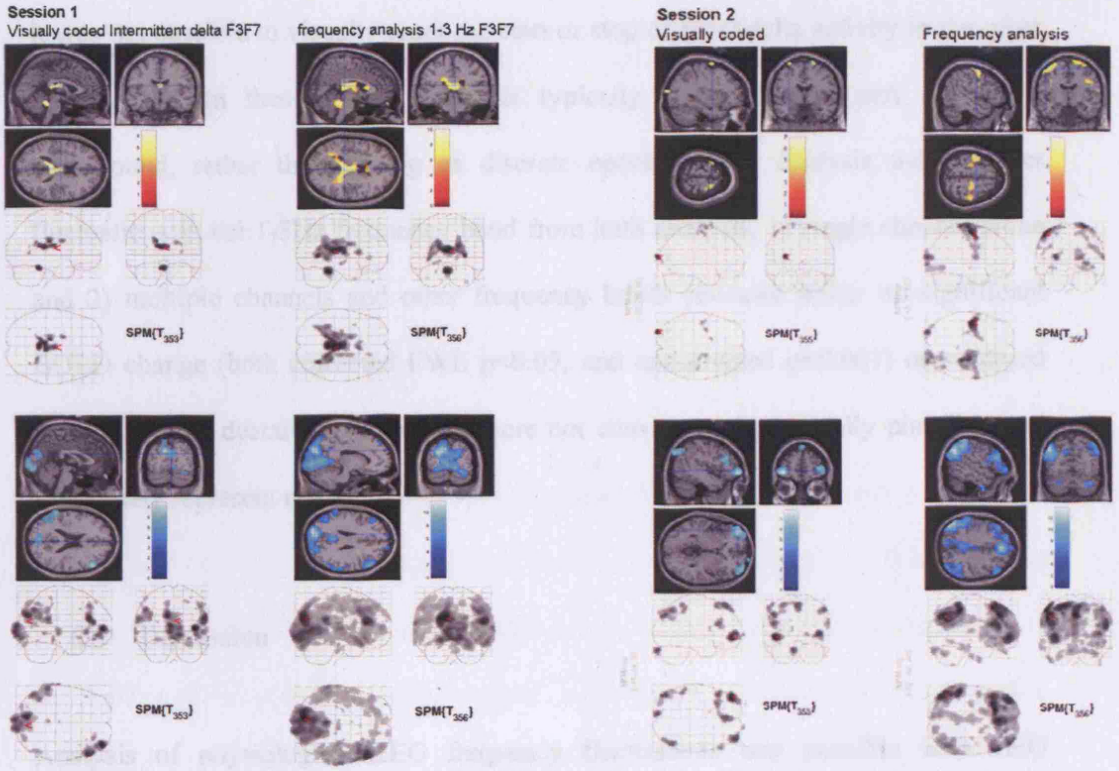


**Figure 6-2 BOLD response to focal delta activity.**

**SPM from patient #2, session 1 and session 2, on the left analysis using regressor from visual coding of EEG (start and stop of intermittent delta), on the right analysis using regressor of power fluctuations of 1-3Hz in channel F3-F7.**

**Session 1, upper panel (yellow) SPM[t] positive hrf, lower panel (blue) negative hrf, shows some periventricular activation and occipital, parieto-temporal and frontal deactivation. The distribution of BOLD changes is similar for both analysis methods; cluster size and significance levels are higher in the power band analysis compared to visually coded analysis.**

**Session 2, upper panel (yellow) SPM[t] positive hrf, lower panel (blue) negative hrf, shows posterior frontal activation, adjacent the central sulcus and characteristic bifrontal, biparietal and posterior cingulate deactivation. The distribution of BOLD changes is similar for both analysis methods; cluster size and significance levels are higher in the power band analysis compared to visually coded analysis.**

It was not possible to visually mark the start or stop of focal delta activity in the other six subjects. In these focal delta was typically persistent and part of resting background, rather than arising as discrete epochs. fMRI analysis using power fluctuations in the 1-3Hz frequency band from both analysis, 1) single channel alone and 2) multiple channels and other frequency bands revealed either no significant BOLD change (both corrected FWE $p<0.05$, and uncorrected $p<0.001$) or scattered activations and deactivations in that were not considered biologically plausible and most likely represent noise.

## 6.5 Discussion

Analysis of physiological EEG frequency fluctuations was possible with EEG recorded in the MRI scanner.

*Case 1*

In one case comparison of analysis using visually coded EEG and analysis of power fluctuations gave similar results with greater statistical significance in the latter. The resulting SPMs suggest changes in resting state brain activity.

*Deactivations*

The difference in findings between the two sessions is difficult to explain with only a single case; however it may represent different levels of alertness between the two sessions. In the first session, there is deactivation of visual and auditory cortices, it is possible that here the patient is more alert and primary cortex influenced by external stimuli, slow wave epochs whilst lying in the scanner therefore results in a decrease or interruption in areas that are most active, i.e. due to visual and auditory sensory input. In the second session the more characteristic decreases in areas of association cortex

were seen but no relative change in acitivity is seen in primary cortex. Independent visual review of EEG by two neurophysiologists and one senior EEG technician found no clear difference in background EEG between the sessions, to suggest drowsiness or sleep in either session.

*Activations*

The ventricular activation in session 1 is similar to the ventricular activations in GSW. It is suspected that this is due to haemodynamic changes in global cerebral blood flow, leading to greater variability in ventricular pulsation. In session 2 there was symmetrical activation in bilateral frontal areas with a left maximum. Whilst this is seemingly concordant with the left sided interictal discharge with bilateral spread seen on EEG; it should not be over interpreted however given the variability of results between these session and the other studies, see below.

*Cases 3 – 6*

There was no consistent BOLD change to suggest physiological activation or deactivation in the other cases. SPMs were inspected at both thresholds, corrected $p<0.05$ and uncorrected $p<0.001$. Using the current analysis strategy power fluctuations in the delta power band failed to detect fMRI activation in those with persistent focal slow activity.

To date most EEG-fMRI analysis in epilepsy, have used visually identified EEG epochs to model the simultaneously acquired fMRI data. An observational comparison of frequency power analysis and the visual analysis was possible here in a patient with distinct epochs of intermittent delta activity arising from background. The patient was scanned over two 20 minute sessions, the SPMs from each session were clearly different (figure 6.2), however there was close correlation between the visual and frequency coded analysis; with similarly located clusters of activation and

deactivation, but greater cluster size in the frequency analysis. The SPM from these two sessions show global BOLD changes, indicative of changes in resting state brain activity, rather than localisation of an epileptogenic focus. In session 1 deactivation is seen in occipital and auditory cortices, suggesting visual and auditory deactivation. There is ventricular activation likely due to global changes in cerebral blood flow and hence altered pulsation at the brain / CSF boundary. Session 2 shows bi-frontal and bi-parietal deactivation i.e. default mode networks. The reason for the difference in the SPMs from these 2 sessions is unclear.

*Limitations*

Case 1 provides a useful validation of the method, however the presence of clear fMRI changes in focal slow was only apparent in this one case where changes clearly arose from background. Focal slow in other cases was persistant without clear temporal demarcation in frequency changes.

The methods employed here were exploratory, but would have been justified by a more positive result. The basis of fluctuations in surface EEG rhythms is not known. As a result it is difficult to know how to model such fluctuations in fMRI data.

Whilst motion was modelled as a confounding covariate, other confounds, respiration, cardiac pulsation were not. It is possible that these confounding covariates shared frequency bands with the covariate of interest, although we would not have expected them to fluctuate to the same degree as epileptogenic or pathological EEG phenomena.

## 6.6 Conclusion

Power fluctuations in EEG frequency bands have been of some value in studying BOLD correlates of alpha rhythm, they did not appear useful in studying focal slow in most cases here. In one case findings suggest that BOLD responses of focal delta represent alterations in resting state brain function during changes in focal EEG. This is not surprising given that surface EEG reflects changes from extensive cortical areas, which are likely to have an influence on brain function as a whole. In essence fMRI is able to detect changes that stand out from a noisy background. It remains to be seen whether more sophisticated mathematical analyses of EEG can provide localising information on the neuronal populations driving abnormal focal changes. Possible avenues for future analysis include exploration of which channels / frequencies best explain variance at regions of interest, or using other measures, for example EEG coherence rather than frequency power band.

# 7 Chapter 7. A Combined EEG-fMRI and MR Tractography Study of Interictal Epileptic Activity.

## 7.1 Abstract

A patient with refractory left temporal lobe epilepsy and very frequent interictal discharges was studied with EEG-fMRI to identify areas of significant activation. A diffusion MRI sequence and probabilistic tractography were used to visualize connecting white matter tracts from a seed point at the location of fMRI activation. The EEG-fMRI demonstrated activation in the left temporal, parietal and occipital lobes in association with left anterior temporal IEDs. Tractography showed connections from the maximum temporal lobe activation to the occipital areas seen on fMRI, demonstrating possible pathways of IED propagation. EEG-fMRI correlated with tractography is a promising tool in investigating cerebral networks in epilepsy.

## *7.2* Introduction

Diffusion weighted MRI evaluates brain microstructure through the 3-D measurement of the passive diffusion of water molecules in tissue, from which connectivity between voxels can be inferred [Conturo *et al.* 1999;Parker *et al.* 2002]. The recent advent of probabilistic tractography algorithms allows the generation of maps of probability of connection from chosen start points [Parker *et al.* 2003;Parker and Alexander 2005], which can be displayed to visualize white matter tracts [Parker *et al.* 2002;Guye *et al.* 2003;Powell *et al.* 2005]. Combining fMRI and tractography

offers an opportunity to study the relationship between brain structure and function in vivo.

## 7.3 Methods

A 23 year old right handed man with refractory complex partial seizures since age seven was studied. Complex partial seizures lasting one to five minutes occurred every other day, and comprised a brief aura (in childhood an abnormal taste or smell, and currently of "abnormal feelings"), an inability to vocalise followed by unresponsiveness with right arm posturing and subsequent bimanual automatisms. Secondarily generalised seizures occurred twice weekly without aura, beginning with tonic extension of the right arm, then asymmetric clonic movements, right greater than left. Interictal EEG showed left antero-temporal excess slow activity and frequent left temporal spikes phase reversing at T3, with no other focal findings (figure 7.1).

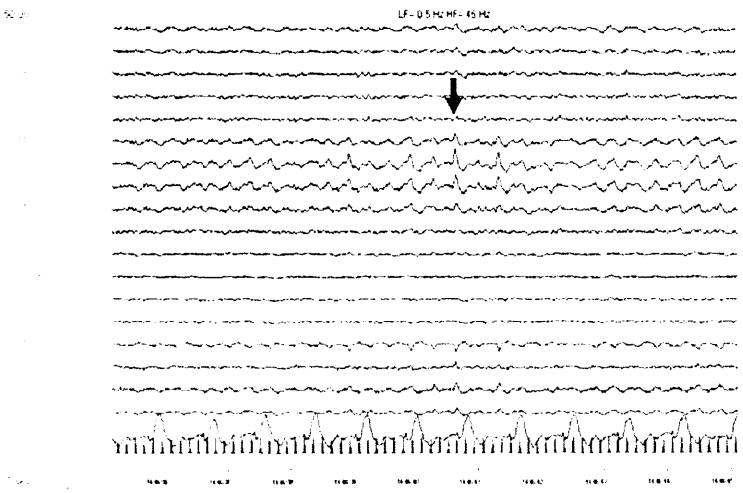

**Figure 7-1 Left temporal spikes on EEG recorded during fMRI scanning.**

**Bi-temporal chain, upper 10 channels referential to Pz, lower 10 bipolar montage) shows persistent left temporal theta with frequent intermixed spikes phase reversing at T3 (bold arrow). OSC channel "sticks" mark scanner gradient switching.**

Ictal video-EEG telemetry showed onset of seizure activity in the left temporal lobe, spreading rapidly to the frontal region and right temporal lobe. Structural MRI showed left hippocampal sclerosis and mild expansion of the left lateral ventricle with signal change in surrounding subependymal tissue.

*MR Imaging.* A GE Horizon echospeed 1.5T MRI scanner (Milwaukee, USA) was used.

*EEG.* Simultaneous EEG and fMRI were acquired over 35 minutes. Ten channels of EEG referenced to Pz and two channels ECG were recorded using the in-house (PA) recording equipment [Allen *et al.* 1998;Allen *et al.* 2000] (see General Methods).

*fMRI.* Seven hundred BOLD sensitive echo planar imaging (EPI) images (TE/TR 40/3000, 21 x 5 mm, interleaved axial slices, FOV 24 x 24 cm, 64x64 matrix) were acquired. An additional four images acquired at the start of each session were discarded to allow for $T_1$ equilibration effects. A vacuum head cushion was used to help secure the EEG leads, minimize motion, and improve patient comfort. SPM2 was used for all image preprocessing and analysis (www.fil.ion.ucl.ac.uk). Images were realigned and spatially smoothed (Gaussian kernel FWHM 8mm)

We used the timing of left temporal spikes (figure 7.1) convolved with the haemodynamic response function (HRF) and its temporal derivative in an event related analysis of the fMRI data. Realignment parameters, from the image realignment step were entered as confounds. The computed SPM[F] and SPM[t] were thresholded at $P < 0.05$ level (corrected for multiple comparisons)

*Tractography.* Whole-brain diffusion imaging data were acquired with a cardiac gated single-shot spin-echo EPI sequence (Wheeler-Kingshott et al., 2002), with TE = 95 ms, 96 x 96 acquisition matrix (reconstructed as 128 x 128), 22 x 22 cm field of view. Sixty contiguous 2.3 mm thick axial slices covering the whole brain were obtained, with a maximum b value of 1148 $mm^2$ $s^{-1}$ ($\delta$ = 34 ms, $\Delta$ = 40 ms, using full gradient strength of 22 mT/m) applied in each of 54 noncolinear directions, along with 6 non-diffusion weighted (b=0) volumes. The reconstructed voxel size was 1.72 x 1.72 x 2.3 $mm^3$. The diffusion data acquisition time for a total of 3600 images was approximately 25 min (depending on the heart rate).

The algorithm of Parker and Alexander [Parker and Alexander 2003] was applied to the diffusion imaging data to identify voxels where the single tensor model of diffusion fits poorly, in which case a mixture of two Gaussian densities was fitted [Alexander *et al.* 2001]. This allows up to two fiber populations to be modeled in any given imaging voxel. In voxels adequately characterized by the diffusion tensor a single fiber population was assumed. Fiber orientation probability density functions were then defined for each voxel for subsequent probabilistic tractography as described in [Parker and Alexander 2003].

The probabilistic index of connectivity (PICo) algorithm [Parker *et al.* 2003;Parker and Alexander 2003], was used, designed to incorporate multiple fibre populations to avoid ambiguities in voxels containing fibre crossings, to track the anatomical connections from the maximum temporal lobe activation obtained from the EEG-fMRI, thresholded at a connection probability of 0.01 [Toosy *et al.* 2004].

The SPM[t] positive HRF image from EEG-fMRI was resliced, reoriented and overlaid onto the b=0 image. A region of interest (ROI) of 31 voxels was drawn around the left mesial temporal fMRI BOLD activation (the temporal activation with

the highest z-score) using MRIcro (www.mricro.com). This was used as a seed region for the PICo tractography analysis (figure 2a). With the smoothing used in fMRI analysis, the ROI includes both grey matter and adjacent white matter, making tractography possible.

## 7.4 Results

There were 177 IED during the 35 minute EEG-fMRI session. Three distinct areas of activation were seen within the left temporal lobe, with maxima in the left parahippocampal gyrus, the left middle temporal gyrus and left superior temporal gyrus. Activations were also seen bilaterally in parietal, and occipital lobes (L>R) including the lingual gyrus (table 7.1 and figure 7.2). Tractography demonstrated connections from the left temporal ROI to the left occipital and orbito-frontal frontal areas (figure 7.2b).

| Region | Talairach Coordinates (voxels) | Cluster size | Z score |
|---|---|---|---|
| Temporal Lobe | | | |
| L Parahippocampal Gyrus | -32 -1 -20 | 1192 | >8 |
| L Middle Temporal Gyrus | -59 -20 -14 | 299 | 6.40 |
| L Middle Temporal Gyrus | -51 8 -31 | 101 | 6.66 |
| L Middle Temporal Gyrus | -46 -62 3 | 231 | 6.11 |
| L Superior Temporal Gyrus | -65 -17 3 | 301 | 5.78 |
| Parietal Lobe | | | |
| L Postcentral Gyrus | -22 -31 72 | 1720 | >8 |
| R Postcentral Gyrus | 48 -19 53 | 1204 | 7.77 |
| Occipital Lobe | | | |
| L Lingual Gyrus | -20 -58 1 | 6292 | 7.65 |
| R Inferior Occipital Gyrus | 28 -91 -4 | 69 | 5.81 |

**Table 7-1. BOLD activation to left temporal spikes.**

**Results of EEG-fMRI analysis giving Talairach coordinates (obtained using software 'mni2tal' (http://www.mrc-cbu.cam.ac.uk/Imaging/mnispace.html), Talairach labels (from Talairach Daemon (http://ric.uthscsa.edu/projects/talairachdaemon.html)) and Z scores of fMRI activations associated with interictal left temporal discharges, SPM[F], corrected $p<0.05$; extent threshold 50.**

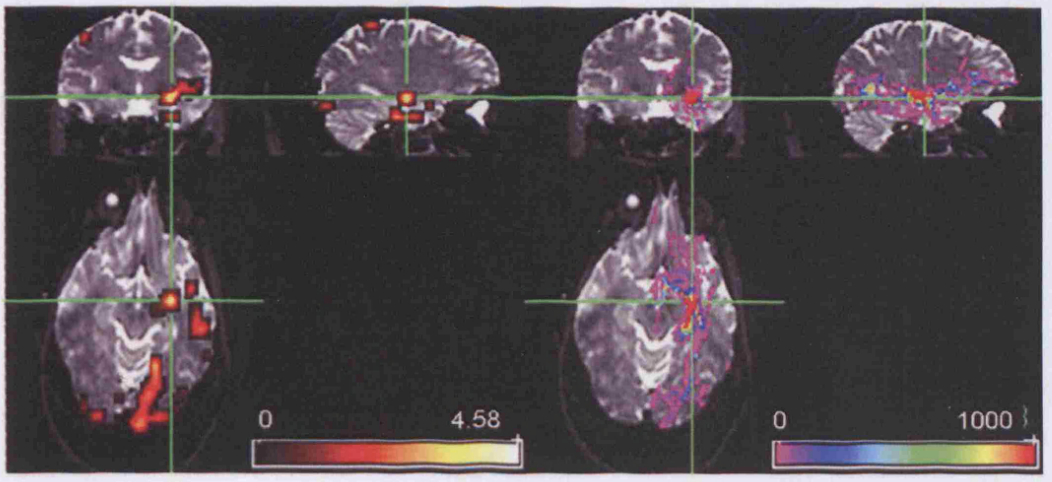


**Figure 7-2 EEG-fMRI activations and tractography from temporal activation. A) Significant anterior temporal IED-related fMRI activations SPM[T] overlaid onto structural echo planar image (b=0), showing left temporal and bilateral occipital fMRI activations. There were no significant deactivations. Scale represents z-score. (B) Tractography findings overlaid onto structural echo planar image, showing white matter connectivity to occipital and frontal areas. Cross hairs at left temporal fMRI maximum and the tractography seed region. The color bar represents a measure of connection probability or connection confidence to the start point. Figure created with MRIcro (http://www.sph.sc.edu/comd/rorden/mricro.html)**

## 7.5 Discussion

Using EEG-fMRI activations to left temporal spikes in left temporal lobe, bilateral parietal and bilateral (L>R) occipital lobes were found. Tractography seeded from the left mesial temporal fMRI maximum demonstrated strong probability of connection to the left occipital, and left orbito-frontal areas. The concordance between the occipital

fMRI activation and temporal-occipital connectivity seen on tractography was striking (figure 7.2). Tractography demonstrates the anatomy of white matter tracts and similar findings would have been seen in a normal subject. Tractography only shows the possible propagation pathways of neural activity; and it is noted that the tractography connection to the frontal lobe was not associated with fMRI activation in the frontal lobe.

Three distinct areas of activation were found (more than 8 mm apart) within the temporal lobe, involving the parahippocampal / hippocampal formation, the superior temporal gyrus and middle temporal gyrus. Well separated sources generating interictal discharges are seen with dipole modeling with propagation from a mesial to lateral temporal source [Baumgartner *et al.* 1995;Tao *et al.* 2005]. The temporal resolution of fMRI, although superior to other functional imaging modalities, cannot distinguish between the presumed primary mesial areas and those of propagation. There was no electro-clinical evidence to support occipital or parietal onset in our case; the clinical semiology, interictal EEG and ictal video EEG findings being consistent with left temporal onset. Areas of fMRI activation distant to the electro-clinically concordant areas are sometimes seen in EEG-fMRI studies [Al Asmi *et al.* 2003], and we propose that, in this study at least, these represent propagated effects from the left temporal lobe, passing via the observed white matter connections to occipital areas.

The propagation of IEDs from their source is well recognized [Baumgartner *et al.* 1995]. The concept of a network of epileptic activity rather than a single site of onset is gaining ground, with much of the evidence obtained from intercranial recordings [Spencer 2002]. Spencer proposes the existence of three specific large human epilepsy networks [Spencer 2002]. The first and most commonly recognised is the medial

temporal/limbic network, that includes the hippocampi, the amygdalae, the entorhinal cortices, lateral temporal neocortices and extratemporal components of the medial thalamus and inferior frontal lobes; the others proposed are a medial occipital/lateral temporal network and the superior parietal/medial frontal network. These network hypotheses cannot be readily applied to the patient studied here in the absence of ictal intracranial recordings, nevertheless the fMRI and tractography findings are in keeping with elements of the latter two networks proposed by Spencer.

MRI methods have two key advantages: they are non-invasive, and allow whole brain imaging of the correlates of interictal discharges, as opposed to the limited spatial sampling of inter-cranial recordings. This has to be set against the fact with fMRI, neural activity is inferred from an indirect measure - the haemodynamic response with its smoothed temporal response.

Tractography methods in healthy volunteers have demonstrated evidence for similar anatomical connections from the anterior parahippocampal gyrus to the occipital lobe [Powell *et al.* 2004] reflecting the inferior longitudinal fasiculus (ILF)[Catani *et al.* 2003]. The ILF passes to the superior, middle and inferior temporal gyri on the lateral surface of the temporal lobe and medially to the uncus/parahippocampal gyrus close to the amygdala and hippocampus [Catani *et al.* 2003]. MR-tractography is blind to the direction of neural propagation, and cannot distinguish between afferent and efferent pathways. The ILF most likely represents fast occipito-temporal access to allow associative processing of visual inputs and temporo-occipital projections that have neuromodulatory effects on the processing of visual stimuli [Morris *et al.* 1998;Pessoa *et al.* 2002].

Functional connectivity analysis of fMRI, for example with dynamic causal modeling (DCM) [Penny *et al.* 2004] may give further useful information regarding the propagation of IEDs.

## 7.6 Conclusion

The combination of fMRI and MR-tractography offers a unique technique for investigating cerebral networks, the advantages being imaging of whole brain activity and non-invasiveness, neither of these aspects are afforded by intracranial recordings. Further studies with corroborative evidence from intracranial recordings and post surgical outcome are needed to validate many of these findings.

# 8 Chapter 8. Discussion

## 8.1 Summary of Findings

Generalised Spike Wave

- GSW associated BOLD fMRI changes are seen in patients with idiopathic (IGE) and secondary generalised epilepsy (SGE)
- There were no clear syndrome specific changes between IGE and SGE or between IGE sub syndromes
- Changes were predominantly, but not exclusively of thalamic BOLD signal increase and cortical signal decrease predominantly in areas of association cortex
- BOLD signal decreases were shown to be due to decreased cerebral perfusion, indicating decreased neural activity either through inhibition or dis-facilitation most likely via thalamocortical circuits
- This decrease in cortical activity is in keeping with the clinical manifestation of absence seizures
- The occurrence of GSW events during scanning is a key limitation of these studies

Focal interictal discharges

- Visually coding IEDs is established in the analysis of EEG-fMRI data, a key limitation being the occurrence of IEDs during scanning, hence the need for methods not reliant on surface recorded IEDs if larger population studies are to be done.

- An alternative analytical strategy of fMRI data alone - temporal clustering analysis – was assessed and found to be prone to false positive errors - due to a circularity in the analysis methods - and correlated poorly with surface recorded IEDs.
- Frequency power analysis of simultaneously recorded EEG with fMRI is possible showing BOLD correlates of changes in resting state brain function; further work is required to determine whether this avenue can aid localisation of epileptogenic areas in focal epilepsy.

Main conclusions

- EEG-MRI allows inferences to be made about neurobiological correlates of EEG phenomena.
- In well selected patients there is concordance of fMRI activations and areas of presumed IED onset.
- The occurrence of interictal discharges in the scanner is currently the main obstacle to EEG-fMRI in epilepsy.
- Known and unknown variables confound fMRI data that at present are impossible to distinguish from true biological signal.
- Whilst carefully designed task based experiments can overcome the above obstacles a greater understanding of the fMRI signal and novel analytical techniques are needed to increase the applicability of EEG-fMRI to a wider population of patients with epilepsy and its use as a clinical tool.

Generalised spike wave activity is associated with decreased BOLD contrast in areas of association cortex. This finding is not syndrome specific and is seen in both idiopathic and secondary generalised epilepsies and with different GSW frequencies, between 2 and 4 Hz. This negative bold response (NBR) correlates with a decreased

cerebral perfusion measured using ASL-fMRI. This likely reflects decreased neural activity in these during GSW. In a number of cases thalamic activation is also seen. Thalamus has an established role in the generation of GSW. The reasons for a lack of thalamic activation in all cases remains unclear but is likely related to experimental efficiency and net metabolic thalamic activity. Comparison between patients studied at 1.5T and a small number at 3T suggests that there is no paradigm shift in the sensitivity of EEG-fMRI, despite the theoretical 4 fold increase in the signal to noise ratio for BOLD fMRI. This is likely due to the confounding effects of intersession variability – motion, physiological noise and other as yet unknown factors. This has also been corroborated by studies aiming for an objective assessment of sensitivity gains between 1.5 and 3T [Fera *et al.* 2004] and [Professor Robert Turner personal communication].

In selected patients EEG-fMRI to study the haemodynamic correlates of GSW is a robust technique, giving reproducible results over long time periods. SPM methods for analysis of EEG-fMRI data however is limited by the model needed for statistical analysis of the fMRI data. In essence this is dictated by the presence of frequently occurring (several per minute for the most efficient statistical models) visually identifiable IED on the surface EEG. Such patients, with active EEGs, of sufficient cognitive abilities to tolerate MRI scanning, or consent for research studies, are few and far between, even in specialist epilepsy centres. For these reasons, large case series with direct clinical applicability have not been demonstrated in the literature since the first descriptions of EEG-fMRI some ten years ago. Nevertheless studies to date have demonstrated a solid proof of principle, that haemodynamic correlates of ictal and interictal discharges are measurable and give localising value. None of the patients in this thesis underwent procedures to increase the frequency of IED. In

patients with idiopathic generalised epilepsy sleep deprivation and drug reduction can increase the frequency of GSW, however without clear clinical benefit to the patient this is difficult to justify ethically, given the potential risk of provoking a seizure. In focal epilepsy whilst drug reduction per se does not increase the frequency of IED, IED may increase after a seizure. Combining EEG-fMRI with pre-surgical monitoring, when patients antiepileptic drugs have been reduced with a view to recording a seizure, or increased IEDs, could therefore increase the yield of EEG-fMRI.

The following discussion highlights the issues that have been raised and conclusions that can be made from the work in this thesis.

## 8.2 General Methodological Considerations

### 8.2.1 fMRI and SPM

#### 8.2.1.1 Clinical Versus Cognitive Neuroscience

BOLD fMRI is qualitative rather than quantitative technique [Liu et al. 2004]. In the published literature fMRI is most commonly used in the field of cognitive neuroscience. Here the experimenter designs a task related paradigm performed by the subject in the scanner. Great efforts are put into such paradigm design to optimise the statistical efficiency of the analysis of fMRI data. Typically the experimenter seeks to answer a specific question about brain function, i.e. which area is involved in such and such task? and more recently investigations have begun into the interaction between areas and how activity in one area modulates the activity in another [Penny *et al.* 2004]. To answer such questions experiments are carried out on groups of subjects,

that ask if the population from which a particular set of subjects is drawn posses a particular effect, or if two populations differ in their response to an effect.

EEG-fMRI in epilepsy asks different sets of questions. Where and what type of brain activity causes surface EEG events or phenomena? Or alternatively can resting state fMRI be used to identify epileptogenic areas not visible on surface EEG? Can resting state fMRI be useful in the diagnosis or classification of epilepsy in a similar way to the surface EEG? Answers to the first question are reliant on the occurrence of these EEG events in the scanner within the frequency range that fMRI is most optimal. The cognitive neuroscientist attempts to circumvent the issues of fMRI noise by designing an experiment that operates within a frequency range outside that of fMRI noise, and / or negate the effects of fMRI noise by comparing two closely related tasks that differ only in the specific component of neural function under investigation. EEG-fMRI requires a greater understanding of the sources of fMRI noise and methods to successfully model these as covariates of no interest. A number of studies have addressed the issues of cardiac and respiratory noise [Liston *et al.* 2006b;Lund *et al.* 2006;Deckers *et al.* 2006] and their implementation in EEG-fMRI are likely to improve statistical analyses.

#### 8.2.1.2 Motion

Motion is a serious confound of fMRI [Hajnal *et al.* 1994]. Current strategies and those employed here involve a realignment pre-processing step, so that all volumes are within the same space. The translations and rotations derived from the realignment steps, and a Volterra expansion of them in the design matrix as covariates of no interest, increases the efficiency of the analysis [Lund *et al.* 2005]. However these strategies do not deal fully with the non-linear effects of subject motion on fMRI data; that include the spin history effects, magnetic field inhomogeneities and between slice

motion. Motion correlated with the task would tend to lead to false negative findings. A question that is often asked amongst neuroimaging researchers is how much motion is too much motion? (http://www.jiscmail.ac.uk/lists/spm.html). In much of the published literature researchers reject a dataset based on the extent or type of motion (eg sudden jerks); however such criteria can only be empirical. Similarly one might exclude an analysis on the basis of an unusual or artifactual appearing SPM. This was one of the difficulties with the GSW series, where ventricular activation lead to exclusion of a subject; however similar findings four years later on a different scanner suggest that the findings are a real effect that nevertheless remains difficult to interpret.

Advances in MRI physics may go some way to address these issues. New structural MRI sequences exist that apply a motion correction in k space, for example the propeller sequence from GE healthcare (www.gehealthcare.com/usen/mr/products/propeller_brainimg.html). Development of a similar process in fMRI acquisition could have a significant impact on the problem of confounding subject motion.

#### 8.2.1.3 Modelling Against Background

The majority of fMRI studies are designed such that a contrast is generated between two closely related tasks to avoid the problems of contrasting against a potentially variable baseline, for example reading real versus nonsense words. In most EEG-fMRI studies the EEG event of interest is modelled against background. Little work has been on the effect of variation in this background on fMRI, and its effect on EEG-fMRI analysis of epileptic activity. This is an important area that deserves further exploration.

#### 8.2.1.4 The Haemodynamic Response

The haemodynamic response is a temporally smoothed correlate of neural activity, peaking at around 4-6 seconds after a stimulus or action, returning to baseline, with an undershoot over approximately 30 seconds, gradually returning to the baseline. The sampling rate of fMRI in this thesis was 3 seconds (i.e. the TR). GSW initiation is likely to occur in the order of a few milliseconds [Lemieux and Blume 1986]. The sampling of a smoothed haemodynamic correlate of the order of several tens of seconds clearly presents inherent problems in trying to capture the onset and evolution of GSW. The contradictions that have arisen from functional imaging studies of GSW with activations seen in some, and predominantly deactivation in others most likely arise from this limited temporal resolution.

The possibility of directly detecting image contrast related to electrical neuronal activity with MRI is compelling. Several groups have shown the feasibility of the detecting ultra weak magnetic field changes with MRI i.e. similar to the order of magnitude of those induced by neuronal electrical current. Most of the work to date has taken place with phantoms. There are currently two theoretical models as how this can take place. 1) a phase change of proton magnetic signal results from neuronal firing that could feasibly be detected [Bodurka *et al.* 1999;Bodurka and Bandettini 2002;Konn *et al.* 2003]. 2) The magnetic field of neural current dipoles result in loss of phase coherence and hence decrease in signal magnitude [Xiong *et al.* 2003], in the similar way to BOLD contrast. The development of this technique remains at an early stage, it remains questionable whether the sensitivity of MRI can truly detect neural current, or whether it is in fact measuring some other phenomena such as components of the haemodynamic response, or cellular metabolic change, rather than neural electrical current

### 8.2.2 EEG

#### 8.2.2.1 EEG Acquisition

Acquisition of EEG during fMRI is now a well established research tool. There are a number of commercially available systems available, within an affordable price range for most medium to large research centres. During the work carried out for this thesis two EEG systems were used, one in-house system, the other commercially available, which used the same principle for dealing with scanner artefact. A number of methodological observations were made. The use of a vacuum head cushion improved patient comfort and the quality of the EEG. Subject motion within the scanner degrades the EEG to the extent that it is not possible to interpret. At 3T, EEG artefact was commonly encountered with the in house system. It was not possible to isolate the source of this artefact. The EEG cables, from electrode disc to the head box were approximately 2 metres long and were brought through the front of the scanner bore and thence to the head box. It was noted that minimal motion of the EEG cables (for example from scanner vibration, or draughts in the scanner room), was sufficient to degrade the EEG to make interpretation difficult. The BrainProducts system used a short (~50cm) flat ribbon cable that connected the cap to the head box / amplifier, through the back of the scanner bore. This was held secure by sandbags and cushions to reduce the effects of motion and vibration. EEG systems in high field MRI need the shortest possible cabling, that can be secured against motion or vibration. If EEG-fMRI had a wider clinical application then future advances could see MRI manufacturers producing MR compatible EEG systems tailored to their particular hardware.

#### 8.2.2.2 EEG Coding

Much of the work described in this thesis was based on the visual coding of EEG. Similarly the majority of publications that use EEG-fMRI to study epilepsy use similar visual coding for analysis. Inter observer variability was accounted for by having two EEGers, myself and a fellow researcher with EEG experience involved in defining the morphology of events and how they should be coded, in some cases after consultation with experienced neurophysiologists or EEG technicians. Patients were selected on the basis of stereotyped events clearly distinguished from background to minimize any ambiguity regarding EEG coding. Whilst published literature suggests a large degree of inter observer variation on clinical EEG this is unlikely in the clearly stereotyped pre-defined events used here.

Automated algorithms are being developed for EEG interpretation. Collaborative work with this thesis showed that automated algorithms can improve the efficiency of EEG-fMRI analyses [Liston *et al.* 2006a].

## 8.3 Inferences

It is worth considering again the methodological aspects of EEG-fMRI in comparison with 'conventional' paradigm driven fMRI. In a conventional fMRI experiment the subject undertakes a particular task, or is provided with a particular stimulus. Consequent fMRI changes can then be attributed to neural activity resulting from this experimental paradigm. By contrast, EEG-fMRI involves measuring two independent correlates of neural activity, the EEG and the BOLD signal. A statistical model derived from the EEG is used to analyse the fMRI data. From this we attempt to make inferences about the origin of the EEG activity. The primary aims of early EEG-fMRI

studies were to localise the irritative zone [Krakow *et al.* 1999;Patel *et al.* 1999]. However findings of subsequent EEG-fMRI studies [Al Asmi *et al.* 2003;Gotman *et al.* 2005;Hamandi *et al.* 2006;Salek-Haddadi *et al.* 2006] show activations and deactivations remote from the site of presumed epileptic activity in focal as well as generalised discharges. The pattern of deactivations is consistent with those seen in normal subjects referred to as the 'default mode', brain areas active during conscious rest. The term 'default mode' however presumes to explain the basis of these observed changes. It is preferable to consider these fMRI changes as alterations in activity in areas of association cortex during activities or states. In fact many use the term 'default mode' to refer merely to the spatial distributon of brain regions, without much functional inference. Three possibilities could explain changes in these areas during GSW, 1) they are involved in the generation of IED, 2) IED alters activity in these areas and 3) altered activity in these areas, for example an increase in drowsiness precedes, and leads to IEDs. Current fMRI studies lack the ability to distinguish cause and effect. To prove one of these hypotheses would probably require the whole brain sampling that fMRI offers, but with a temporal resolution on the millisecond scale.

## 9 Conclusion

EEG-fMRI shows novel information relating to interictal epileptic discharges and other EEG phenomena. In well selected cases with focal epilepsy EEG-fMRI shows localisation of brain areas from which these discharges are presumed to originate, however findings perhaps are far more complex, reflecting the fact that epileptic discharges are unlikely to originate form a single point in the brain. Whilst focal epileptic discharges and seizures may originate from a specific abnormal brain area, there are no doubt wider network areas involved in their generation and interaction.

The temporal resolution of fMRI, whilst far superior to the imaging modalities of PET and SPECT, remains several orders of magnitude higher than the few milliseconds of neuronal activity. More sophisticated modelling techniques and combining information with MEG may provide answers to these problems.

Debate continues as to the origin of GSW discharges despite many decades of neurophysiological basic science research in this area. At present EEG-fMRI does not have the temporal resolution to distinguish a thalamic from cortical onset. In addition EEG-fMRI most likely shows the effect of discharges on resting brain function. This is interesting from a cognitive neuroscience perspective but such changes are a potential confound to identifying epileptic activity. Further work is required to determine whether there are unique BOLD signatures of epileptic versus normal brain activity.

The signal to noise ratio of fMRI necessitates simultaneous recording of EEG for modelling of epileptic activity. Exploratory fMRI analysis should be treated with caution particularly if clinical decisions are anticipated from the results. At present EEG-fMRI has unproven sensitivity, specificity and reproducibility to make it a clinical tool. These three parameters are difficult to measure. The main constraint on EEG-fMRI is the occurrence of IED events in the scanner; this in turn is determined by patient selection. Further, if EEG-fMRI offered direct clinical benefit to the individual patient under investigation, reducing antiepileptic drugs or using other measures to provoke discharges would be ethically acceptable. Such measures would be likely to increase the yield of any EEG-fMRI study. Modelling of other aspects of the interictal EEG, for example abnormal EEG slowing would also increase the yield of EEG-fMRI.

## 9.1 Future Work

Future EEG-fMRI studies would benefit from additional physiological measures during the study. This would include respiratory rate, using a respiratory belt, and possibly expired $CO_2$ to assess ventilatory status. Cardiac and respiratory confounds should be modelled and analytic tools are now freely available for this. A video camera, possibly with an eye tracker, synchronised with the EEG-fMRI acquisition would provide accurate information on eye movement, eye opening and any possible subtle clinical correlate of IEDs.

Modelling EEG frequency changes as 'baseline' changes in fMRI signal due to changes in physiological brain states, may improve sensitivity. In conjunction with this a systematic examination of the relationship between frequencey changes on the EEG and fMRI as a result of motion, drift and machine noise are necessary.

Combining BOLD with ASL fMRI with whole brain coverage will allow more precise measurement of the temporal evolution of blood flow. Repeat studies at time intervals in a larger number of patients with GSW will give greater confidence in the conclusion, that BOLD changes to GSW are patient specific.

Further advances in both electrophysiology and MRI technology are inevitable. Simultaneous intracranial EEG with fMRI has been carried out in rats and monkeys, without reports of adverse incidents related to EEG in the MRI environment. Safety studies are already underway for the use of intracranial EEG with fMRI in humans, as well as MRI of patients with implanatable brain stimulators. A number of international centres have open intraoperative MRI in neurosurgical operating theatres with fMRI capabilities. Intrcranial electrodes exist that allow single cell recordings that have been applied to study higher cortical functions in patients undergoing monitoring for epilepsy surgery. The combination of electrophysiological and fMRI

techniques therefore offers enormous potential in understanding human brain function in health and disease.

# 10 Appendices

## 10.1 Appendix 1. ILAE Classification of Seizures

**Partial seizures beginning locally**

- Simple (consciousness not impaired)
  - With motor symptoms
  - With somatosensory or special sensory symptoms
  - With autonomic symptoms
  - With psychic symptoms
- Complex (with impairment of consciousness)
  - Beginning as simple partial seizure (progressing to complex seizure)
  - Impairment of consciousness at onset
  - a) Impairment of consciousness only
  - b) With automatism

**Partial seizures becoming secondarily generalised**

**Generalised seizures**

- Absence seizures
  - Typical
  - Atypical
- Myoclonic seizures
- Clonic seizures
- Tonic seizures
- Tonic-clonic seizures
- Atonic seizures

## 10.2 Appendix 2. ILAE Classification of Epileptic Syndromes and Epilepsies

**Localisation related (local, focal, partial) epilepsies and syndromes**

Idiopathic (with age related onset)
- Benign childhood epilepsy with centrotemporal spikes
- Childhood epilepsy with occipital paroxysms
- Primary reading epilepsy

Symptomatic
- Chronic progressive Epilepsia partialis continua
- Syndromes characterised by seizures with specific modes of precipitation
  - Temporal lobe epilepsies
  - Frontal lobe epilepsies
  - Parietal lobe epilepsies
  - Occipital lobe epilepsies
- Cryptogenic

**Generalised epilepsies and syndromes**

Idiopathic (with age related onset)
- Benign neonatal familial convulsions
- Benign myoclonic epilepsy in infancy
- Childhood absence epilepsy
- Juvenile absence epilepsy
- Juvenile myoclonic epilepsy
- Epilepsy with generalised tonic clonic seizures on wakening
- Other generalised idiopathic epilepsies
- Epilepsies with seizures precipitated by specific modes of action

**Cryptogenic or symptomatic**
- West syndrome
- Lennox-Gastaut syndrome
- Epilepsy with myoclonic-astatic seizures
- Epilepsy with myoclonic absences
- Early myoclonic encephalopathy
- Early infantile epileptic encephalopathy with burst suppression
- Other symptomatic generalised epilepsies, Non-specific aetiology

**Specific syndromes**
- Epileptic seizures complicating other diseases
- Epilepsies and syndromes undetermined whether focal or generalised
- Neonatal seizure
- Severe myoclonic epilepsy of infancy
- Epilepsy with continuous spike and slow waves during slow wave sleep
- Acquired epileptic aphasia
- Other undetermined epilepsies without unequivocal generalised or focal features

**Special syndromes**
- Situation related seizures, febrile convulsions
- Isolated seizures or isolated status epilepticus
- Seizures occurring only with acute metabolic or toxic events

## 11 References

Reference List


1. Abou-Khalil BW, Siegel GJ, Sackellares JC, Gilman S, Hichwa R, Marshall R. Positron emission tomography studies of cerebral glucose metabolism in chronic partial epilepsy. Ann Neurol 1987; 22: 480-486.

2. Aghakhani Y, Bagshaw AP, Benar CG *et al.* fMRI activation during spike and wave discharges in idiopathic generalized epilepsy. Brain 2004; 127: 1127-1144.

3. Aghakhani Y, Kobayashi E, Bagshaw AP *et al.* Cortical and thalamic fMRI responses in partial epilepsy with focal and bilateral synchronous spikes. Clin Neurophysiol 2005.

4. Aguirre GK, Detre JA, Zarahn E, Alsop DC. Experimental design and the relative sensitivity of BOLD and perfusion fMRI. NeuroImage 2002; 15: 488-500.

5. Aguirre GK, Zarahn E, D'Esposito M. The variability of human, BOLD hemodynamic responses. Neuroimage 1998; 8: 360-369.

6. Ajmone MARS. Electrographic aspects of "epileptic" neuronal aggregates. Epilepsia 1961; 2: 22-38.

7. Al Asmi A, Benar CG, Gross DW *et al.* fMRI activation in continuous and spike-triggered EEG-fMRI studies of epileptic spikes. Epilepsia 2003; 44: 1328-1339.

8. Alarcon G, Guy CN, Binnie CD, Walker SR, Elwes RD, Polkey CE. Intracerebral propagation of interictal activity in partial epilepsy: implications for source localisation. J Neurol Neurosurg Psychiatry 1994; 57: 435-449.

9. Alexander AL, Hasan KM, Lazar M, Tsuruda JS, Parker DL. Analysis of partial volume effects in diffusion-tensor MRI. Magn Reson Med 2001; 45: 770-780.

10. Allen PJ, Josephs O, Turner R. A Method for Removing Imaging Artifact from Continuous EEG Recorded during Functional MRI. NeuroImage 2000; 12: 230-239.

11. Allen PJ, Polizzi G, Krakow K, Fish DR, Lemieux L. Identification of EEG Events in the MR Scanner: The Problem of Pulse Artifact and a Method for Its Subtraction. NeuroImage 1998; 8: 229-239.

12. Altay EE, Fessler AJ, Gallagher M *et al.* Correlation of severity of FDG-PET hypometabolism and interictal regional delta slowing in temporal lobe epilepsy. Epilepsia 2005; 46: 573-576.

13. Anami K, Mori T, Tanaka F *et al.* Stepping stone sampling for retrieving artifact-free electroencephalogram during functional magnetic resonance imaging. NeuroImage 2003; 19: 281-295.

14. Anami K, Saitoh O, Yumoto M. Reduction of ballistocardiogram with a vacuum head-fixating system during simultaneous fMRI andmulti-channel monopolar EEG recording. Int. Congr. Se. 1232. Recent Adv Hum Brain Mapp 2002; 1232: 427-431.

15. Andermann F, Berkovic SF. Idiopathic generalized epilepsy with generalized and other seizures in adolescence. Epilepsia 2001; 42: 317-320.

16. Archer JS, Abbott DF, Waites AB, Jackson GD. fMRI "deactivation" of the posterior cingulate during generalized spike and wave. NeuroImage 2003a; 20: 1915-1922.

17. Archer JS, Briellman RS, Abbott DF, Syngeniotis A, Wellard RM, Jackson GD. Benign epilepsy with centro-temporal spikes: spike triggered fMRI shows somato-sensory cortex activity. Epilepsia 2003b; 44: 200-204.

18. Archer JS, Briellmann RS, Syngeniotis A, Abbott DF, Jackson GD. Spike-triggered fMRI in reading epilepsy: Involvement of left frontal cortex working memory area. Neurology 2003c; 60: 415-421.

19. Ashburner J, Friston KJ. Nonlinear spatial normalization using basis functions. Hum Brain Mapp 1999; 7: 254-266.

20. Assaf BA, Ebersole JS. Continuous source imaging of scalp ictal rhythms in temporal lobe epilepsy. Epilepsia 1997; 38: 1114-1123.

21. Attwell D, Iadecola C. The neural basis of functional brain imaging signals. Trends in Neurosciences 2002; 25: 621-625.

22. Avoli M, Rogawski MA, Avanzini G. Generalized epileptic disorders: an update. Epilepsia 2001; 42: 445-457.

23. Bagshaw AP, Aghakhani Y, Benar CG *et al.* EEG-fMRI of focal epileptic spikes: analysis with multiple haemodynamic functions and comparison with gadolinium-enhanced MR angiograms. Hum Brain Mapp 2004; 22: 179-192.

24. Bandettini PA, Wong EC, Hinks RS, Tikofsky RS, Hyde JS. Time course EPI of human brain function during task activation. Magn Reson Med 1992; 25: 390-397.

25. Barkley GL. Controversies in neurophysiology. MEG is superior to EEG in localization of interictal epileptiform activity: Pro. Clin Neurophysiol 2004b; 115: 1001-1009.

26. Barkley GL. Controversies in neurophysiology. MEG is superior to EEG in localization of interictal epileptiform activity: Pro. Clin Neurophysiol 2004a; 115: 1001-1009.

27. Bartenstein PA, Duncan JS, Prevett MC *et al.* Investigation of the opioid system in absence seizures with positron emission tomography. J Neurol Neurosurg Psychiatry 1993; 56: 1295-1302.

28. Baumgartner C. Controversies in clinical neurophysiology. MEG is superior to EEG in the localization of interictal epileptiform activity: Con. Clin Neurophysiol 2004; 115: 1010-1020.

29. Baumgartner C, Lindinger G, Ebner A *et al.* Propagation of interictal epileptic activity in temporal lobe epilepsy. Neurology 1995; 45: 118-122.

30. Benar CG, Gross DW, Wang Y *et al.* The BOLD response to interictal epileptiform discharges. NeuroImage 2002; 17: 1182-1192.

31. Benbadis SR, Pallagi J, Morris GL, Collier BD, Hellman RS. Ictal SPECT findings in typical absence seizures. Journal of Epilepsy 1998; 11: 187-190.

32. Berkovic SF, Andermann F, Andermann E, Gloor P. Concepts of absence epilepsies: discrete syndromes or biological continuum? Neurology 1987; 37: 993-1000.

33. Berkovic SF, McIntosh AM, Kalnins RM *et al.* Preoperative MRI predicts outcome of temporal lobectomy: an actuarial analysis. Neurology 1995; 45: 1358-1363.

34. Bode H. Intracranial blood flow velocities during seizures and generalized epileptic discharges. Eur J Pediatr 1992; 151: 706-709.

35. Bodurka J, Bandettini PA. Toward direct mapping of neuronal activity: MRI detection of ultraweak, transient magnetic field changes. Magn Reson Med 2002; 47: 1052-1058.

36. Bodurka J, Jesmanowicz A, Hyde JS, Xu H, Estkowski L, Li SJ. Current-induced magnetic resonance phase imaging. J Magn Reson 1999; 137: 265-271.

37. Bonmassar G, Purdon PL, Jaaskelainen IP *et al.* Motion and ballistocardiogram artifact removal for interleaved recording of EEG and EPs during MRI. NeuroImage 2002; 16: 1127-1141.

38. Boor S, Vucurevic G, Pfleiderer C, Stoeter P, Kutschke G, Boor R. EEG-related Functional MRI in Benign Childhood Epilepsy with Centrotemporal Spikes. Epilepsia 2003; 44: 688-692.

39. Born AP, Law I, Lund TE *et al.* Cortical deactivation induced by visual stimulation in human slow-wave sleep. NeuroImage 2002; 17: 1325-1335.

40. Brazier MAB. The Emergence of Electrphysiology as an Aid to Neurology. 1980.

41. Bruggemann JM, Som SS, Lawson JA, Haindl W, Cunningham AM, Bye AM. Application of statistical parametric mapping to SPET in the assessment of

intractable childhood epilepsy. Eur J Nucl Med Mol Imaging 2004; 31: 369-377.

42. Buchheim K, Obrig H, Pannwitz W *et al.* Decrease in haemoglobin oxygenation during absence seizures in adult humans. Neurosci Lett 2004; 354: 119-122.

43. Buckner RL, Bandettini PA, O'Craven KM *et al.* Detection of cortical activation during averaged single trials of a cognitive task using functional magnetic resonance imaging. Proc Natl Acad Sci 1996; 93: 14878-14883.

44. Buxton RB. The elusive initial dip. NeuroImage 2001; 13: 953-958.

45. Buxton RB. Brain Activation. Introduction to Funtional Neuroimaging. Cambridge University Press; 2002. p. 41-61.

46. Buxton RB, Frank LR. A model for the coupling between cerebral blood flow and oxygen metabolism during neural stimulation. J Cereb Blood Flow Metab 1997; 17: 64-72.

47. Buzaki G, Traub RD. Physiological Basis of EEG Activity. In: Engel JJ, Pedley TA, editors. Epilepsy: A Comprehensive Textbook. Lippencott-Raven; 1997. p. 819-30.

48. Caplan LR, Brass LM, DeWitt LD *et al.* Transcranial Doppler ultrasound: present status. Neurology 1990; 40: 696-700.

49. Catani M, Jones DK, Donato R, Ffytche DH. Occipito-temporal connections in the human brain. Brain 2003; 126: 2093-2107.

50. Chassoux F, Semah F, Bouilleret V *et al.* Metabolic changes and electro-clinical patterns in mesio-temporal lobe epilepsy: a correlative study. Brain 2004; 127: 164-174.

51. Cohen D. Magnetoencephalography: evidence of magnetic fields produced by alpha-rhythm currents. Science 1968; 161: 784-786.

52. Cohen D, Cuffin BN, Yunokuchi K *et al.* MEG versus EEG localization test using implanted sources in the human brain. Ann Neurol 1990; 28: 811-817.

53. Cohen MS, Bookheimer SY. Localization of brain function using magnetic resonance imaging. Trends Neurosci 1994; 17: 268-277.

54. Conturo TE, Lori NF, Cull TS *et al.* Tracking neuronal fiber pathways in the living human brain. Proc Natl Acad Sci 1999; 96: 10422-10427.

55. Cooper R. Research at the Burden Neurological Institute, Bristol. Biomed Eng 1972; 7: 220-225.

56. Cooper R, Winter AL, Crow HJ, Walter WG. Comparison of subcortical, cortical and scalp activity using chronically indwelling electrodes in man. Electroencephalogr Clin Neurophysiol 1965; 18: 217-228.

57. Critchley MCEA. John Hughlings Jackson, father of English neurology. New York: Oxford University Press; 1998.

58. Czisch M, Wehrle R, Kaufmann C *et al.* Functional MRI during sleep: BOLD signal decreases and their electrophysiological correlates. Eur J Neurosci 2004; 20: 566-574.

59. De Simone R, Silvestrini M, Marciani MG, Curatolo P. Changes in cerebral blood flow velocities during childhood absence seizures. Pediatr Neurol 1998; 18: 132-135.

60. Deckers RH, van GP, Ries M *et al.* An adaptive filter for suppression of cardiac and respiratory noise in MRI time series data. NeuroImage 2006; 33: 1072-1081.

61. Deichmann R, Schwarzbauer C, Turner R. Optimisation of the 3D MDEFT sequence for anatomical brain imaging: technical implications at 1.5 and 3 T. NeuroImage 2004; 21: 757-767.

62. Deppe M, Ringelstein EB, Knecht S. The investigation of functional brain lateralization by transcranial Doppler sonography. Neuroimage 2004; 21: 1124-1146.

63. Desmond JE, Glover GH. Estimating sample size in functional MRI (fMRI) neuroimaging studies: statistical power analyses. J Neurosci Methods 2002; 118: 115-128.

64. Detre JA, Alsop DC. Perfusion magnetic resonance imaging with continuous arterial spin labeling: methods and clinical applications in the central nervous system. Eur J Radiol 1999; 30: 115-124.

65. Detre JA, Alsop DC, Aguirre GK, Sperling MR. Coupling of cortical and thalamic ictal activity in human partial epilepsy: demonstration by functional magnetic resonance imaging. Epilepsia 1996; 37: 657-661.

66. Detre JA, Sirven JI, Alsop DC, O'Connor MJ, French JA. Localization of subclinical ictal activity by functional magnetic resonance imaging: correlation with invasive monitoring. Ann Neurol 1995; 38: 618-624.

67. Devous MDSr, Thisted RA, Morgan GF, Leroy RF, Rowe CC. SPECT brain imaging in epilepsy: a meta-analysis. J Nucl Med 1998; 39: 285-293.

68. Diehl B, Knecht S, Deppe M, Young C, Stodieck SR. Cerebral hemodynamic response to generalized spike-wave discharges. Epilepsia 1998; 39: 1284-1289.

69. Diehl B, Salek-Haddadi A, Fish DR, Lemieux L. Mapping of spikes, slow waves, and motor tasks in a patient with malformation of cortical development using simultaneous EEG and fMRI. Magn Reson Imaging 2003; 21: 1167-1173.

70. Dreifuss FE. Classification of reflex epilepsies and reflex seizures. Adv Neurol 1998; 75: 5-13.

71. Duffy FH, Burchfiel JL. Eye movement-related inhibition of primate visual neurons. Brain Res 1975; 89: 121-132.

72. Duncan JS. Imaging and epilepsy. Brain 1997; 120 ( Pt 2): 339-377.

73. Dupont P, Van PW, Palmini A *et al.* Ictal perfusion patterns associated with single MRI-visible focal dysplastic lesions: implications for the noninvasive delineation of the epileptogenic zone. Epilepsia 2006; 47: 1550-1557.

74. Ebersole JS. Defining epileptogenic foci: past, present, future. J Clin Neurophysiol 1997; 14: 470-483.

75. Ehrhardt JC, Lin CS, Magnotta VA, Fisher DJ, Yuh WT. Peripheral nerve stimulation in a whole-body echo-planar imaging system. J Magn Reson Imaging 1997; 7: 405-409.

76. Ellingson ML, Liebenthal E, Spanaki MV, Prieto TE, Binder JR, Ropella KM. Ballistocardiogram artifact reduction in the simultaneous acquisition of auditory ERPS and fMRI. Neuroimage 2004; 22: 1534-1542.

77. Engel J, Jr. A proposed diagnostic scheme for people with epileptic seizures and with epilepsy: report of the ILAE Task Force on Classification and Terminology. Epilepsia 2001; 42: 796-803.

78. Engel J, Jr., Brown WJ, Kuhl DE, Phelps ME, Mazziotta JC, Crandall PH. Pathological findings underlying focal temporal lobe hypometabolism in partial epilepsy. Ann Neurol 1982a; 12: 518-528.

79. Engel J, Jr., Kuhl DE, Phelps ME. Patterns of human local cerebral glucose metabolism during epileptic seizures. Science 1982b; 218: 64-66.

80. Engel J, Jr., Lubens P, Kuhl DE, Phelps ME. Local cerebral metabolic rate for glucose during petit mal absences. Ann Neurol 1985; 17: 121-128.

81. Federico P, Abbott DF, Briellmann RS, Harvey AS, Jackson GD. Functional MRI of the pre-ictal state. Brain 2005; 128: 1811-1817.

82. Fell J, Klaver P, Lehnertz K *et al.* Human memory formation is accompanied by rhinal-hippocampal coupling and decoupling. Nat Neurosci 2001; 4: 1259-1264.

83. Fell J, Widman G, Rehberg B, Elger CE, Fernandez G. Human mediotemporal EEG characteristics during propofol anesthesia. Biol Cybern 2005; 92: 92-100.

84. Fera F, Yongbi MN, Van Gelderen P, Frank JA, Mattay VS, Duyn JH. EPI-BOLD fMRI of human motor cortex at 1.5 T and 3.0 T: sensitivity dependence on echo time and acquisition bandwidth. J Magn Reson Imaging 2004; 19: 19-26.

85. Fernandez G, Hufnagel A, Van RD *et al.* Safety of intrahippocampal depth electrodes for presurgical evaluation of patients with intractable epilepsy. Epilepsia 1997; 38: 922-929.

86. Field AS, Yen YF, Burdette JH, Elster AD. False cerebral activation on BOLD functional MR images: study of low-amplitude motion weakly correlated to stimulus. AJNR Am J Neuroradiol 2000; 21: 1388-1396.

87. Fox PT, Raichle ME. Focal physiological uncoupling of cerebral blood flow and oxidative metabolism during somatosensory stimulation in human subjects. Proc Natl Acad Sci 1986; 83: 1140-1144.

88. Fox PT, Raichle ME, Mintun MA, Dence C. Nonoxidative glucose consumption during focal physiologic neural activity. Science 1988; 241: 462-464.

89. Frahm J, Bruhn H, Merboldt KD, Hanicke W. Dynamic MR imaging of human brain oxygenation during rest and photic stimulation. J Magn Reson Imaging 1992; 2: 501-505.

90. Frahm J, Kruger G, Merboldt KD, Kleinschmidt A. Dynamic uncoupling and recoupling of perfusion and oxidative metabolism during focal brain activation in man. Magn Reson Med 1996; 35: 143-148.

91. Frahm J, Merboldt KD, Hanicke W, Kleinschmidt A, Boecker H. Brain or vein--oxygenation or flow? On signal physiology in functional MRI of human brain activation. NMR Biomed 1994; 7: 45-53.

92. Friston KJ, Frith CD, Liddle PF, Dolan RJ, Lammertsma AA, Frackowiak RS. The relationship between global and local changes in PET scans. J Cereb Blood Flow Metab 1990; 10: 458-466.

93. Friston KJ, Frith CD, Liddle PF, Frackowiak RS. Comparing functional (PET) images: the assessment of significant change. J Cereb Blood Flow Metab 1991; 11: 690-699.

94. Friston KJ, Holmes AP, Price CJ, Buchel C, Worsley KJ. Multisubject fMRI studies and conjunction analyses. NeuroImage 1999; 10: 385-396.

95. Friston KJ, Josephs O, Zarahn E, Holmes AP, Rouquette S, Poline J. To smooth or not to smooth? Bias and efficiency in fMRI time-series analysis. NeuroImage 2000; 12: 196-208.

96. Friston KJ, Stephan KE, Lund TE, Morcom A, Kiebel S. Mixed-effects and fMRI studies. NeuroImage 2005; 24: 244-252.

97. Friston KJ, Williams S, Howard R, Frackowiak RS, Turner R. Movement-related effects in fMRI time-series. Magn Reson Med 1996; 35: 346-355.

98. Gambardella A, Gotman J, Cendes F, Andermann F. Focal intermittent delta activity in patients with mesiotemporal atrophy: a reliable marker of the epileptogenic focus. Epilepsia 1995; 36: 122-129.

99. Gao JH, Yee SH. Iterative temporal clustering analysis for the detection of multiple response peaks in fMRIMag21(1. Magnetic Resonance Imaging 2003; 21: 51-53.

100. Garraux G, Hallett M, Talagala SL. CASL fMRI of subcortico-cortical perfusion changes during memory-guided finger sequences. NeuroImage 2005; 25: 122-132.

101. Gastaut H. Clinical and electroencephalographical classification of epileptic seizures. Epilepsia 1970; 11: 102-113.

102. Gastaut H, Roger J, Soulayrol R, Tassinari CA, Regis H, Dravet C. Childhood epileptic encephalopathy with diffuse slow spike-waves (otherwise known as "petit mal variant") or Lennox syndrome. Epilepsia 1966; 7: 139-179.

103. Geyer JD, Bilir E, Faught RE, Kuzniecky R, Gilliam F. Significance of interictal temporal lobe delta activity for localization of the primary epileptogenic region. Neurology 1999; 52: 202-205.

104. Gibbs FA, Gibbs EL, Lennox WG. The electroencephalogram in epilepsy and in conditions of impaired conciousness. Arch Neurol Psychiatry 1935; 34: 1135-1148.

105. Glaser DE, Penny WD, Henson RN, Rugg MD, Friston K. Correcting for non-sphericity in imaging data using classical and Bayesian approaches. NeuroImage 2001; 13: S127.

106. Gloor P. Berger lecture. Is Berger's dream coming true? Electroencephalogr Clin Neurophysiol 1994; 90: 253-266.

107. Gloor P. Generalized cortico-reticular epilepsies. Some considerations on the pathophysiology of generalized bilaterally synchronous spike and wave discharge. Epilepsia 1968; 9: 249-263.

108. Gloor P, Ball G, Schaul N. Brain lesions that produce delta waves in the EEG. Neurology 1977; 27: 326-333.

109. Goldman RI, Stern JM, Engel J, Jr., Cohen MS. Acquiring simultaneous EEG and functional MRI. Clin Neurophysiol 2000; 111: 1974-1980.

110. Goldman RI, Stern JM, Engel J, Jr., Cohen MS. Simultaneous EEG and fMRI of the alpha rhythm. Neuroreport 2002; 13: 2487-2492.

111. Goncalves SI, De Munck JC, Pouwels PJ *et al.* Correlating the alpha rhythm to BOLD using simultaneous EEG/fMRI: inter-subject variability. Neuroimage 2006; 30: 203-213.

112. Goodridge DM, Shorvon SD. Epileptic seizures in a population of 6000. I: Demography, diagnosis and classification, and role of the hospital services. Br Med J (Clin Res Ed) 1983a; 287: 641-644.

113. Goodridge DM, Shorvon SD. Epileptic seizures in a population of 6000. II: Treatment and prognosis. Br Med J (Clin Res Ed) 1983b; 287: 645-647.

114. Gotman J, Grova C, Bagshaw A, Kobayashi E, Aghakhani Y, Dubeau F. Generalized epileptic discharges show thalamocortical activation and suspension of the default state of the brain. Proc Natl Acad Sci 2005; 102: 15236-15240.

115. Guye M, Parker GJ, Symms M *et al.* Combined functional MRI and tractography to demonstrate the connectivity of the human primary motor cortex in vivo. NeuroImage 2003; 19: 1349-1360.

116. Haas LF. Hans Berger (1873-1941), Richard Caton (1842-1926), and electroencephalography. J Neurol Neurosurg Psychiatry 2003; 74: 9.

117. Haginoya K, Munakata M, Kato R, Yokoyama H, Ishizuka M, Iinuma K. Ictal cerebral haemodynamics of childhood epilepsy measured with near-infrared spectrophotometry. Brain 2002; 125: 1960-1971.

118. Hajnal JV, Myers R, Oatridge A, Schwieso JE, Young IR, Bydder GM. Artifacts due to stimulus correlated motion in functional imaging of the brain. Magnetic Resonance in Medicine 1994; 31: 283-291.

119. Hamandi K, Salek-Haddadi A, Laufs H *et al.* EEG-fMRI of idiopathic and secondarily generalized epilepsies. NeuroImage 2006; 31: 1700-1710.

120. Handwerker DA, Ollinger JM, D'Esposito M. Variation of BOLD hemodynamic responses across subjects and brain regions and their effects on statistical analyses. Neuroimage 2004; 21: 1639-1651.

121. Heeger DJ, Ress D. What does fMRI tell us about neuronal activity? Nat Rev Neurosci 2002; 3: 142-151.

122. Henry TR, Engel J, Jr., Mazziotta JC. Clinical evaluation of interictal fluorine-18-fluorodeoxyglucose PET in partial epilepsy. J Nucl Med 1993; 34: 1892-1898.

123. Henry TR, Mazziotta JC, Engel J, Jr. *et al.* Quantifying interictal metabolic activity in human temporal lobe epilepsy. J Cereb Blood Flow Metab 1990; 10: 748-757.

124. Henry TR, Votaw JR. The role of positron emission tomography with [18F]fluorodeoxyglucose in the evaluation of the epilepsies. Neuroimaging Clin N Am 2004; 14: 517-35, ix.

125. Henson R. Analysis of fMRI time series. In: Frackowiak RS, Friston K, Frith CD *et al*, editors. Human Brain Function. Academic Press; 2003.

126. Henson RN, Price CJ, Rugg MD, Turner R, Friston KJ. Detecting latency differences in event-related BOLD responses: application to words versus nonwords and initial versus repeated face presentations. NeuroImage 2002; 15: 83-97.

127. Hill RA, Chiappa KH, Huang-Hellinger F, Jenkins BG. EEG during MR imaging: differentiation of movement artifact from paroxysmal cortical activity. Neurology 1995; 45: 1942-1943.

128. Ho SS, Berkovic SF, Newton MR, Austin MC, McKay WJ, Bladin PF. Parietal lobe epilepsy: clinical features and seizure localization by ictal SPECT. Neurology 1994; 44: 2277-2284.

129. Hoffmann A, Jager L, Werhahn KJ, Jaschke M, Noachtar S, Reiser M. Electroencephalography during functional echo-planar imaging: detection of epileptic spikes using post-processing methods. Magn Reson Med 2000; 44: 791-798.

130. Hoge RD, Atkinson J, Gill B, Crelier GR, Marrett S, Pike GB. Linear coupling between cerebral blood flow and oxygen consumption in activated human cortex. Proc Natl Acad Sci 1999b; 96: 9403-9408.

131. Hoge RD, Atkinson J, Gill B, Crelier GR, Marrett S, Pike GB. Investigation of BOLD signal dependence on cerebral blood flow and oxygen consumption: the deoxyhemoglobin dilution model. Magn Reson Med 1999a; 42: 849-863.

132. Holmes GL, McKeever M, Adamson M. Absence seizures in children: clinical and electroencephalographic features. Ann Neurol 1987; 21: 268-273.

133. Huang-Hellinger FR, Breiter HC, McCormack G *et al.* Simultaneous functional magnetic resonance imaging and electrophysiological recording. Human Brain Mapping 1995; 3: 13-23.

134. Huppertz HJ, Hof E, Klisch J, Wagner M, Lucking CH, Kristeva-Feige R. Localization of interictal delta and epileptiform EEG activity associated with focal epileptogenic brain lesions. Neuroimage 2001; 13: 15-28.

135. Hutton C, Bork A, Josephs O, Deichmann R, Ashburner J, Turner R. Image Distortion Correction in fMRI: A Quantitative Evaluation. NeuroImage 2002; 16: 217-240.

136. ILAE. Proposal for revised clinical and electroencephalographic classification of epileptic seizures. From the Commission on Classification and Terminology of the International League Against Epilepsy. Epilepsia 1981; 22: 489-501.

137. ILAE. Proposal for classification of epilepsies and epileptic syndromes. Commission on Classification and Terminology of the International League Against Epilepsy. Epilepsia 1985; 26: 268-278.

138. ILAE. Proposal for revised classification of epilepsies and epileptic syndromes. Commission on Classification and Terminology of the International League Against Epilepsy. Epilepsia 1989; 30: 389-399.

139. International Federation of Societies for Electroencephalography and Clinical Neurophysiology. A glossary of terms most commonly used by clinical electroencephalographers. Electroencephalogr Clin Neurophysiol 1974; 37: 538-548.

140. Ives JR, Warach S, Schmitt F, Edelman RR, Schomer DL. Monitoring the patient's EEG during echo planar MRI. Electroencephalography and Clinical Neurophysiology 1993; 87: 417-420.

141. Jackson GD, Connelly A, Cross JH, Gordon I, Gadian DG. Functional magnetic resonance imaging of focal seizures. Neurology 1994; 44: 850-856.

142. Jager L, Werhahn KJ, Hoffmann A *et al.* Focal Epileptiform Activity in the Brain: Detection with Spike-related Functional MR ImagingùPreliminary Results. Radiology 2002; 223: 860-869.

143. Jan MM, Sadler M, Rahey SR. Lateralized postictal EEG delta predicts the side of seizure surgery in temporal lobe epilepsy. Epilepsia 2001; 42: 402-405.

144. Janszky J, Schulz R, Ebner A. Clinical features and surgical outcome of medial temporal lobe epilepsy with a history of complex febrile convulsions. Epilepsy Res 2003; 55: 1-8.

145. Jasper H. Report of the Committee on Methods of Clinical Examination in Electoencephalography. Electroencephalogr Clin Neurophysiol 1958; 10: 370-375.

146. Jasper H, Drooglever-Fortuyn J. Experimental studies on the functional anatomy of petit mal epilepsy. Res Publ Assoc Nerv Ment Dis 1947; 26: 272-298.

147. Jefferys JG. Models and mechanisms of experimental epilepsies. Epilepsia 2003; 44 Suppl 12: 44-50.

148. Jezzard P, Clare S. Sources of distortion in functional MRI data. Hum Brain Mapp 1999; 8: 80-85.

149. Joynt RJ, Cape CA, Knott JR. Significance of focal delta activity in adult electroencephalogram. Arch Neurol 1965; 12: 631-638.

150. Kaminska A, Chiron C, Ville D *et al.* Ictal SPECT in children with epilepsy: comparison with intracranial EEG and relation to postsurgical outcome. Brain 2003; 126: 248-260.

151. Kapucu LO, Serdaroglu A, Okuyaz C, Kose G, Gucuyener K. Brain single photon emission computed tomographic evaluation of patients with childhood absence epilepsy. J Child Neurol 2003; 18: 542-548.

152. Kemna LJ, Posse S. Effect of respiratory CO(2) changes on the temporal dynamics of the hemodynamic response in functional MR imaging. NeuroImage 2001; 14: 642-649.

153. Kilner JM, Mattout J, Henson R, Friston KJ. Hemodynamic correlates of EEG: a heuristic. NeuroImage 2005; 28: 280-286.

154. Kim KH, Yoon HW, Park HW. Improved ballistocardiac artifact removal from the electroencephalogram recorded in fMRI. Journal of Neuroscience Methods 2004; 135: 193-203.

155. Kim SG. Quantification of relative cerebral blood flow change by flow-sensitive alternating inversion recovery (FAIR) technique: application to functional mapping. Magn Reson Med 1995; 34: 293-301.

156. Kim SG, Ogawa S. Insights into new techniques for high resolution functional MRI. Curr Opin Neurobiol 2002; 12: 607-615.

157. Klingelhofer J, Bischoff C, Sander D, Wittich I, Conrad B. Do brief bursts of spike and wave activity cause a cerebral hyper- or hypoperfusion in man? Neurosci Lett 1991; 127: 77-81.

158. Knowlton RC, Shih J. Magnetoencephalography in epilepsy. Epilepsia 2004; 45 Suppl 4: 61-71.

159. Kobayashi E, Bagshaw AP, Grova C, Dubeau F, Gotman J. Negative BOLD responses to epileptic spikes. Hum Brain Mapp 2006; 27: 488-497.

160. Kobayashi E, Bagshaw AP, Jansen A *et al.* Intrinsic epileptogenicity in polymicrogyric cortex suggested by EEG-fMRI BOLD responses. Neurology 2005; 64: 1263-1266.

161. Kochen S, Giagante B, Oddo S. Spike-and-wave complexes and seizure exacerbation caused by carbamazepine. Eur J Neurol 2002; 9: 41-47.

162. Koepp MJ, Noppeney U, Salek-Haddadi A, Price CJ. Functional Imaging in Reading Epilepsy. In: Wolf P, Inoue Y, Zifkin B, editors. Reflex Epilepsies. Paris: John Libbey Eurotext; 2004. p. 71-8.

163. Koepp MJ, Richardson MP, Brooks DJ, Cunningham VJ, Duncan JS. Central benzodiazepine/gamma-aminobutyric acid A receptors in idiopathic generalized epilepsy: an [11C]flumazenil positron emission tomography study. Epilepsia 1997; 38: 1089-1097.

164. Koepp MJ, Richardson MP, Brooks DJ *et al.* Cerebral benzodiazepine receptors in hippocampal sclerosis. An objective in vivo analysis. Brain 1996; 119 ( Pt 5): 1677-1687.

165. Konn D, Gowland P, Bowtell R. MRI detection of weak magnetic fields due to an extended current dipole in a conducting sphere: a model for direct detection of neuronal currents in the brain. Magn Reson Med 2003; 50: 40-49.

166. Koutroumanidis M, Binnie CD, Elwes RD *et al.* Interictal regional slow activity in temporal lobe epilepsy correlates with lateral temporal hypometabolism as imaged with 18FDG PET: neurophysiological and metabolic implications. J Neurol Neurosurg Psychiatry 1998a; 65: 170-176.

167. Koutroumanidis M, Koepp MJ, Richardson MP *et al.* The variants of reading epilepsy. A clinical and video-EEG study of 17 patients with reading-induced seizures. Brain 1998b; 121 ( Pt 8): 1409-1427.

168. Koutroumanidis M, Martin-Miguel C, Hennessy MJ *et al.* Interictal temporal delta activity in temporal lobe epilepsy: correlations with pathology and outcome. Epilepsia 2004; 45: 1351-1367.

169. Krakow K, Allen PJ, Symms MR, Lemieux L, Josephs O, Fish DR. EEG recording during fMRI experiments: image quality. Hum Brain Mapp 2000; 10: 10-15.

170. Krakow K, Lemieux L, Messina D *et al.* Spatio-temporal imaging of focal interictal epileptiform activity using EEG-triggered functional MRI. Epileptic Disord 2001; 3: 67-74.

171. Krakow K, Woermann FG, Symms MR *et al.* EEG-triggered functional MRI of interictal epileptiform activity in patients with partial seizures. Brain 1999; 122 ( Pt 9): 1679-1688.

172. Krings T, Reinges MH, Erberich S *et al.* Functional MRI for presurgical planning: problems, artefacts, and solution strategies. J Neurol Neurosurg Psychiatry 2001; 70: 749-760.

173. Krings T, Topper R, Reinges MH *et al.* Hemodynamic changes in simple partial epilepsy: a functional MRI study. Neurology 2000; 54: 524-527.

174. Kwong KK, Belliveau JW, Chesler DA *et al.* Dynamic magnetic resonance imaging of human brain activity during primary sensory stimulation. Proceedings of the National Academy of Sciences of the United States of America 1992; 89: 5675-5679.

175. Lai S, Hopkins AL, Haacke EM *et al.* Identification of vascular structures as a major source of signal contrast in high resolution 2D and 3D functional activation imaging of the motor cortex at 1.5T: preliminary results. Magn Reson Med 1993; 30: 387-392.

176. Laich E, Kuzniecky R, Mountz J *et al.* Supplementary sensorimotor area epilepsy. Seizure localization, cortical propagation and subcortical activation pathways using ictal SPECT. Brain 1997; 120 ( Pt 5): 855-864.

177. Lantz G, Grave dP, Spinelli L, Seeck M, Michel CM. Epileptic source localization with high density EEG: how many electrodes are needed? Clin Neurophysiol 2003; 114: 63-69.

178. Laufs H, Hamandi K, Walker MC *et al.* EEG-fMRI mapping of asymmetrical delta activity in a patient with refractory epilepsy is concordant with the epileptogenic region determined by intracranial EEG. Magn Reson Imaging 2006a; 24: 367-371.

179. Laufs H, Holt JL, Elfont R *et al.* Where the BOLD signal goes when alpha EEG leaves. Neuroimage 2006b; 31: 1408-1418.

180. Laufs H, Kleinschmidt A, Beyerle A *et al.* EEG-correlated fMRI of human alpha activity. NeuroImage 2003a; 19: 1463-1476.

181. Laufs H, Krakow K, Sterzer P *et al.* Electroencephalographic signatures of attentional and cognitive default modes in spontaneous brain activity fluctuations at rest. Proc Natl Acad Sci 2003b; 100: 11053-11058.

182. Laufs H, Lengler U, Hamandi K, Kleinschmidt A, Krakow K. Linking generalized spike-and-wave discharges and resting state brain activity by using EEG/fMRI in a patient with absence seizures. Epilepsia 2006c; 47: 444-448.

183. Laureys S, Owen AM, Schiff ND. Brain function in coma, vegetative state, and related disorders. The Lancet Neurology 2004; 3: 537-546.

184. Lazeyras F, Blanke O, Perrig S *et al.* EEG-triggered functional MRI in patients with pharmacoresistant epilepsy. J Magn Reson Imaging 2000; 12: 177-185.

185. Lazeyras F, Zimine I, Blanke O, Perrig SH, Seeck M. Functional MRI with simultaneous EEG recording: feasibility and application to motor and visual activation. J Magn Reson Imaging 2001; 13: 943-948.

186. Lee SK, Yun CH, Oh JB *et al.* Intracranial ictal onset zone in nonlesional lateral temporal lobe epilepsy on scalp ictal EEG. Neurology 2003; 61: 757-764.

187. Lemieux JF, Blume WT. Topographical evolution of spike-wave complexes. Brain Res 1986; 373: 275-287.

188. Lemieux L, Allen PJ, Franconi F, Symms MR, Fish DR. Recording of EEG during fMRI experiments: patient safety. Magnetic Resonance in Medicine: Official Journal of the Society of Magnetic Resonance in Medicine / Society of Magnetic Resonance in Medicine 1997; 38: 943-952.

189. Lemieux L, Salek-Haddadi A, Josephs O *et al.* Event-related fMRI with simultaneous and continuous EEG: description of the method and initial case report. Neuroimage 2001; 14: 780-787.

190. Lemieux L, Salek-Haddadi A, Krakow K. The nature of MR signal changes. Radiology 2003; 226: 922-923.

191. Lennox WG, DAVIS JP. Clinical correlates of the fast and the slow spike-wave electroencephalogram. Pediatrics 1950; 5: 626-644.

192. Lesser RP. MEG: good enough. Clin Neurophysiol 2004; 115: 995-997.

193. Liston AD, De Munck JC, Hamandi K *et al.* Analysis of EEG-fMRI data in focal epilepsy based on automated spike classification and Signal Space Projection. Neuroimage 2006a; 31: 1015-1024.

194. Liston AD, Lund TE, Salek-Haddadi A, Hamandi K, Friston KJ, Lemieux L. Modelling cardiac signal as a confound in EEG-fMRI and its application in focal epilepsy studies. NeuroImage 2006b; 30: 827-834.

195. Liu JZ, Zhang L, Brown RW, Yue GH. Reproducibility of fMRI at 1.5 T in a strictly controlled motor task. Magn Reson Med 2004; 52: 751-760.

196. Liu Y, Gao JH, Liu HL, Fox PT. The temporal response of the brain after eating revealed by functional MRI. Nature 2000; 405: 1058-1062.

197. Llinas RR. The intrinsic electrophysiological properties of mammalian neurons: insights into central nervous system function. Science 1988; 242: 1654-1664.

198. Logothetis NK, Pauls J, Augath M, Trinath T, Oeltermann A. Neurophysiological investigation of the basis of the fMRI signal. Nature 2001; 412: 150-157.

199. Loring DW, Meador KJ, Allison JD *et al.* Now you see it, now you don't: statistical and methodological considerations in fMRI. Epilepsy Behav 2002; 3: 539-547.

200. Luh WM, Wong EC, Bandettini PA, Hyde JS. QUIPSS II with thin-slice TI1 periodic saturation: a method for improving accuracy of quantitative perfusion imaging using pulsed arterial spin labeling. Magn Reson Med 1999; 41: 1246-1254.

201. Lund TE, Madsen KH, Sidaros K, Luo WL, Nichols TE. Non-white noise in fMRI: does modelling have an impact? NeuroImage 2006; 29: 54-66.

202. Lund TE, Norgaard MD, Rostrup E, Rowe JB, Paulson OB. Motion or activity: their role in intra- and inter-subject variation in fMRI. NeuroImage 2005; 26: 960-964.

203. MacDonald BK, Cockerell OC, Sander JW, Shorvon SD. The incidence and lifetime prevalence of neurological disorders in a prospective community-based study in the UK. Brain 2000; 123 ( Pt 4): 665-676.

204. Malonek D, Grinvald A. Interactions between electrical activity and cortical microcirculation revealed by imaging spectroscopy: implications for functional brain mapping. Science 1996; 272: 551-554.

205. Mansfield P. Multi-planar image formation using N.M.R. spin echoes. J Phys 1977; 10: L55-L58.

206. Marcus EM, Watson CW. Bilateral synchronous spike wave electrographic patterns in the cat. Interaction of bilateral cortical foci in the intact, the bilateral cortical-callosal, and adiencephalic preparation. Arch Neurol 1966; 14: 601-610.

207. Marcus EM, Watson CW. Symmetrical epileptogenic foci in monkey cerebral cortex. Mechanisms of interaction and regional variations in capacity for synchronous discharges. Arch Neurol 1968; 19: 99-116.

208. Markand ON. Alpha rhythms. J Clin Neurophysiol 1990; 7: 163-189.

209. Martins dS, Aarts JH, Binnie CD *et al.* The circadian distribution of interictal epileptiform EEG activity. Electroencephalogr Clin Neurophysiol 1984; 58: 1-13.

210. Mazoyer B, Zago L, Mellet E *et al.* Cortical networks for working memory and executive functions sustain the conscious resting state in man. Brain Res Bull 2001; 54: 287-298.

211. McKeown MJ. Detection of consistently task-related activations in fMRI data with hybrid independent component analysis. NeuroImage 2000; 11: 24-35.

212. McKeown MJ, Makeig S, Brown GG *et al.* Analysis of fMRI data by blind separation into independent spatial components. Hum Brain Mapp 1998; 6: 160-188.

213. Meencke HJ. Neuron density in the molecular layer of the frontal cortex in primary generalized epilepsy. Epilepsia 1985; 26: 450-454.

214. Meeren HK, Pijn JP, Van Luijtelaar EL, Coenen AM, Lopes da Silva FH. Cortical focus drives widespread corticothalamic networks during spontaneous absence seizures in rats. J Neurosci 2002; 22: 1480-1495.

215. Moosmann M, Ritter P, Krastel I *et al.* Correlates of alpha rhythm in functional magnetic resonance imaging and near infrared spectroscopy. NeuroImage 2003; 20: 145-158.

216. Moran NF, Lemieux L, Maudgil D, Kitchen ND, Fish DR, Shorvon SD. Analysis of temporal lobe resections in MR images. Epilepsia 1999; 40: 1077-1084.

217. Morgan VL, Price RR, Arain A, Modur P, Abou-Khalil B. Resting functional MRI with temporal clustering analysis for localization of epileptic activity without EEG. NeuroImage 2004; 21: 473-481.

218. Morocz IA, Karni A, Haut S, Lantos G, Liu G. fMRI of triggerable aurae in musicogenic epilepsy. Neurology 2003; 60: 705-709.

219. Morris HH, Luders H. Electrodes. In: Gotman J, Ives J, Gloor P, editors. Long-term Monitering in Epilepsy. Elsevier Science; 1985. p. 3.

220. Morris JS, Friston KJ, Buchel C *et al.* A neuromodulatory role for the human amygdala in processing emotional facial expressions. Brain 1998; 121 ( Pt 1): 47-57.

221. Muri RM, Felblinger J, Rosler KM, Jung B, Hess CW, Boesch C. Recording of electrical brain activity in a magnetic resonance environment: distorting effects of the static magnetic field. Magn Reson Med 1998; 39: 18-22.

222. Natsume J, Kumakura Y, Bernasconi N *et al.* Alpha-[11C] methyl-L-tryptophan and glucose metabolism in patients with temporal lobe epilepsy. Neurology 2003; 60: 756-761.

223. Negishi M, Abildgaard M, Nixon T, Todd Constable R. Removal of time-varying gradient artifacts from EEG data acquired during continuous fMRI. Clinical Neurophysiology 2004; 115: 2181-2192.

224. Nehlig A, Valenti MP, Thiriaux A, Hirsch E, Marescaux C, Namer IJ. Ictal and interictal perfusion variations measured by SISCOM analysis in typical childhood absence seizures. Epileptic Disord 2004; 6: 247-253.

225. Nehlig A, Vergnes M, Marescaux C, Boyet S, Lannes B. Local cerebral glucose utilization in rats with petit mal-like seizures. Ann Neurol 1991; 29: 72-77.

226. Nehlig A, Vergnes M, Waydelich R *et al.* Absence seizures induce a decrease in cerebral blood flow: human and animal data. J Cereb Blood Flow Metab 1996; 16: 147-155.

227. Nersesyan H, Herman P, Erdogan E, Hyder F, Blumenfeld H. Relative changes in cerebral blood flow and neuronal activity in local microdomains during generalized seizures. J Cereb Blood Flow Metab 2004a; 24: 1057-1068.

228. Nersesyan H, Hyder F, Rothman DL, Blumenfeld H. Dynamic fMRI and EEG recordings during spike-wave seizures and generalized tonic-clonic seizures in WAG/Rij rats. J Cereb Blood Flow Metab 2004b; 24: 589-599.

229. Newton MR, Austin MC, Chan JG, McKay WJ, Rowe CC, Berkovic SF. Ictal SPECT using technetium-99m-HMPAO: methods for rapid preparation and optimal deployment of tracer during spontaneous seizures. J Nucl Med 1993; 34: 666-670.

230. Niedermeyer E. Frontal lobe epilepsy: the next frontier. Clin Electroencephalogr 1998; 29: 163-169.

231. Niedermeyer E, Laws ER, Jr., Walker EA. Depth EEG findings in epileptics with generalized spike-wave complexes. Arch Neurol 1969; 21: 51-58.

232. Niedermeyer E, Lopes Da Silva F. Electroencephalography, Basic Principles, Clinical Applications and Related Fields. Lippincott Williams and Wilkins; 1998.

233. Normand MM, Wszolek ZK, Klass DW. Temporal intermittent rhythmic delta activity in electroencephalograms. J Clin Neurophysiol 1995; 12: 280-284.

234. Nöth U, Meadows GE, Kotagima R, Deichmann R, Corfield DR, Turner R. Cerebral vascular response to hypercapnia: determination with perfusion MRI at 1.5 and 3.0 Tesla using a pulsed arterial spin labelling technique. 2006.

235. O'Brien TJ, So EL, Mullan BP *et al.* Subtraction ictal SPECT co-registered to MRI improves clinical usefulness of SPECT in localizing the surgical seizure focus. Neurology 1998; 50: 445-454.

236. Ochs RF, Gloor P, Tyler JL *et al.* Effect of generalized spike-and-wave discharge on glucose metabolism measured by positron emission tomography. Ann Neurol 1987; 21: 458-464.

237. Ogawa S, Lee TM, Kay AR, Tank DW. Brain magnetic resonance imaging with contrast dependent on blood oxygenation. Proc Natl Acad Sci 1990a; 87: 9868-9872.

238. Ogawa S, Lee TM, Nayak AS, Glynn P. Oxygenation-sensitive contrast in magnetic resonance image of rodent brain at high magnetic fields. Magn Reson Med 1990b; 14: 68-78.

239. Ogawa S, Tank DW, Menon R *et al.* Intrinsic signal changes accompanying sensory stimulation: functional brain mapping with magnetic resonance imaging. Proceedings of the National Academy of Sciences of the United States of America 1992; 89: 5951-5955.

240. Opdam HI, Federico P, Jackson GD *et al.* A sheep model for the study of focal epilepsy with concurrent intracranial EEG and functional MRI. Epilepsia 2002; 43: 779-787.

241. Panayiotopoulos CP. A Clinical Guide to Epileptic Syndromes and their Treatment. Bladon Medical Publishing; 2002a.

242. Panayiotopoulos CP. Reflex Seizures and Reflex Epilepsies. A Clinical Guide to Epileptic Syndromes and their Treatment. Bladon Medical Publishing.; 2002b. p. 215.

243. Panet-Raymond D, Gotman J. Asymmetry in delta activity in patients with focal epilepsy. Electroencephalogr Clin Neurophysiol 1990; 75: 4742-481.

244. Parker GJ, Alexander DC. Probabilistic Monte Carlo based mapping of cerebral connections utilising whole-brain crossing fibre information. Lecture Notes Computer Sci 2003; 2737: 684-695.

245. Parker GJ, Alexander DC. Probabilistic anatomical connectivity derived from the microscopic persistent angular structure of cerebral tissue. Philos Trans R Soc Lond B Biol Sci 2005; 360: 893-902.

246. Parker GJ, Haroon HA, Wheeler-Kingshott CA. A framework for a streamline-based probabilistic index of connectivity (PICo) using a structural interpretation of MRI diffusion measurements. J Magn Reson Imaging 2003; 18: 242-254.

247. Parker GJ, Stephan KE, Barker GJ *et al.* Initial demonstration of in vivo tracing of axonal projections in the macaque brain and comparison with the human brain using diffusion tensor imaging and fast marching tractography. NeuroImage 2002; 15: 797-809.

248. Parkes LM, Fries P, Kerskens CM, Norris DG. Reduced BOLD response to periodic visual stimulation. NeuroImage 2004; 21: 236-243.

249. Patel MR, Blum A, Pearlman JD *et al.* Echo-Planar Functional MR Imaging of Epilepsy with Concurrent EEG Monitoring. AJNR Am J Neuroradiol 1999; 20: 1916-1919.

250. Pauling L, Coryell CD. The Magnetic Properties and Structure of Hemoglobin, Oxyhemoglobin and Carbonmonoxyhemoglobin. 1936. p. 210-6.

251. Penny WD, Stephan KE, Mechelli A, Friston KJ. Modelling functional integration: a comparison of structural equation and dynamic causal models. NeuroImage 2004; 23 Suppl 1: S264-S274.

252. Pessoa L, McKenna M, Gutierrez E, Ungerleider LG. Neural processing of emotional faces requires attention. Proc Natl Acad Sci 2002; 99: 11458-11463.

253. Powell HW, Guye M, Parker GJ *et al.* Noninvasive in vivo demonstration of the connections of the human parahippocampal gyrus. NeuroImage 2004; 22: 740-747.

254. Powell HW, Parker GJ, Alexander DC *et al.* MR tractography predicts visual field defects following temporal lobe resection. Neurology 2005; 65: 596-599.

255. Prevett MC, Duncan JS, Jones T, Fish DR, Brooks DJ. Demonstration of thalamic activation during typical absence seizures using H2(15)O and PET. Neurology 1995a; 45: 1396-1402.

256. Prevett MC, Lammertsma AA, Brooks DJ *et al.* Benzodiazepine-GABAA receptors in idiopathic generalized epilepsy measured with [11C]flumazenil and positron emission tomography. Epilepsia 1995b; 36: 113-121.

257. Prevett MC, Lammertsma AA, Brooks DJ, Cunningham VJ, Fish DR, Duncan JS. Benzodiazepine-GABAA receptor binding during absence seizures. Epilepsia 1995c; 36: 592-599.

258. Raichle ME, MacLeod AM, Snyder AZ, Powers WJ, Gusnard DA, Shulman GL. A default mode of brain function. Proc Natl Acad Sci 2001; 98: 676-682.

259. Reiher J, Beaudry M, Leduc CP. Temporal intermittent rhythmic delta activity (TIRDA) in the diagnosis of complex partial epilepsy: sensitivity, specificity and predictive value. Can J Neurol Sci 1989; 16: 398-401.

260. Reutens DC. Imaging Monoamine Oxidase B Receptor Mapping. In: Henry TR, Duncan JS, Berkovic SF, editors. Functional Imaging in the Epilepsies. Lippicott Williams & Wilkins; 2000. p. 173-6.

261. Rosenow F, Luders H. Presurgical evaluation of epilepsy. Brain 2001; 124: 1683-1700.

262. Roy CS, Sherrington CS. On the regulation of the blood supply of the brain. Joural of Physiology 1890; 11: 85-118.

263. Salek-Haddadi A, Diehl B, Hamandi K *et al.* Hemodynamic correlates of epileptiform discharges: an EEG-fMRI study of 63 patients with focal epilepsy. Brain Res 2006; 1088: 148-166.

264. Salek-Haddadi A, Friston KJ, Lemieux L, Fish DR. Studying spontaneous EEG activity with fMRI. Brain Res Rev 2003a; 43: 110-133.

265. Salek-Haddadi A, Lemieux L, Merschhemke M, Friston KJ, Duncan JS, Fish DR. Functional magnetic resonance imaging of human absence seizures. Ann Neurol 2003b; 53: 663-667.

266. Salek-Haddadi A, Merschhemke M, Lemieux L, Fish DR. Simultaneous EEG-Correlated Ictal fMRI. NeuroImage 2002; 16: 32-40.

267. Sanada S, Murakami N, Ohtahara S. Changes in blood flow of the middle cerebral artery during absence seizures. Pediatr Neurol 1988; 4: 158-161.

268. Savic I, Pauli S, Thorell JO, Blomqvist G. In vivo demonstration of altered benzodiazepine receptor density in patients with generalised epilepsy. J Neurol Neurosurg Psychiatry 1994; 57: 797-804.

269. Savic I, Persson A, Roland P, Pauli S, Sedvall G, Widen L. In-vivo demonstration of reduced benzodiazepine receptor binding in human epileptic foci. Lancet 1988; 2: 863-866.

270. Savic I, Thorell JO, Roland P. [11C]flumazenil positron emission tomography visualizes frontal epileptogenic regions. Epilepsia 1995; 36: 1225-1232.

271. Savic I, Widen L, Thorell JO, Blomqvist G, Ericson K, Roland P. Cortical benzodiazepine receptor binding in patients with generalized and partial epilepsy. Epilepsia 1990; 31: 724-730.

272. Seeck M, Lazeyras F, Michel CM *et al.* Non-invasive epileptic focus localization using EEG-triggered functional MRI and electromagnetic tomography. Electroencephalogr Clin Neurophysiol 1998; 106: 508-512.

273. Shmuel A, Augath M, Oeltermann A, Logothetis NK. Negative functional MRI response correlates with decreases in neuronal activity in monkey visual area V1. Nat Neurosci 2006; 9: 569-577.

274. Shmuel A, Yacoub E, Pfeuffer J *et al.* Sustained negative BOLD, blood flow and oxygen consumption response and its coupling to the positive response in the human brain. Neuron 2002; 36: 1195-1210.

275. Snead OC, III. Basic mechanisms of generalized absence seizures. Ann Neurol 1995; 37: 146-157.

276. Spencer SS. Depth electroencephalography in selection of refractory epilepsy for surgery. Ann Neurol 1981; 9: 207-214.

277. Spencer SS. Neural networks in human epilepsy: evidence of and implications for treatment. Epilepsia 2002; 43: 219-227.

278. Spencer SS, Berg AT, Vickrey BG *et al.* Initial outcomes in the Multicenter Study of Epilepsy Surgery. Neurology 2003; 61: 1680-1685.

279. Sperling MR, Skolnick BE. Cerebral blood flow during spike-wave discharges. Epilepsia 1995; 36: 156-163.

280. Stefanovic B, Warnking JM, Kobayashi E *et al.* Hemodynamic and metabolic responses to activation, deactivation and epileptic discharges. NeuroImage 2005; 28: 205-215.

281. Steinlein OK, Mulley JC, Propping P *et al.* A missense mutation in the neuronal nicotinic acetylcholine receptor alpha 4 subunit is associated with autosomal dominant nocturnal frontal lobe epilepsy. Nat Genet 1995; 11: 201-203.

282. Talairach J, Bancaud J. Lesion, "irritative" zone and epileptogenic focus. Confin Neurol 1966; 27: 91-94.

283. Tanaka N, Kamada K, Takeuchi F. Ictal magnetoencephalographic study in a patient with ring 20 syndrome. J Neurol Neurosurg Psychiatry 2004; 75: 488-490.

284. Tao JX, Ray A, Hawes-Ebersole S, Ebersole JS. Intracranial EEG substrates of scalp EEG interictal spikes. Epilepsia 2005; 46: 669-676.

285. Temkin O. The Falling Sickness. The John Hopkins Press; 1971.

286. Tenney JR, Duong TQ, King JA, Ferris CF. FMRI of brain activation in a genetic rat model of absence seizures. Epilepsia 2004; 45: 576-582.

287. Tenney JR, Duong TQ, King JA, Ludwig R, Ferris CF. Corticothalamic modulation during absence seizures in rats: a functional MRI assessment. Epilepsia 2003; 44: 1133-1140.

288. Thadani VM, Siegel A, Lewis P *et al.* Validation of ictal single photon emission computed tomography with depth encephalography and epilepsy surgery. Neurosurg Rev 2004; 27: 27-33.

289. Theodore WH, Brooks R, Margolin R *et al.* Positron emission tomography in generalized seizures. Neurology 1985; 35: 684-690.

290. Thulborn KR, Waterton JC, Matthews PM, Radda GK. Oxygenation dependence of the transverse relaxation time of water protons in whole blood at high field. Biochim Biophys Acta 1982; 714: 265-270.

291. Timofeev I, Steriade M. Neocortical seizures: initiation, development and cessation. Neuroscience 2004; 123: 299-336.

292. Toczek MT, Carson RE, Lang L *et al.* PET imaging of 5-HT1A receptor binding in patients with temporal lobe epilepsy. Neurology 2003; 60: 749-756.

293. Toosy AT, Ciccarelli O, Parker GJ, Wheeler-Kingshott CA, Miller DH, Thompson AJ. Characterizing function-structure relationships in the human visual system with functional MRI and diffusion tensor imaging. NeuroImage 2004; 21: 1452-1463.

294. Turner R, Le Bihan D, Moonen CT, Despres D, Frank J. Echo-planar time course MRI of cat brain oxygenation changes. Magn Reson Med 1991; 22: 159-166.

295. Van Paesschen W, Dupont P, Van HB *et al.* Self-injection ictal SPECT during partial seizures. Neurology 2000; 54: 1994-1997.

296. Vanrumste B, Jones RD, Bones PJ, Carroll GJ. Slow-wave activity arising from the same area as epileptiform activity in the EEG of paediatric patients with focal epilepsy. Clin Neurophysiol 2005; 116: 9-17.

297. Velasco M, Velasco F, Velasco AL, Lujan M, Vazquez dM. Epileptiform EEG activities of the centromedian thalamic nuclei in patients with intractable partial motor, complex partial, and generalized seizures. Epilepsia 1989; 30: 295-306.

298. Wade AR. The negative BOLD signal unmasked. Neuron 2002; 36: 993-995.

299. Walczak TS, Jayakar P. Interictal EEG. In: Engel JJ, Pedley TA, editors. Epilepsy: A Comprehensive Textbook. Lippincott-Raven; 1997. p. 831-48.

300. Wang J, Aguirre GK, Kimberg DY, Roc AC, Li L, Detre JA. Arterial spin labeling perfusion fMRI with very low task frequency. Magn Reson Med 2003; 49: 796-802.

301. Warach S, Ives JR, Schlaug G *et al.* EEG-triggered echo-planar functional MRI in epilepsy. Neurology 1996; 47: 89-93.

302. Wenzel R, Wobst P, Heekeren HH *et al.* Saccadic suppression induces focal hypooxygenation in the occipital cortex. J Cereb Blood Flow Metab 2000; 20: 1103-1110.

303. Williams D. A study of thalamic and cortical rhythms in petit mal. Brain 1953; 76: 50-69.

304. Williams DS, Detre JA, Leigh JS, Koretsky AP. Magnetic resonance imaging of perfusion using spin inversion of arterial water. Proc Natl Acad Sci 1992; 89: 212-216.

305. Woermann FG, Free SL, Koepp MJ, Sisodiya SM, Duncan JS. Abnormal cerebral structure in juvenile myoclonic epilepsy demonstrated with voxel-based analysis of MRI. Brain 1999; 122 ( Pt 11): 2101-2108.

306. Wong EC, Buxton RB, Frank LR. Implementation of quantitative perfusion imaging techniques for functional brain mapping using pulsed arterial spin labeling. NMR Biomed 1997; 10: 237-249.

307. Wood ML, Wehrli FW. Principles of Magnetic Resonance Imaging. In: Stark DD, Bradley WG, editors. Magnetic Resonance Imaging. Mosby; 1999. p. 1-14.

308. Wu DH, Lewin JS, Duerk JL. Inadequacy of motion correction algorithms in functional MRI: role of susceptibility-induced artifacts. J Magn Reson Imaging 1997; 7: 365-370.

309. Xiong J, Fox PT, Gao J-H. Directly mapping magnetic field effects of neuronal activity by magnetic resonance imaging. 2003. p. 41-9.

310. Yee SH, Gao JH. Improved detection of time windows of brain responses in fMRI using modified temporal clustering analysis. Magnetic Resonance Imaging 2002; 20: 17-26.

311. Yeni SN, Kabasakal L, Yalcinkaya C, Nisli C, Dervent A. Ictal and interictal SPECT findings in childhood absence epilepsy. Seizure 2000; 9: 265-269.

312. Yoshinaga H, Ohtsuka Y, Watanabe Y *et al.* Ictal MEG in two children with partial seizures. Brain Dev 2004; 26: 403-408.